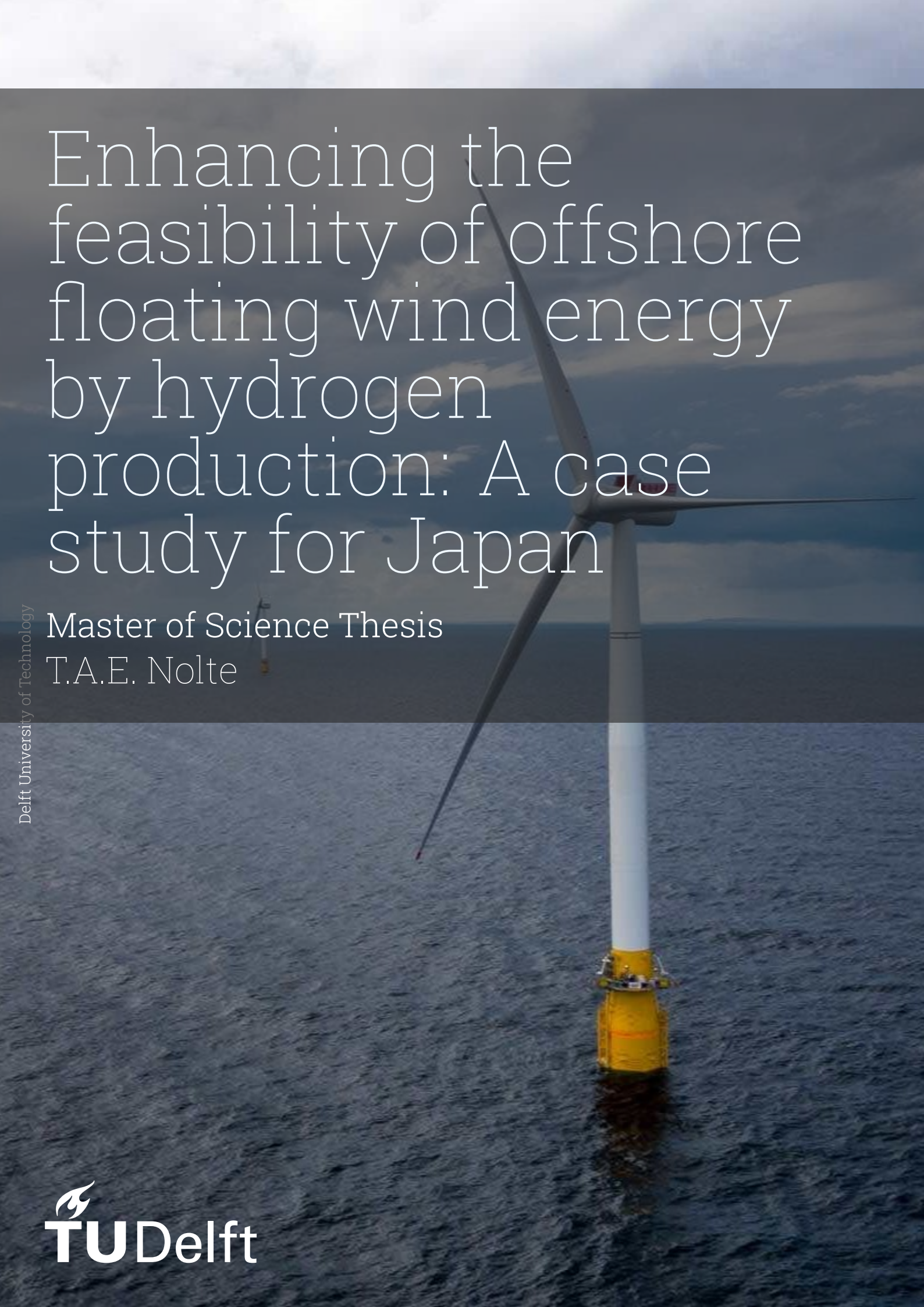

Enhancing the feasibility of offshore floating wind energy by hydrogen production: A case study for Japan

Master of Science Thesis

T.A.E. Nolte

Delft University of Technology

TU Delft

Enhancing the feasibility of offshore floating wind energy by hydrogen production: A case study for Japan

by

T.A.E. Nolte

Student Number 4465105

to obtain the degree of Master of Science
at the Delft University of Technology,
to be defended publicly on Friday May 3, 2024 at 10:00 AM.

Thesis committee:	Prof. dr. Ir. E. B. H. J. van Hassel
	Ir. A. C. M. van der Stap
	Dr. Ir. A. Jarquin Laguna
Daily Supervisor:	Dr. Ir. J. Breukels
Faculty:	Civil Engineering and Geosciences (CITG), Delft

Cover: https://reneweconomy.com.au/explainer-how-offshore-floating-wind-farms-work/

TU Delft

Preface

Over the past 11 months, various persons have contributed to this Master Thesis. First of all, I want to thank all the industry experts that I consulted for the interesting discussions on their expertise connected to the project. In addition, I want to extend my thanks some people in particular. To start with, I would like to express my gratitude to Edwin van Hassel and Andre van der Stap from the TU Delft for their guidance throughout my thesis journey. Andre's enthusiasm, drive, and expertise have been key in shaping the direction of my research. Especially when times were tough and I did not know what to do anymore, his insightful consult motivated me to get going again and elevated the quality of my thesis. Similarly, Edwin's mentorship and consistent availability and feedback have been extremely valuable. I am truly grateful for their dedication and contributions. Furthermore, I want to extend my appreciation to Antonio Jarquin Laguna for his role as a committee member. I am grateful for his interest in my research and for taking the time to assess the work. I would also like to acknowledge Jeroen Breukels for his role as supervisor from the Innovations Department at Allseas Engineering. I would like to thank Jeroen for his constant support, daily advise and for connecting me to various industry experts. To Andre, I would like to express my gratitude for introducing me to this thesis subject, teaching me about the shortcomings of offshore floating wind energy, and providing high-level project guidance. Lastly, I want to express my contentment with the choice for the Masters program Offshore and Dredging Engineering. This program has proven to be an excellent background for performing an integrated system study, as is done in this thesis. On top of that, I can honestly say that I enjoyed every bit of the program.

T.A.E. Nolte
Delft, April 2024

Summary

Offshore Floating Wind Energy (OFWE) remains an underdeveloped sector compared to its fixed-bottom alternative due to heightened engineering requirements and a lack of standardization, resulting in highly elevated costs. However, its potential advantages are noteworthy, especially in its characteristic that is it not restricted by water depth. This restriction does limit the applicability of fixed-bottom systems. Consequently, OFWE offers over four times the available ocean area, enabling deployment further offshore where wind speeds are higher and more consistent. Despite these advantages, this renewable energy technology's viability is currently dependent on governmental subsidies.

Recognizing the need for affordable, scalable, and transportable renewable energy storage solutions, Integrated Systems (IS) offer a promising new perspective. An IS combines an offshore wind farm, either fixed-bottom or floating, with a hydrogen production system. The primary focus of this research is to assess whether this integration can overcome the economic gap for OFWE, enhancing the Techno-Economic Performance (TEP) of a OFWE system potentially rendering it feasible.

To investigate this, a base case was modelled of Japan's Goto City Wind Farm (WF), the nation's first commercial Offshore Floating Wind Farm (OFWF). Japan was chosen as a case study due to its ambitious wind energy goals, limited areas suitable for fixed-bottom wind energy, and its desire towards integrating hydrogen as a key component of its energy mix. The base case would simulate the TEP of the WF over its operational lifetime of 25 years, employing a set of Key Performance Indicators (KPIs) to assess its TEP. Hourly wind speed data and power prices from the Japanese Electrical Power Exchange (JEPX), along with future estimations on both parameters derived from literature, were utilized to obtain hourly revenue generated by the system.

Results indicated that the base case Goto City WF was not economically viable over its operational lifetime, with revenue from power generation failing to outweigh expenses. Subsequently, the Goto City WF was converted into an IS by integrating additional components for Hydrogen (H2) production: desalination, electrolysis, and hydrogen carrier configuration units. The IS adopted a non-dedicated operational strategy, dynamically allocating generated power between grid supply and hydrogen production based on prevailing market conditions and a predetermined switchprice. Given the non-dedicated operational strategy of the IS and the requirement for a grid connection, a decentralized orientation was chosen. This entails locating the hydrogen production system onshore rather than offshore. Additional offshore operations would result in an even higher cost structure.

Various analyses were conducted to examine the TEP of the system comprehensively. These included examining the influence of four different hydrogen carrier configurations of which the Compressed Gaseous H2 (CGH2) was used as a reference case. Next, a capacity analysis was conducted to examine if installing the maximum amount of electrolyser capacity would yield maximum profit. Thirdly, scenario analysis was performed to investigate the influence of possible future scenarios on the TEP of the system. Finally, a sensitivity analysis was performed to analyse parameter deviation on TEP.

Results revealed that hydrogen production during periods of low power prices significantly enhanced the TEP of the Goto City WF based on the set criteria, rendering it feasible by the end of its operational lifespan. Moreover, the ability to switch between hydrogen production and grid supply provides a hedge against potential uncertainties considering power prices in the future. Wind farm capacity, particularly the type of turbines utilized, emerged as a crucial factor affecting TEP. Results underscored the significance of employing wind turbines with higher capacity for optimal performance, though adding turbines with equal characteristics also contributed to improved TEP.

In conclusion, under the analysed conditions, the addition of an H2 production system to OFWE does add to the TEP performance of the system when H2 is produced during hours of low power prices and consequently ensures system feasibility. Besides enhancing the TEP, it also mitigates risks of future uncertainties with respect to hydrogen and power prices. Under the condition that the OFWF uses WTs with a large capacity or the WF would be located at a location with more favorable wind conditions, feasibility can even be achieved for both the IS and the WF.

Contents

Nomenclature

Abbreviations

Abbreviation	Definition
AEL	Alkaline Electrolyte Electrolysers
CAPEX	Capital Expenditure
CGH2	Compressed Gaseous Hydrogen
CF	Cash Flow
CO2	Carbon Dioxide
EM	Electricity Mode
FC	Fuel Cell
FiT	Feed-in Tariff
FM	Forward Market
GH2	Gaseous Hydrogen
GW	Gigawatt
H2	Hydrogen
HB	Haber-Bosch (process)
HHV	Higher Heating Value
HM	Hydrogen Mode
HVAC	High Voltage Alternating Current
HVDC	High Voltage Direct Current
IPP	Independent Power Producers
ISA	International Standard Atmosphere
IS	Integrated System
JEPX	Japanese Electrical Power Exchange
KPIs	Key Performance Indicators
kWh	kilowatthour
LCOA	Levelized Cost of Ammonia
LCOE	Levelized Cost of Electricity
LCOH	Levelized Cost of Hydrogen
LH2	Liquid Hydrogen
LHV	Lower Heating Value
LOHC	Liquid Organic Hydrogen Carrier
LT	Lifetime
MCH	Methylcyclohexane
MW	Megawatt
NH3	Ammonia
NPV	Net Present Value
OFWE	Offshore Floating Wind Energy
OFWF	Offshore Floating Wind Farm
O&M	Operations and Maintenance
OPEX	Operational Expenditure
P2A	Power-to-Ammonia
PBP	Payback Period
PEM	Proton Exchange Membrane
PEMEL	Proton Exchange Membrane Electrolyser
RAO	Response Amplitude Operator
RES	Renewable Energy Source
SD	Success Difference

Abbreviation	Definition
SEC	Specific Energy Consumption
SM	Spot Market
SOEC	Solid Oxide Electrolysers
SWRO	Seawater Reverse Osmosis
TA	Technical Analysis
TEA	echno-Economical Analysis
TEF	Techno-Economic Feasibility
TEP	Techno-Economic Performance
VED	Volumetric Energy Density
W2H	Wind-to-Hydrogen
WF	Wind Farm
WT	Wind Turbine

1

Introduction

The transition from fossil fuels to a carbon free energy sources in transport, industry and electricity is one of the largest challenge mankind faces in the modern world. The goal is to be completely carbon neutral by 2050 [120] and therefor fossil fuels must be replaced by renewable energy sources (RES). Although the use of renewable energy sources has increased dramatically over the past few years, we are still behind the set target of reducing the rise in global temperature [119, 2]. One of the renewable energy sources that will play a key role in this transition is wind energy. Wind energy offers several advantages as a renewable energy source: it is abundant, inexhaustible, and widely distributed across the globe, providing a consistent and reliable source of electricity, without producing greenhouse gas emissions or air pollutants during operation. However, wind energy has a couple of drawbacks since it is an intermittent, weather-dependent energy source. As a consequence, power supply can not always be constant and will vary from time to time. In addition to this, the available areas for wind turbines onshore can be limited due to infrastructure, governmental regulations and human interaction. Therefor vast areas for WTs are also developed offshore. This brings additional advantages compared to onshore WTs. Apart from the not applicable previously named limitations, offshore WTs experience higher and more constant wind speeds resulting in more energy generation [2]. Also offshore wind energy is a highly developed RES making its price per kWh relatively low compared to other RES.

Offshore wind energy can be divided in to two configurations: fixed-bottom wind energy and floating wind energy. Fixed-bottom wind energy systems encompass turbines which are mounted directly to the seabed by a supporting structure. Floating wind energy systems have the turbines mounted on a floating structure which is anchored to the seabed. Whereas fixed-bottom wind energy systems are highly developed, floating wind energy is only in the early stage of commercial exploitation. From the total installed 57 GW of offshore wind energy capacity, only 140 MW is generated form floating wind energy systems [129]. This is because there is fewer floating wind farm equipment manufacturers and thus a lack of supply chain. Also, the technological challenges compared to the largely standardized fixed-bottom WTs are higher for floating wind energy. These factors result in elevated costs for floating wind energy compared to fixed-bottom. Given that about 80% of the ocean area suitable for offshore wind energy is too deep for fixed-bottom wind energy [129], ensuring that floating wind energy becomes a more developed RES could help the global energy industry significantly in order to contribute to the goals of the Paris Agreement.

Because of the intermittency of RES and the demand for energy being lower during the day, electricity prices tend to be much lower during the day than during the night [28]. Where this is normally not beneficial for the economics of offshore wind energy projects, it does provide an opportunity to see if there are other uses for the generated power during these hours of low prices. One of these uses can be production of hydrogen through electrolysis. The advantage of hydrogen compared to most RES is that it is not intermittent like wind and solar and can be stored for later use.

H2 is expected to play an essential role in the global transition from fossil fuels [56]. One nation that is expected to be a large consumer of H2 in the near future is Japan. Being one of the world's important economies, Japan is currently a large importer of energy sources since its own possibilities to produce energy is limited. Japan does not have a domestic supply of fossil fuels and its available area for deployment new RES is also limited due to

mountainous, inaccessible terrain and high population density, making available areas for RES scarse. The nation aims to be self-sufficient in the future and not dependent on other nations for its energy [98]. Besides the strive for independence, Japan also want to diversify its energy sources. After the Fukushima nuclear disaster, the nation decided to be less reliable on one primary source of energy for its electricity. Since RES are intermittent and because of the global climate goals Japan agreed on, its needs to find another source of energy other than fossil fuels when RES are unable to meet demand.

Another characteristic of Japan is that is has very deep seas along a very large proportion of its shores. This makes Japan not an ideal place for offshore wind energy since fixed-bottom wind energy is not a suitable option for a large part of Japan's coastal waters. However, Japan does aim to be one of the leading producers of offshore wind energy by 2030 [58]. To achieve this goal Japan is bound to use floating wind energy for some locations if it want to provide certain areas with offshore wind energy. A first initiative in exploring this form of wind energy is the Goto City wind farm. This project started out as a experiment using a 2.1 MW floating offshore WT and will be expanding to 8 WTs combining for 16.8 MW and will be commercially active from January 2024 [42]. Although this initiative is not expected to generate positive economics successes, Japan, like most governments when investing in RES, covers this by ensure the wind farm with a Feed in Tariff. This is a subsidy that the investors in this project will receive for each produced kWh [59].

Japan presents itself as an promising country for experimentation aimed at enhancing the feasibility of floating wind energy through the addition of hydrogen production during periods of relatively low electricity market prices. Successful outcomes of such trials could lead to heightened enthusiasm and financial commitment from all stakeholders, including energy corporations, investors, global sector regulators and local governments toward the advancement of floating wind energy technologies. Consequently, this would amplify the floating wind energy supply chain, therefor mitigating technological challenges and financial risks, which will result in a decrease in overall costs and subsequent more positive return on investment associated with offshore floating wind energy.

1.1. Problem Analysis

As the introduction states, Japan's ambition to increase the energy generation from offshore wind is largely restricted by its very deep seas along largest part of the shoreline. Only very small percentage of the available sea area is suitable for fixed-bottom offshore wind turbines. For this reason, if Japan aims to achieve its goals on offshore wind energy production, the nation is confined to resort to offshore floating wind energy. This is not necessarily an unfavourable situation, as OFWE has the upper hand in terms of performance compared to its fixed-bottom alternative. OFWE often has a higher capacity factor, meaning that the maximum power output is reached more often [20]. This is the result of constant higher wind speeds. Besides the elevated performance, the area of availability is also much larger since the deployment of Offshore Floating Wind Farms (OFWF) is less restricted to sea depth. Compared to its fixed-bottom alternative, there is around four times more available ocean area suitable for OFWE [20].

However, OFWE currently has a highly elevated Levelized Cost of Energy (LCOE) compared to fixed-bottom due to it higher expenses. LCOE is the average price of all the generated power of a Wind Farm (WF) over its operational lifetime. Whereas the LCOE of OFWE varies between €100-250/MWh [23, 88, 135, 13], the average LCOE of a WF in the North Sea is approximately €50/MWh [65]. Notably OFWE, even with a higher capacity factor compared to fixed-bottom, is still an intermittent source of energy since it is dependent the variance of wind speeds. This means that power generation is also volatile. The profitability of OFWE also depends on power market dynamics which are the prices at which power is sold to the electricity grid. Since this is a market based on supply and demand, power prices tend to be high when there is an abundant supply of electricity and vice versa. These three aspects make that OFWE is an energy source which is techno-economically not feasible e.g. the income does not outweigh the expenses and is therefor not a viable investment.

In order to identify the problem of non-feasibility of OFWE, it is paramount that a set OFWF, namely the Goto City Wind Farm, needs to be modeled and its performance needs to be simulated. In this study, the performance of the Goto City Wind Farm will be assessed based on key performance indicators which will later be introduced and elaborated. The model should be able to identify the shortages of OFWE in terms of its elevated cost structure and why the LCOE is so much higher compared to fixed bottom. More importantly, the model should identify how these shortages can be contained or even overcome by hydrogen production, making a set Feed-in Tariff obsolete. Hydrogen production via electrolysis only requires pure water and electricity to form hydrogen. For this reason, electricity generated from OFWF, especially during hours of high wind speeds and low power prices, proposes to

be a potential advocate for hydrogen production. The main research question of this research is depicted below.

"How can H2 production add value to offshore floating wind energy?"

Since this is a high level research question, meaning that it seeks to advance knowledge in the particular areas without necessarily having any immediate applications in mind, and the concepts of both hydrogen and OFWE are broad, setting boundaries on the depth of both these concepts is crucial. The scope of this research therefor extends to determining if the techno-economic feasibility of OFWE for Japan can be enhanced by producing hydrogen during hours where the price of hydrogen is higher than the price of electricity per kWh.

1.2. Structure

The initial chapter provide a contextual background on offshore floating wind energy and detail the foundational aspects of the base case model, establishing the groundwork for this study. The latter chapter will also discuss acquired results and draw conclusions which explain the motive behind this research. Following this, Chapter 4 outlines the research proposal, while Chapter 2.2 delves into the fundamentals of hydrogen and will provide the necessary knowledge of the topic for the following research. Chapter 2.3 elaborates on the concept of an integrated system and its application in this research. The modeling methodology for the integrated system is explained in Chapter 6. Subsequently, Chapter 7 discusses the results derived from the integrated system model. Lastly, Chapter 8 draws conclusions and offers recommendations for further studies based on the obtained results.

2

Literature Study

2.1. Offshore Floating Wind Energy

This section provides a description of the fundamental aspects surrounding OFWE. It provides explanation on the pivotal elements that form the building blocks of an offshore floating wind farm. A detailed examination of the operational processes within such installations is presented, with a particular focus on the Goto City Wind Farm in Japan, positioned as the nation's pioneering OFWF.

To comprehensively assess the viability of OFWE as a RES, a contextual understanding of the power market is imperative. This chapter initiates the discussion by delving into the crucial elements and procedural steps in offshore floating wind farms, described in Section 2.1.1. Subsequently, Section 2.1.2 provides an overview of the characteristics of the Goto City Wind Farm. Finally, the power market of Japan is explained in Section 2.1.3, offering insights into the dynamics present in the trade of electricity in Japan.

2.1.1. Fundamentals

Offshore floating wind energy denotes a renewable energy source generated by wind turbines which are floating on water. Consisting of a wind turbine and a floater keeping the turbine in place, it is the most efficient and developed technique of electricity generation offshore. The offshore location affords heightened wind speeds with increased stability and consistency, rendering it a superior environment for energy extraction. Furthermore, the absence of infrastructural constraints and minimal human interference allows for the construction of larger and more concentrated wind turbines, contributing to enhanced operational efficiency [16]. It is also expected that because of increasing economies of scale, more competitive supply chains and further technological improvements, the costs of wind energy will decrease of the coming years [2].

Power Conversion

A wind turbine operates through the utilization of aerodynamic forces exerted on its rotor blades, functioning like the lift-producing wings of an aircraft. The pressure differentials acting on either side of the blades induce rotational motion, propelling the rotor. Subsequently, this rotational energy is harnessed through a direct connection or gearbox linkage to a generator, facilitating the conversion of kinetic energy into electricity. Wind turbines exhibit operational characteristics such as cut-in speeds, representing the minimum wind velocity required to initiate rotor rotation and power generation.

As wind speeds increase, the electricity output proportionally increases until reaching a maximum known as the rated power. Beyond this threshold, despite increased wind speeds, the power output stabilizes until it reaches the cut-out speed. This critical point prompts an automatic turbine shutdown, a precautionary measure aimed at reducing the risk of large stresses on the rotor system. The graphical representation of this generation curve is depicted in Figure 2.1a.

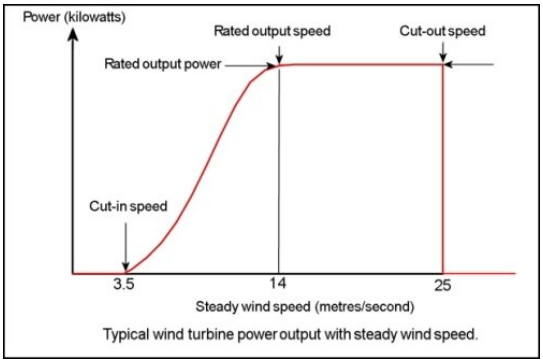

(a) Rated power graph of a wind turbine [48]

(b) Wake of offshore wind turbines [128]

The hub height of the turbine is also of importance to power conversion. Wind speeds increase with increasing height above sea level [90]. As a result, the wind speed at 10 meter height is different from 100 meter height. If height at which measurements have been conducted do not match, the wind speed at the desired height has to be extrapolated. The computational steps required to extrapolate the available wind speeds to the turbine hub height are given in equation 2.1 [77].

$$v_{hub} = v_r(\frac{H_{hub}}{H_r})^{\alpha} \tag{2.1}$$

Where v_{hub} is the wind speed at hub height, v_r is the reference wind speed at elevated height, H_{hub} is the hub height and H_r is the reference height. The α is the power law exponent. In engineering applications, the value of α is determined by the terrain type and generally is estimated to range from 0.1 to 0.4 [3]. Here, the general value of α for coastal topography is set to 0.15 based on former studies [3].

The presence of other wind turbines in the same WF influences the wind flow of the area. This disturbed wind flow is called wake and is visualized in Figure 2.1b. Current practices in turbine spacing for optimal wind utilization involve maintaining a distance of approximately seven times the diameter (7D) of the rotor area. However, empirical investigations, as indicated in a study by Meyers et al. [66], suggest that a significantly larger inter-turbine spacing, approximately 15D, may be more effective.

Floater

There are a number of different methods to mount offshore wind turbines. The depth of the water is determinative to choose which method is best applicable. For deeper waters (>50m) three predominant foundation types are employed for supporting wind turbines: the tension leg platform (TLP), the semi-submersible (SSP) platform, and the spar buoy (SB). All these foundations are suitable for deep sea wind farms but the spar buoy and semi-submersible have proven the be more viable in economic terms [23].

The spar buoy foundation, particularly suitable for regions with mild environmental conditions, features a singular column tethered to the seabed. Comprising a steel or concrete cylinder filled with ballast, this design ensures a low center of gravity, strategically positioned beneath the center of buoyancy, thereby facilitating buoyancy-driven stability. The spar buoy configuration is specifically designed so the turbine to float and maintain in the upright position [82].

A SSP is a platform consisting mostly of three or four floaters interconnected by rods. This result in a larger waterline area and thus a larger stabilizing moment in waves [67]. Other designs for semi-submersible platforms exist but these are generally still in the design stage at the moment and are not yet implemented [78]. Another advantage of the semi-sub is that is can be constructed onshore and towed to the offshore location reducing installation costs [82].

The platforms need to be moored to the sea bottom in order to keep them in position. The platform of a TLP is held in position by vertical tendons anchored by suction piles, driven piles or a template foundation. The tension in the tendons provides righting stability. Spar buoys and semi-subs are moored with a spread mooring system with catenary or taut lines. A drag anchor is attached to the end of each line providing resistance against displacement of the platform when experiencing wave and current forces. The distance of the anchor to the platform where it

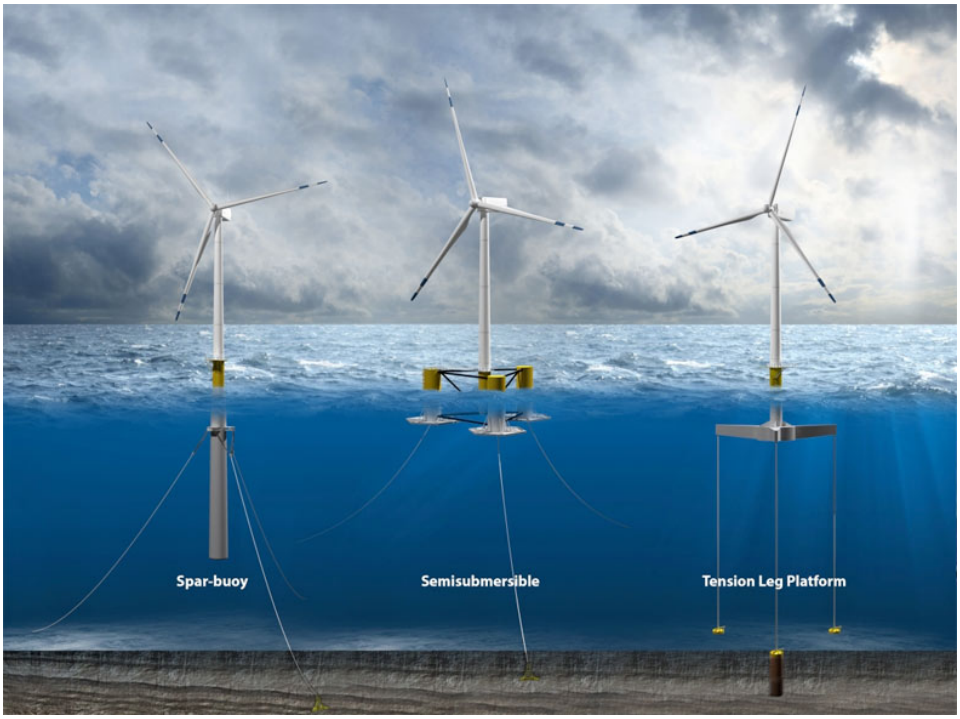

Figure 2.2: Three types of deep sea mooring for offshore wind turbines [92]

is stationary on the sea bottom, the so called *anchor radius*, is between 4-8 times the water depth. A large part of the chain lies on the sea bottom and is called *ground chain*. The catenary mooring leg has the ground chain resting on the seafloor to provide the restoring forces when getting lifted by the motion of the vessel or excursion [82].

Electrical Infrastructure

The transmission of electricity from offshore wind farms necessitates the utilization of high voltages to facilitate the efficient transmission of large-scale electric power over extended distances [53]. In general terms, large electric transmission systems fall into two categories: High Voltage Alternating Current (HVAC) and High Voltage Direct Current (HVDC). HVAC systems, characterized by fewer losses and enhanced economic viability compared to HVDC, are typically preferred compared to HVDC systems. However, HVAC cables with the same amperage require a larger section due to skin effect and self-induced reactance, making HVDC more cost-effective over extended transmission distances beyond 60 kilometers [121].

The collective electricity yield from all wind turbines is channeled to an offshore substation, where the voltage is increased before onward transport to an onshore substation [53]. Onshore substations subsequently convert the voltage for compatibility with the power grid. Notably, offshore substations can assume either a fixed-bottom configuration or, in recent applications, be fixed to a floater. The latter configuration allows for centralized placement within the wind farm, particularly advantageous in deep-sea conditions, thereby minimizing losses and reducing cable-related costs [38]. The schematic depiction of the electricity transmission process is illustrated in Figure 2.3.

2.1.2. Goto City Wind Farm

As Japan strives to diversify its energy sources and embrace sustainable alternatives [58, 98], the Goto City Wind Farm is a groundbreaking initiative, positioning itself as the nation's first commercial offshore floating wind farm. Driven by a commitment to diversify its energy matrix and reduce dependence on fossil-fuel based energy sources, the construction of this wind farm off the coast of Goto City signifies a strategic leap towards achieving Japan's renewable energy ambitions.

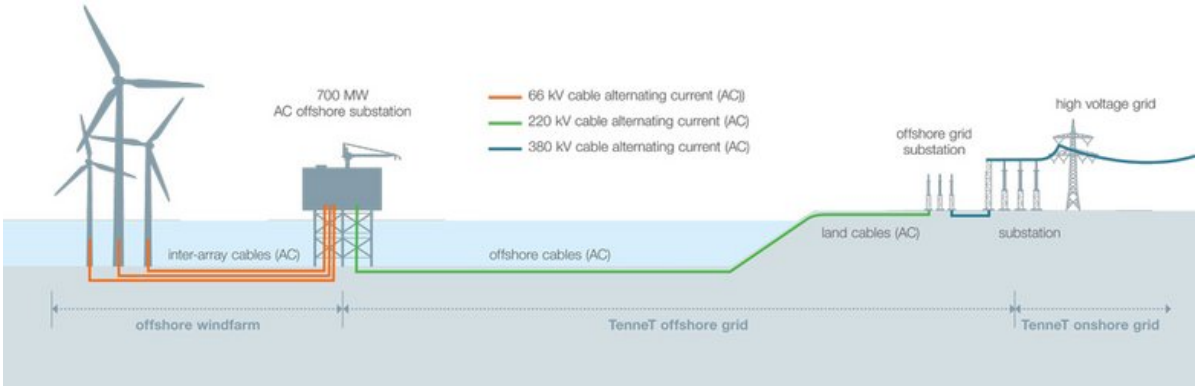

Figure 2.3: Schematic overview of the transmission of generated electricity to the power grid through off- and onshore substations [95]

Motives

The motives behind the construction of the Goto City Wind Farm are rooted in Japan's overarching energy strategy. Faced with the need to mitigate environmental impact, reduce carbon emissions, and increase energy security, Japan is using its coastal resources to harness the vast potential of offshore wind. However, Japan's shores a characterized by the rapidly increasing water depth the further from the coast. Only a very select number of regions harness the possibility of using fixed-bottom wind energy [106] . By opting for floating wind turbines, the Goto City Wind Farm aims to overcome the constraints of water depth, thereby expanding the geographical scope for offshore wind energy projects.

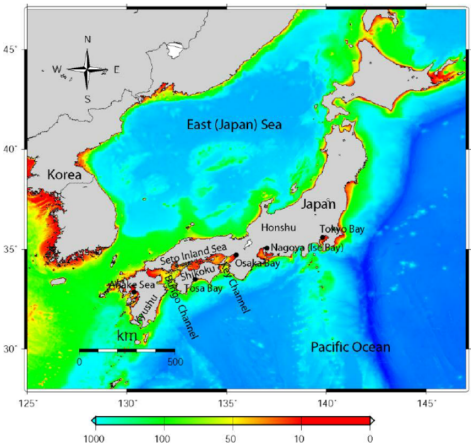

(a) Coastal topography of Japan [72]

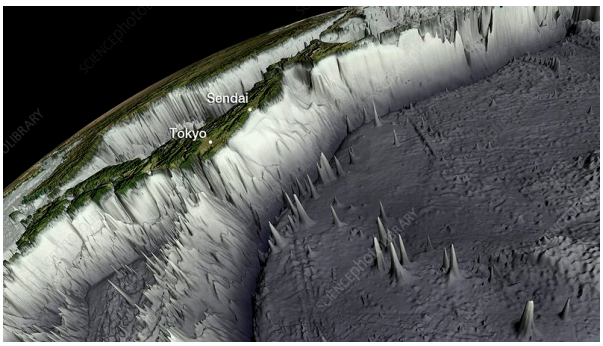

(b) Rapidly decreasing sea depth near the shore of Tokyo [63]

Deployment

The deployment strategy of the Goto City Wind Farm involves the installation of SPAR-buoy floater in the waters surrounding Goto City. The project takes into account the unique challenges posed by deeper waters, employing advanced floaters that ensure the stability and efficient operation of the turbines. The first of the eight SPAR-type floating foundations has been loaded onto the semi-submersible spud barge at Fukue Port and transported to the wind farm site offshore Kabashima where the unit is undergoing installation. This is depicted in Figure 2.5a. This foundation will be extensively tested and monitored before further deployment of floaters.

(a) Deployment of the first SPAR-buoy floater used for the Goto City Wind Farm [94]

(b) Hitachi 2.1 MW wind turbine used in the Goto City Wind Farm [62]

Characteristics

The Goto City Wind Farm boasts distinctive characteristics that set it apart as a trailblazer in Japan's renewable energy landscape. The utilization of state-of-the-art floaters and optimized turbine spacing aims to mitigate the wake effects caused by neighboring turbines, enhancing overall energy extraction efficiency. An overview of the park lay-out is shown in Figure 2.6. The Goto City Wind Farm utilises eight 2.1 MW Hitachi wind turbines, resulting in a combined power output of 16.8 MW [44]. The turbines are installed on hybrid SPAR-type, three-point mooring floating foundations [94]. The wind farm is planned to deliver electricity until December 2043. The used wind turbines are illustrated in Figure 2.5b.

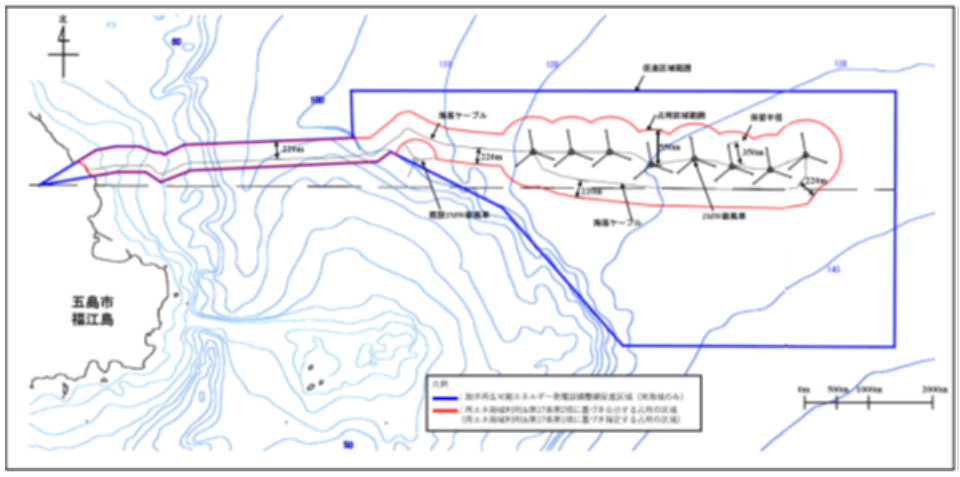

Figure 2.6: Lay-out of the Goto City Wind Farm in terms of turbine spacing [101]

2.1.3. Power Market

The power market in Japan is a complex and regulated system that has undergone significant changes in recent years to enhance competition and promote renewable energy sources [44]. After the 2011 Fukushima nuclear disaster, the Japanese government implicated the Basic Energy Plan (BEP). This discussed a long-term national energy policy for Japan. It has reaffirmed the importance of nuclear power generation as a base load capacity in Japan and it emphasizes it is necessary to increase use of various renewable energy sources in the future. Consequently, Japan has introduced a FiT to support the growth of RES including wind and particularly offshore wind energy [59]. A FiT is a guaranteed payment by the government per unit of power to a supplier of RE, thus providing a stable and attractive financial environment for investors and project developers. RE projects are rarely profitable in the first stages of deployment [114, 80]. Therefor the government used a FiT in order to make investment in this project more accessible and attract developers. By offering a predictable revenue stream, FiTs

play an important role in accelerating the development of OFWE. It causes that the electricity grid is provided by more electricity generated from OFWE and it advances the global transition towards RES.

The newly revised Japanese Power Market consists of three components: 1. Generation, 2. Transmission and 3. Distribution.

1. **Power Generation** in Japan is dominated by a mix of resources. The generated power is provided to the grid by Independent Power Producers (IPP) and traditional utilities operate power plants [44, 96]. After the Fukushima nuclear disaster, all nuclear power generation was shut down. This resulted in a self-sufficient energy rate of only 4% for Japan consisting mostly of RES which can be volatile. The low rate is the result of Japan not having domestic sources of fossil fuels. All fossil-fuels must be imported to sustain a constant power generation since Japan is also not connected to the electricity network of other Asian countries. This is a consequence of Japan being an island isolated by the sea.
2. **Transmission** of the generated power is managed by the Japan Electric Power Exchange (JEPX). This is a government-regulated entity which plays a crucial role in ensuring a stable supply of electricity by coordinating electricity flows across the country [97]. JEPX offers two types of trading: a day-ahead trading system called Forward Market (FM) as the main marketplace for energy, and a real-time, intra-day trading system called Spot Market (SM) as the adjustment market for bulletin board products.

   The FM was introduced to give both generators and distributors a last-minute opportunity to balance their demand and supply, and thus avoid penalties for failing to do so. It is the market where the electricity to be delivered the next day is traded. 48 products are traded every 30 minutes in a 24-hour period. The bidding is done through a system called *Blind Single Price Auction*, where the price is traded at the contracted price regardless of the bid price. For example, if a bid is placed at ¥10/kWh, but the contract price is ¥15/kWh, it will be sold at ¥15/kWh. The "blind" refers to the fact that one cannot see the bids of other participants at the time of bidding. On the following day, after electricity is traded in the FM, unforeseen power generation problems or demand surges may occur during the period between the planned and actual delivery. The SM is designed to address such unforeseen supply-demand mismatches that occur after the next day's plan is formulated. The contract is executed as a continuous session.
3. The **Distribution** of electricity is carried out by various regional utilities, each serving a specific area of Japan. These regional utilities are responsible for delivering electricity to end-users. Within each region specific electricity retailers are operational which purchase electricity from generators and sell it to end-users, including households and businesses. The retail market was liberalized in 2016, allowing consumers to choose their electricity supplier [44].

2.2. Hydrogen

In pursuit of a cleaner and more sustainable energy future, hydrogen has emerged as a promising player, offering a versatile and eco-friendly alternative to conventional energy sources. Besides its sustainable properties, hydrogen is a materialistic RES. This means that, like oil and gas, it can be temporarily stored and does not have to be used as energy at the moment of production.

This section delves into the fundamentals of hydrogen, exploring its production methods and its compatibility as an additional energy production system to offshore floating wind energy. It begins by elaborating the diverse methods of hydrogen production in today's industry. A critical examination of these production techniques lays the foundation for finding a suitable method for offshore wind applications. Section 2.2.3 will give a more detailed description of the desalination process, which is required before seawater can be utilized for hydrogen production. Hydrogen can be stored in different form, dependent on its application or preference of transport. Finally, Section 2.2.4 delves into the four most used hydrogen carrier configurations used today to give a better understanding of how these might apply to offshore floating wind.

2.2.1. Fundamentals

At its fundamental level, hydrogen is the lightest and most abundant element in the universe. Consisting a single proton and a lone electron, H2 exhibits unique physical and chemical characteristics that render it a versatile energy carrier. One of hydrogen's defining features is its remarkable energy content per unit mass. When combusted or utilized in fuel cells, hydrogen releases energy with high efficiency, providing a potent source of power. Moreover, the combustion of hydrogen produces only water vapor as a byproduct, avoiding the emission of greenhouse

gases making hydrogen environmentally a much desired energy carrier.

Hydrogen's adaptability extends beyond its role as a fuel. Its applications span various sectors, including industry, transportation, and energy storage. In industry, hydrogen serves as a crucial feedstock for the production of ammonia and is integral in refining processes. As a transportation fuel, it can power fuel cell electric vehicles, offering a clean alternative to conventional internal combustion engines. Furthermore, hydrogen plays a vital role in energy storage, offering a means to store excess renewable energy generated during periods of abundance for use during times of high demand.

Hydrogen does not appear in on earth in pure form. This means that hydrogen carriers must be split in order to obtain hydrogen. This primarily done in three ways each characterizing the obtained hydrogen by a different color.

1. **Grey hydrogen** is hydrogen that is won by reforming methane gas. This is currently the most common way to gain hydrogen. However the reforming process still uses fossil fuels and emit green house gasses in the atmosphere. It is therefor not a sustainable way to win hydrogen.
2. **Blue hydrogen** is won by the same reforming process as grey hydrogen only the emitted CO_2 is captured so it barely effects global warming. However it still uses fossil fuels as a base material and is therefor not sustainable.
3. **Green hydrogen** is hydrogen won by electrolysis using renewable energy sources to provide electricity. This type of hydrogen is sustainable and should be the main type of hydrogen used in a carbon neutral future.

In essence, the fundamentals of hydrogen lie in its abundance, simplicity, and potential to serve as a clean and versatile energy carrier. As global efforts intensify to transition away from fossil fuels and combat climate change, hydrogen stands as a cornerstone in the quest for a more sustainable and resilient energy future.

2.2.2. Production

Hydrogen production -green hydrogen at least- is done using electrolysers. Electrolyser systems generate H2 gas through the process of electrolysis, which involves the splitting of water molecules (H2O) into oxygen (O2) and hydrogen (H2) utilizing an electric current. This process involves two basic principles: the Faraday's laws of electrolysis and the Nernst equation.

The Faraday's laws of electrolysis describe the relationship between the amount of electricity passed through an electrolyte and the amount of chemical reaction that occurs. The laws state that the amount of chemical reaction that occurs is directly proportional to the amount of electricity passed through the electrolyte. Thus, the amount of H2 gas produced is directly proportional to the amount of electricity passed through the electrolyte.

The Nernst equation is a mathematical tool that predicts how the electrical voltage affects the concentration of chemicals generated by a chemical reaction in cells. The equation is shown below.

$$E = E^o - (\frac{RT}{nF}) * ln(Q) \tag{2.2}$$

Where E is the voltage, E^o is the standard voltage for the reaction, which is a constant value for a specific chemical reaction at standard conditions, R is the gas constant, T is the temperature, n is the number of electrons involved in the reaction, F is Faraday's constant and Q is the ratio of the concentrations of the reactants and products.

The efficiency of an electrolyser cell is defined by the theoretical amount of energy required for the splitting of water, W_{split}, and the amount of energy that is consumed in the process, W_r. The efficiency can be subdivided into lower and higher heating efficiency. Calculations on efficiency use respectively the Higher Heating Value (HHV) and the Lower Heating Value (LHV). HHV is the energy needed for splitting water at 1 bar at 25 C°. The LHV is the HHV minus the energy needed for the evaporation of water. With regard to the electrolysis of water to form H2, the LHV is used more commonly.

$$\eta_{cell} = \frac{W_{split}}{W_r} \tag{2.3}$$

Three conventional electrolysis techniques presently operational in industrial applications contribute systematic consideration at a system level. A comprehensive understanding of each technique is of essence selecting an electrolyser suitable for integration with offshore floating wind systems.

Alkaline

Alkaline electrolysers (AEL) have a relatively easy design and manufacturing process. They operate in a potassium hydroxide (KOH) solution which it uses as an electrolyte. It uses a zirconium dioxide (ZrO_2) diaphragms as separators and nickel (Ni) coated stainless-steel electrodes. In alkaline electrolysers the hydroxyl ion (OH^-) is the ionic charge carrier. KOH and water permeate through the porous structure of the diaphragm to provide functionality for the electro-chemical reaction. This does allow the produced gases to mix with the electrolyte which limits the lower power-operating range and the ability to operate at high pressure. To prevent this, the diaphragms are thickened. However, this consequently leads to higher resistance and lower efficiencies for the electrolysis process.

To reduce the mixing of gasses with the electrolyte manufacturers sometimes include spacers between the diaphragms and electrolyte. Modern AELs use zero-gap electrodes, thin diaphragms and different electrocatalysts concepts to reduce their performance gap in comparison to PEM electrolysers. This does however reduce the durability of the AEL which could normally reach to more than 30 years.

AEL requires for the electrolyte to be recirculated in and out of the stacks components. This does negatively affect the efficiency of the electrolyser since the circulation creates a pressure drop that requires specific pumping characteristics.

If the AEL does not have pumps the alkaline solution and mixed gasses need to be separated when it leaves the stack. This is done in gas-water separators placed above the electrolyser stack. The gases are removed at the top and the water/KOH mixture is removed at the bottom and flows back into the stack.

AEL stacks are generally more difficult to operate in different pressure compared to PEM electrolysers due to the requirement to balance charges between anode and cathode. However, they can operate at pressure up to 200 bar. But more resistant and balance of plant materials are needed which results in higher CAPEX compared to unpressurized AEL.

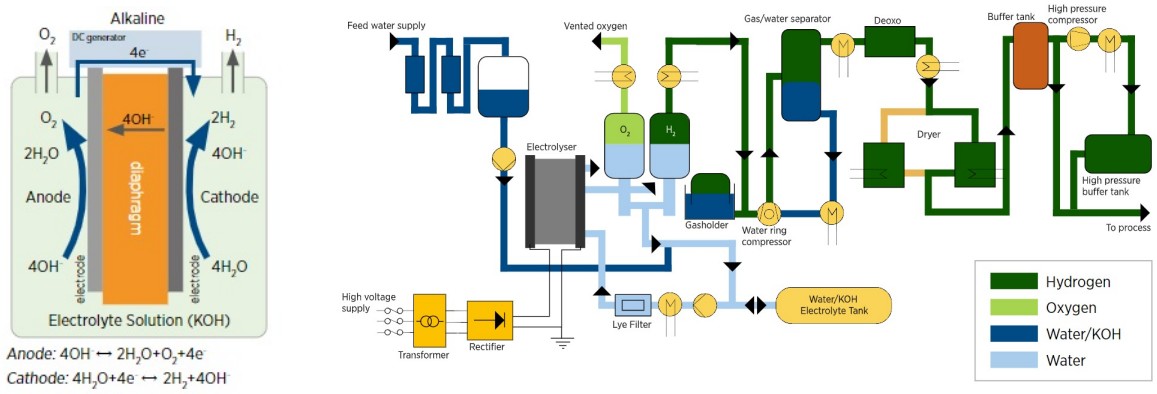

(a) AEL cell

(b) AEL system

Proton exchange membrane

PEM electrolysers do not use a electrolyte solution but a perfluorosulfonic acid (PFSA) membrane. This unique membrane composition facilitates superior efficiency and higher pressure differentials when compared to AEL systems. PEM cells can operate at pressures up to 70 bar, with the oxygen side maintained at 1 bar. Despite their efficiency advantages, PEM cells present certain drawbacks, particularly their elevated cost. Because it operates in an acidic environment caused by the membrane, high voltages and oxygen evolution in the anode creates a harsh oxidative environment. Therefor the catalysts of noble metals, titanium based materials and coatings are

necessary. These tend to be expensive and therefor the manufacturing of PEM cells is more expensive compared to AEL. However, the compactness and heightened efficiency of PEM cells stand out as advantages in their favor.

In contrast to a AEL, the principle of a PEM electrolyser is more simple. It only requires circulation pumps, pressure control, heat exchangers and monitoring device only at the anode side (oxygen). At the cathode side (H2) it requires a gas separator, a de-oxygenation component, gas dryer and a compressor.

Besides, PEM electrolysers have more design modes compared to AEL. There is a configuration choice for pressure. It can be atmospheric, balanced or differential. There is however no option to change the choice when designed. This reduces system complexity, maintenance and the costs.

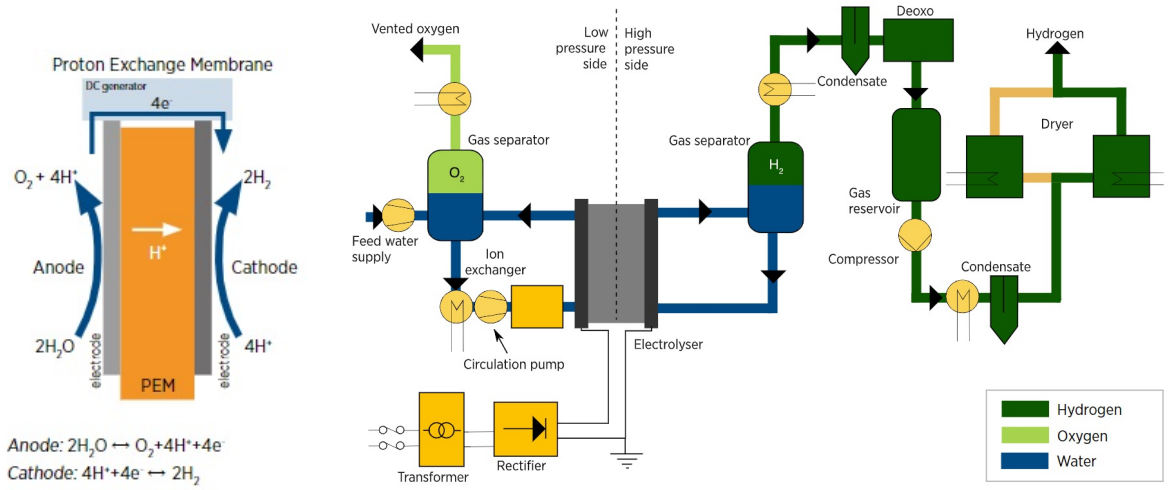

(a) PEM cell

(b) PEM system

Solid oxide

Solid oxide electrolysers (SOEC) are relatively new compared to PEM and AEL. They operate at very high temperatures ranging between 700 and 850 C°. The primary benefit lies in the reduction of energy demand for electrolysis, as a portion of the needed energy for the separation process is supplied in the form of heat. Consequently, cost-effective nickel electrodes, like those employed in AEL systems, can be utilized in SOECs. Additionally, SOECs exhibit the potential for reversibility, enabling their operation both as electrolysers and as fuel cells. A disadvantage of a SOEC is that these high temperatures result in faster degradation of the cells. Thermo-chemical cycling during shutdown and ramping periods causes large temperature differences which affect the electrodes. This results in a relatively short lifetime.

SOEC systems can be coupled with heat-producing technologies to increase the system efficiency. For higher temperatures, the electrolysis of water is increasingly endothermic and thus the process requires less energy in the form of electricity. The heat needed for water vaporization can be provided by sources other than electricity like waste-heat from industry or solar power plants.

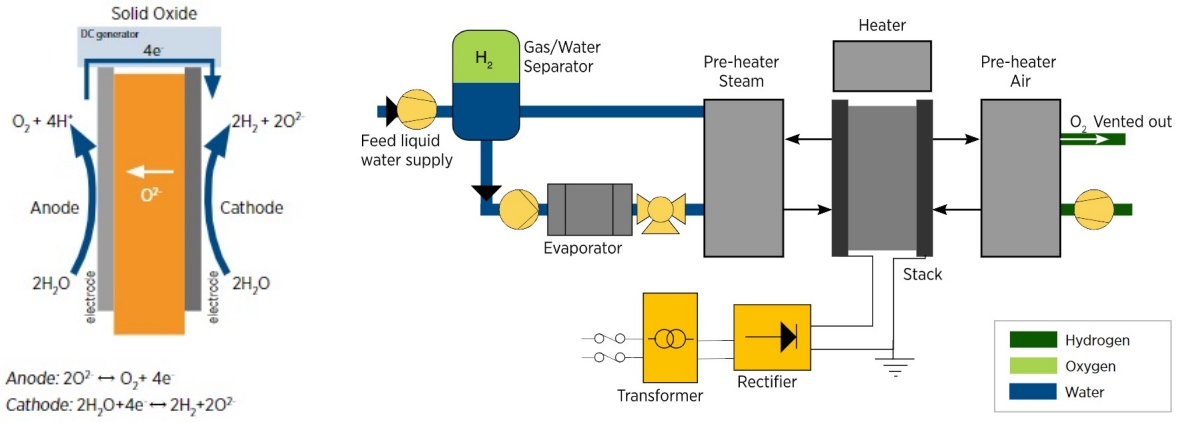

(a) SOEC cell

(b) SOEC system

Comparison

In Table 2.1 a comparison is made of the three different electrolyser technologies. The three different electrolyser technologies are now compared. This comparison shows the different characteristics and values of each of these systems and in relation to each other. The values indicated in the table are the current characteristics of the different techniques and are expected to improve significantly in the coming years [57].

	AEL	PEM	SOEC
Operating temperature	70-90 [56]	50-80 [56]	700-850 [56]
Operating pressure	1-30 [56]	<70 [56]	1 [56]
Electrolyte	KOH (5-7 molL^-1) [56]	PFSA membranes [56]	Yttria-stabilized Zirconia (YSZ) [56]
Separator	ZrO_2 stabilized with PPS mesh [56]	PFSA membranes [56]	YSZ [56]
Electrode/catalist (oxygen side) [56]	Ni coated perforated stainless steel [56]	Iridium oxide [56]	Perovskite-type [56]
Electrode/catalist (H2 side)	Ni coated perforated stainless steel [56]	Platinum nanoparticles on carbon black [56]	Ni/YSZ [56]
Porous transport layer anode	Ni mesh [56]	Platinum coated sintered porous titanium [56]	Coarse Ni mesh or foam [56]
Porous transport layer cathode	Ni mesh [56]	Sintered porous titanium or carbon cloth [56]	-
Efficiency	43-67% [50]	40-67% [50]	63-82% [50]
Specific energy consumption	55-65 [kWh/kg]	55-65 [kWh/kg]	45-50 [kWh/kg]
Start-up time	Cold: 15 min Warm: 1-5 min [50]	Cold: <15 min Warm: seconds [50]	Cold: hours Hot from standby: minutes [50]
Flexibility	Minimum partial load 10-40% [50]	Suitable for partial and variable load [50]	>40% partial load [50]
Main advantage	Reliability	High purity product	High efficiency
Main disadvantage	Inflexibility	Expensive	High degradation
Costs	800-1500 [19]	1400-2100 [19]	>2000 [19]

Table 2.1: Comparison between the three discussed electrolyser technologies. The grey cells indicate that there is significant variation among manufacturers [56]

2.2.3. Desalination

This research considers the use of seawater for the production of hydrogen. Seawater can not directly be used for HE because of its salinity. These relatively large salt and other dirt particles are to be filtered out before the water is suitable for electrolysis. Desalination is therfor an essential process in the of hydrogen production form seawater. This desalination process is called reverse osmosis and is elaborated in the following paragraph.

Reverse osmosis

In order to desalinate the seawater used by the electrolysers, a technique called *Seawater Reverse Osmosis* (SWRO) is used. Seawater is pumped to a purifying station containing a reverse osmosis (RO) unit utilizing a membrane barrier and pumping energy to separate the salts from the seawater. The pumps create a high pressure in the inflow of seawater so the water is forced through the membranes that consist of a dense separation

layer (thin film composite membrane). This filter allows for pure water molecules to pass through while rejecting the larger molecules like salts and sediment [68]. A schematic drawing of a RO filter and process is shown in Figure 2.10.

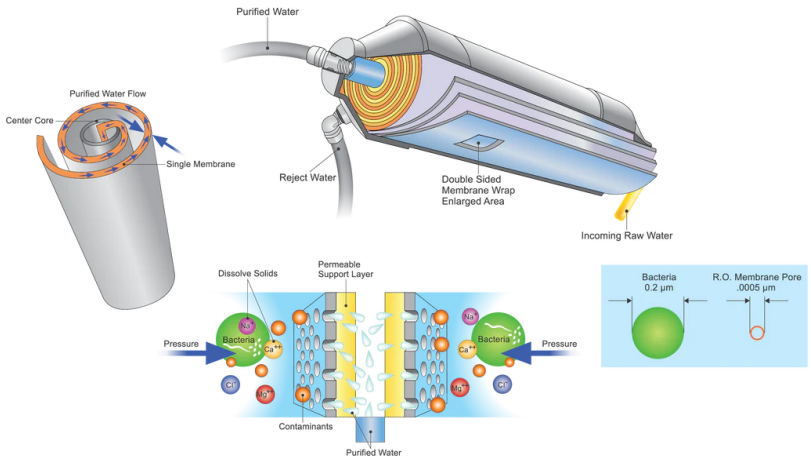

Figure 2.10: Reverse osmosis filter [103]

To mitigate scaling in RO processes in SWRO stations, a comprehensive pretreatment process is required. This regimen encompasses various attributes addressing both physical and chemical impurities in the seawater, ensuring its suitability for high-capacity membrane filtration. Physical pretreatment involves the utilization of sediment and carbon filters, as well as low-pressure filters such as ultrafiltration. Simultaneously, chemical pretreatment methods are employed, involving the application of polymers, acids, and dechlorination agents [68].

The selection and configuration of pretreatment attributes are of importance upon the specific quality of seawater used at the offshore location. A correct combination of these pretreatment techniques, coupled with passage through RO membranes, yields a product that surpasses a 99% removal efficiency for total dissolved solids [68]. This treated water is suitable for employment in electrolysis processes.

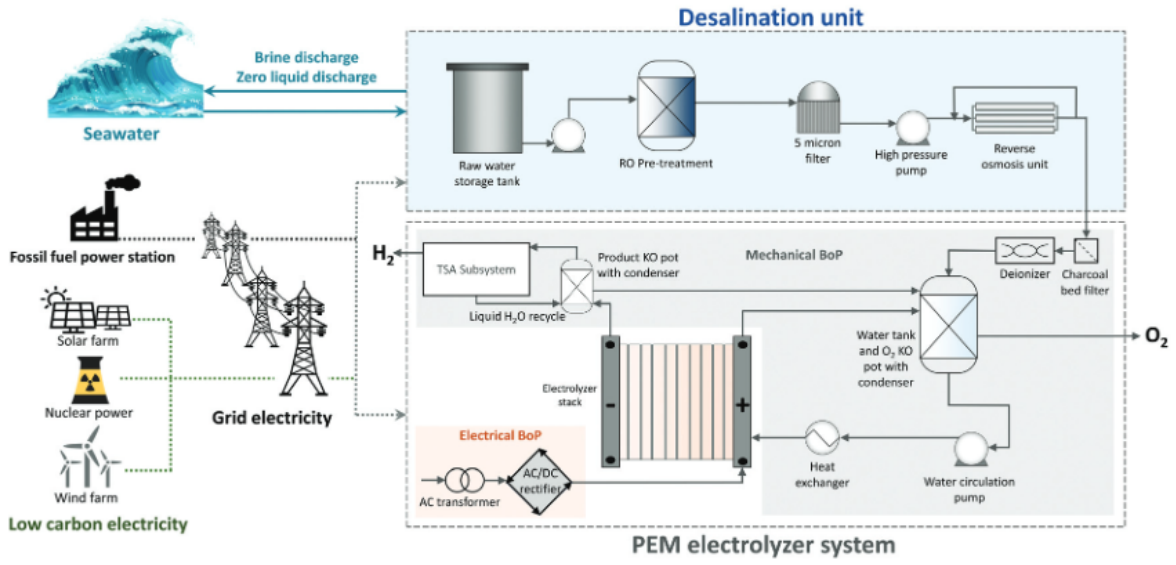

Figure 2.11: Schematic drawing of an 50 ton/day SWRO-PEM installation [68]

2.2.4. Hydrogen configurations

H2 can be stored and thus transported by converting it to a H2 carrier. This research considers the most applied carriers in industry today which are *Compressed Gaseous Hydrogen* (CGH2), *Liquid Hydrogen* (LH2), *Ammonia*

(NH3) and *Methylcyclohexane* (MCH) [9]. These are considered because of their characteristics, application feasibility, and economic performance. Each of these H2 carriers has advantages and disadvantages over the others and each carrier has its own challenges. This subsection will elaborate on the basic characteristics and requirements for each carrier to better understand how it affects the techno-economic feasibility of being used after production from offshore floating wind energy.

Compressed Gaseous Hydrogen

CGH2 is the simplest configuration of H2 after production since H2 is in gaseous form at room temperature and at 1 bar. At these ambient conditions the gas has a very low density at 0.0899 g/L making it the lightest gas known [134]. This property contributes to its high buoyancy, causing it to rise rapidly in the global atmosphere when released. Due to its low density, it diffuses quickly and can escape through small openings, requiring careful containment measures.

GH2 possesses a high level of flammability, readily undergoing combustion in the presence of an ignition source or oxygen. This combustion process generates a clean and intensely hot flame. While the flammability of H2 renders it advantageous for multiple applications, it also raises safety concerns. Proper handling and storage are of vital importance, particularly in industrial and scientific contexts, to mitigate potential risks associated with its combustibility.

The exceptional flammability of GH2 makes it as a viable alternative in combustion systems, potentially replacing traditional fuels such as petrol or natural gas. This application underscores its role in facilitating the transition of the transport sector toward sustainability. Besides its combustion properties for transportation, H2 finds application in fuel cells, where it combines with oxygen to generate electricity. This characteristic extends its utility to stationary power generation, particularly during periods when no power is being generated.

The primary drawback associated with GH2 is its low energy density, necessitating high-pressure storage solutions for practical applications. It is commonly stored in containers with pressures reaching 700 bar. The compression of GH2 is an adiabatic process that consumes a substantial amount of energy. The energy required for compressing H2 to 700 bar is notably higher compared to the compression of natural gas. Specifically, this process demands energy equivalent to 13% of the Higher Heating Value (HHV) of H2, as indicated by Bossel et al. [17].

Another disadvantage of GH2 is that is causes metal embrittlement. Because H2 is a very small atom it is very volatile. This results in it being able to go into micro cracks in the metal that transports it. In these cracks during temperature changes it can expand and retract resulting in the crack growing. This causes embrittlement weakening the metal and making it more prone to failure.

Liquid Hydrogen

LH2 exhibits a significantly higher volumetric energy density compared to GH2. Even at a pressure of 700 bar, LH2 possesses an energy density nearly twice that of GH2 [10]. Therefor, to optimize energy storage, H2 can be liquefied after electrolysis. This approach offers greater versatility in distribution since larger quantities of energy can be transported at a time.

LH2 is an odorless, tasteless and colorless fluid. The foremost characteristic of LH2 is its extremely low temperature in liquid state. H2 has a boiling point of -253 C° [10]. However, in liquid state it has a far higher energy density compared to gaseous form at 1 bar which amounts to around 848 times higher [10]. This gives LH2 a high gravimetric energy density of 33.3 kWh/kg. But because H2 is such a small molecule it is, like CGH2, very volatile and therefor prone to leak during storage. This in combination with the characteristic of LH2 to be extremely flammable makes it a dangerous substance.

H2 has two different spin isomers that coexist in liquid form: ortho- and para-hydrogen. The concentration of these spin isomers is dependent on the temperature. For lower temperatures the concentration para-hydrogen is larger. The spin isomer and concentration percentage of both isomers is shown in Figure 2.12. At low temperatures, ortho-hydrogen, especially in LH2, is unstable and changes to a more stable para-hydrogen. This isomer change leads to heat generation [10] and promotes vaporization of LH2.

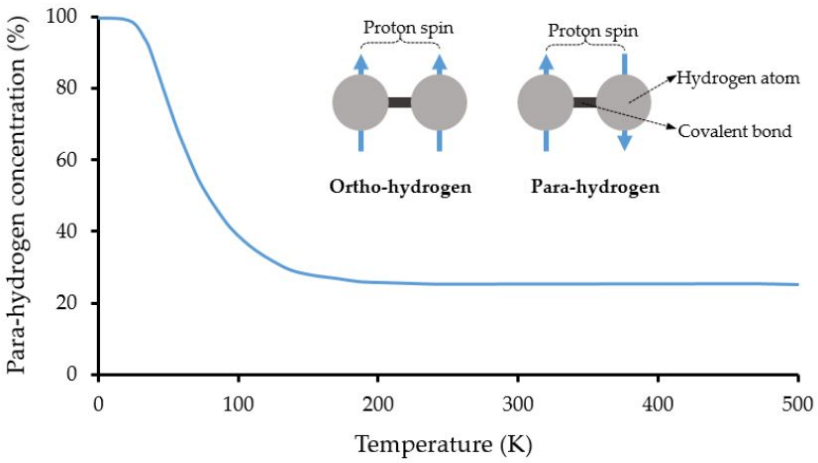

Figure 2.12: Ortho- and para-hydrogen spin and concentration as a function of temperature

LH2 is produced through the cooling of GH2 to its boiling point, and various processes can achieve this. The *Linde-Hampson process* stands out as the most fundamental method, relying on the isenthalpic effects of Joule-Thompson expansion. The *Joule-Thompson process* involves forcing a gas under high pressure through a porous material, inducing a sudden expansion that leads to cooling.

In the Linde-Hampson process, H2 gas is initially compressed under ambient conditions. This compressed gas undergoes Joule-Thompson expansion as it passes through a throttling valve, resulting in rapid cooling on the other side of the valve. This cycle is repeatedly performed until the gas reaches a low enough temperature to transition into a liquid state. However, due to the inherent property of H2 to warm up during expansion at room temperature and ambient pressure, not all gas reaches the liquid state simultaneously. Consequently, cooled gas is recirculated for subsequent cooling processes.

To further cool the H2 following expansion, it must first be brought down to its inversion temperature (-73 C° at 1 bar). This preliminary cooling is accomplished by employing liquid nitrogen as a coolant. The schematic representation of the Linde-Hampson process is depicted in Figure 2.13.

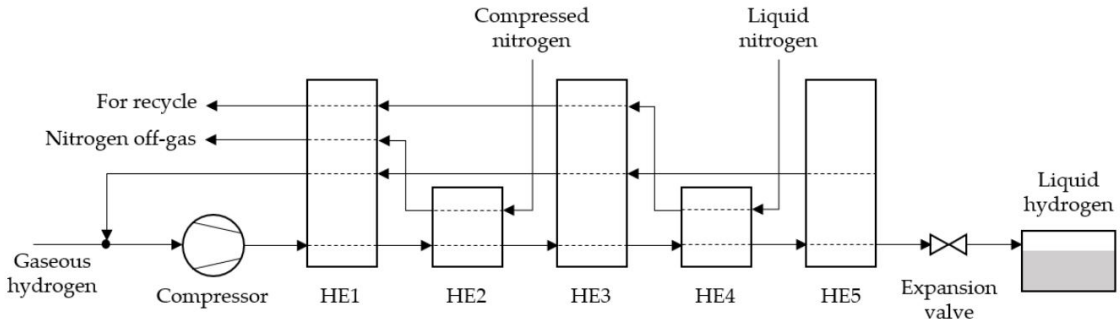

Figure 2.13: Basic schematic of the Linde-Hampson process

Commercialized H2 liquefiers today have a specific energy consumption ranging between 10-20 kWh/kg H2 [10]. This value changes with the plant's capacity, illustrated in figure 2.14. A larger capacity results in a lower specific energy consumption per kg H2.

Theoretically the minimum required energy for the thermodynamically ideal H2 liquefaction cycle is approximately 3 kWh/kg [93]. However, because of the large energy losses due to relatively high ambient temperature the average specific energy consumption of liquefaction plants globally amounts to 13.83 kWh/kg [93]. Today however, optimized liquefaction cycles can deliver much lower energy consumption sometimes below 6 kWh/kg. But like stated earlier this is dependent on the capacity of the plant. Energy consumption of plants can be optimized by:

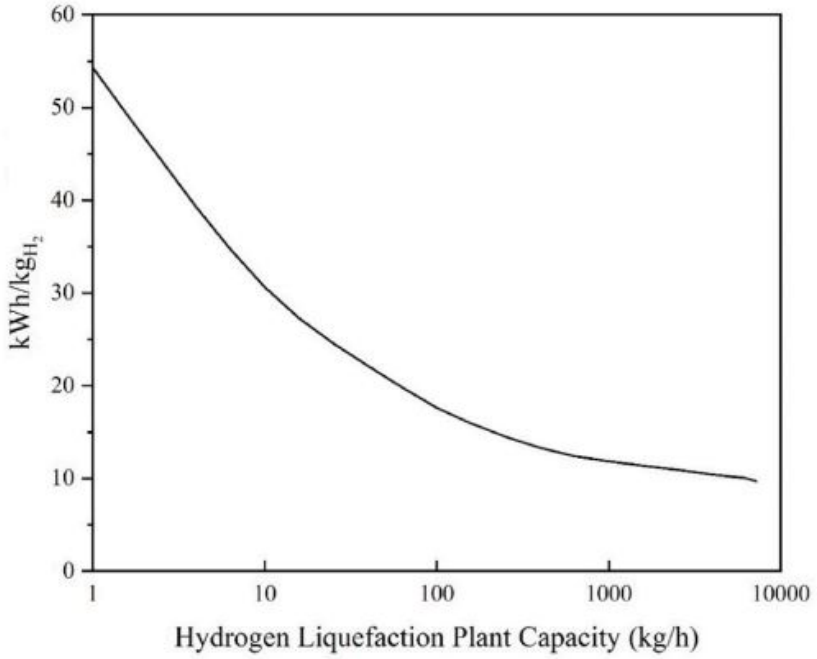

Figure 2.14: SEC of a H2 liquefaction plant versus the capacity [17]

- Upgrade the H2 liquefaction configurations currently used in the industry to more efficient and energy-saving configurations
- Optimise the scale/capacity of the H2 liquefaction plants.
- Recover the high-grade cold energy released during LH2 transportation and utilization (boil-off, regasification and para-to-ortho conversion) and reuse it in the liquefaction process.

Ammonia

Ammonia (NH3) emerges as a notable H2 carrier, synthesized through the reaction of GH2 with nitrogen. Despite being colorless, ammonia is highly toxic, irritating, corrosive, and possesses a suffocating odor. However, its appeal lies in its high gravimetric H2 density, reaching 17.7% [116]. Given the potential challenges and expenses associated with storing H2 in its pure form, H2 carriers like ammonia are increasingly considered as viable alternatives [125].

NH3 exhibits the highest volumetric H2 density when compared to LH2 and MCH. Nonetheless, its toxicity and corrosiveness requires careful and high-quality storage and transportation protocols. Notably, NH3 is the second largest synthetic commodity globally, with 80% of its production used in the fertilizer industry. The nitrogen component of NH3 contributes to the production of nitrogen fertilizers, crucial for sustaining approximately half of the world's population. Leveraging existing infrastructure, the fertilizer industry is already well-established, reducing the need for substantial new investments compared to LH2. NH3 is traditionally produced through the Haber-Bosch process, involving the reaction of nitrogen and steam-reformed natural gas. GH2 can substitute natural gas in this process, aligning with sustainability goals [49]. This combined application of water electrolysis and the Haber-Bosch process is commonly referred to as *power-to-ammonia* (P2A) technology. The chemical reaction of this process is expressed below:

$$N_2 + 3H_2 \rightleftharpoons 2NH_3$$

NH3 has several clear advantages as synthetic fuel and energy storage. It contains no carbon and therefor its combustion does not produce CO2. It can be easily as liquid stored in atmospheric pressure by cooling to -33 C° or pressurized at 9 bar in room temperature [27]. The cost of storage is low and can be densely stored for large energy amounts without any significant losses. For example: a typical liquid NH3 storage tank in the Corn Belt, USA, has a capacity of 30,000 Mt, equal to 190 GWh as H2 reformed from NH3, with estimated capital cost of

only 0.1US$/kWh [73]. The specific energy consumption to form NH3 from pure H2 gas is 0.64 MWh/tNH3 [54].

Methylcyclohexane

MCH is a Liquid Organic Hydrogen Carrier (LOCH), possessing several advantageous characteristics including low cost, high safety, high H2 storage density, ease of handling, and excellent reversibility. MCH is synthesized through the hydrogenation of toluene, where toluene, a liquid, is vaporized and combined with H2 to form MCH. This reaction occurs at temperatures ranging from 180 to 300 C° and pressures between 10 and 50 bar [116, 69].

MCH has a gravimetric H2 density of approximately 6.2%, existing in a liquid state over a temperature range spanning from -127 to 101 degrees Celsius. This extensive liquid temperature range enhances its suitability as an LOHC for storage and transportation, given its remarkable stability under varying conditions. The chemical reaction is shown below.

$$C_7H_8 + 3H_2 \rightleftharpoons C_7H_{14}$$

MCH is currently used in the industry as an industrial solvent due to its abilities to dissolve in a wide range on non-polar compounds like coating and resins. It is also used in the petroleum industry as a fuel additive. MCH is thus socially accepted and there are no needs for new regulations for storage and transportation. Japan houses the first toluene-hydrogen hydro- and dehydrogenation plant. This plant is however a pilot project and the focus of development is on the scaling up to the industrial scale [116].

Comparison

The four configurations of H2 are compared to each other in Table 2.2. The comparison shows definitive characteristics of each configuration, certain advantages and challenges the configuration faces. The goal is to illustrate why one might prefer a certain configuration because of the advantages or disadvantages it has over the other configurations.

Characteristic	GH2 (700 bar)	LH2	NH3	MCH
Boiling point	-253	-253	-33	101
Density	42	70.8	682	769
Gravimetric density H2	100	100	17.7	6.16
Volumetric density H2	100	100	120.3	47.1
Physical (compared to m^3 GH2 at 1 bar)	467	800	1200	500
Infrastructure	Possibility to use current NG infrastructure	Needs development for large scale application	Possibility to use current propane infrastructure	Possibility to use current gasoline infrastructure
Application	- H2 combustion - Fuel cell	- H2 combustion - Fuel cell	- Direct combustion - Fuel cell - Fertilizer	- H2 combustion - Fuel cell
SEC	5	13.8	5	0.363
Advantages	- High purity - Requires no dehydrogenation or purification	- High purity - Requires no dehydrogenation or purification	- Existing storing infrastructure - Existing regulations - No losses during transport - Safe - Stored at ambient conditions	- Existing storing infrastructure - Existing regulations - No losses during transport - Safe - Stored at ambient conditions
Development level	Small scale: application stage Large scale: infrastructure development is carried out Regulation for transportation	Small scale: application stage Large scale: infrastructure development is carried out Regulation for transportation	R&D stage Partially demonstration stage	Demonstration stage
Future perspective	Development GH2 engines Application in existing NG pipelines	Development in engines Loading/unloading systems Efficiency liquefaction	Higher energy efficiency in synthesis Fuel cell with direct NH3	Catalyst for both de- and hydrogenation Energy dehydrogenation

Table 2.2: Comparison of different H2 configurations [75, 99, 69, 17, 14, 10, 36, 100, 105]

2.3. Integrated System

Now that the basic knowledge of OFWE, the power market, desalination, electrolysis and a variety of H2 carriers has been explained, this section will combine these elements and zoom out to the broader scope

of this research. This includes looking at an integrated wind-to-hydrogen (W2H) system influenced by the power market. An integrated W2H system, also called an Integrated System (IS), is a system which uses electricity generated from on- or offshore wind farms to power electrolysis cells that produce green hydrogen. While a fully operational W2H system is yet to be realized, numerous studies have explored its potential applications.

A literature research was conducted on offshore wind-hydrogen combinations. An overview is given in Table 2.3. Found studies are divided into two different types: Technical Analysis (TA) and Techno-Economical Analysis (TEA). To comprehend the choices made in research, it is essential to elaborate on certain definitions related to integrated W2H systems. The terms *centralized* and *decentralized* are crucial for understanding the orientation of the IS, while *dedicated* and *non-dedicated* are pivotal for assessing operationality.

2.3.1. Centralized and Decentralized definition

Integrated offshore W2H concepts are categorized into centralized and decentralized systems. In the centralized approach, power generation and H2 production are both done on the offshore location. This centralized concept can be further classified into centralized and individual electrolyser technologies.

In the centralized scenario, all electrolysers are situated on a single platform where the generated power from wind turbines is combined and transformed to supply the electrolysers. On this platform, the produced H2 is compressed and subsequently transported to an onshore location either via pipeline or tanker. On the other hand, individual electrolyser technology, exemplified by the Dolphyn concept [31], entails each wind turbine platform having its own electrolyser. The output from all electrolysers is collected through a manifold, which then transports the H2 to an onshore location.

Conversely, decentralized concepts generate electricity offshore using wind turbines, but the electrical power is transmitted to an onshore location where H2 is produced. A schematic overview of centralized versus decentralized W2H concepts is illustrated in Figures 2.15a, 2.15b, and 2.15c. These provide a visual representation of the structural variations between centralized and decentralized W2H configurations.

Author, Year	Type	Category	Concept and application	Results
Bonacina et al. 2022	TEA	CE	Offshore LH2 production facility from a 50-190 MW wind farm for ship refuelling.	For a capacity ratio of 80-90% payback time is minimum, LCOH of 5-7 euro/kg. Total cost of plant is euro340M
Baardsen 2022	TA	CE	Offshore floating LH2 production, storage and offloading	Deck area of 21.000 m^2, storage capacity of 41.300 m^3 for a 400MW electrolysis capacity with LH2 storage for 17 days and 172 tons/day production.
Ibrahim et al. 2022	TA	CE/DCE	Three options for hydrogen production to onshore storage	List of advantages and disadvantages for each of the discussed options
Nguyen Dinh et al. 2021	TEA	CE	Case study on offshore hydrogen production from a 101.3 MW wind farm of the coast of Ireland	Offshore wind farm to hydrogen production profitable in 2030 for price of euro5/kg. Short term storage economically better
Wang et al. 2021	TEA	CE	Offshore green ammonia production from based on demand in ton/day and distance to shore	LCOA varying 1000-1200$/t for demand between 300-1500t/day for fixed WTB and between 1300-1900$/t depending on water depth
Calado et al. 2021	TEA	CE/DCE	Comparison of offshore and onshore H2 production AEL and PEMEL for different wind farm power outputs	LCOH varying between 2-9.17euro/kg for AEL and 2.26-11.75euro/kg for PEMEL
Luo et al. 2022	TEA	CE	Hydrogen production for offshore wind power in South China	Price of 1 Nm^3 H2 varies between 2.75-3.5 CNY
Lee et al. 2023	TA	CE	Design optimization for a LH2 production FPSO	For a 600MW electrolysis sytem a combined area of 8623 m^2 is need from top view. For side view it amounts to 7775 m^2
Babarit et al. 2018	TEA	CE/DCE	Comparison between four options for far offshore hydrogen production using different WECs	LCOH is around 5euro/kg for offshore production plants and ranges from 3.3-7.5 for onshore production
Morgan et al. 2017	TEA	DCE	Green ammonia production from US offshore wind farms	LCOA varies around 1224$/t of a power installation of 122.75 MW depending on various economic assumptions
Yan et al. 2021	TEA	CE/DCE	Scenario comparison for offshore green hydrogen production for various distances to shore	LCOH varies between 3.4-21.42$/kg when using a pipeline depending on distance to shore and 4.77-4.79$/kg for ship distribution
Giampieri et al. 2023	TEA	CE/DCE	Assesment of wind-to-hydrogen scenarios for the UK	LCOH varies between 2.71-184 pound/kg depending on power output, system concept, distance to shore and year

Table 2.3: Overview of previous research done of the concept of offshore wind-to-hydrogen

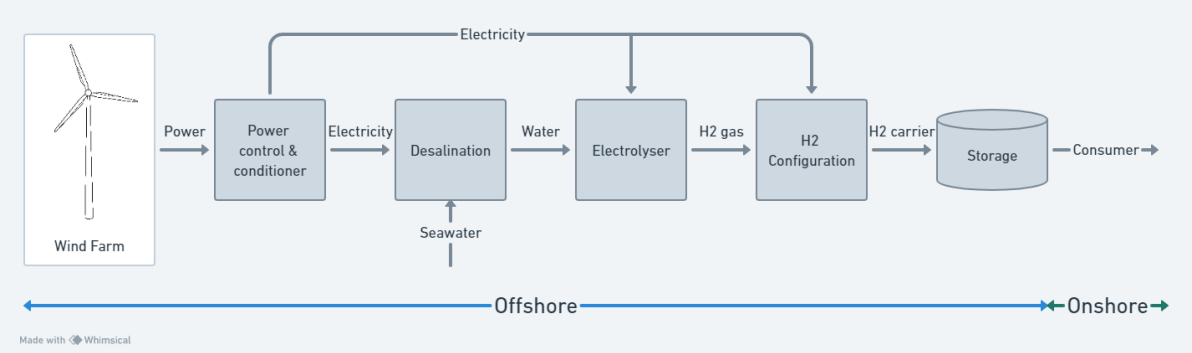

(a) Schematic overview centralized integrated W2H system

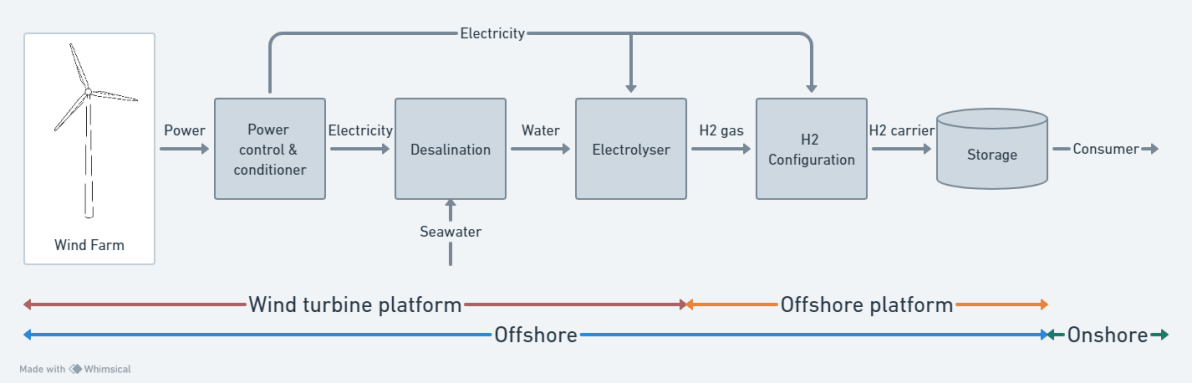

(b) Schematic overview individual centralized integrated W2H system

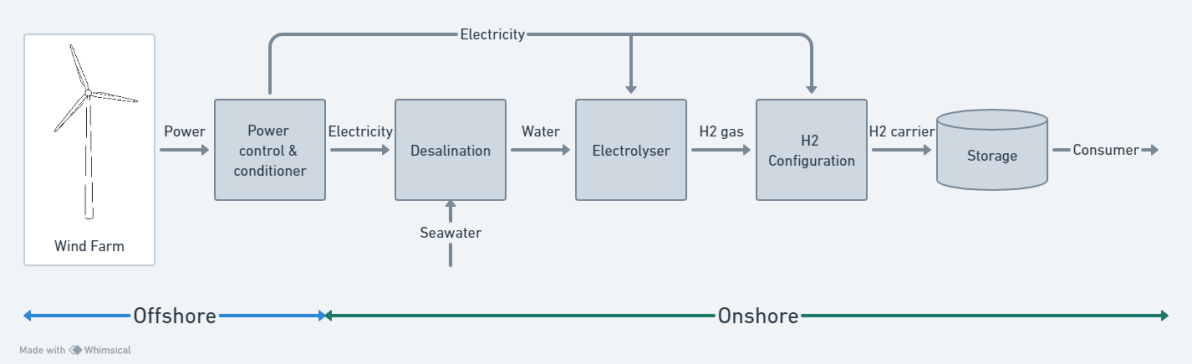

(c) Schematic overview decentralized integrated W2H system

2.3.2. Centralized application

The centralized configuration is the one that is most researched since it brings the most challenges[53, 21, 11, 131, 40]. Nguyen et al. [30] considers an offshore wind farm for GH2 production off the coast of Ireland. The product is stored in underground caverns below the seabed. This is in accordance with technology advancements. The stored product is periodically offloaded on tanker ships and is transported to mainland. All the revenue comes from H2 sales since there is no grid connection. It does not consider different hydrogen configurations and only considers offloading scenarios in evaluating its payback period and NPV. An overview of the conceptual design of the system is shown in Figure 2.16.

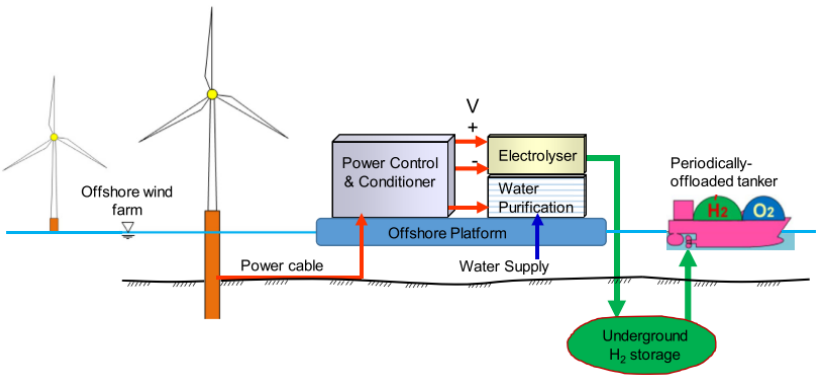

Figure 2.16: Conceptual system proposed in Nguyen et al. [30]

Bonacina et al. [15] proposes an offshore wind warm providing electricity to an offshore LH2 production plant in the Mediterranean Sea. The produced LH2 is intended to fuel ships that transport goods between countries that border the Mediterranean Sea. The research analyses influence of the wind farms capacity on the LCOH. It considers capacities in the range of 50-190 MW. It also considers the electrolyser to wind farm capacity ratio, and it is found that at a capacity ratio between 80-90% the Payback Period (PBP) is lowest with around 13 years. This indicates that as a result of the dependability of electrolysers on wind conditions, the techno-economic feasibility of the park is maximum when the installed capacity of electrolysers is between 80-90% of the capacity of the wind farm. This research does not take into account predicted future wind speeds and the wake of turbines. The LCOH is between 5-7€/kg H2. The conceptual design is illustrated in Figure 2.17.

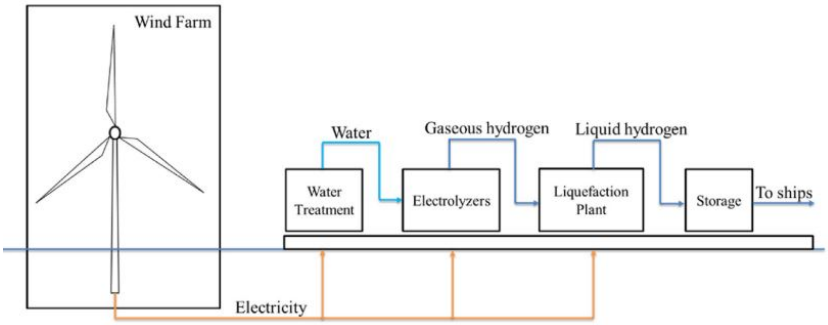

Figure 2.17: Conceptual system for an offshore LH2 production plant for ship refueling proposed by Bonacina et al [15]

Luo et al. [81] considers an offshore wind farm off the coast of South China. It considers four system configurations for centralized and decentralized hydrogen production. The first configuration analyses a system where power is delivered partially to the grid and partially to a small PEM electrolyser system compared to wind farm capacity. An AE system is connected to the electricity grid and provides constant hydrogen production. The second configuration analyses partial H2 production where the installed capacity of electrolyser is equal to that of the WF. H2 production in this configuration is only active when the grid capacity is full and can not take the generated power of the WF. Generated power will then be used for H2 production. The third and fourth configuration considers an offshore wind farm solely coupled to a H2 production system and not the grid where one configuration is centralized and the other one is decentralized. The research focuses mostly on option for configurations and prices of electricity compared to gas and leaves out techno-economic details on specific system configurations. It gives a LCOH in gaseous form between 2.75-3.5 CNY/Nm^3 H2. A schematic overview of the research is shown in Figure 2.18.

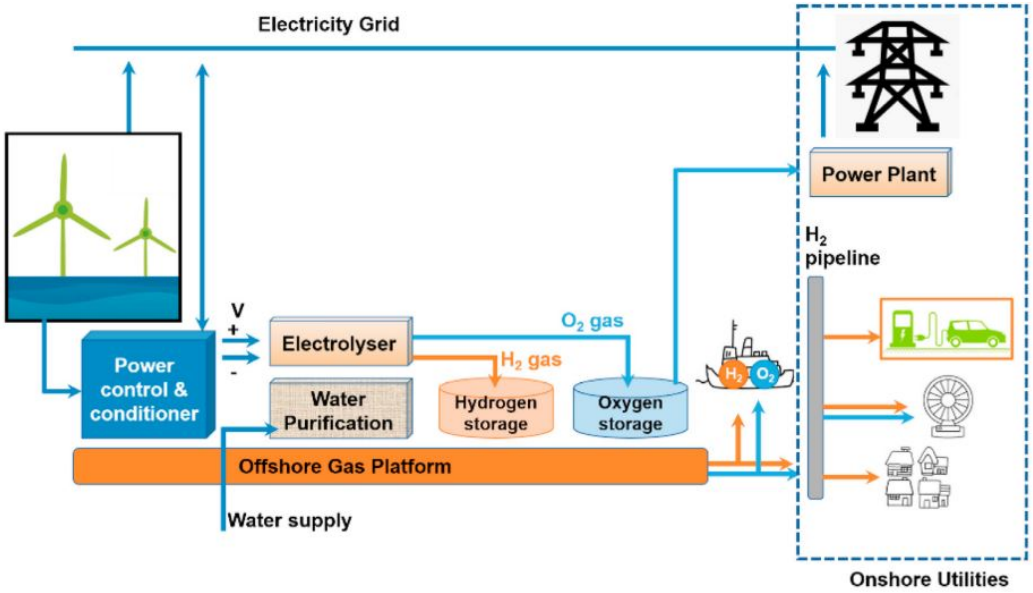

Figure 2.18: Schematic overview of H2 configurations off the coast of South China proposed by Luo et al [81]

Giampieri et al [40] analyses several system configurations for an offshore wind farm off the coast of the UK. The farm produces power for a centralized or decentralized H2 production facility. It considers five system configurations: centralized GH2 production, decentralized GH2 production, centralized LH2 production, centralized NH3 production and centralized MCH production. For each configuration it considers scenarios where proportions of the electricity generated are used for H2 production and how that influences the LCOH. It also takes in to account the total costs in different years with expected prices and efficiencies for equipment. The different concepts are shown in Figure 2.19.

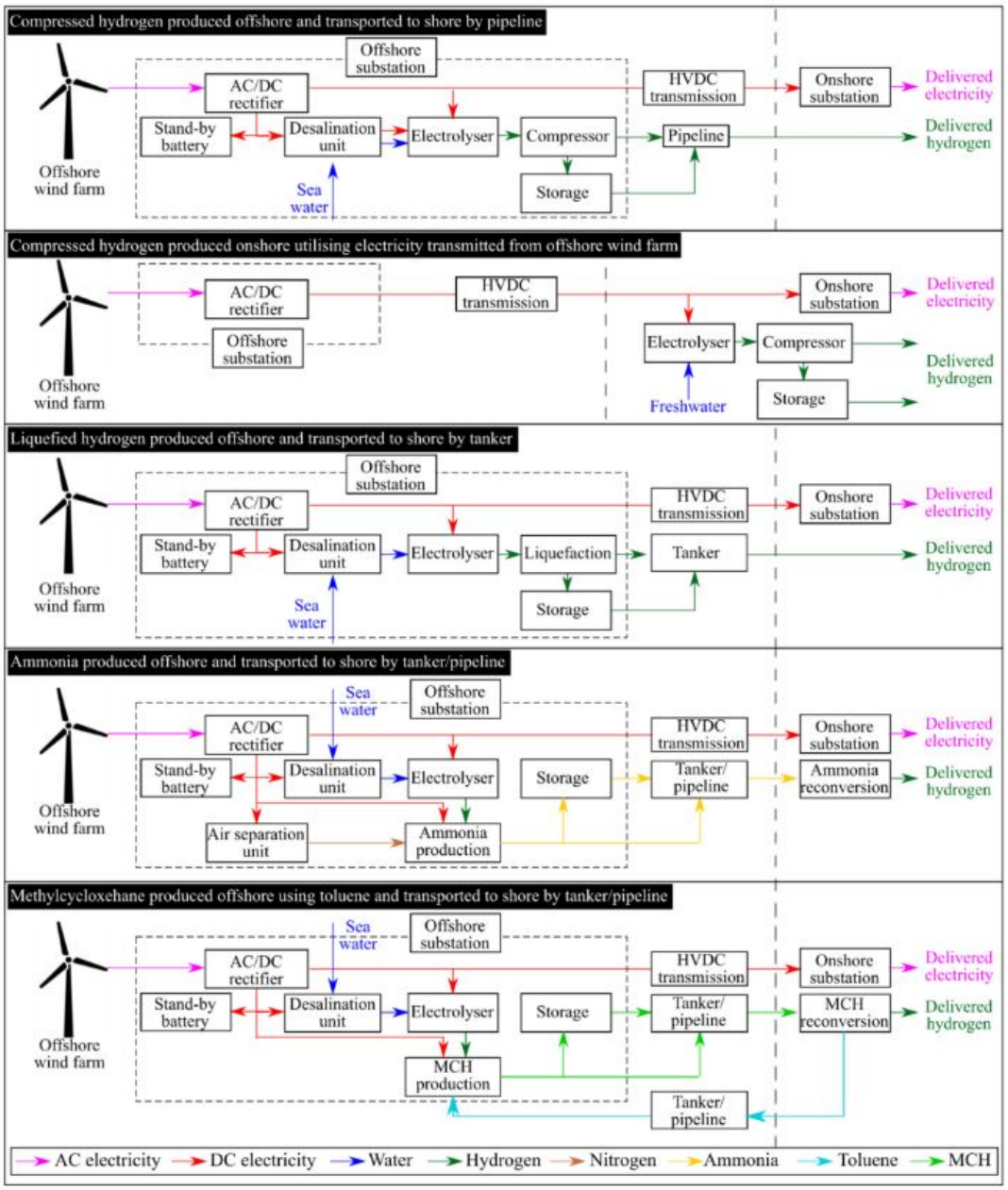

Figure 2.19: The different configurations for H2 production off the coast of the UK as proposed by Giampieri et al. [40]

2.3.3. Decentralized application

The decentralized application involves H2 production onshore with power from offshore wind farms. Three decentralized system applications are discussed in this subsection. Ibrahim et al. [53] discusses three options for hydrogen production from floating offshore wind farms to onshore storage. It assesses technologies and projects beyond state-of-the-art and evaluates advantages and disadvantages of centralized and decentralized H2 production from offshore floating wind energy. The research is solely a technical analysis and does not include economic values to indicate economic performance of different typologies. The three proposed typology concepts are shown in Figure 2.20.

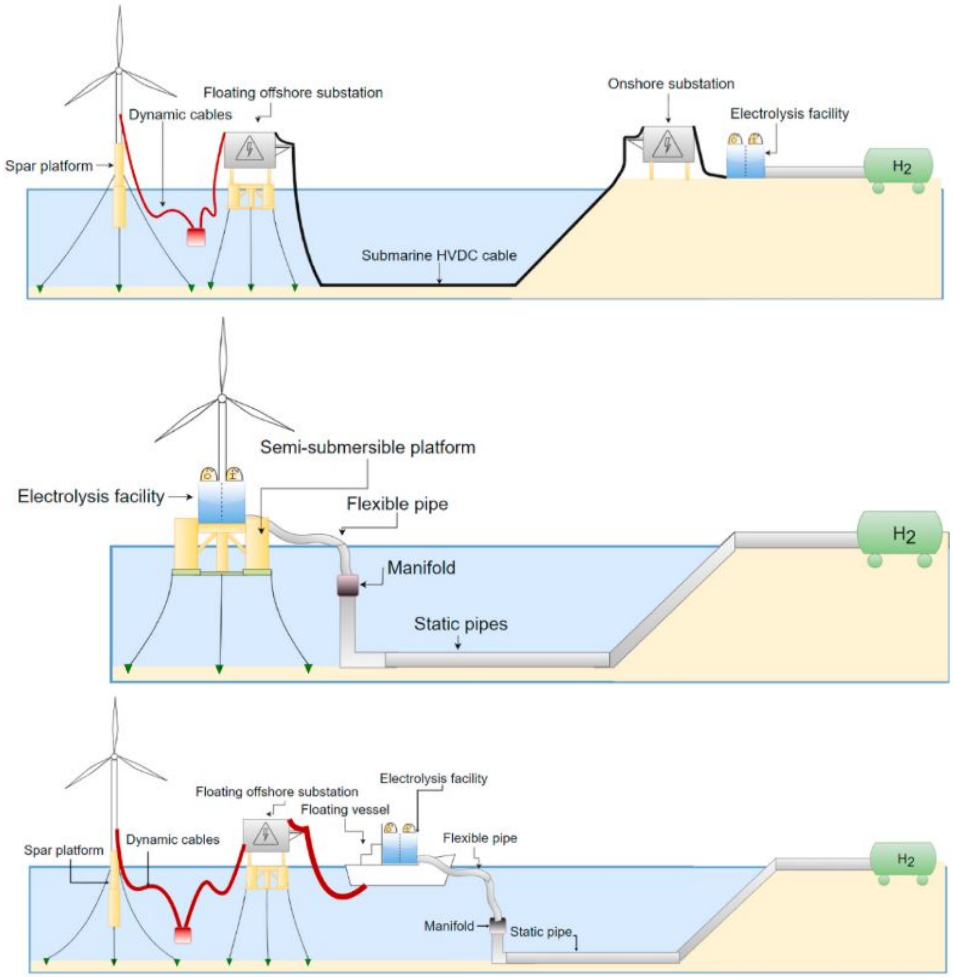

Figure 2.20: Three typologies analysed by Ibrahim et al. [53]

Morgan et al. [87] analyses green ammonia production from offshore wind farm off the US shore. It elaborates on state-of-the-art ammonia synthesis and the requirements for a facility that produces ammonia from offshore wind energy. It also does an economic analysis of the entire system. However, it considers a constant electricity supply by grid connection rather than delivering the surplus of power from the wind farm to the grid. A sensitivity analysis is conducted to evaluate which economic parameters influence the Levelized Cost of Ammonia (LCOA). The LCOA is concluded at around $1224/t NH3. A schematic overview of the concept is shown below in Figure 2.21.

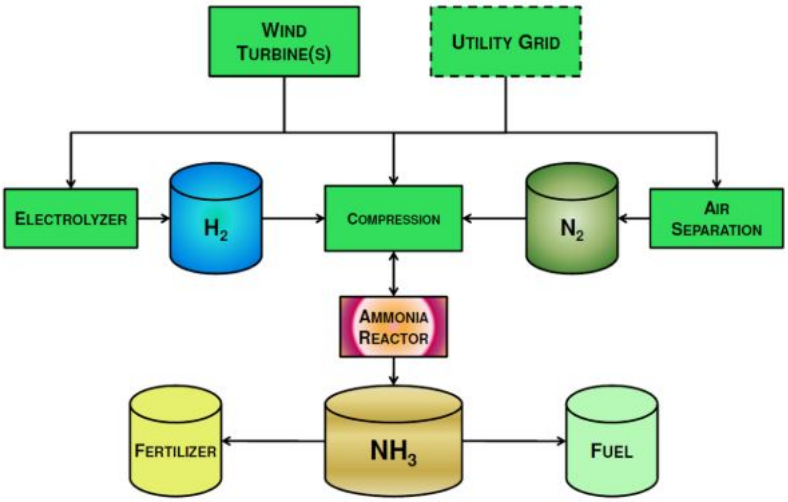

Figure 2.21: Schematic overview of the concept proposed in Morgan et al. [87]

Calado et al. [21] analyses the current situation of wind-to-hydrogen systems from AEL and PEMEL for varying wind farm capacities. It also analyses the cost-effectiveness of centralized production compared to decentralized. It discusses future scenarios for electrolysers and wind energy and how they influence the LCOH. Finally, it discusses the various uses of the produced H2 in the near future. LCOH varying between €2-9.17/kg for AEL and €2.26-11.75/kg for PEMEL.

2.3.4. Dedicated and Non-dedicated definition

Wind farms of an integrated system can be classified in two categories based on the operational strategy of the farm: *dedicated systems* and *non-dedicated systems*.

In *dedicated systems*, the power generated from the offshore wind farm is exclusively allocated for the auxiliaries of the H2 production facility. This operational strategy aligns with one of the challenges of wind energy, namely its volatility. As RES are intermittent, periods of low or no wind speeds result in zero H2 production [40, 15, 30]. While dedicated wind farms may still maintain a grid connection, the power produced by the WT is exclusively purposed for H2 production. The grid connection serves the purpose of providing a continuous power supply for the auxiliaries, ensuring uninterrupted operation during periods of low or no wind, thereby mitigating the intermittency of wind energy.

In a *non-dedicated* operational strategy, the wind farm serves a dual purpose by supplying electricity not only to the electrolysers and other auxiliaries but also to the electricity grid. Unlike dedicated strategies that prioritize H2 production, non-dedicated strategies aim to use the wind farm's capacity for electricity generation as primary goal, with H2 production as a secondary, opportunistic goal. Research on non-dedicated wind farms is relatively limited compared to dedicated strategies.

2.3.5. Dedicated operational strategy applications

Most studies consider a dedicated wind-to-hydrogen system [40, 15, 30, 81, 126, 21, 11, 84, 131] [87, 115]. Some studies suggests a connection to the electricity grid in order to maintain a constant supply of power for the electrolyser units. Luo et al. [81] considers a large AE unit and a small PEMEL. The large AE unit is constantly powered by the grid and by the wind farm when grid can not supply all the power. The PEMEL units are intended for the surplus of electricity when the WF's power generation exceeds the capacity of the AE unit. For these periods the PEMEL units use the surplus to produce extra GH2. Morgan et al. [87] also talks about a grid connection for stable power supply for constant ammonia production. Both studies base their energy supply on the electricity demand of its auxiliaries. However, both of these studies do not consider providing electricity to the connected grid.

Most of the other studies leave out the grid connection and focus solely on the power generated by the wind farm. Tomasini et al. [115] considers the wind energy potential off the coast of Uruguay to assess how much H2 can be

produced. This is the potential of two regions which in total could produce 11.2 Mton H2/yr. This research only considers using the wind potential for H2 production.

2.3.6. Non-dedicated operational strategy application

Non-dedicated operational strategies also apply for onshore wind energy systems. Buffo et al. [18] uses a rSOC electrolyser and a connection to the grid to switch between H2 production and providing to the electricity grid. It takes in to account the prices for chemicals for the electrolysis system and the electrical demand while also considering the price of electricity on the grid. It uses a switchprice which is the price where providing electricity to the grid is equally beneficial per kWh as production 1 kWh of H2. If the price of electricity on the grid is higher than the switchprice, the system will provide power to the grid. If the price is lower than the switchprice, the system will produce H2.

In conclusion, the research on wind-to-hydrogen systems has predominantly focused on dedicated operational strategies. However, there is a growing recognition of the advantages of non-dedicated operational strategies. Non-dedicated operational strategies, as exemplified by Buffo et al.[18], offer several advantages. They provide flexibility in managing the intermittent nature of wind energy by allowing power to be supplied to the grid when electricity prices are favorable. This approach can lead to more efficient resource utilization and potentially better economic outcomes.

While dedicated strategies ensure a consistent H2 production output, they may underutilize the wind farm's capacity and miss opportunities to generate revenue by selling excess electricity to the grid. Non-dedicated strategies, on the other hand, offer the potential to maximize the overall value of offshore wind installations by simultaneously serving the needs of both H2 production and the electricity grid. This approach aligns with the broader goal of optimizing the economic and operational benefits of renewable energy systems.

2.3.7. Conclusion

Green hydrogen emerges as a great potential RES because of its high gravimetric energy density and its emissions during production are equal to zero. It does embody some dangers, as it is a extremely flammable substance. Combined with the characteristic that is it volatile, operations involving hydrogen require a very high safety standard. Of the three considered hydrogen production methods via electrolysis, PEM electrolysis emerges as the most suitable for the applications of offshore wind energy operations because of its reduces start-up time and variable operating range. These characteristics make it the best alternative when the power supply is dependent on variable wind speeds. Four different hydrogen carrier configurations have been considered since they are the most used and show the greatest promise for future applications. Each of the four carriers, namely CGH2, LH2, ammonia and MCH, have their own unique set of characteristics which make them suitable for numerous applications depending on the preference of the user.

3

Base Case Model

Since the Goto City Wind Farm is still not operational, the floating wind farm system will be modeled in order to obtain the required data on the performance of the wind farm. Modeling the Goto City wind farm considers multiple factors to ensure an as accurate as possible representation of electricity generation. This involves accounting for wind speed and direction at the designated location, the type of wind turbines utilized, and the manner in which they are positioned and interconnected by cables. This model forms a base case for the overarching goal of this research which will be discussed in the coming chapters.

3.1. Characteristics

This section will give an overview of the characteristics of the Goto City Wind Farm that are applied in the model to simulate the performance. These characteristics can be found in Table 3.1. The subsequent sections will get in to more detail on how these characteristics are used in the corresponding processes in the model.

Component	Property	Value	Unit	Source
Wind Turbine	Capacity	2.1	MW	[94]
	Cut-in Speed	4	m/s	[46]
	Rated Power	13	m/s	[46]
	Cut-out Speed	25	m/s	[46]
	Rotor Diameter	80	m	[46]
	Swept Area	4978	m^2	[46]
	Hub Height	78	m	[46]
	Lifetime	25	years	[94]
	Floater	SPAR-buoy	-	[94]
Park Lay-Out	No. WT	8	-	[94]
	Distance Between Turbines	1200	m	[101]
	Distance Offshore Substation to Shore	15	km	[101]
	Water Depth	100	m	[25]
Electrical Infrastructure	Cross section	95	mm^2	[74]
	Resistance	0.25	Ω/km	[74]
	Capacity	26	MW	[74]

Table 3.1: Overview of the characteristics of the Goto City Wind Farm

3.2. Processes

In an offshore floating wind farm, a series of processes work together to transform the kinetic energy from ocean winds into a sustainable source of electricity. This paragraph will break down how these processes are simulated

in the model to accurately depict the dynamics that result in the generation of electricity and how this electricity is transported to be provided to the power grid.

3.2.1. Electricity Generation

For electricity generation by the wind turbines, two elements are considered of vital importance to the contribution of the energy output in this research. These elements are wind speed and wind direction. The chosen methodology for modeling these factors should be capable of providing a realistic depiction of the OFWF's performance. The accuracy of the wind speed and direction modeling directly influences the reliability of the subsequent electricity generation simulations. Since the Goto City Wind Farm is positioned to minimize the wake induced by wind turbines on each other, in this model wake is considered to be 0 and therefor wind directions do not influence the performance of the wind turbines. Note that for most large wind farms that consist of multiple rows of turbines, wake induced by turbines has a significant influence on the overall performance of the wind farm [5].

To model wind speeds for the designated location, historic hourly wind data can be obtained from Copernicus [35]. These datasets provide the average wind speed per hour at a chosen location and 100 m height above sea level. This is not the same as hub height and should therefor be extrapolated to achieve the correct wind speeds. However, using equation 2.1, wind speed differences at hub height and reference height of 100 meters above sea level differ only 4%. Since wind speed differences are low, it is assumed that the reference wind speed is equal to the wind speed at hub height. By associating these wind speeds with the power curve of the offshore WT, the hourly power generation can be calculated.

Wind turbines have specific characteristics depending on manufacturer as described in Subsection 2.1.1. The most important in terms of power generation for the considered modeling approach are the rated power, the cut-in and out speeds and the rated speed, the rotor swept area of the blades and the power coefficient. The power output as a function of the of the wind speed can be modeled using Equation 3.1 [8].

$$P(v) = \frac{1}{2} C_p \rho_{air} A v^3 \tag{3.1}$$

Where C_p is the power coefficient, ρ_{air} the density of the air at the designated location which is equal to 1.225 kg/m^3, A the rotor swept area and v the wind speed. The power coefficient represents the efficiency of energy transfer between the wind and the blades an is usually in the range of 25% and 45% [8]. Because the rated power of the wind turbine is 2.1 MW at a wind speed of 13 m/s, the resulting C_p is approximately 0.32 (32%). This power coefficient is therefor assumed in calculations on power generation. The power curve of the wind turbine can be represented by the Equation 3.2.

$$P_T = \begin{cases} 0, & v \leq v_{cin} \\ P(v), & v_{cin} < v < v_r \\ P_r, & v_r \leq v < v_{cout} \\ 0, & v \geq v_{cout} \end{cases} \tag{3.2}$$

Where v is the hourly wind speed, v_{cin} is the cut-in wind speed, v_r is the rated wind speed and v_{cout} the cut-out wind speed.

In addition to historic wind speeds, estimating future wind speeds is conducted to analyze the future performance of the system. Wind profiles typically follow a Weibull distribution [124]. It is assumed that by analyzing the wind profile of the previous year, the model can extrapolate future wind speeds by applying the Weibull distribution to these historical wind speeds. This estimating methodology does not take in to account deviations in wind speed as a result of day- and night time or deviations caused by the seasons. Because the wind profile for the first year does not show to be influenced by these factors, estimations on future wind speeds are assumed not to be effected by them as well.

As previously stated in Subsection 2.1.1, wind direction can significantly influence the performance of a wind farm. WTs possess the capability to orient their hubs toward the incoming wind direction, ensuring that the angle of attack, the angle at which the wind strikes the hub, remains perpendicular to the rotor blades, optimizing lift. However, due to the specific layout of the turbines in the Goto City Wind Farm, as depicted in Figure

2.6, and considering that wind direction only impacts performance when the angle of attack is precisely 0°or 180°(corresponding to westerly or easterly winds), wake-induced wind speeds are not factored into the model.

3.2.2. Transmission

The electrical cables responsible for transporting the electric current have resistance, resulting in inevitable electrical losses from the wind turbine to the substations. Opting for a higher inter-array cable voltage offers clear advantages in terms of transportation, installation, and maintenance requirements compared to nominal voltage inter-array cable systems. Therefor, for modeling purposes, the inter-array cable operates at a voltage of 66 kV [71]. The length of the cables between turbines can be estimated based on the location of the wind turbine, as provided by [42].

The Goto City WF in this research is modeled without an offshore substation to transform the voltage of the combined power for further transportation. Offshore wind farms generally do not require an offshore substation when the park capacity is below 100 MW or the farm is within 15 km of the shore [32]. All generated electricity is combined by an export cable and transported to an onshore substation without additional transformation. The length of the export cable from the offshore substation to the onshore transmission station can be calculated using Equation 3.3. It's important to note that the current-converting processes occurring at the offshore- and onshore substations are not modeled in detail, as such processes fall outside the scope of this research.

$$l_{export} = d_{substation} + L_{ss-tr} \tag{3.3}$$

An overview of the different inter array cable characteristics is shown in Table 3.2. Since the Goto City WF has a capacity of just 16.8 MW, the cable with the smallest girth is used between turbines.

	Inter-array					
Cross section [mm^2]	95	150	300	400	630	800
Resistance [Ω/km]	0.25	0.158	0.078	0.059	0.037	0.029
Cost [€/m]	220	300	423	475	554	683
Capacity [MW]	26	31	44	51	62	71

Table 3.2: Inter-array cable characteristics [74]

The power losses from transmission at a certain hour t in the cables can be calculated using Equation 3.4.

$$P_{loss}(t) = I^2(t) \sum_{i=1}^{n} R(i) * l(i) \tag{3.4}$$

Where $I(t)$ is the current in the cable at hour t that can be calculated using Equation 3.5, $R(i)$ is the resistance of the cable i with length $l(i)$

$$I(t) = \frac{P(t)}{V} \tag{3.5}$$

Where $P(t)$ is the combined power of the wind turbines at hour t and V the voltage in the cable.

3.2.3. Wave Interaction

The wave conditions at the location of the wind farm can exert significant forces on the turbine foundation. For fixed-bottom WTs, heavy wave conditions can lead to waves slamming onto the monopile or jacket foundation, potentially causing structural damage [12]. Over time, frequent exposure to heavy waves may also decrease the fatigue life of the structure, increasing the risk of failure before the end of its operational lifespan. However, fixed-bottom turbines offer limited displacement because of their rigid foundations, which reduces motion resulting from wave interaction.

In contrast, WTs placed on floating foundation are more dependent on the interaction between floater and prevailing wave conditions as they are not anchored to the seabed but rely on mooring systems. As floaters are

not mounted to the seabed but moored instead, their motion is highly influenced by wave conditions, and consequently the motion of the wind turbine. This relationship, known as the *Response Amplitude Operator* (RAO), characterizes the turbine's motion response to wave forces across different frequencies and degrees of freedom, including heave, pitch, and roll [127].

SPAR-buoy floaters, such as those used in the Goto City wind farm, are particularly sensitive to wave conditions [76]. Operating in rough waves may induce significant turbine response motions, potentially resulting in structural damage.

However, it's important to note that this research primarily focuses on how hydrogen production can enhance the techno-economic performance of offshore floating wind energy, rather than the dynamic interaction between waves and the floater and WT. While it's recognised that wave conditions at the designated location could potentially damage power-generating WTs, leading to temporary shutdowns, this aspect is not considered in this particular case study. The study prioritizes analyzing the benefits of hydrogen production and thus does not go into further detail on the dynamic response of floaters to wave forces.

3.3. Operational strategy

Since there is no alternative for a floating wind farm, all the generated electricity will be delivered directly to the power grid. Because of transmission losses the generated electricity of the WTs will not be the same as the electricity provided to the grid. The delivered power to the grid is therefor assumed to be the hourly power generation minus the electrical losses.

3.3.1. Japan Electric Power Exchange

In this operational strategy, the FiT is not considered. Since the goal of this research is to analyse if the techno-economic performance of OFWE can be enhanced by hydrogen production, initial performance of the wind farm is considered without governmental aid. Instead, the hourly average power prices of the JEPX are utilized in the operational strategy as they impose a better representation of the systems self-sufficiency.

Hourly electricity generated is paired with corresponding hourly electricity prices from the JEPX. In the base case, it is assumed that all the produced power can be fed into the grid. As most electrical contracts prioritize energy supplied by RES first [70], even during hours of low prices, indicating a high supply compared to demand, all the electricity is assumed to be sold for the corresponding price. This assumption is made to streamline the analysis and focus on evaluating the potential performance of the Goto City Wind Farm. Realistically, power is traded differently at and these average prices do not accurately represent the real price an independent power generator could get for its delivered power. These prices depend on the bids of other power generators and the supply-demand mismatch traded on the intra-day market. Since this is very hard to accurately match with power generation in the model and impossible to estimate for the remainder of the operational lifetime, the hourly average price is assumed instead.

A dataset with half-hour prices from April 2022 to April 2023 is obtained, as illustrated in Figure 3.1. The JEPX provides the dataset for a full year of prices from April 1 to March 31, and wind speeds from the dataset are matched with the corresponding dates to account for any seasonal effects. The average of each two half hours is calculated and used to maintain the same number of values in the electricity price matrix. It's important to note that these prices may vary over the years due to various external influences. Due to the complexity of accurately predicting day-ahead market prices for electricity, the power market is modeled based on previous electricity prices.

To analyze the performance of the system over its lifetime, predicted wind speeds in the wind model are linked with predictions on electricity prices. However, accurately modeling future electricity prices is an extremely challenging task, as stated above. Therefor, future predictions on electricity prices are estimated based on rough expectations of averages. Due to the significant increase in RES in Japan, which are prone to intermittency, the number of hours with negative prices is expected to rise substantially in the years leading up to 2030 [34]. This is projected to result in an annual increase of 20% in negative hours. After 2030, the increase is anticipated to decrease to 5% per year [83, 34]. Simultaneously, during this substantial rise in hours with negative electricity prices, the average price of electricity per kWh is expected to decrease by only 2% per year [83]. This is attributed to the growing presence of RES with intermittency, causing electricity prices to become more volatile. As a result, there will be more hours with low prices, but conversely, the hours with high prices will also be higher. To estimate future prices, the prices of 2022 are used as a reference. The previously mentioned percentages are applied to

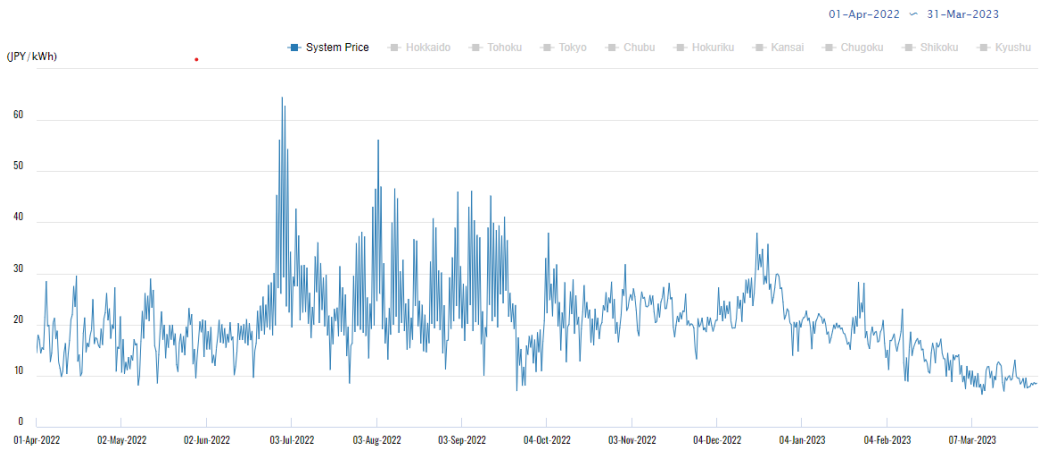

Figure 3.1: Half hour electricity prices April 2022 - April 2023 [28]

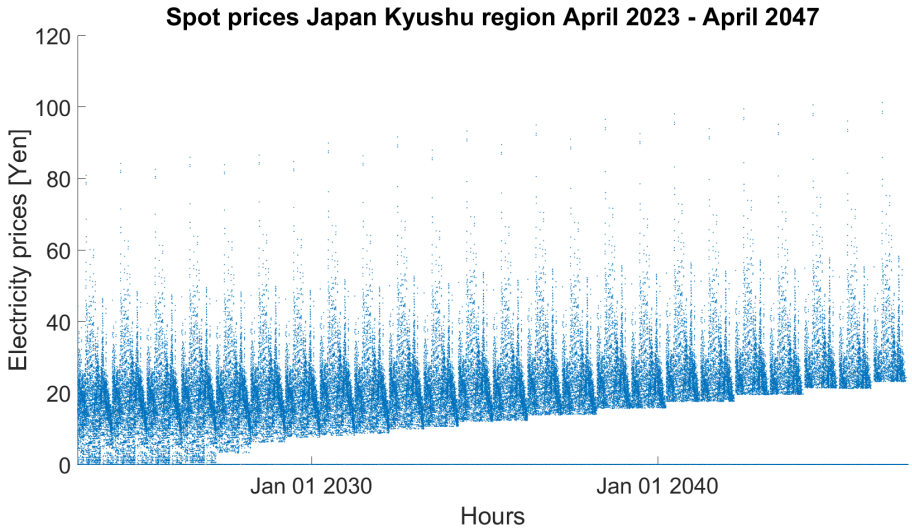

Figure 3.2: Prediction on the future electricity prices for Japan during the lifetime of the Goto City Wind Farm

this dataset, and the results are illustrated in Figure 3.2.

3.4. Technical challenges

The application of an offshore floating wind farm, especially when it is Japan's first commercial one, can come with a significant amount of technical challenges.As previously discussed (see Subsection 3.2.3), SPAR-buoy floaters can be subjected to large wave forces, potentially causing increased downtime and decreased power generation. Moreover, the unique nature of this wind energy approach may demand more maintenance efforts. This challenge can be underscored by a structural defect that was experienced in the pilot phase of the Goto City Wind Farm, resulting in a delay of its commercial launch from 2024 to 2026 [111].

In addition to wave interactions and maintenance concerns, other technical challenges for offshore floating wind energy could be issues related to anchoring systems, dynamic positioning, cable connections, and extreme weather resilience. All these aspects require consideration to ensure proper operation of an OFWF.

However, while all of these technical challenges are acknowledged that they could impose problems during operations, the main focus of this research is to assess if the techno-economic feasibility of OFWE can be enhanced since it is currently not a viable form of energy. While these challenges might occur for different system, the technical systems used in the Goto City WF have all been proven on technical feasibility as they are applied in commercial industry. It is recognised that still optimization of various techniques such as dynamic positioning

of floaters or anchoring of SPAR-buoy can be investigated, but this is not the goal of this research. The goal is to examine if H2 production can enhance the techno-economic feasibility of OFWE systems, resulting in the assessment of technical feasibility taking on a secondary role as their feasibility has already been proven to a certain extend becasue they are already commercially applied.

However, while it is acknowledged that the potential operational challenges posed by various technical aspects of OFWE, this research primarily focuses on evaluating whether the techno-economic feasibility of OFWE can be improved. Currently, OFWE is not considered a financially viable energy source. However, the technical systems used in the Goto City Wind Farm have already been proven in commercial industries [51, 52, 130], mitigating concerns regarding their technical feasibility. While it is recognised that optimization can be done for techniques such as dynamic positioning and SPAR-buoy anchoring, this research does not seek to investigate these challenges. Instead, the objective is to investigate whether H2 production can enhance the techno-economic feasibility of OFWE systems. Therefore, while technical feasibility remains important, the assessment of technical feasibility takes a secondary role, given that these systems have already demonstrated a certain level of feasibility through their commercial application.

3.5. Economics

The economic definitions used in this research might vary in different industries. This section will elaborate those used definitions to better translate the economic performance of the system.

3.5.1. CAPEX, OPEX and discount rate

CAPEX stands for Capital Expenditure. It refers to the costs of investment in, in this case, equipment and technology.

The discount rate is used in CAPEX to determine the present value of future cash flows generated by the investment. This helps in assessing the profitability and feasibility of the investment project. A lower discount rate indicates a higher present value for future cash flows, thus making long-term investments more attractive.

OPEX stands for Operating Expenses. These are the day-to-day costs associated with running a system and maintaining its ongoing operations. OPEX are recurring and generally short-term costs. OPEX includes items such as utilities, salaries, insurance and other routine expenditures necessary for the regular functioning of a system. OPEX of each system component are based on production rate or percentage of CAPEX.

When considering OPEX, the discount rate is used to calculate the present value of future operating expenses. This helps in evaluating the cost efficiency of projects or investments, as it accounts for the time value of money. A higher discount rate implies greater importance given to immediate costs over future costs.

3.5.2. KPIs

The characteristics of the model discussed in Section 3.1 and the way of modeling in 3.2 and 3.3 are used to assess the Techno-Economic Performance (TEP) of the system. The TEP of the system can be analysed and expressed in Key Performance Indicators (KPIs). This section gives an insight on the different KPIs used in this study, how they are relevant and how they are calculated.

LCOE

The LCOE represents the average cost of electricity over lifetime of a system. It is expressed in a value per unit energy, often €/MWh. These costs include all cost over lifetime of the power system so CAPEX and OPEX. For the Goto City Wind Farm it is calculated using Equation 3.6.

$$LCOE = \frac{CAPEX_{OFWF} + \sum_{1}^{LT} OPEX_{OFWF}}{P_{input,grid}} \tag{3.6}$$

Cash Flow

Cash Flow (CF) refers to the movement of revenues and expenses of a system over the lifetime. It's a crucial measure of a systems financial health to sustain ongoing operations. A positive overall CF indicates that a system is bringing in more money than it is costing. Conversely, negative CF may signal a failing system economically. CF is calculated using Equation 3.7 where i indicates the year during the lifetime.

$$CF(i) = R(i) - OPEX_{OFWF}(i) \tag{3.7}$$

PBP

The payback period (PBP) is calculated by dividing the initial investment cost by the annual cash inflow generated by the investment. The result is the number of years it will take to recover the initial investment. Its Equation is shown below 3.8.

$$PBP = \frac{CAPEX_{OFWF}}{CF(i)} \tag{3.8}$$

An important remark for the PBP in this research is that when the net present value of the system is below zero at the end of lifetime, signifying that the system is not viable, the PBP is calculated by using the average CF over lifetime of the system.

NPV

Net Present Value (NPV) is a metric that assesses the profitability of an investment by comparing the present value of expected cash inflows with the present value of expected cash outflows. It takes into account the time value of money, recognizing that revenue received in the future is worth less than revenue received today. The NPV can be calculated using Equation 3.9. Calculatation of the NPV utilizes a discount rate r. The discount rate serves as a tool to evaluate the financial viability of both OPEX and CAPEX by factoring in the time value of money and helping in comparing costs and benefits over time. In this research the discount rate is set to 4% e.g. $r = 0.04$. This value is based on found literature on offshore floating wind farms and integrated systems summarized in table 2.3 which often assumes this value for discount rate.

$$NPV = \sum_{i=1}^{LT} \frac{CF(i)}{(1+r)^i} - C_{investment} \tag{3.9}$$

A positive NPV indicates that the investment is expected to generate more revenue than costs, and is generally considered a financially sound decision. A negative NPV suggests that the investment may not meet the required rate of return and may not be economically viable. NPV in this research represents the development of the value of the system between start and end of lifetime. Graphs will thus indicate the trajectory of the value of the system to reach its final value. This KPI is the definitive factor that indicates if the TEP of the system is enhanced

3.5.3. Economic Properties

The economic values used for calculations on the TEP of the Goto City Wind Farm are summed up in Table 3.3. Note that these are estimations based on found literature. Expenditures on the Goto City Wind Farm are either not published or non existent since the wind farm is not yet commercially active.

System	Expense	Component	Value	Unit	Source
Wind farm	CAPEX				
		Wind turbines	1210	€/kW	[20, 84, 88]
		Floating platform	2.75	M€/WT	[84, 88]
		Mooring	528	k€/WT	[84, 135]
		Anchoring	18.9	k€/WT	[84]
		Turbine and platform installation	325.2	k€/WT	[84, 88]
		Mooring and Anchoring installation	169.6	k€/WT	[84]
	OPEX				
		O&M floating	68	k€/MW/year	[84, 88, 20]
Electrical Infrastructure	CAPEX				
		Inter-array cable	220	€/m	[74]
		Onshore cable	83	€/m	[84]
		Onshore Substation	55.12	k€/MW	[84, 20]
		Inter-array cable installation	848	€/m	[84, 135]
		Onshore Substation installation	8320	€/MW	[84, 135]

Table 3.3: CAPEX and OPEX estimations of the Goto Floating Wind Farm

3.6. Results

The retrieved dataset consisting hourly wind speeds at the specified location undergoes a transformation within the model, resulting in the derivation of a nominal wind speed associated with a designated wind direction. This process yields a wind profile, which is visually represented through a wind speed graph (Figure 3.3) and a wind rose (Figure 3.5).

The wind speed graph offers a clear depiction of how wind speeds at different hours throughout the year compared to the characteristics of the wind turbine. Notably, the graph reveals that the designated location does not show seasonal or daily variations in wind speed. An important observation is that the average wind speed fluctuates around 7.5 m/s, and the wind turbine's rated power is not frequently reached. This insight implies that the chosen location for the wind farm may not be particularly suited to the deployment of an OFWF, as the wind conditions do not consistently align with the optimal operating range of the turbines. This results in a low capacity factor, indicating poor power generation performance.

Future wind speeds are estimated using the method described in Section 3.2.1. The resulting profile is illustrated in Figure 3.4.

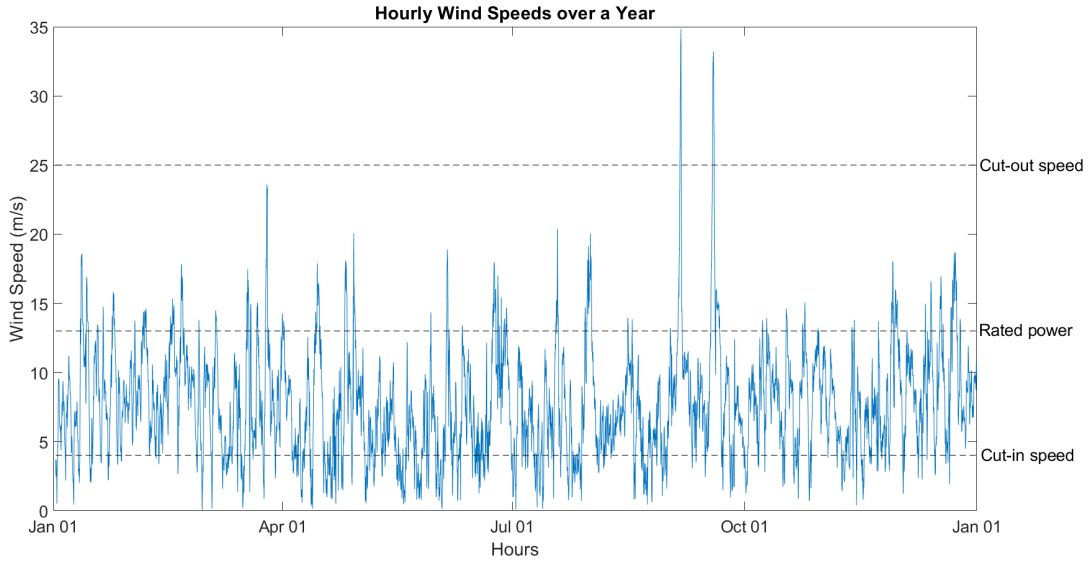

Figure 3.3: Graph of hourly wind speeds at location of the Goto City wind farm in 2022

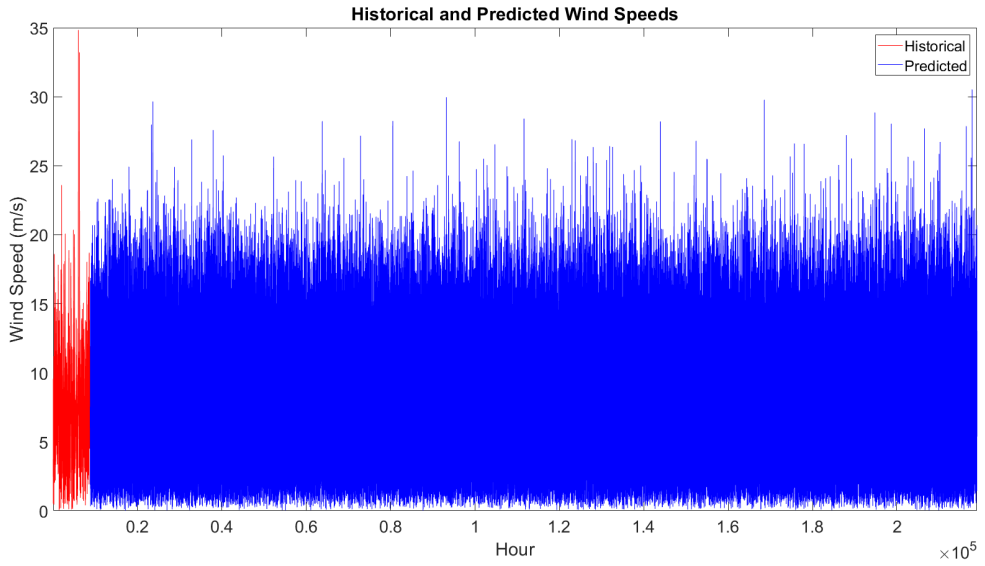

Figure 3.4: Graph of hourly future wind speeds at location of the Goto City Wind Farm

A wind rose is a graphical tool that displays the distribution of wind speeds and directions at a specific location over a set period. It consists of concentric circles representing different wind speed ranges and radial lines indicating wind directions, providing a visual summary of the wind profile. The axis on the circle refer to percentages and indicate the share of wind speeds from the direction in question. The wind rose for the Goto City wind farm is shown in Figure 3.5. Values on the wind rose represent directions the wind is coming from and not the direction the wind is headed toward.

The wind rose analysis reveals that less than 1% of the annual prevailing winds exhibit velocities exceeding the cut-in speed and originate precisely from the west or east directions. Consequently, the dismissal of wake-induced wind speeds and the assumption of their negligible impact on the technical performance of the Goto City wind farm are substantiated.

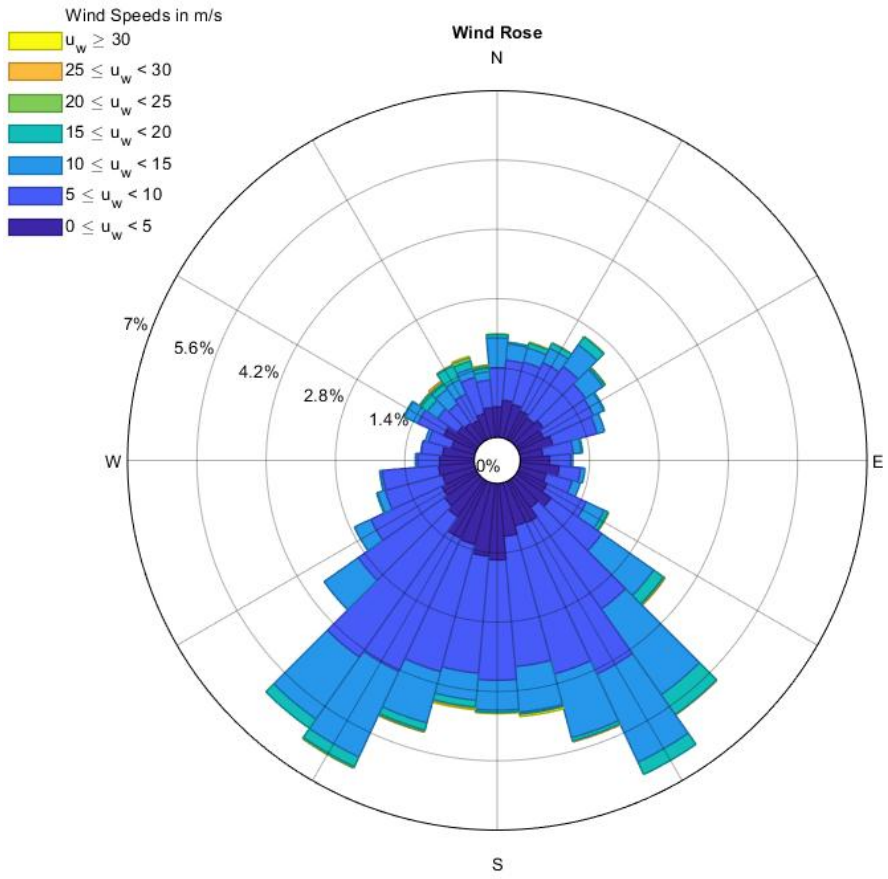

Figure 3.5: Wind rose of the location of the Goto City wind farm for 2022

The power output of each turbine is subsequently computed by integrating the wind speeds and the power curve of the WT. For wind speeds between cut-in and rated wind speed, power output is calculated by utilizing Equation 3.1. All the generated power from the OFWF, after transformation at the onshore substation, is directly supplied to the grid. Figure 3.3 indicates that a significant amount of hours the wind speed is below cut-in wind speed. This results in a relative high amount of down time of the OFWF. Figure 3.6 shows the total power output of the wind farm during the year. As a result of this the capacity factor of the wind farm amount to just 0.314.

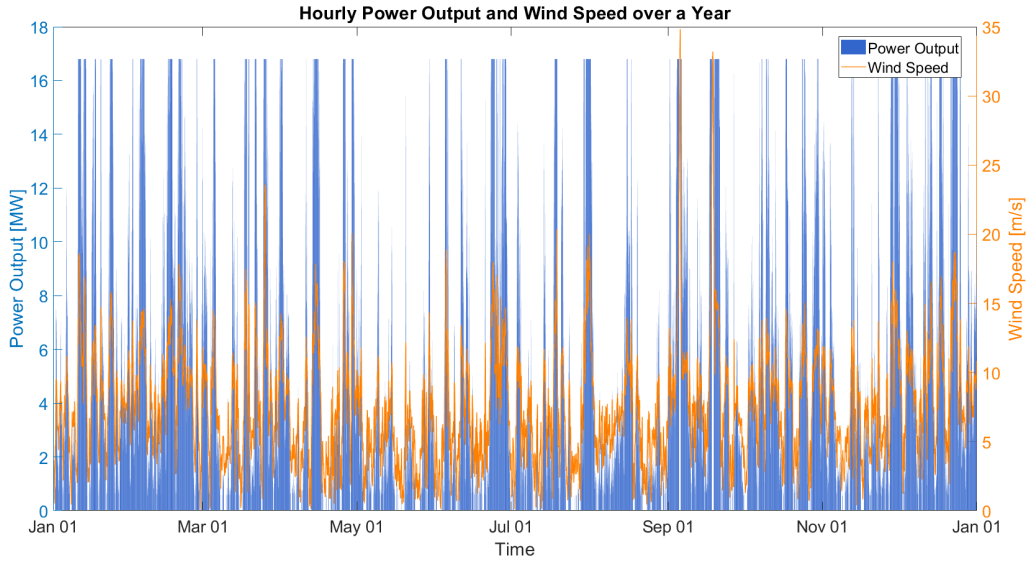

Figure 3.6: Hourly power output of the Goto City Wind Farm in 2022. The blue bars indicate the output in watts [W] with the corresponding wind speeds (orange).

3.7. Assumptions

In the previous sections on modeling of the Goto City Wind Farm that form a base case of this research, various assumptions derived from literature were considered. These assumptions serve as boundaries for specific aspects within this research, which is recommended given the broad scope of both OFWE and H2 concepts. Furthermore, they provide additional opportunities for further discussion. All the assumptions made in this model until this point are summarized in Table 3.4.

Category	Assumption
Wind	Since the wind speed at hub height is only 3.3% lower than the wind speed from the retrieved data set, the difference in power output as a result of height deviation is assumed negligible. Since less than 1% of the annual prevailing winds are coming from 0 or 180 degrees direction and those that do are barely above cut-in speed, the influence of wake on the power output of the wind farm is not considered. Since annual wind speeds typically follow a Weibull distribution, future wind speeds are estimated by applying a Weibull distribution over the retrieved 2022 dataset. Since the retrieved 2022 dataset for wind speeds shows very limited seasonal and daily variations, these factors are not considered to influence estimations on future wind speeds. The power coefficient is assumed to be constant at 32% when calculating the power output, regardless of the wind speed. Since the dynamic response of the SPAR-buoy floaters as a result of the prevailing wave conditions is assumed to be of limited value on the overarching goal of assessing if H2 production can enhance the TEP of OFWE, the influence of wave conditions is not taken into account.
Electrical	Since the OFWF is located around 15 km offshore and the combined power output is 16.8 MW, an offshore substation is assumed to be redundant. Since the voltage at the onshore substation is equal to the voltage of the grid, it is assumed that there are no transmission losses at the onshore substation. The onshore substation is assumed to be located 10 km from the shore.
Technical	While it is acknowledged that the OFWE system poses several technical challenges, the primary role of this research is to examine if H2 production can enhance the techno-economic feasibility of OFWE systems, as the technical systems used have all been proven on technical feasibility as they are applied in commercial industry.
Economics	FiT is not considered in analysis on TEP of the system. Hourly average power prices are used and matched with corresponding power output. Future estimations on power prices are based on literature, which considers a significant increase in RES until 2030. Consequential development of power prices is applied to the 2022 dataset. Since the Goto City Wind Farm is not realised yet and no information can be found on the economics regarding the system, capital and operating expenses used in the model are retrieved from literature on offshore floating wind farms. Discount rate used in calculations regarding CAPEX, OPEX and NPV is based on found literature and is set equal to 4%.

Table 3.4: Assumptions for the base case model

3.7.1. KPI results

The power generated by the wind farm is traded at the corresponding prices outlined in Subsection 3.3.1, resulting in a revenue stream that is visually represented in the graph presented in Figure 3.7.

To enhance understanding of how this revenue is derived, Figure 3.8 provides a detailed depiction of the hourly revenue over a two-day period, correlating power output and power prices. The blue line signifies the wind speed for each hour, while the green bars indicate the corresponding hourly power output from the wind farm in MW. The red bars overlaying the green bars represent the revenue generated from supplying the generated electricity to the grid under the assumption that all generated electricity can be sold to the grid for the hourly average price of the JEPX. This visual representation underscores the relationship between electricity generation, wind speed, and revenue, emphasizing the codependency of revenue on power prices. The figure serves as a valuable illustration of how power prices significantly influence the overall financial performance of the wind farm, underlining the interplay between electricity generation and market dynamics.

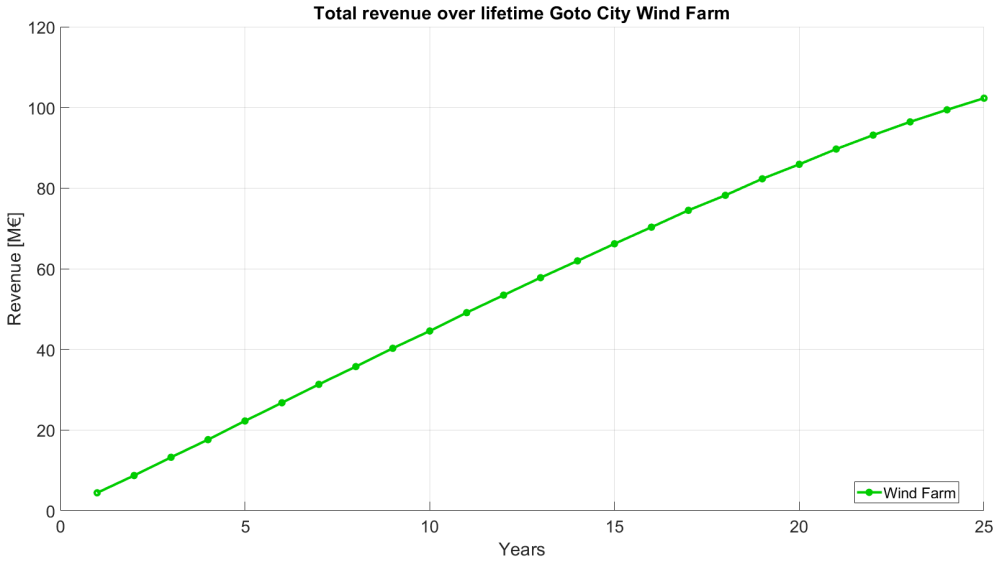

Figure 3.7: Revenue gained from the Goto City Wind Farm over its lifetime

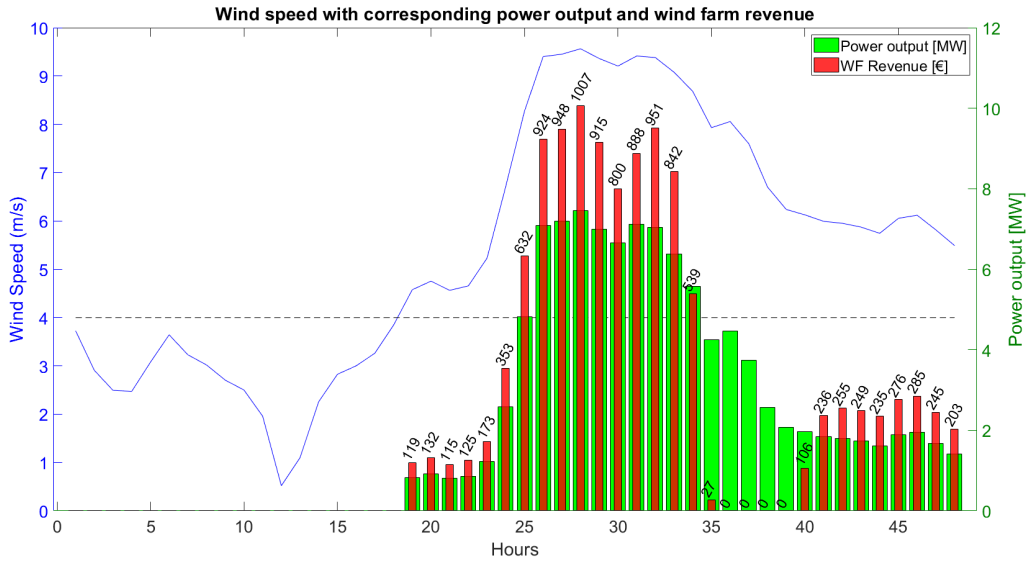

Figure 3.8: Power generation and corresponding revenue from providing electricity to the grid for the corresponding wind profile for the first 2 days of operation

The annual NPV of the OFWF is depicted in Figure 3.9b. Two remarkable features are of interest in this graph. Firstly, there is convergence observed approximately at the 17th year of the OFWF's operational LT. This convergence results from a substantial increase in the number of hours during which power prices exhibit negativity or zero valuation. Such negative pricing results in the absence of a revenue stream despite the generation of power.

Secondly, it is noteworthy that at the end of its operational life, the NPV of the OFWF remains negative. This signifies that the revenue from the wind farm has failed to surpass the corresponding expenses. This finding underscores the assumption that OFWE is an underdeveloped form of RES because it is not an economically viable form of energy source. This is primarily due to its high cost structure, resulting in a lower starting point for the NPV curve. Therefor, the establishment of a FiT by the Japanese government, which is set at ¥38/kWh (±€0.25/kWh) [33], proves to be a necessary measure for incentivizing investments in OFWE. This is visualized in Figures 3.9a and 3.9b, showing a clear increase in annual cashflow of the WF. This results in a highly positive

NPV at the end of lifetime, meaning that the Goto City Wind Farm with FiT is economically viable and consequently a wise investment. An overview of the KPI results in for the base case under the specified conditions is shown in Table 3.5. Note that since the NPV is below zero, the PBP is higher than the operational lifetime of the system.

KPI	Revenue	Average CF	PBP	NPV	LCOE
Value	€102.0M	€2.94M	27.6 years	€-7.62M	€88.7/MWh

Table 3.5: Overview of the results on KPIs for the base case

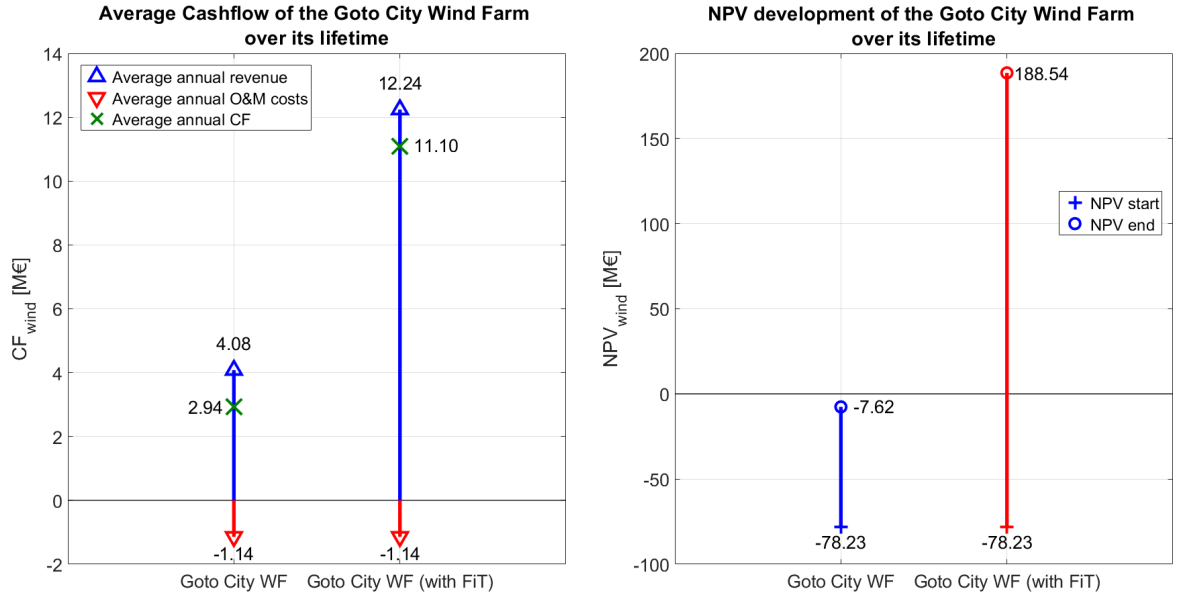

(a) Cashflow

(b) NPV

Figure 3.9: Average CF (a) and NPV development (b) of the Goto City Wind Farm over its operational lifetime. The right plot in the graph underscores the importance of a Feed-in Tariff by the Japanese Government.

3.8. Verification and Validation

The robustness and reliability of the obtained results is of vital importance, particularly when using data analyses and simulation models. To conclude the modeling processes run accurately, the identification of key results is paramount. A promising observation is derived from the graphical representation in Figure 3.6, which illustrates that the hourly power output of the Goto City Wind Farm does not exceed the maximum of 16.8 MW. This observation suggests that the power output of each turbine does not surpass the rated power, thus suggesting the model's simulations represent correct operational parameters. Moreover, Figure 3.8 indicates that the power output remains at zero when wind speeds fall below the cut-in speed of 4 m/s. This alignment with expected operational behavior provides further verification of the model's accuracy.

The validation of the Goto City Wind Farm model presents a challenge, as traditional validation methods rely on comparisons with real-world data or experimental results. However, given that the farm has not yet been constructed and thus the lack of associated performance or economic data for the Goto City Wind Farm, an alternative approach is adopted for result validation. This study resorts to cross-referencing with existing literature to validate the resultant LCOE for the Goto City Wind Farm.

To validate the model's accuracy in predicting power output, the simulation is extended to replicate the operational year of 2022 for an established wind farm in the North Sea with similar characteristics. This simulation involves replicating the environmental conditions and comparing the model's power output with the realized output of the reference wind farm. A successful match between the simulated and actual power outputs would indicate the model's capability to accurately simulate the Goto City Wind Farm.

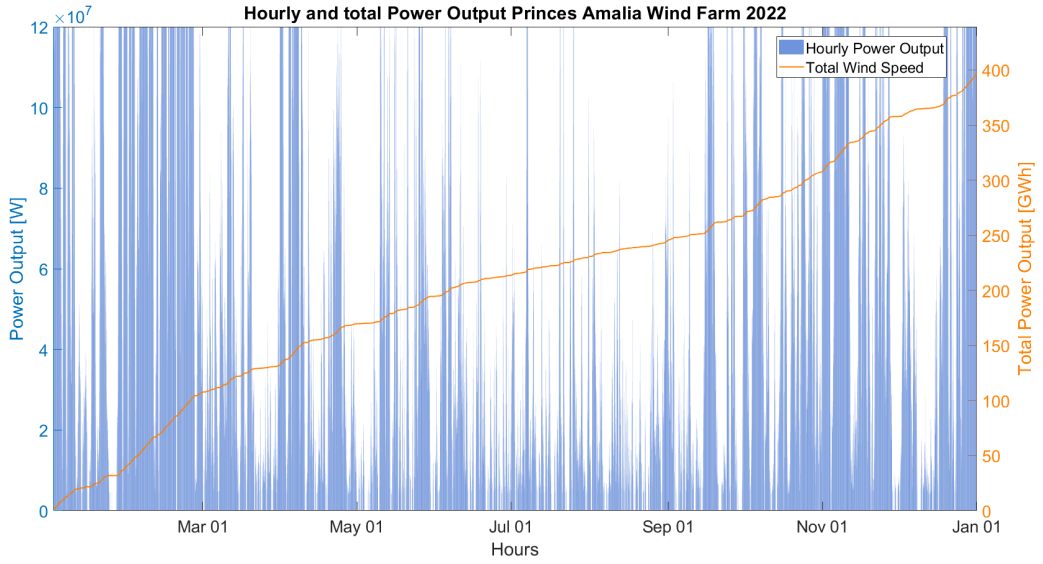

Figure 3.10: Hourly and total power output of the Princes Amalia Wind Farm off the coast of Egmond aan Zee in the Netherlands

For the validation of the annual power output, the model is compared against the Princes Amalia Wind Park off the coast of Egmond aan Zee in the Netherlands [102]. This wind farm, like the Goto City Wind Farm, utilizes 2 MW wind turbines with comparable cut-in and cut-out speeds and a slightly higher rated power of 15 m/s [122]. The Princes Amalia Wind Park, comprising 60 turbines with a combined capacity of 120 MW, registers an annual power output of around 422 GWh, dependent on conditions and downtime [102]. When applying the corresponding wind profile to the model and adjust the appropriate parameters to match the reference wind farm, the resultant power output of the model approximates 395 GWh, as depicted in Figure 3.10. This finding shows to be promising in terms of power output of the model. Considering uncertainties in a simulation model with respect to real time operations, as more parameters are of influence on the output of a wind farm other than the WT characteristics and wind speed, one can state that the simulation model depicts a fairly accurate representation of other wind farm power output with a margin of error of 6.4%.

For the evaluation of the LCOE for the Goto City Wind Farm model, the resulting value is compared to existing literature. The LCOE resulting from the model amounts to €88.7/MWh, aligning with findings in studies conducted by Maeinza et al., Myhr et al., and Castro-Santos et al. [23, 88, 84]. These investigations explore various alternatives, including the Hywind floater, which corresponds to the SPAR buoy floater utilized in the Goto City Wind Farm. The literature provides a range of LCOE values for wind farms employing similar floaters for offshore wind turbines. It is noteworthy that the resulting LCOE from the model falls at the lower limit of the reported LCOE ranges in the cited studies. This is explicable by the fact that the referenced research primarily deals with theoretical wind farms featuring significantly higher capacities than those employed in this model and larger distances from shore.

As stated in 3.2.2, this system does not require an additional offshore substation to convert the power for further transport, which is required when a wind farm capacity exceeds 100 MW and is located more than 15 km from the coast. The absence of an offshore station results in a lower cost structure. The addition of an offshore substation in a OFWF system significantly adds to the CAPEX of the system and therefor LCOE mutually increased as well.

The observation that the model's results yield a LCOE for the wind farm system within the range of existing literature, be it on the lower limit, suggests a promising level of accuracy in the simulation of an OFWF. However, it's important to note that no definitive validation of the model can be conducted by the unavailability of real-life data from the Goto City Wind Farm. Therefore, while the model's results show similarity with existing literature and thus provides a degree of accuracy, further validation with actual operational data would be necessary to strengthen its reliability and to ensure correct representation of operational performance.

3.9. Conclusion

In conclusion, the base case model for the Goto City Wind Farm provides a correct representation of the wind farm's performance, taking into account factors such as wind speed, turbine characteristics, electrical infrastructure, and operational strategy. The characteristics of the wind farm, as outlined in Table 3.1, serve as the foundation for the model's processes and calculations as described in Section 3.2. The utilization of historic wind speed data, along with future wind speed extrapolation, ensures a realistic depiction of energy production. The transmission losses in the electrical cables, as well as the incorporation of electricity prices from the JEPX market, contribute to the overall resulting wind farm's economic performance.

As the results and figures clearly indicate, the economic performance of the Goto City Wind Farm, under the set conditions and assumptions for current and future scenarios, is inadequate. This signifies the importance of the FiT set by the Japanese government. Without this FiT, the Goto City Wind Farm is not economically viable and demonstrates substandard KPIs as described in Section 3.7.1. KPis such as LCOE, Cash Flow, Payback Period, and NPV are essential metrics for evaluating the techno-economic performance of the system over its operational lifetime.

The results of the model are validated through comparisons with existing wind farms and literature. The power output of the Goto City Wind Farm model closely aligns with the observed data from the Princes Amalia Wind Park in the North Sea, providing confidence in the model's ability to simulate real-world scenarios. The resulting LCOE is in line with literature, considering the differences in capacity and wind speed profiles.

In summary, the base case model lays the groundwork for further analysis and optimization, providing valuable insights into the potential challenges and economic considerations of the Goto City Wind Farm. The model's accuracy and reliability are supported by comparisons with real-world data and existing literature, enhancing its credibility as a tool for assessing offshore floating wind farm performance.

4

Research Proposal

4.1. Hypothesis and relevance

H2 production for offshore floating wind farms can provide and additional revenue stream besides supplying the grid, which is desired considering the high cost of technology. Because of the increase in RES in the future, the volatility of energy supply is expected to increase and a need for a stable and constant supply will be higher [83]. Because of this the reward for flexible consumption and generation of energy will most likely be higher resulting in higher prices per kWh. This lead to the following hypothesis for this research: *"H2 production can improve the techno-economic performance of offshore floating wind farms, mitigating investment risks by governments and corporations and providing a hedge against volatile power prices"*. This reduced risk might kick-start the large-scale implementation of floating wind energy.

4.2. Research gaps

At the start of this research a literature study was conducted to identify various research gaps. A summary of those gaps is listed below. These gaps were identified by analysing applications of offshore wind-hydrogen combinations. After that literature was analysed on how these systems where modeled and finally how the techno-economic analysis of offshore wind-hydrogen systems was reviewed.

Research gaps:

- Investigating the influence of future wind speed and direction estimations derived from historical measurements for accurate lifetime calculations in wind energy systems.
- Assessing the impact of hourly electricity prices on the economic viability an integrated wind-to-hydrogen system and investigating potential differences between electricity prices and H2 production costs.
- Examining the use of an active dynamic production schedule of an integrated system to maximize profits while considering fluctuations in power prices.
- Investigating the influence of different H2 carrier configurations on the improvement of floating integrated system.
- Evaluating the NPV and PBP based on expected future electricity prices characterized by higher volatility.

4.3. Research objective

The research objective of this study is to determine if the techno-economic performance of the concept offshore floating wind energy for Japan can be enhanced by installing an additional hydrogen production system. Hydrogen will be produced during hours where the prevailing market price of hydrogen is higher per kWh than the price of electricity per kWh. This is translated into a research question and sub-questions to approach the research question methodically.

"How can H2 production add value to the techno-economic feasibility of offshore floating wind energy?"

This research question will be examined by answering the following subquestions:

1. What components are essential for an H2 production facility and how do all the processes of these components work?
2. What configurations of H2 carriers exist and how do they influence the case of adding a H2 production system to offshore floating wind for the Goto City Wind Farm?
3. At what electricity price per kWh is the production of hydrogen economically more beneficial than feeding electricity to the electricity grid?
4. What elements within the power of design of an integrated system are variable and can be altered to enhance the system under the set conditions?
5. How do possible future scenarios affect the decision to add H2 production to offshore floating wind?
6. What is the minimum number of hours per year the H2 production system must be active to economically enhance the concept of offshore floating wind at a prevalent H2 price per kg?
7. Which internal parameters of the integrated system have the most impact on enhancing to the concept of floating wind?

4.4. Methodology

In pursuit of the research objective, a modeling methodology is employed. To model the integrated wind-to-hydrogen system as accurately as possible, the computational tool MATLAB is used. The Goto City WF is used as the base case due to its status as Japan's premier OFWF, setting a tone for future floating wind energy projects. The modeling process encompasses the incorporation of the hourly wind profile at the designated location with hydrogen production and providing the grid with electricity. The prevailing wind profile at the site, stated in Chapter 3, is gathered from an open-source database, named Copernicus [35]. Subsequently, the power output of the wind turbines is translated in the form of an hourly electricity generation graph.

The simulation extends to the electricity grid, involving the evaluation of hourly market prices. These are gathered from the JEPX. During hours where the active market price of electricity per kWh falls below a set threshold value per kWh, the floating wind farm shifts its operation to hydrogen production instead of electricity feed-in to the grid. This threshold value is yet to be determined and is called the *switchprice*, similar to the research of Buffo et al. [18].

The hydrogen production plant components are modeled in MATLAB, incorporating parameters such as energy consumption, efficiency and size. These characteristics are compliant with the wind farm's output and the active production hours of the facility. In addition, different H2 carrier configuration are compared to investigate their influence on the improvement of techno-economic performance. Configurations include compressed gaseous hydrogen, liquid hydrogen, ammonia, and MCH.

The initial simulation of the integrated system with set operational conditions, using a CGH2 configuration as a final product, will be set as the reference case. CGH2 will be used as a reference case due to its reduced steps to form the final product and therefor its reduced losses. Future scenarios consider changes in circumstances with respect to the reference case which influence the performance of the system over its lifetime. In a scenario analysis study on the integrated system, a conservative, pessimistic and optimistic future scenarios are examined for parameters outside the power of design to assess their impact on the economic viability of the system. This is to examine if H2 addition can enhance the economic viability of offshore floating wind energy for different future scenarios under the set conditions. The economic characteristics of the H2 production plant, linked with the produced volume of H2, result in determining the LCOH. This is an indicator in assessing the overall economic viability of the H2 production system.

The techno-economic performance of the conventional and integrated system is indicated in this research by means of KPIs. These are the results of certain techno-economic characteristics of the systems, indicating if the addition of H2 production to offshore floating wind energy can enhance its feasibility based on the criteria of KPI improvement.

In order to complete this methodology and achieve the set goal of answering the research questions, some insights are required to conduct this research in an educated way. Validation of the various outputs must be ensured to simulate the operations of an integrated system accurately and realistically. Validation and verification of the model strengthens the credibility of the model en therefor the research. Besides that, insights into power

price market fluctuations and a deeper understanding in the changing conditions for hydrogen production would enhance the simulation's robustness.

5

Goto City Integrated System

In order to enhance the performance of the Goto City WF, the technical implications of building a proposed IS need to be addressed. This chapter will describe the how the conventional Goto City Wind Farm is modeled in to an IS. It will discuss the additional components for the system for H2 production, where these will be placed within the system and what new operational strategy will be adopted to maximize profits. Note that the newly modeled system's performance will be simulated under the same conditions and with the same assumptions as the base case model. The question raised in 4.3, Subquestion 1, will be answered and reads: *"What components are essential for an H2 production facility and how do all the processes work?"*

This section will elaborate further on this specific question. First the orientation and characteristics of the proposed system will be described, followed by the operational modes of the system. Subsequently, the system build-up will be explained and visualized. Finally, the economic implications that come with the additional components will be discussed.

5.1. System Set-up

As the goal of this research is to optimize the performance of the proposed Goto City IS, the adoption of a non-dedicated operational strategy is recommended. In this research, the IS is configured to possess dual connectivity, enabling it to interface with the electrical grid and a H2 production system. Electricity output is allocated either to the grid or the H2 production infrastructure. This allocation of electricity is dependent upon the prevailing market conditions at the operational hour, specifically the power pricing dynamics within the local spot market of Japan. When power prices are at high levels, the power generated by the WT is supplied to the grid, contributing to revenue generation from electricity. Vice versa, during periods of low electricity prices, the power is redirected towards the production of H2. The H2 will be sold against the price of H2 at that specific time. Again, it is assumed that all the generated power by the wind farm can directly be sold to the grid for the prevailing hourly average markets prices, similarly to the base case model. This dynamic operational strategy is anticipated to yield an optimal revenue stream.

Given that the primary objective of this research is to enhance the feasibility of OFWE through H2 production, the orientation of the Goto City IS takes on a secondary role in comparison to the more relevantly considered operational strategy. As the chosen operational strategy is non-dedicated, the electricity generated is destined for delivery to the grid in one of the two operational modes. Therefor, the construction of inter-array cables connecting the wind farm to the onshore substation is required either way.

Consequently, in order to reduce the already elevated costs of OFWE compared to fixed-bottom, and reduce the associated risks that come with the construction of an offshore platform for auxiliary components, a decentralized system configuration is employed. Onshore construction typically presents a more cost-effective alternative compared to offshore installations [21, 53]. It is assumed that under the circumstances of the Goto City Wind Farm, the additional offshore operations will result in elavated expenses compared the onshore operations. This would further decrease the value and viability of the already non-feasible system. Offshore H2 production and storage may offer certain advantages regarding the distribution as well as the spatial management. However,

these advantages are not directly related to the research's core objective.

5.2. System Characteristics

The total system consists of three essential components besides the already discussed Goto City WF of which basic knowledge has been given previously. Characteristics on each of these components will now be discussed.

5.2.1. Desalination

For this research it is assumed that to prepare water for electrolysis, only seawater needs to be desalinated. The desalination installation will use SWRO like described in Section 2.2.3. The water intake is dependent on the production of H2 from the electrolysers.

5.2.2. Electrolysis

Literature study on electrolyser techniques conducted in Section 2.2.2 reveals that the three considered electrolyser techniques each excel in its own regard. Based on the criteria for the proposed IS, the PEM electrolyser emerges as the most suitable technique for OFWE applications. This is primarily due to its high flexibility and low start-up time. Given the volatile nature of electricity supply resulting from fluctuating wind speeds, it is crucial for the electrolyser to swiftly adapt to these changing currents. Similarly, volatile power market prices during the day cause for a preference for PEM electrolysis. The start-up times must be very short to maximize the operational time of the IS when power prices drop below the set threshold. The PEM electrolyser excels in this regard, offering rapid response capabilities. Because of this fast response time, the electrolysis unit does not need an additional battery system to keep the electrolysers within operating range.

Furthermore, the choice of PEM electrolyser over alternatives like AEL or SOEC is motivated by the high purity of the H2 gas it delivers. Since the H2 gas might undergo liquefaction or conversion to a H2 carrier in the subsequent step, the purity of the electrolyser's product becomes crucial. By employing the PEM technique, the resulting product after conversion exhibits lower levels of oxygen contamination. The installed capacity of the electrolysers is equal to that of the Goto City WF, namely 16.8 MW.

5.2.3. H2 Configuration

The product of the integrated system will be in one of the four discussed forms of H2 carriers in 2.2.4. The addition of processes for each of the four configurations and the extra energy consumption and losses that come with the configuration must be added to analyse the total performance of the system. Respectively, the four configurations use an electric compression pump (CGH2), a H2 liquefier (LH2), an air separation and ammonia synthesis installation (NH3) and a MCH synthesis and decomposition installation (MCH).

- **Compressed Gaseous Hydrogen** - The H2 carrier configuration of CGH2 is used as a reference case because of its reduced steps to form the final product compared to other configurations. The focus of the research is on evaluating the potential enhancement of the OFWE concept through H2 utilization, rather than an in-depth study on H2 carriers. To simplify the configuration and streamline the processes post-electrolysis, a straightforward approach is adopted.

  In this research, it is assumed that the produced CGH2 will be used in the steel industry of Japan. Japan is a large producer of steel and the process of producing steel requires a heat source in gaseous form. Since the production of H2 is expected to be relatively low compared to the demand for a steel mill [60], purchases of CGH2 by the steel industry will be bi-daily. The amount of storage for the compressed gas is therefor assumed to be needed for two days of maximum production. The produced CGH2 will be stored in high-pressure tnks on the onshore production facility. The CGH2 will be sold for the prevailing H2 market price.
- **Liquid Hydrogen** - The use of LH2 is envisioned to be for the storage of energy in the future [26, 10, 56]. Storage of energy is needed for when there is a shortage of supply which is often characterized by high energy prices. Figure 3.1 visualizes those shortages on the electricity market. Because of this expected role LH2 is envisioned to have, this research assumes that the produced LH2 will not be sold as a product on itself but it will be stored. This will be done in a cryogenic tanker on the onshore facility and re-gasified back to gaseous form and used in fuel cells to produce electricity during hours of high prices.
- **Ammonia** - NH3 already has an existing infrastructure and market since it is the most used feedstock in the fertilisation industry. For that reason, it is assumed that the produced NH3 will have the same application as

CGH2 and will directly be sold to consumers. In this context those consumers are the fertilization industry.

- **MCH** - For MCH, a similar principle as for LH2 is employed. The produced MCH is stored for a week, and in the following week, it is converted back to electricity to be supplied to the power grid. The re-gasification process of MCH requires additional energy input and installations. To convert the MCH back to toluene and GH2, a decomposition unit is required. The remnant toluene is sold for the same price it was bought.

5.2.4. Operational modes

The integrated system has two operational modes: *Electricity Mode* (EM) and *Hydrogen Production Mode* (HM). In the first mode the system solely supplies electrical power to the grid. In the second mode the generated power is solely used for the production of H2. The system can also be in standby mode. This is when there is no wind, the wind speeds are below the cut-in speed of the WT or the wind speed is above cut-out speed of the WT. As a result no power is generated by the WT.

5.2.5. System build up

The system build up for both operational modes is shown in Figure 5.1. The green blocks and lines indicate the system operational in conventional OFWF mode. The blue blocks and lines indicate the system operational in W2H mode. The blue, lightblue, orange and purple lines represent the different H2 carrier configurations.

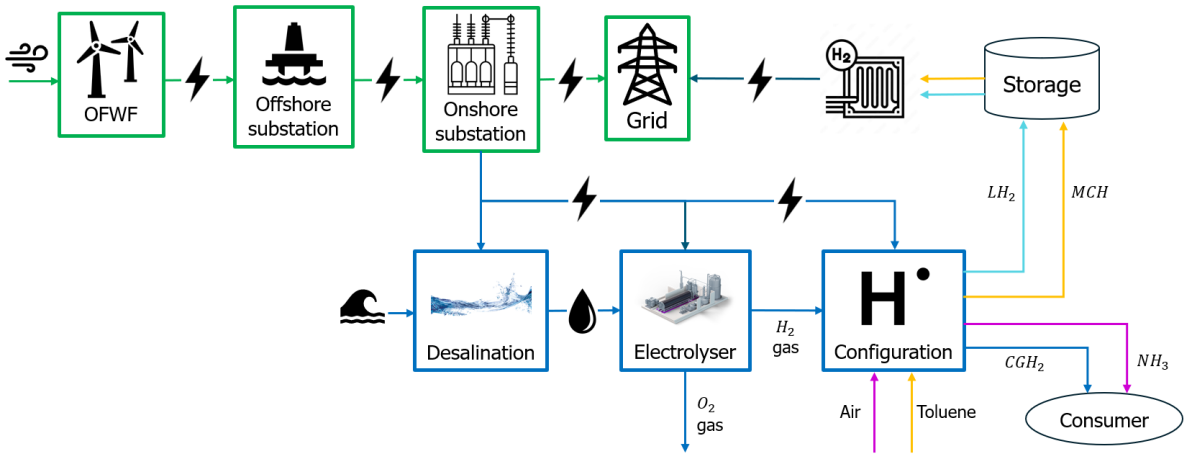

Figure 5.1: System build-up in conventional OFWF mode (Green) and in W2H mode (Blue)

5.3. Technical challenges

The integration of a hydrogen production system into OFWE system can pose several technical challenges. Firstly, the PEM electrolyser technique utilized in this research to convert seawater into hydrogen gas requires consideration of sizing and energy conversion efficiency. The first of these considerations will be analysed using a capacity analysis, similar to the one performed by Bonacina et al. [15], which will be further explained in Section 6.4.

The second consideration, regarding the energy conversion efficiencies, will be discussed in Section 6.2. Additionally, the storage and transportation of hydrogen offshore necessitate specialized infrastructure, including storage tanks and suitable transportation vessels, adding complexity to the overall system design will also be discussed in the last referred section.

While this research addresses some technical challenges, not every key technical challenge is considered in this research, such as the efficiency of the PEM electrolyser unit. While energy conversion efficiencies are discussed, it's noted that challenges like degradation and optimization still exist for this technology, with expectations of future improvements. Also, transportation of the final product, at least for two of the considered H2 carrier configurations, is assumed to be handled by the consumers of the product. Transportation can come with serious complications that could interfere with the overall performance of the IS [133, 29, 24, 10].

However, as outlined in Section 3.4, the primary focus of this study is to examine if H2 production can enhance the techno-economic feasibility of OFWE systems, specifically for Japan's Goto City WF. Further investigation on the

technical feasibility of such a proposed IS falls outside the scope of this research. Although some components of the H2 production system may require additional technical assessment for performance enhancement, most have already been proven in commercial applications and are assumed to require no further investigation in this study.

5.4. Economic Implications

The addition of a H2 production system to the Goto City WF also brings additional investment and operating costs. Based on found literature, CAPEX and OPEX estimations for the Goto City IS are shown in Table 5.1. This table does not consider the conversion of the produced H2 gas to one of the four considered carriers yet. These economics will be discussed in the subsequent chapter.

The flow of economics of the wind farm and the integrated system is illustrated in Figure 5.2. As stated in the above segment, the CAPEX of certain CAPEX values is assumed to be dependent on the maximum production of the electrolyser component. Maximum production of this component is based on the prevailing wind conditions en consequently the resulting generated power.

The electrolyser CAPEX consists two components: the Stack and the Balance of Plant (BoP). The Stack serves as the core system where the electrolytic process between water and the cathode/anode takes place. Conversely, the BoP encompasses all supplementary components necessary for ensuring the efficient and safe operation of the electrolyser, as illustrated in Figure 2.8b.

Traditionally, PEMEL stacks are anticipated to require replacement approximately every 20 years due to stack degradation [40, 56]. This exceeds operational lifetime of the IS and should therefor be replaced within this timeframe. However, given that the system with be varying in operating conditions, it is assumed in this research that the degradation of the electrolyser stacks does not necessitate replacement after 20 years of operation.

System	Expense		Value	Unit
Desalination [55, 68, 118, 22]	Capital			
		SWRO unit	1917	€/(m^3/d)
	Operating			
		Maintenance	49.53	€/MWh
		Chemicals	37.6	€/MWh
Electrolysis [56, 86]	Capital			
		Electrolyser Stack	420	€/kW
		Electrolyser BoP	330	€/kW
	Operating			
		O&M	0.22	€/kg H2
		Stack replacement	12	% Capital

Table 5.1: CAPEX and OPEX estimations of the integrated H2 production system for the Goto Floating Wind Farm.

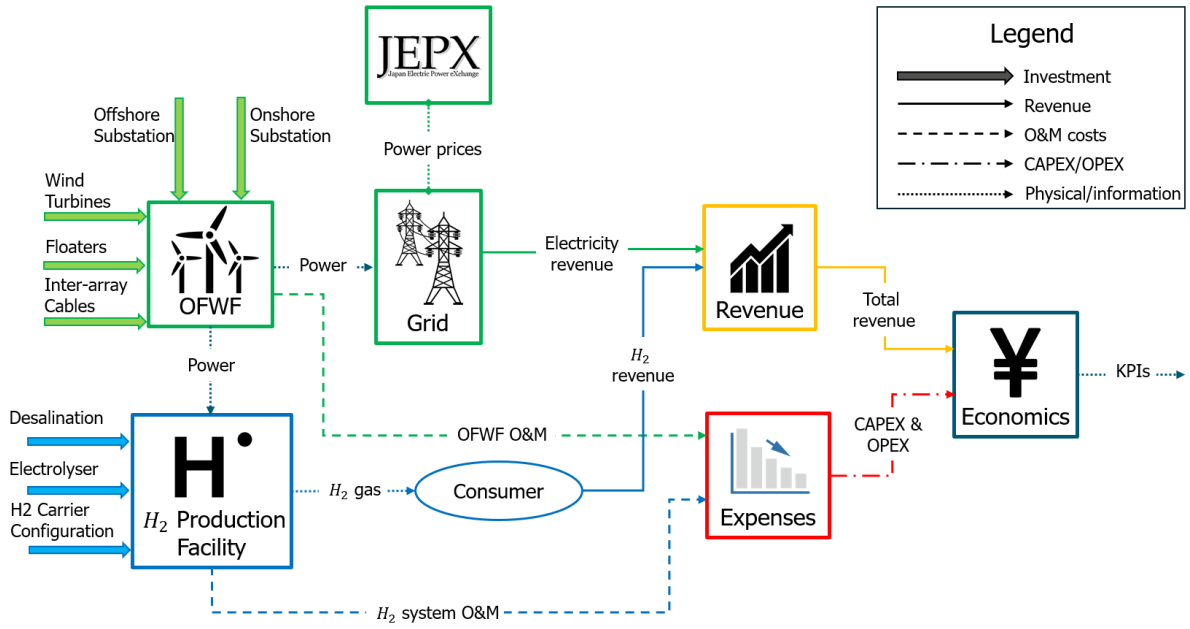

Figure 5.2: Flow diagram of the economics of the OFWF (Green) and the integrated system (Blue). Striped lines indicate expenses and solid lines indicate income. Dotted lines indicate physical flows or information.

Both systems of the Goto City IS that can generate revenue require investment, as indicated with the bold arrows in Figure 5.2. These are the essential components for respectively the OFWF and the H2 production system. This economic flow diagram is based on the reference case, meaning that the produced and compressed H2 gas directly sold to the consumer. For the other configurations that are considered in this research, the following chapter will elaborate further on the applications.

However, the goal of this figure is to illustrate the economic dynamic of the Goto City IS. The combined investment and Operating and Maintenance (O&M) costs form the system CAPEX and OPEX. Combining that with the revenue gained from providing the grid and H2 production results in the KPIs of the system.

6

Methodology

This chapter details the methodology employed to address the research questions outlined in the study. The primary objective of this methodology is to identify and visualize potential improvements in the OFWE concept through H2 production during periods of low electricity prices. The methodology encompasses the evaluation of various H2 configurations, as discussed in Section 2.2.4, and an extensive scenario analysis that tests the influence of multiple future scenarios on the integration of H2 production into the base case. An overview of the methodology is presented in Figure 6.1.

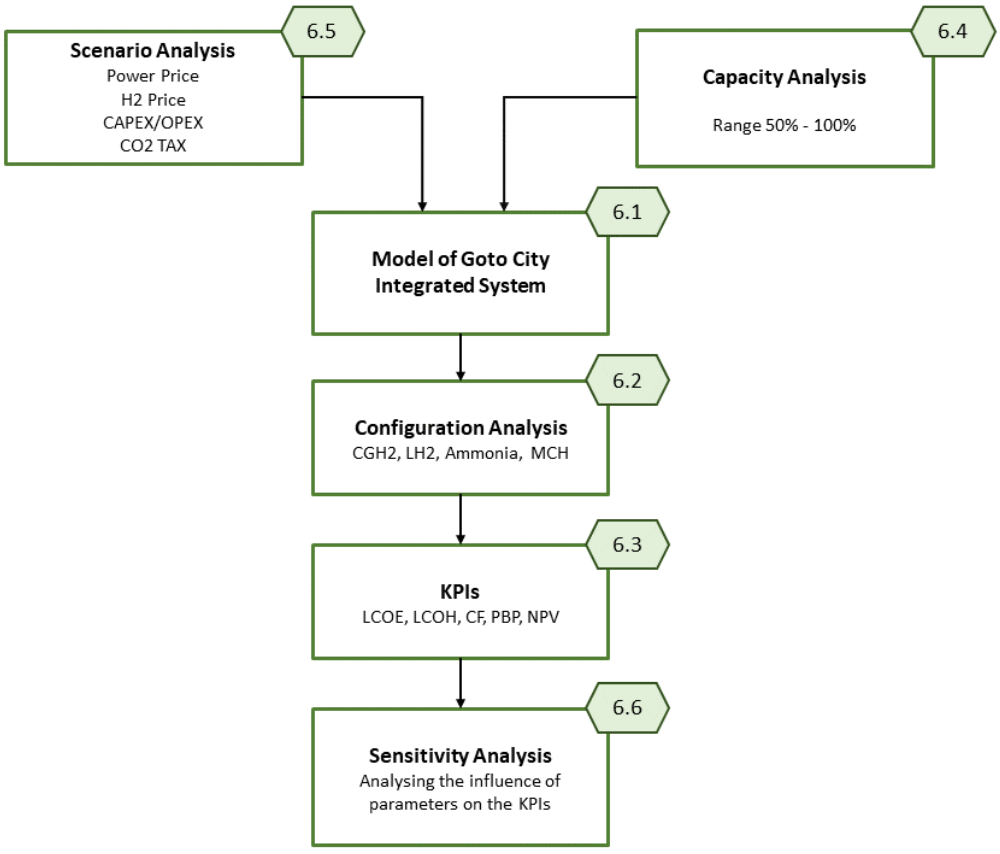

Figure 6.1: Structure of Methodology

The model conducts a extensive simulation of the integrated system, covering its operational span of 25 years and analysing its performance. The initial Section, 6.1, delves into the reference case of the model,

aiming to provide a detailed understanding of the Goto City IS with compressed gaseous H2 production. This serves as a benchmark for assessing the impact of integrating H2 production into the conventional model and presenting the methods and assumptions for each component of the integrated system.

Following the analysis of the reference case, Section 6.3 discusses the assessment of system performance using proposed KPIs. Subsequently, Section 6.2 introduces how different H2 carrier configurations influence the KPIs of the integrated system. In Section 6.4, a capacity analysis is introduced, exploring the notion that installing the same capacity for the electrolysers as for the wind farm yields optimal results. Given the 25-year lifespan of the integrated system, Section 6.5 introduces four scenarios that could significantly influence the system's performance. Finally, Section 6.6 entails a sensitivity analysis, quantifying the impact of parameter changes on the KPIs.

6.1. Modeling the Integrated System

The integrated system is modeled where the choices on components of the system are based on characteristic described in Section 5.2. Additionally, some other choices for components are made which are further explained in each of the following subsections. Modeled components of the integrated system can be seen in Figure 5.1. Each block represents one of the components described in the subsections.

6.1.1. Desalination

Modeling the auxiliary components of the system such as the desalination, electrolyser units and H2 configuration auxiliaries is strongly dependent on the power supply of the wind farm. Furthermore these components are mutually dependent. SWRO requires a significantly lower amount of energy in this model since the only power required by the units is for pumps circulating water and forcing seawater through filters [68]. Desalination modeling can be calculated using Equation 6.1.

$$E_{desal} = V_{H_2O} * e_{des} = (\sum_{i=1}^{24} W_{H2,elec,theor}(t) * Q_{H_2O} * \rho_{H_2O}) * e_{des} \tag{6.1}$$

In which V_{H_2O} is the daily volume of water required by the production facility, Q_{H_2O} the water consumption per kg of produced H2. This is set to 15 [109]. ρ_{H_2O} is the density of the seawater which is set equal to 1025 kg/m^3. e_{des} is the specific energy consumption of the desalination unit per m^3 of desalinated water and is assumed to be 3.5 kWh/m^3 [109]. The first component, V_{H_2O}, is set for maximum daily production since it is assumed that the system should be able to cope with maximum H2 production for 24 hours.

6.1.2. Electrolysers

Electrolysis demands the highest power consumption among all the auxiliaries. For this research, the NEL electrolyser is selected, with a power consumption of 4.5 kWh/Nm^3 [91]. The weight of 1 m^3 of H2 gas is 0.0848 kg [123]. The equation is presented below. The resulting in a total energy consumption for the first operational hour before degradation of the electrolyser stack is 53.17 kWh/kg of H2.

$$E_{el} = \frac{E_{el,gas}}{\rho_{H2,gas}} \tag{6.2}$$

An essential aspect to model for the auxiliary systems is that if the power supply is below 10% of the electrolyser's SEC, the system will not be operational, as the electrolysers have an operating range between 10-100% [91]. The downtime of the electrolysers does not significantly impact their performance, as the startup time from being cold for 24 hours is less than 5 minutes. Therefor production losses as a result of start-up time are assumed to be negligible.

Additionally, the degradation of the electrolysers' performance needs to be considered. After a certain number of production hours, it is assumed the electrolysers experience a reduction in performance, which may be as low as 0.1%/1000 hours [132]. Over the life expectancy of 25 years for the IS, this degradation has a notable impact on production. The performance of the electrolysers can be calculated using Equation 6.3.

$$\eta_{el}(t+1) = \eta_{el}(t) * (1 - \frac{\eta_{deg}}{1000} * B(t))^{OH(t)} \tag{6.3}$$

In which $B(t)$ is a Boolean parameter and is 1 for when the electrolyser is on and 0 if it is off due to low wind speed. OH is the number of operational hours of the electrolyser since installation and is calculated using Equation 6.4.

$$OH = \sum_{t=1}^{LT} B(t) \tag{6.4}$$

The new performance of the electrolyser is then

$$E_{el}(t+1) = E_{el}(t) * \eta_{el}(t+1) \tag{6.5}$$

6.1.3. Operational strategy

The critical aspect of this research is to analyze whether a non-dedicated strategy for an OFWF can enhance its techno-economic performance. Therefor, the operational strategy of the system in this research is considered of vital importance: at which active hours, where the wind farm generates electricity, will the generated electricity be supplied to the grid, and at which hours will it be used to produce H2? This section will seek to answer Subquestion 3: *"At what electricity price per kWh is the production of hydrogen economically more beneficial than feeding electricity to the electricity grid?"*. An important note here is that the primary objective of the system is that it operates as a conventional OFWF. This means that supplying the grid with power is the system's priority, and H2 production will only occur if electricity prices allow it.

PEMEL used in this study have an operating range of 10-100%, like stated in Section 6.1.2. This means that when the power generated by the OFWF is below 10% of the installed capacity of the electrolyser unit, it is not operational. During hours where the wind speeds are so low that generated power is below 10% installed capacity, it is assumed that the generated power will be supplied to the grid, regardless of the price of electricity at that hour.

Switchprice

The crucial factor in this strategy is the price of electricity per hour, as it determines whether power is supplied to either a). the electrolysers or b). the grid. The price of electricity is given in ¥/kWh. However, the modeling of H2 production, as described in the previous sections, is given in kWh/kg H2. Therefor, H2 must be expressed in kWh to determine the price at which it is more beneficial to produce H2 than to feed it to the grid. This price is defined as the so-called switchprice.

A kg of pure H2 has a gravitational energy density of 33.32 kWh/kg, its LHV [79]. It takes however more energy to produce H2 as shown in Section 6.1.1 and Section 6.1.2. Therefor the energy density of a kg of produced H2 must be equal to the amount of power that is used to produce it in order compare it with the initial purpose of the generated power and supply the grid.

Finally, the price for 1 kg of H2 is needed. Currently, in 2024, this price is $8/kg green H2 in Japan. This price is expected to decrease over time because the market for H2 will grow. It is expected that by 2030 the price of green H2 will be $5-3/kg and by 2050 $3-2/kg [61, 112]. Besides the expected gradual decrease in green H2 price over time, this price will also fluctuate as a result of supply and demand at certain periods of time. Since this is primarily influenced by external factor en therefor impossible to accurately estimate, much like power prices, this research assumes a stable H2 price each year based on literature. The switchprice during each year of the lifetime of the system can be calculated using Equation 6.6.

$$\chi_{switch}(t) = \frac{\chi_{H2}(t)}{E_{total,prod}} \tag{6.6}$$

Where $\chi_{switch}(t)$ is the switchprice at time t, $\chi_{H2}(t)$ is the market price of 1 kg green H2 at time t and $E_{total,prod}$ is the total required energy in kWh to produce 1 kg of H2.

A schematic overview of the operational strategy is shown in Figure 6.2. This research involves an operational strategy for the IS which is only dependent on the power generation by the wind farm and the prevailing switchprice.

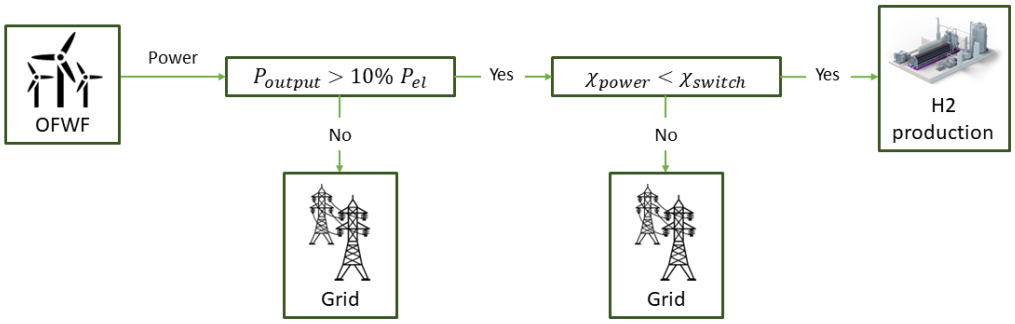

Figure 6.2: Schematic overview of the decisions that lead to the operational strategy of the integrated system.

JEPX

The resulting switchprice for the first operational year, based on a hydrogen price of ¥1282/kg (±€8/kg) [64], is ¥23.76 (±€0.16), assuming a currency ratio Yen to Euro of 150 to 1. Subsection 6.1.3 states that the price of H2 will vary over the operational lifetime of the system. As a result, so will the switchprice. When the switchprices for each operational year are implemented in the power price dataset and the estimations on future power prices (3.1, 3.2, the operational hours of the IS will become clear.

6.2. H2 carrier configuration

The modeling of different H2 carrier configurations in this research is mainly based on the Specific Energy Consumption (SEC). This is the energy required by the installed installation to produce 1 kg of the carrier. Each subsection will elaborate on how that is translated in the production of the H2 carrier in question.

The motive behind conversion is often related to transport convenience or the application of the product. Produced H2 gas has a very low Volumetric Energy Density (VED) [10]. Conversion is often done to increase the VED so larger amounts of energy can be transported at one time. This requires more energy to be put into the product since conversion requires additional power or another substance to form a H2 carrier. Besides the increased total energy consumption, it also requires additional investment for machinery or other installations.

Since the switchprice is based on the energy content of a kg of H2 and not he volume of the carrier, the expected KPIs will therefor be negative with respect to no conversion. The efficiency of each of the analysed configurations is calculated by dividing the energy content of a kg of final product, e.g. the LHV, by the required energy to form it. This is expressed in Equation 6.7. The final efficiencies and SEC of each of the configurations is shown in Table 6.1.

$$\eta_{H2,config} = \frac{LHV_{H2,config}}{E_{H2,config}} \tag{6.7}$$

CGH2

Compressed gas requires relatively low additional energy. The compression of H2 gas is done using a pressure pump with a SEC of around 10% the energy to produce H2 from electrolysis [105]. Since this amounts to approximately 50 kWh/kg 6.1.2, the SEC of the pressure pump is assumed to be 5 kWh/kg of H2 gas. This results in a

combined SEC of 58.17 kWh/kg CGH2, making the theoretical efficiency of configuration 57.38%. This H2 gas is compressed to 700 bar.

As stated in section 6.2.1, in the CGH2 configuration the final product is assumed to be stored for two days whereafter it is assumed the steel industry of Japan will acquire the product. This requires additional storage infrastructure, in this case high pressure tanks, suitable to store the maximum produced CGH2 over a two day period over the system's lifetime. The model will analyse each of the hourly production rates of the facility over its lifetime and the 48 consecutive hours with the highest total production of CGH2 will be the threshold value for storage capacity.

Such high pressure tanks come with additional cost which are based on the storage capacity of the tanks. For high pressure tanks capable of withstanding 700 bar, additional investment amount to approximately $400/kg H2 (€375/kg H2) [47, 107].

LH2

Liquefaction can be difficult to accurately model [10, 133, 15, 11, 40]. Its SEC differs between the used liquefaction process and the size of the liquefaction unit. Like stated in Section 2.2.4, the SEC of a liquefaction plant reduces when the production increases. There is no governing equation to determine the energy consumption of the liquefaction units. Theoretical minimum energy requirements for liquefaction of 1 kg of H2 is 2.88 kWh, but because of large energy losses this has not been achieved in practice. Today for large quantities it is in the range of 8-12 kWh/kg of LH2 [40].

In the system the SEC for liquefaction will be modeled based on the SEC of real commercialized liquefaction plants described by Zhang et al. [133]. If production does not come close to commercialized liquefaction plants, the SEC will be iterated within a the range 10-20 kWh/kg to match the closest resemblance with an existing plant like stated by Zhang et al. [133]. As production is expected to be relatively low compared to the plants considered by Zhang et al., the SEC of liquefaction is assumed to be 20 kWh/kg LH2. Therefor efficiency of the LH2 will be 45.6%.

However, LH2 might be the final product but this will not be the final form of energy that is delivered to the consumer since the LH2 will be stored and transformed back in to electricity. This configuration uses a fuel cell to transform the regasified H2 back to electricity which is assumed to have an efficiency of around 60% [117]. The total efficiency of this configuration for that reason is 27.36%.

The storage infrastructure for this configuration must be able to store the maximum weekly produced LH2 over the lifetime of the system. Again the model will analyse each of the hourly production rates of the facility over its lifetime, only now the 168 consecutive hours with the highest LH2 production will be the threshold value for storage capacity.

The additional investment of the LH2 storage infrastructure is based on the volume of the storage tank that is required. The investment of such a cryogenic storage tank, able to handle temperatures of -253 C°, is estimated at around $2250/m^3 (€2113/m^3) [4]. The addition of an alkaline fuel cell also brings additional investment which is estimated at €370/kW installed power [37]. The installed fuel cell capacity is assumed equal to the electrolyser capacity.

Ammonia

Ammonia production is less energy consuming compared to liquefaction [87, 126, 110]. The Haber-Bosch process requires around 8-17% of the total required power for H2 electrolysis [110]. For simplicity the assumed SEC of ammonia is set to 10% of the SEC of the PEM electrolysers and is therefor 5 kWh/kg H2. This includes energy required for the air separation unit. This process requires thus 58.17 kWh to form 5.06 kg of NH3, taking in to account the efficiency of the HB process of 90%. The LHV of NH3 is 5.17 kWh/kg. The resulting theoretical efficiency of the configuration amounts to 45.05%.

Besides electricity the Haber-Bosch process also requires nitrogen gas to react with H2 and form NH3. As indicated before, it is assumed in this research that the supply of nitrogen is infinite since this outside the scope of this research. Only the financial aspects of this supply will be considered.

The storage infrastructure required for this configuration is similarly determined with respect to the CGH2 configuration. However, since ammonia storage does not require extreme handling conditions and ammonia storage tanks are widely applied globally, there is a large investment difference. Additional investment cost of the ammonia storage infrastructure is estimated at ±€1/kg NH3 [89].

MCH

MCH production, like ammonia, is also a less energy consumption process since it relies on a chemical reaction between two molecules to form a H2 carrier [45, 6, 116, 69, 113]. It is stated that the electrical energy requirement to form 1 kWh of H2 equivalent it takes 0.011 kWh of electrical energy [113]. As stated in Section 2.2.2, the LHV of 1 kg of H2 is around 33 kWh. This means the model should imply a SEC for MCH forming of 0.363 kWh/kg H2.

The chemical process also requires toluene fluid to react with H2 and form MCH. As described earlier, for simplicity reasons the supply of toluene is assumed to be infinite since this has been excluded from the scope of this research. Only the financial aspects of this supply will be considered. However not all the toluene reacts with the H2 gas to form MCH. The efficiency of the reaction is around 90%. Production of MCH is therefor 10% lower considering its SEC. The toluene that has not reacted with H2 is recirculated into the process.

The efficiency of the formation of MCH amounts to a total of 56.12%, considering a required energy of 53.43 kWh to form 14.62 kg of MCH. However, this is the efficiency of the final product but not the delivered form of energy to the consumer. Decomposition of MCH requires an additional 1.5 kWh/kg MCH with an efficiency of 89%. Combined with the same FC efficiency as the LH2 configuration the total efficiency of the process amounts to 29.2%.

The storage infrastructure required for this configuration is similarly determined with respect to the LH2 configuration. However, since MCH storage does not require extreme handling conditions, there is a large investment difference. Additional investment cost of the MCH storage infrastructure is estimated at €6.4/kg MCH [6]. Besides the storage infrastructure, the configuration also requires additional investment for the MCH decomposition unit and alkaline fuel cell. The first requires an investment of €1372/ (kg MCH/h) [40]. and the latter is already stated in the LH2 configuration.

An overview of the additional expenditure for each of the four considered configurations is shown in figure 6.2

Configuration	**SEC Final Product** [kWh/kg]	**Efficiency** [%]	**SEC Conversion** [kWh/kg]	**Efficiency** [%]	**Total Efficiency** [%]
CGH2	58.07	57.38	-	-	57.38
LH2	73.07	45.6	16.67	60	27.36
NH3	11.48	45.05	-	-	45.05
MCH	3.66	56.12	3.36	61.3	29.2

Table 6.1: SEC for each or the four considered configurations and the corresponding efficiencies.

System	Expense		Value	Unit
Compression [36, 105, 100, 107, 37]	Capital			
		Compression pump	170000	€
		Storage tank	375	€/kg
	Operating			
		O&M	5	% Capital
Liquefaction	Capital			
[10, 133, 15, 11, 40, 4]		Liquefaction unit	36797	€/(kg/h)
		Cryogenic tank	2113	€/m^3
		Fuel cell	370	€/kW
	Operating			
		O&M	4	% Capital/y
Ammonia synthesis [40, 89]	Capital			
		Air separation unit	1435	€/(kg N2/h)
		Synthesis unit	47670	€/(kg H2/h)
		Efficiency	90	%
		Storage tank	1	€/kg
	Operating			
		O&M synthesis unit	4	% Capital/yr
MCH synthesis [40]	Capital			
		MCH synthesis unit	4850	€/(kg/h)
		Storage tank	6.4	€/kg
		MCH decomposition unit	1372	€/(kg/h)
		Fuel cell	370	€/kW
	Operating			
		Toluene cost	0.7	€/kg
		Ratio toluene to H2	4	-
		Efficiency	90	%
		O&M synthesis unit	4	% Capital/yr

Table 6.2: Addditional CAPEX and OPEX estimations of the four considered H2 carrier configurations

6.2.1. Applications

The discussed carrier configurations above have different uses in industry that affect the contribution to the concept of floating wind. Section 6.2 already stated that converting GH2 into a H2 carrier is primarily done to increase the VED or for transport convenience [26]. Fot the produced H2 by the electrolyser, it is not assumed that it can be sold directly to some sort of H2 grid like the proposed Hydrogen Backbone [7]. Therefor each of the four different carrier configuration has their own proposed application in the Japanese industry based on the most local use.

CGH2

The CGH2 is assumed to be sold for the active H2 market price and the transportation cost will be neglected since these are modeled to be for the costumer.

LH2

The produced LH2 will not be sold as a product but is assumed to be stored and re-gasified back to gaseous form and used in fuel cells to produce electricity during hours of high prices. This process comes with additional losses that need to be considered [116]. For simplicity it is assumed that the LH2 can be directly converted to electricity in the same hour as the above-threshold electricity price. As a fuel cell, an alkaline fuel cell with a efficiency of 60% is used to convert the GH2 to electricity [29]. The total produced LH2 of the current week is used and sold as electricity to the grid against the mean of power prices above switchprice of the following week.

NH3

The produced NH3, like CGH2, is assumed to be sold weekly to the fertilisation market against active NH3 prices.

MCH

To convert the MCH back to toluene and GH2, a decomposition unit is required, which has a SEC of 1.5 kWh/kg of MCH. Besides the specific energy consumption, it also has an efficiency of 89%. For this configuration, an alkaline fuel cell is used to convert the gas to power with an efficiency of 60%. The toluene is sold for the same price it was bought [99].

6.2.2. Economic definitions

This research uses various economic definitions that might vary in different industries. This section will elaborate those used definitions to better translate the economic performance of the integrated system.

CAPEX

The total CAPEX of the system is calculated by Equation 6.8.

$$CAPEX_{system} = CAPEX_{OFWF} + CAPEX_{desal} + CAPEX_{el} + CAPEX_{H2,config} \tag{6.8}$$

Where each item represents the capital expenses of respectively the total integrated system, the offshore floating wind farm, the desalination unit, the electrolysers and the additional installations required for the H2 carrier configuration used.

OPEX

OPEX of each system component are based on production rate or percentage of CAPEX. As can be seen from Table 5.1, configuration OPEX is usually expressed in percentage of CAPEX. However, the CAPEX of those installations is again dependent on production. This results in larger OPEX for a higher production of H2. OPEX of the OFWF on the other hand is dependent solely on the installed capacity. Total OPEX is calculated using Equation 6.9.

$$OPEX_{system} = OPEX_{OFWF} + W_{H2}(OPEX_{desal} + OPEX_{el}) + W_{H2/hr}(OPEX_{H2,config}) \tag{6.9}$$

Where each $OPEX$ represents the operational expenditure of respectively the total integrated system, the offshore floating wind farm, the desalination unit, the electrolysers and the additional installations required for the H2 carrier configuration used. The W_{H2} and $W_{H2/hr}$ are the produced H2 in kg and the capacity for H2 production per hour respectively. The OPEX of the desalination and electrolysers is thus dependent on the produced H2 and the OPEX of the carrier configuration is dependent on the production rate of the installation.

Finally, a new term is introduced called the success difference (SD). At hours where H2 is produced, the electricity could also have been sold to the grid for a non-zero price. However, it is assumed that as these hours H2 production is more profitable. The SD is the difference in H2 price and price of electricity at any hour of H2 production and therefor the increased revenue of the system due to H2 production. The hourly SD can be calculated using Equation 6.10.

$$SD(t) = \chi_{H2}(t) * \frac{P_{input}(t)}{E_{total}} - P_{input}(t) * \chi_{grid}(t) \tag{6.10}$$

Where $SD(t)$ is the success difference at any hour t of H2 production, $\chi_{H2}(t)$ the market price of 1 kg of green H2 at hour t, $P_{input}(t)$ is the power input to the H2 production system at hour t, E_{total} is the energy required to produce 1 kg of H2 and $\chi_{grid}(t)$ is the price for 1 kWh of electricity at hour t.

6.3. KPIs

The characteristics of the model discussed in Section 5.2 and the way of modeling in 6.1 are used to assess the TEP of the system. The TEP of the system in this research is expressed in KPIs. This section gives an insight on the different KPIs used in this study, how they are relevant and how they are calculated.

6.3.1. LCOE

The LCOE represents the average cost of electricity over lifetime of a system. It is expressed in a value per unit energy, often €/MWh. These costs include all cost over lifetime of the power system so CAPEX and OPEX. For the proposed integrated system it is calculated using Equation 6.11.

$$LCOE = \frac{CAPEX_{OFWF} + \sum_1^{LT}(OPEX_{OFWF} - R_{H2})}{P_{input,grid}} \tag{6.11}$$

Where R_{H2} is the revenue gained from H2 production and $P_{input,grid}$ the total delivered electricity to the grid.

This is not a conventional method of calculating the LCOE of an energy system. This is because not all generated power is used for the same purpose namely supplying the electricity grid. Since a significant share is used to produce H2 this must be considered calculating the LCOE. The annual revenue gained for H2 production is therefor subtracted from the OPEX in order to achieve a relevant and realistic LCOE.

6.3.2. LCOH

The Levelized Cost Of Hydrogen (LCOH) represents the average cost of 1 kg of H2 over the lifetime of the production system. It is expressed in value per unit weight, often €/kg. These costs include all cost over lifetime of the H2 production system so CAPEX and OPEX. For the proposed integrated system it is calculated using Equation 6.12.

$$LCOH = \frac{(CAPEX_{desal} + CAPEX_{el} + CAPEX_{H2,config}) + \sum_1^{LT}(OPEX_{desal} + OPEX_{el} + OPEX_{H2,config})}{W_{H2}} \tag{6.12}$$

In this equation the revenue from power supply is here not subtracted from the costs since the hydrogen production system is assumed as an addition to an existing WF and the operational strategy of the IS is non-dedicated. For that reason, it is assumed that for the calculation of the LCOH, CAPEX and OPEX of the WF are not taken into account.

6.3.3. Cash Flow

Cash Flow refers to the movement of revenues and expenses of a system over the lifetime. It's a crucial measure of a systems financial health to sustain ongoing operations. A positive overall CF indicates that a system is bringing in more money than it is costing. Conversely, negative CF may signal a failing system economically. CF is calculated using Equation 6.13 where i indicates the year during the lifetime.

$$CF(i) = R(i) - OPEX_{total}(i) \tag{6.13}$$

6.3.4. PBP

The payback period (PBP) is calculated by dividing the initial investment cost by the annual cash inflow generated by the investment. The result is the number of years it will take to recover the initial investment. Its equation is shown below 6.14.

$$PBP = \frac{CAPEX_{total}}{CF(i)} \tag{6.14}$$

6.3.5. NPV

Net Present Value (NPV) is a metric that assesses the profitability of an investment by comparing the present value of expected cash inflows with the present value of expected cash outflows. It takes into account the time value of money, recognizing that revenue received in the future is worth less than revenue received today. The NPV can be calculated using Equation 6.15. Again, like the calculations on NPV for the base case, the discount rate is set to 4%.

$$NPV = \sum_{i=1}^{LT} \frac{CF(i)}{(1+r)^i} - C_{investment} \tag{6.15}$$

A positive NPV indicates that the investment is expected to generate more revenue than costs resulting that it is generally considered a financially sound decision. A negative NPV suggests that the investment may not meet the required rate of return and may not be economically viable. The same assumption is made for the NPV of the IS as the one made in 3.5.

6.4. Capacity Analysis

Bonacina et al. [15] employ a capacity analysis to optimize the model with respect to the scale of the H2 production system. The study reveals that achieving a 100% capacity factor for the electrolysers, wherein the electrolyser capacity matches that of the wind farm, does not necessarily result in optimal system profitability. Notably, the investigation indicates that the most economically advantageous electrolyser capacity lies in the range of 80-90% of the wind farm's capacity. Thus, the study by Bonacina et al. underscores the importance of considering an optimal balance in capacity allocation for electrolysers within the H2 production system to maximize overall profitability.

These observations imply the feasibility of conducting an optimization study to examine the optimal electrolyser capacity factor for an IS. This investigation is particularly interesting in the context of a dynamic operating schedule, where operational hours are dependent not only on wind speed but also electricity prices. The uncertainty surrounding the operational hours of the electrolyser further necessitates this optimization task. The optimization, executed through solver-based techniques in MATLAB, involves the manipulation of parameters influencing a specified objective function. The objective is either the minimization or maximization of a predetermined variable. All parameters affecting this function will then be programmed for different values within certain constraints. These constraints define the boundaries within which the software can give values to parameters.

The range for the electrolyser capacity spans from 50% to 100%, with increments of 10% at each iteration. The reason behind this selection lies in alignment with the strategic goals of Japan, specifically directed towards domestic H2 production in accordance with the Basic Hydrogen Strategy [98]. The chosen range is based on the understanding that a smaller electrolyser capacity, such as 20%, would yield insignificant contributions to the overarching goal, particularly with the relatively modest installed capacity of the wind farm. It is important to note that the remaining properties of the integrated system remain constant, serving as foundational parameters maintaining consistency with the base case scenario.

The capacity analysis indicates that not the entirety of generated power is used for H2 production. Excess power is directed to the grid and traded at the prevailing active power price during the hour of operation. Consequently, even in instances where the electricity price is below the established switchprice, surplus power is channeled to the grid during capacity analysis iterations where the electrolyser capacity is less than 100%. This approach results in operation hours characterized by multiple revenue streams, thereby enhancing the economic viability of the integrated system.

6.5. Scenario Analysis

In order to estimate the future performance of the system, a scenario analysis is performed. This involves four external aspects of the system and analyses various values for these aspects based on future predictions: a). the power prices; b). the H2 price; c). CAPEX/OPEX of the system and d). the CO2 emissions and tax rates. This is done to investigate how they influence the KPIs of the system. The scenario analysis is carried out for four external aspects of the integrated system of which each will be discussed in the subsections below. Besides the considered scenarios, all other parameters as assumed the same as the reference case.

6.5.1. Power Price

The reference case of the model discussed in Section 6.1 considers the dataset of day-ahead market prices for Kyushu region, Japan from April 2022 to April 2023. The effect of the power prices on the TEP of the system is analysed by proposing three scenarios based on previous yearly averages and the expected in- and decrease of respectively negative hours and average power price. Again, it must be stated that these prediction and estimations on prices are not entirely accurate and are thus rough estimations, since power prices are hard to predict as they are influenced by many external factors other than the (primary) source of energy.

The analysis of power prices encompasses three distinct scenarios (*conservative, pessimistic and optimistic scenario*), each based on the average power prices observed over the previous five years. These scenarios are constructed to enclose a spectrum of economic conditions, characterized as conservative, pessimistic, and optimistic

Property	Conservative	Pessimistic	Optimistic
Average price per kWh [28]	€0.06	€0.14	€0.05
Increase $\leq$ 2030 [112, 34]	20%	10%	25%
Increase > 2030 [112, 34]	5%	2%	7%
Decrease average [112, 34]	2%	1%	4%

Table 6.3: Three scenarios for power prices in Euros and the future estimates on in- and decrease rates

Property	Conservative	Pessimistic	Optimistic
Price/kg 2023	€8	€8	€8
Price/kg 2030	€4	€5	€3
Price/kg 2050	€2.50	€3	€2

Table 6.4: Three scenarios for power prices in Euros and the future estimates on in- and decrease rates

datasets.

- The *conservative* dataset aligns with the pricing parameters employed in the reference case, as explicated in Section 6.1. These prices, while reflective of recent trends, exhibit a relatively high average compared to power prices from five years ago.
- The *pessimistic* scenario is the dataset spanning April 2020 to April 2021. This period notably includes the onset of the Russo-Ukrainian war, during which geopolitical tensions contributed to a surge in gas prices. While acknowledging the exceptional nature of this timeframe, it is deemed relevant due to the potential conflict between nations because of resource scarcity, as posited by Mansson et al. [85]. The escalation of energy prices in countries heavily reliant on fossil fuel imports, such as Japan, is considered a plausible option in future scenarios.
- Conversely, the *optimistic* case is characterized by the dataset covering April 2018 to April 2019. This interval records the lowest average power price per kWh at ¥7.93 ($\pm$€0.05). This selection provides a counterpoint to the conservative and pessimistic scenarios, offering a representation of more favorable economic conditions.

In addition to the power price datasets, the increase and reduction of negative hours, along with variations in average power prices, are modeled for both pessimistic and optimistic assumptions. The pessimistic scenario involves an increase in negative hours by 10% until 2030 and a subsequent 2% increase thereafter, coupled with a 1% reduction in average power prices. Conversely, the optimistic scenario anticipates a 25% rise in negative hours until 2030, followed by a 7% increase thereafter, accompanied by a 4% decline in average power prices. The discussed power price scenarios are shown in Table 6.3. All these scenarios and their increase- and decrease rate are visualized in Figures B.11 and B.12.

6.5.2. H2 Price

As stated in 6.1.3 the price of H2 is expected to be fluctuating over the entire lifetime of the system. The price of a kg of green H2 in the future is unsure since it is largely dependent on the development and deployment of green H2 production systems and supply-demand mismatch [56, 112]. Although deployment is expected to increase significantly, the growth might not directly trigger green H2 prices to drop. Since demand of H2 can also significantly increase in the operating years of the system, the supply-demand curve may not look like expected.

For the H2 price the three scenarios mentioned earlier are analysed. All scenarios assume the current price of €8/kg H2 at the start of the analysis [64]. The first scenario is the conservative scenarios which follows the expected decrease in price for green H2 that is used in the reference case. The pessimistic scenario wields a H2 sell price of €5/kg by 2030 and €3/kg by 2050. The optimistic scenario wields a H2 sell price of €3/kg by 2030 and €2/kg by 2050 [61, 112].

6.5.3. CAPEX/OPEX

The goal of this research is to improve the concept of floating wind energy and therefor to stimulate the deployment of other integrated systems. Therefor a CAPEX/OPEX scenario is analysed for the theoretical construction of the integrated system in 2030. In this scenario, it is assumed that the model analyses the reference case based on

KPIs but with expected CAPEX and OPEX for 2030.

For this analysis the values taken from Table 3.3 and 5.1 are considered to be conservative. The expected percentage of reduction is taken and used to estimate the CAPEX/OPEX. The result used in this analysis are shown in Table 6.5. Pessimistic scenario will be when no decrease in CAPEX or OPEX occurs. This scenario will be considered equal to the reference case.

Component	Expense	Conservative	Optimistic
Wind Farm [38, 40]	CAPEX	-8%	-35%
	OPEX	-8%	-35%
Desalination [22, 40]	CAPEX	-16%	-30%
	OPEX	0	0
Electrolyser [56, 41, 40]	CAPEX	-45%	-80%
	OPEX	-35%	-35%

Table 6.5: Two scenarios for CAPEX and OPEX and the future estimates on in- and decrease rates

6.5.4. CO2 tax

The final scenario analysis centers on the influence of governmental policies related to CO2 emissions and the associated tax rates. Currently, Japan is subject to a *Total Carbon Content Method* (TCCM) tax rate of ¥289 (±€1.93) per ton of CO2 [104]. Considering Japan's ambitious target to cut CO2 emissions by nearly 50%, there is a strong expectancy that these CO2 emission taxes will increase significantly. This strategic approach aims to trigger corporations to turn towards sustainable energy solutions.

It is noteworthy that the integrated system, by design, operates without emitting CO2. Consequently, one might wonder for the reason behind conducting an analysis related to CO2 taxes. However, the significance of this analysis lies in the anticipation of a substantial rise in CO2 taxes. Such an elevation in tax rates is expected to come with heightened interest and investment in solutions that are free from CO2 emissions, aligning with the overarching objectives of environmental sustainability and emissions reduction.

In evaluating the performance of the integrated system within this analysis, a so-called *Reduced Emissions Bonus* (REB) is employed. The REB represents the cost savings associated with avoiding CO2 taxes with respect to energy generation through fossil fuels. In this specific analysis, natural gas is selected as the representative fossil fuel due to its relatively low emission rate and it is anticipated to have a significant share in Japan's power generation mix even in the future [1].

The determination of the REB involves the assessment between the energy generated by the integrated system and the emissions corresponding to an equivalent amount of energy produced by a natural gas turbine for electricity generation. The financial equivalent of the CO2 tax that a conventional natural gas turbine would have cost for the emissions is then incorporated into the revenue of the integrated system as the REB. In essence, the REB is the economic benefit derived from the integrated system's capacity to avoid CO2 taxes that would otherwise be deducted from revenue for conventional natural gas-based power generation.

The CO2 tax is modeled in a conservative and an optimistic way. The conservative expectancy of the TCCM tax rate by 2030 is approximately ¥11315/t CO2 (±€75.43/t CO2) [104, 43]. For the optimistic analysis a TCCM tax rate of ¥22630/t CO2 (±€150.87/t CO2) is used to calculate the REB [104, 43].

6.6. Sensitivity Analysis

Finally, a sensitivity analysis is performed. Conducting a sensitivity analysis can be valuable for a research for several reasons:

- It helps to understand the impact of varying input parameters on the model results, revealing key factors of influence.
- Sensitivity analysis also aids in model validation, ensuring accuracy and alignment with observations.
- Additionally, it prioritizes data collection and model refinement.

The sensitivity analysis is conducted with two variations. First, a selection of parameters is done. The selected parameters are chosen because of their expected influence on performance of the model. After this the values of

the parameters will be altered and the change in KPIs will be analysed.

The first variation is the percentage analysis where the parameters are each either increased or decreased by 10% or, if the specific parameter has can not be in- or decreased simply by 10%, then characteristics of the parameter 1 tier up of down will be used. for example the voltage in the inter-araay cable. cables utilizing a voltage of 72600 doe not exist. Therefor the parameter change for the voltage has a lower bound of 33000 V and a higher bound of 132000 V. Subbsequently, the absolute change in KPIs is analysed.

The second variation is the percentage deviation. In this analysis the percentage change of KPIs will be analysed. This analysis analyses how the parameter deviation changes the evolution KPIs by percentage with respect to the evolution change of KPIs in the reference case. For example, if the NPV goes from -€50 to €50 in the reference case and by a certain parameter change from -€100 to €100, the percentage change will be +100%.

A parameter of special interest in this analysis is the OFWF capacity. This parameter can not be generally increased or decreased by a certain percentage but rather by the number of wind turbines or a different type of wind turbine with a larger power output. In this analysis the OFWF capacity will thus not be scaled by a percentage but the parameters *number of wind turbines* and *rated power* will be deviated.

The resulting parameters and their deviations are shown in Table 6.6

Component	Parameter	Description	Lower bound	Higher bound	Unit
Wind Farm	$n_{turbines}$	Number of WTs	4	16	-
	P_{rated}	Rated power WT	2.1	8	MW
	$P_{windfarm}$	Wind farm capacity	$n_{turbines,low}$ $P_{rated,low}$	$n_{turbines,high}$ $P_{rated,high}$	MW
	v_{wind}	Wind speed	-10%	+10%	m/s
	v_{cut-in}	Cut-in wind speed	3	5	m/s
	v_{rated}	Rated wind speed	10	15	m/s
	$v_{cut-out}$	Cut-out wind speed	20	30	m/s
Transmission	V	Voltage	33000	132000	V
	Ω_{cable}	Ohmic resistance	0.15	0.35	Ω
Desalination	E_{desal}	Energy consumption desalination	40	60	Wh/kg
Electrolyser	E_{el}	Energy consumption electrolyser	40	60	kWh/kg
	P_{el}	Operating power electrolyser	5%	15%	MW
JPEX	p_{grid}	Electricity prices	-10%	+10%	€
Economics	$CAPEX_{total}$	Integrated system CAPEX	-10%	+10%	€
	$OPEX_{total}$	Integrated system OPEX	-10%	+10%	€/year
	r	Discount rate	3	7	-

Table 6.6: Parameter variation for sensitivity analysis

6.7. Assumptions

All the assumptions made in the model for the integrated system are summarized in Table 6.7. Note that the assumptions for the base case, discussed in Section 3.7, still hold.

Category	Assumption
System set-up	Since it is anticipated that having an active dynamic operational schedule yields the most profitable results, a non- dedicated strategy is adopted. Since additional offshore operations come with elevated cost compared to onshore operations, the non-dedicated strategy means there is a grid connection anyway and the goal of thisresearch is to enhance the TEP of OFWE, a decentralized system orientation is adopted.
Desalination	Since the system should be able to cope with maximum production for 24 hours, the SEC of the desalination unit is based on the maximum water intake for 24 hours.
Electrolyser	The characteristics of a NEL PEM electrolyser are used in the model. At least 10% of the installed electrolyser capacity must be supplied in order for the system to be operational. Since degradation of stacks is lower because of a non-dedicated strategy and the intermittency of power supply as a result of wind speed volatility, it is assumed that electrolyser stack do not need to be replaced during the lifetime of the system. Since the start-up time of PEMEL is so fast, it is assumed that the electrolysers start production of hydrogen immediately when the generated power is allocated to the H2 production system. This also means that no storage of power is required to keep the electrolysers within operation range.
Configurations	Compressed gaseous hydrogen is used as a reference case for the model. All analyses except H2 carrier analyses are conducted using this configuration. After production, it is assumed that CGH2 and NH3 will directly be sold to the consumer. LH2 and MCH will be stored for a week and than converted back the electricity and sold to the highest power price that week. The supply of nitrogen and toluene is assumed to be infinite.
Operational strategy	The operational strategy of the system is dependent only on the hourly generated power and the switchprice. Since the electrolyser operating range is between 10-100%, it is assumed that below 10% power generation this power is supplied to the grid. Switchprice is assumed to be the price where it is either more profitable to supply power to the grid or produce hydrogen. This price is dependent on the prevailing market price for H2 and the requried energy to produce the preferred H2 carrier per kg. Currency ratio Yen to Euro is assumed to be constant over lifetime and 150 to 1.
Technical	While it is acknowledged that the integration of a H2 production system into a OFWE system poses several technical challenges, the primary goal of this research is to examine if H2 production can enhance the techno-economic=feasibility of OFWE systems, as most the technical systems used have been proven on technical feasibility as they are applied in commercial industry.
Economics	The success difference is the increased revenue of the system compared to conventional OFWE operations. The LCOE is calculated by subtracting the revenue made by H2 production from the OPEX of the OFWF since not all generated power from the wind farm is used to provide the grid. Calculation of the LCOH does not include expenses related to the OFWF since the H2 production system is considered an addition to the system and its strategy is non-dedicated. Discount rate used in calculations regarding CAPEX, OPEX and NPV is based on found literature and is set equal to 4%.
Analyses	Scenario analyses assume a conservative, optimistic and pessimistic scenario for external influences outside the power of design.

Table 6.7: Assumptions for the Goto City Integrated System

7

Results & Discussion

This chapter encompasses a comprehensive discussion of the outcomes derived from the analysis of reference case and its various specialized assessments. The primary objective of this chapter is to provide the necessary information for addressing the research questions in a substantiated manner. Subsequent sections provide detailed insights into distinct facets of the analysis.

First, verification and validation of the model will be done in a similar manner as per Section 3.8. Section 7.2 elaborates on the results from the model of the Goto City Integrated System. It gives a clear insight on output of the OFWF and how that energy is used at each hour of operation. It will analyse the TEP of the system based on the set KPIs. In Section 7.3 the influence of the H2 carrier configuration on the performance on the system is stated. Section 7.4 investigates the varying installed capacity of the electrolysers on the KPIs. Furthermore, the sensitivity analysis in Section 7.6 shows the influence of the set parameters from Table 6.6 on the results of the model. The results of the scenario analysis are discussed in Section 7.5. Finally, with all the results gathered, the conditions under which H2 production improves the concept of OFWE are discussed.

7.1. Verification and Validation

Verification of the Goto City IS model involves ensuring that critical indicators align with expected outcomes.

The first indicator relates to hydrogen production, specifically verifying the characteristic of the PEMEL unit. The electrolyser is characterized by the fact that operation ceases when power input falls below 10% of its capacity. Figure 7.1 demonstrates that the model reflects this behavior. During hours when power input exceeds 10% capacity, the system resorts to H2 production in the expected quantities. However, during the 9th hour, where power input drops below 10%, the model correctly shows no hydrogen production, thereby verifying the functionality of the hydrogen production process.

The second indicator focuses on the accurate allocation of generated electricity to either the power grid or the H2 production system based on the switchprice. Figure 7.2 illustrates that the model correctly responds to spot-market prices for electricity. When the market price surpasses the switchprice threshold, the generated electricity is allocated to the grid; otherwise, H2 is produced and sold to consumers.

Validation of the Goto City IS, like the base case model, proves challenging due to the absence of real-world implementations and comparisons with similar systems. Since the concept of an integrated system is not yet widely deployed globally, comparing the model with existing systems is not possible. Consequently, validation is based on comparing critical indicators such as the LCOH and H2 production patterns in relation to operational hours with relevant research findings.

LCOH comparison is difficult due to variations in research methodologies and system configurations. In order to validate the LCOH of the model, the Goto City IS is modeled as a dedicated system, resulting in a LCOH of €6.41/kg. This aligns reasonably well with findings from Bonacina et al., who estimate a LCOH for a dedicated offshore floating wind-to-hydrogen system in the Mediterranean Sea in the range of €5-7/kg [15]. Note that this research considers a LH2 configuration for ship refuelling, lowering the efficiency of H2 production process. In

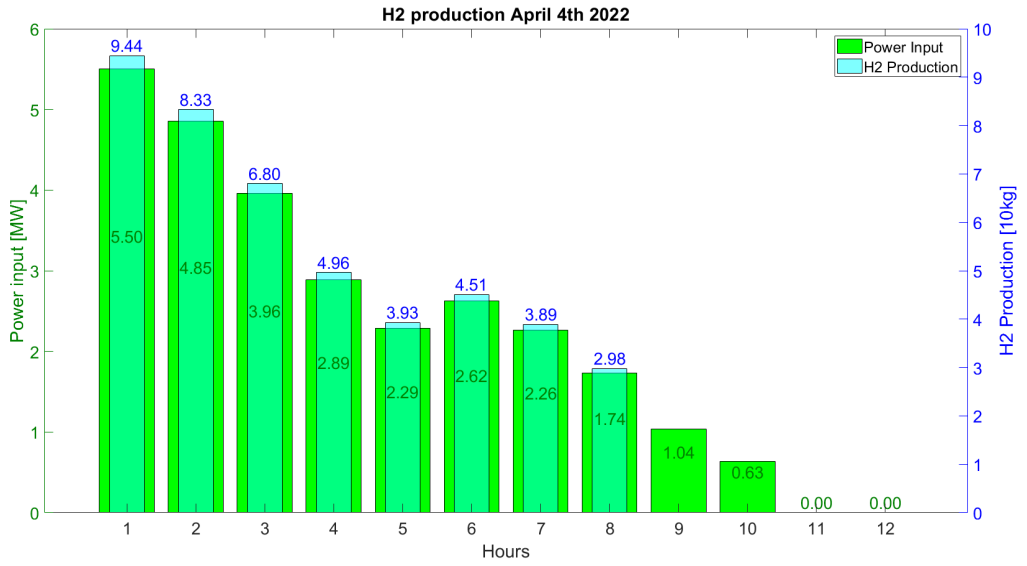

Figure 7.1: H2 production of the Goto City IS over a 12 hour period on the 4th of April in the first production year.

spite of that, the modeled wind farm considered by Bonacina et al. has a capacity of 150 MW which far exceeds that of the farm modeled in this research. Higher production rates might result in a relatively lower LCOH even with lower efficiency.

Additionally, Giampieri et al. provide a comparable LCOH of £8.97/kg for a similar orientation but also with a 150 MW offshore wind farm configuration [40]. The LCOH range in their study, from £4.87/kg (€5.68/kg) to £18.88/kg (€22.01/kg), covers various optimistic and pessimistic scenarios.

Finally, Calado et al. [21] also provides a range of LCOH for hydrogen production from different energy sources obtained from literature review. These ranges are dependent on the installed capacity of the energy sources and the energy source itself. For PEMEL with offshore wind as energy source, the LCOH ranges between €3.77-€11.75/kg H2. Again, the resulting LCOH for a dedicated Goto City IS falls within this range.

The calculated LCOH in this research aligns with these literature findings, suggesting that modeling of the cost and production of H2 by the Goto City IS model shows signs of accuracy compared to the resulting range of LCOH from studied literature.

However, it needs to be stated that no definitive validation of the model can be conducted as real-life figures from the Goto City IS or other similar integrated offshore floating wind-to-hydrogen systems is not available yet.

7.2. Reference Case

The incorporation of a H2 production system into the OFWF yields an additional revenue stream. This addition, however, is accompanied by an increase in overall system expenses, leading to an alteration in the CAPEX and OPEX. Section 7.2.1 provides an elaboration of the outcomes from the operational scheme of this integrated system. The TEP analysis, indicated by KPIs, is explained in Section 7.2.2. Notably, the CGH2 carrier configuration is chosen as the reference case due to its minimal procedural steps and necessary additional installations for the acquirement of the desired H2 product.

7.2.1. Operational Hours

The operational hours of the integrated system for April 2022 to April 2023 are shown in Figure 7.3. Each dot in the graph indicates the hourly power price from the first year of operation in ¥. The red line in the graph represents the set switchprice at ¥23.76/kWh (±€0.16/kWh) as calculated in Section 6.1.3. Blue dots indicate the hours where power prices are below the switchprice and the integrated system is producing H2. Green dots indicate hours where the generated power is supplied to the grid.

For the reference case, as stated in Section 6.5.2, the market price of H2 will follow the expected trajectory of

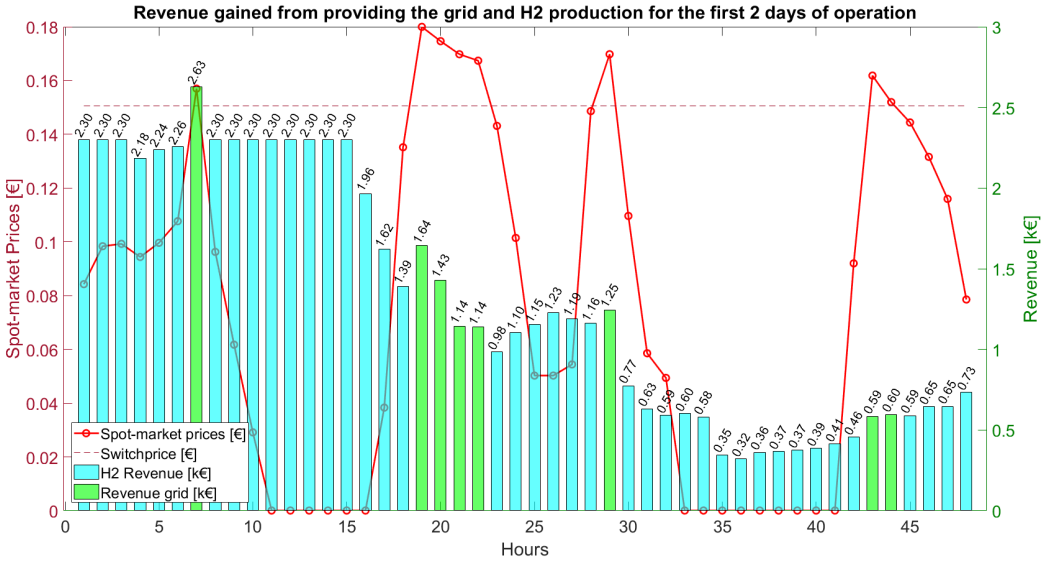

Figure 7.2: Revenue of either H2 production or providing the grid in the first 2 days of operation of the Goto City IS based on the switchprice at the operational hour.

price decrease. This gradually reduced price of H2 results in a reduced switchprice as this is dependent on the H2 market price. The switchprice over the operational lifetime of the IS is again indicated in the graph with the red line. Decreasing switchprice results in an increase in operational hours in EM, visible by a larger share of green dots in the graph. The graph representing the future operational hours is shown in Figure 7.4.

7.2.2. KPI Results

The operational schedule described in the previous subsection serves as the initial indicator of the impact of integrating H2 production into OFWE on the TEP of the system. It shows that the system predominantly operates in HM in the first operational years for over two thirds of the hours, signifying a higher revenue yield compared to the conventional EM. As a reference case the CGH2 configurations is chosen. In later operational years of the system, this predominance in operational hours shifts to proving the grid as the market price of H2 reduces.

The first assessments of improvement show promising trends. Examination of Figure 7.5 reveals that the revenue derived from the integrated system surpasses that of the conventional OFWF and is increased by around 25%. Additionally, Figure 7.6a also shows that operating and maintenance cost deviate little from that of the Goto City WF, indicating that the OPEX of the OFWF substantiate the largest share in OPEX of the IS. For this reason, the increased revenue from H2 production outweigh the increased operating cost causing a elevated cashflow for the system. This increase in revenue translates to a substantially increased cashflow by around 35%.

Of particular interest is the graph in Figure 7.6b, which illustrates a marked increase in the NPV of the project at the end of the operational lifespan, with a turning point at approximately the 17th operational year. This turning point is visualized in the yearly NPV development of the system, illustrated in Figure B.4. The NPV of the integrated system over its operational lifetime is increased by €7.8 million. The lower initial point of the integrated system's NPV (depicted by the plus-sign), results from the additional investments incurred in comparison to the conventional OFWF. The turning point at year 17 signifies that the incorporation of H2 production into a conventional OFWF could enhance the TEP of the concept after 17 years under the prevailing conditions. Additionally, and even more noteworthy, the NPV of the integrated system reaches positive values, indicating that revenue surpasses expenses of the system, rendering the system economically viable. The addition of a H2 production system to the Goto City WF would make the combined system techno-economically feasible under the set conditions. A comparison between the KPIs of the WF and IS configuration is indicated in table 7.1.

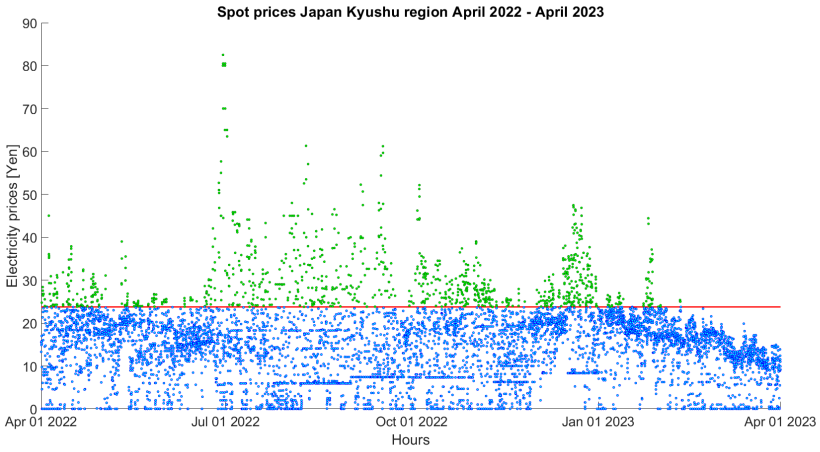

Figure 7.3: Operational hours of the integrated system from April 2022 to April 2023 with a switchprice of ¥23.76/kWh (±€0.16/kWh, Red line). Dot below the line (Blue) indicate hours of H2 production. Dots above the line (Green) indicate hours of grid delivery

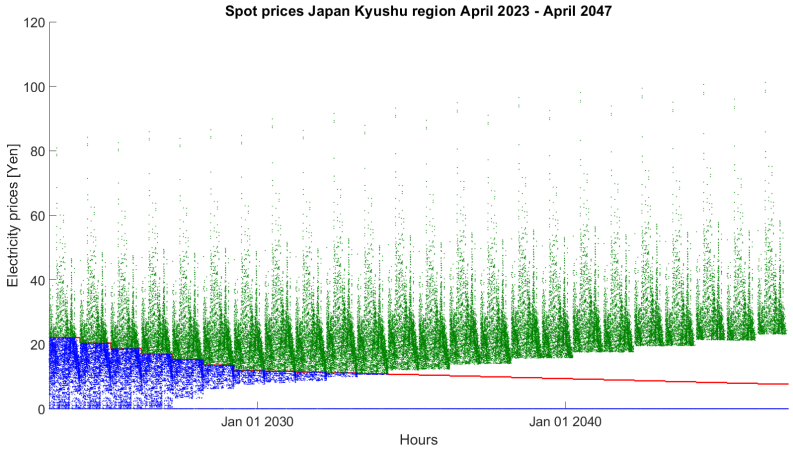

Figure 7.4: Operational hours of the integrated system during its lifetime with a varying switchprice(Red line). Dot below the line (Blue) indicate hours of H2 production. Dots above the line (Green) indicate hours of grid delivery

Figure 7.5: Revenue stream over total lifetime of the integrated system compared to conventional OFWF

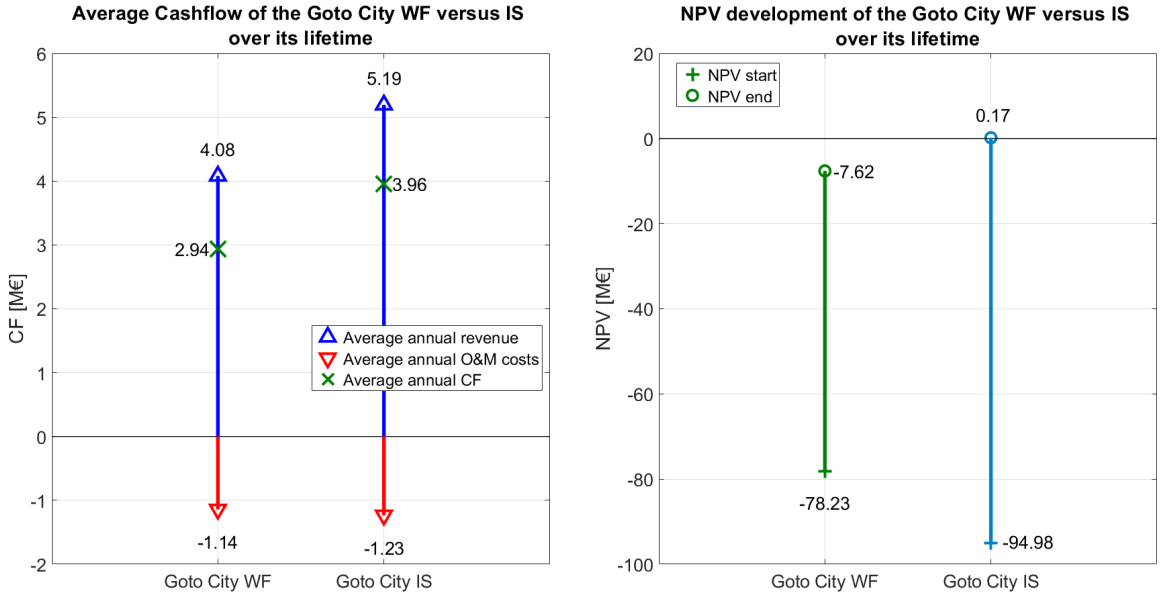

(a) Cashflow

(b) NPV

Figure 7.6: Average CF (a) and NPV development (b) of the Goto City Wind Farm versus the Integrated System over its operational lifetime.

	Goto City WF	Goto City IS	Unit
LCOE	88.7	53.3	€/MWh
LCOH	-	1.59	€/kg
Total Revenue	102.0M	129.8M	€
Average CF	+2.94M	+3.96M	€
PBP	27.6	24.5	years
Final NPV	-7.62M	+0.17M	€

Table 7.1: KPIs for both the Goto City WF and the Goto City IS

7.3. Configuration Analysis

The decision on what to do with the produced hydrogen and therefor which H2 carrier configuration was most beneficial for enhancing the OFWE concept, proved to be of vital importance in determining the TEP of the system. Section 6.2 introduced the use of each hydrogen carrier configuration after production from electrolysis and the arguments behind these uses.

Naturally, each of these different configurations were characterized by different KPI with respect to the reference case of CGH2. The main contributor in the deviation of results were the OPEX of each configuration. Increased OPEX for some of the configurations was due to the number of steps required before the desired form of energy was delivered. Increasing the number of steps and processes of a system subsequently leads to higher losses making the system more inefficient with respect to the reference case.

The primary objective of this subsection is to address the Subquestion 2: *"What configurations of H2 carriers exist and how do they influence the case of adding a H2 production system to offshore floating wind?"*. Visualization of the increased OPEX for some configurations is shown in Figures 7.7 and 7.8.

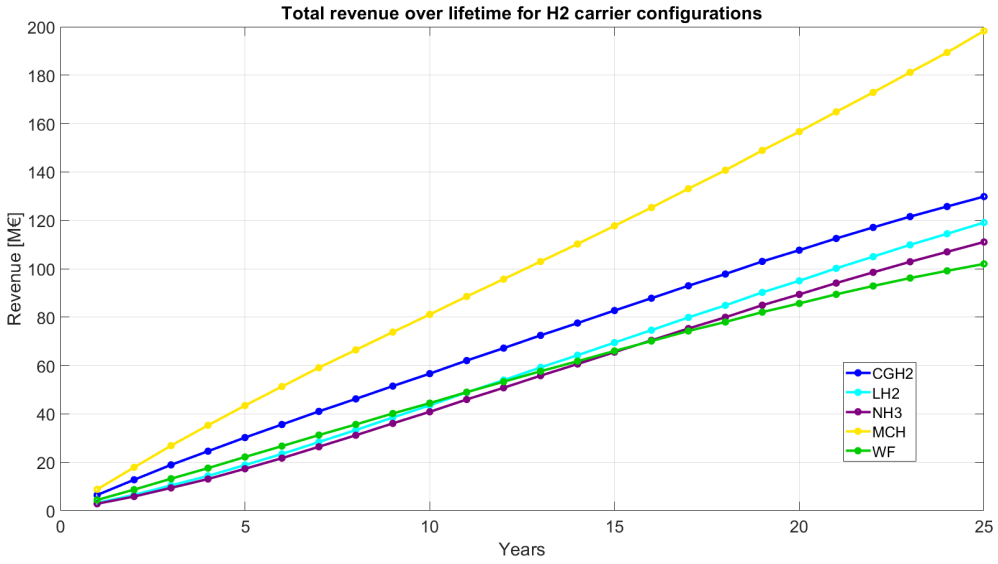

Figure 7.7: Revenue stream for different hydrogen carrier configurations.

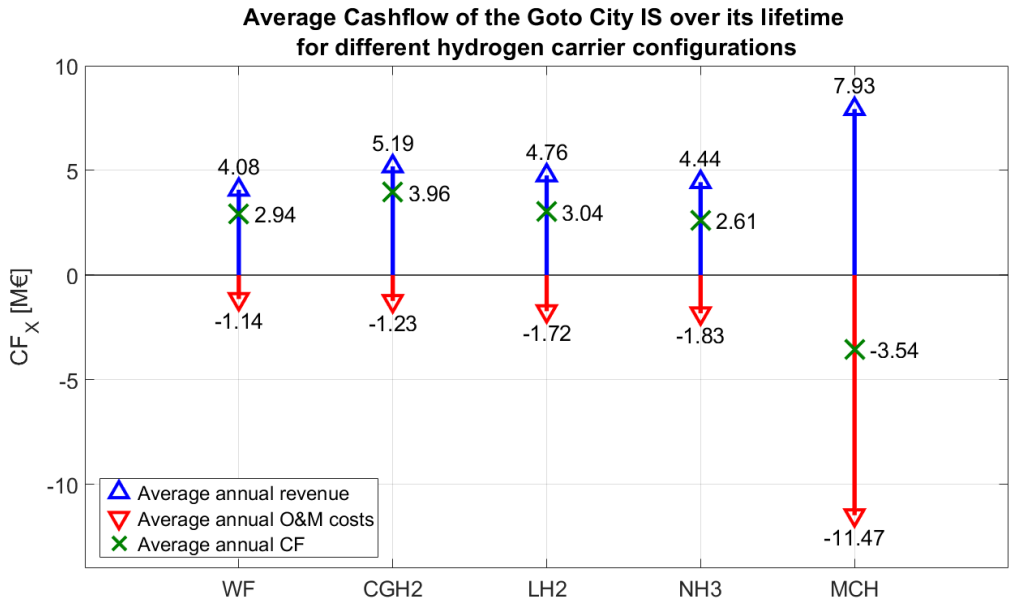

Figure 7.8: Cashflow for different hydrogen carrier configurations.

Revenue differences are predominantly due to the increased losses of the system configurations as indicated above. LH2 for example, has an added liquefaction and re-gasification process, leading to a lower system efficiency compared to CGH2. Added revenue gained from providing the grid with electricity obtained from stored LH2 is not so different from the conventional OFWF, indicating that the revenue stream in this configuration is dominated by revenue from supplying the grid.

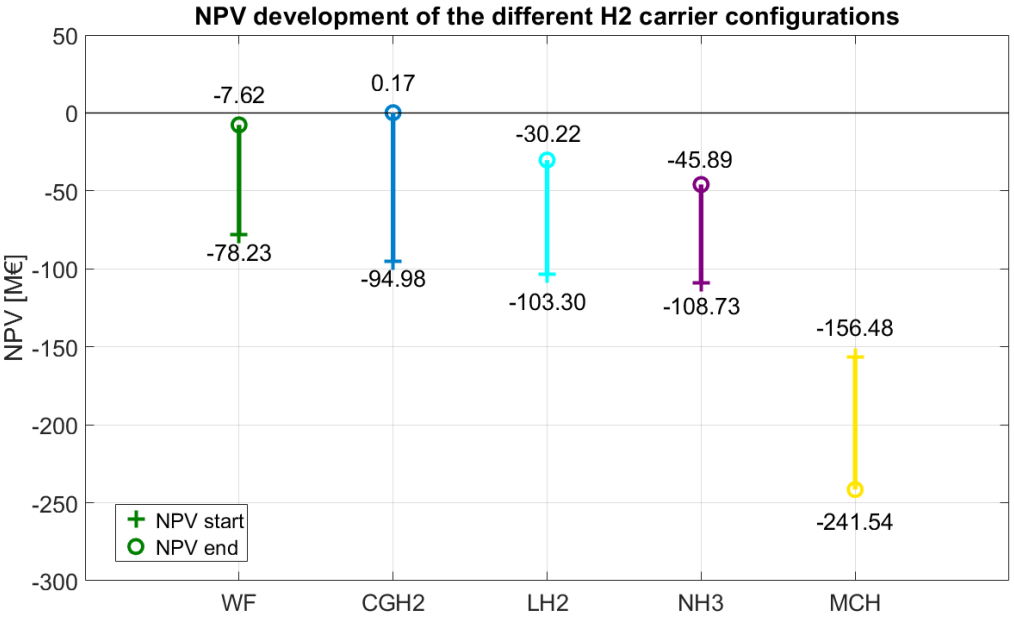

Figure 7.9: NPV for different hydrogen carrier configurations.

Contrary to LH2, the MCH configuration is a much more efficient system, characterized by a revenue stream significantly higher than that of LH2. However, the OPEX results in a negative cashflow for the MCH configuration. NH3 and LH2 configurations do have a positive CF but does not differ much from the Wind Farm configuration.

For LH2, the reason is that revenue is dominated by grid supply and higher OPEX. For NH3, since the industry already exists and the sell price for a kg of NH3 is relatively low, its CF is lower compared to that of the reference case.

The H2 carrier configuration that emerges as the best configuration from the simulations in term of system value increase is the CGH2 configuration. This is therefor the configurations that is advised for the Goto City WF to adopt when it would convert to an integrated system. Not surprisingly, that the resulting NPV of each of the configurations is proportionally lower than the reference and the base case, leading to the conclusion that CGH2 is the preferred configuration for an integrated system if the goal is to increase the feasibility of OFWE. Of course, when different uses for the produced hydrogen are envisioned, other hydrogen carrier configurations from an integrated system may be preferred.

7.4. Capacity Analysis

In this section, an investigation into the installed capacity of the H2 production system within the integrated system is conducted. This investigation focuses on the impact of installed electrolyser capacity on the set KPIs. The objective is to provide elaboration upon the Subquestion 4: *"What elements within the power of design of an integrated system are variable and can be altered to enhance the system?"*. The outcomes of the capacity analysis are depicted through Figures 7.10, 7.11, and 7.12.

Figure 7.10 demonstrates that a reduction in the installed H2 production capacity corresponds to a decrease in annual revenue. This observation aligns logically with the operational dynamics, as a lower installed capacity limits the production of H2 during HM. Consequently, the integrated system generates less revenue from H2 production in comparison to the revenue generated through power supply to the grid. Conversely, higher installed capacities enable increased H2 production during these hours, thereby increase the overall revenue potential.

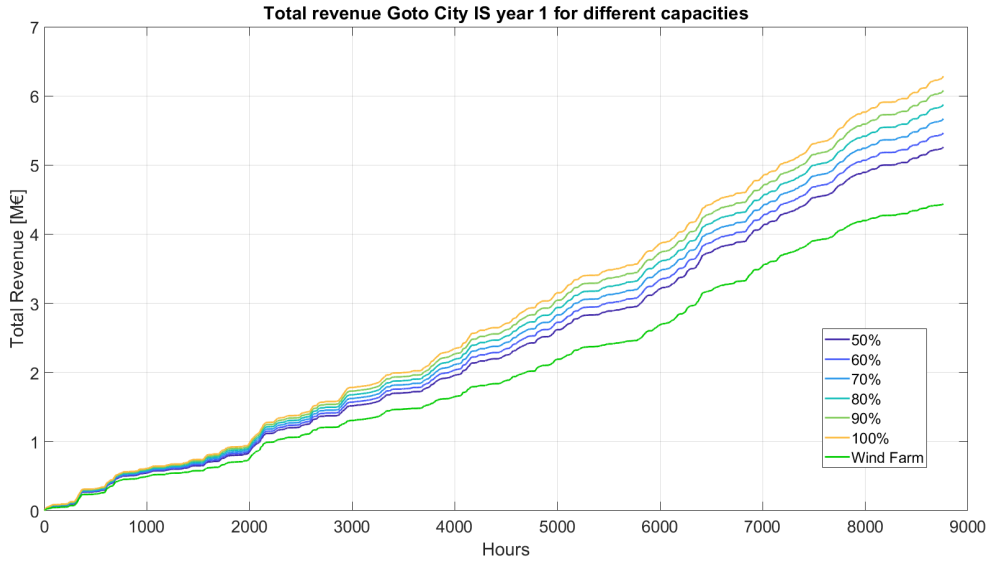

Figure 7.10: Revenue in the first operational year for different installed H2 production capacities

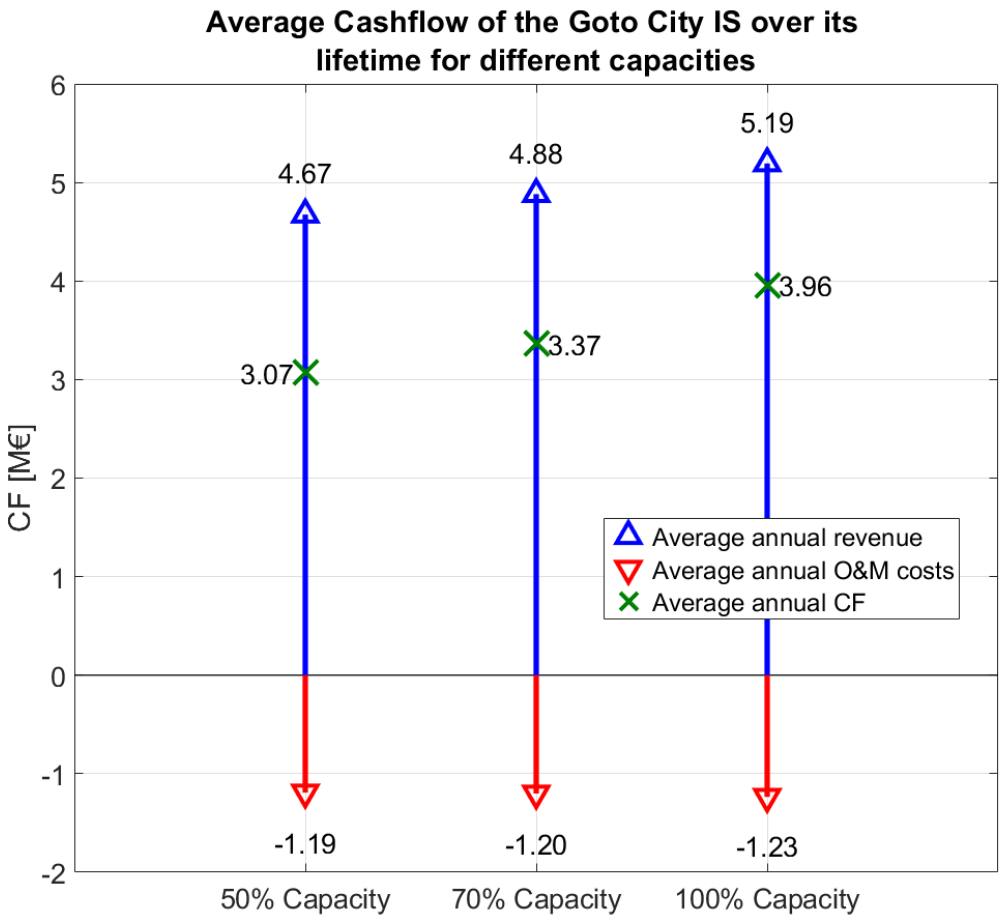

Figure 7.11: Cash Flow of the integrated system over its lifetime for different installed H2 production capacities

The observed rise in revenue corresponds to a parallel increase in CF, as depicted in Figure 7.11. As explained in 7.2.2, the predominant contributor to the OPEX of the integrated system in this model is the OFWF. Consequently, the CF graph demonstrates relatively minor variations across different capacities, underscoring the limited impact of the H2 production system's capacity on CF dynamics.

This statement is further supported by the fact that the revenue difference in the first operational year for the set variety of capacities is approximately €1 million, illustrated in the annual Cashflow graph in Figure B.7. Notably, the OPEX associated with the electrolyser unit, do not play a substantial role in influencing the CF performance.

As anticipated from the results concerning revenue and CF, the NPV of the integrated system exhibits a matching increase with the highest installed capacity. While the NPV initiates at a lower value due to elevated capital costs, the greater H2 production at higher capacities ultimately results in the highest NPV.

Although the differences are very small it is no surprise that the LCOH for a reduced installed capacity is higher than 100% capacity. Higher capacity results in more product and because of relatively low increase CAPEX and OPEX that come with higher installed capacity electrolysers, the LCOH is lower for higher capacities.

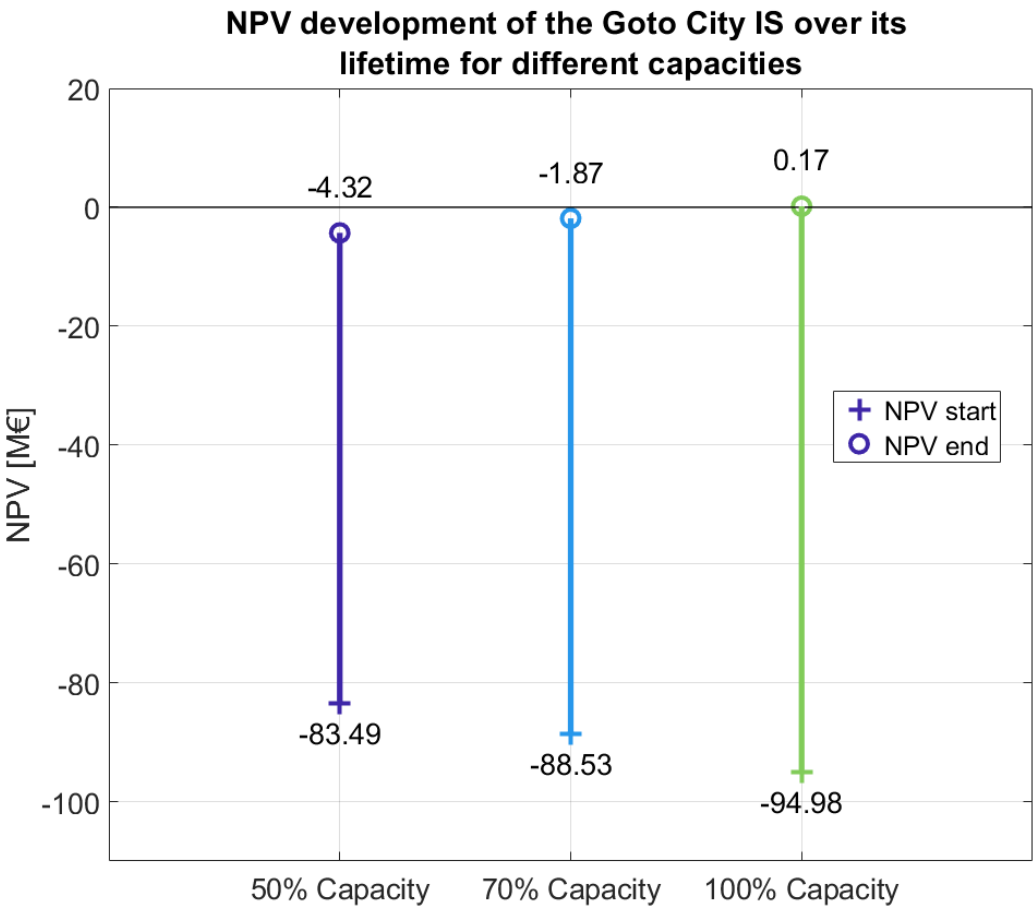

Figure 7.12: NPV of the integrated system over its lifetime for different installed H2 production capacities

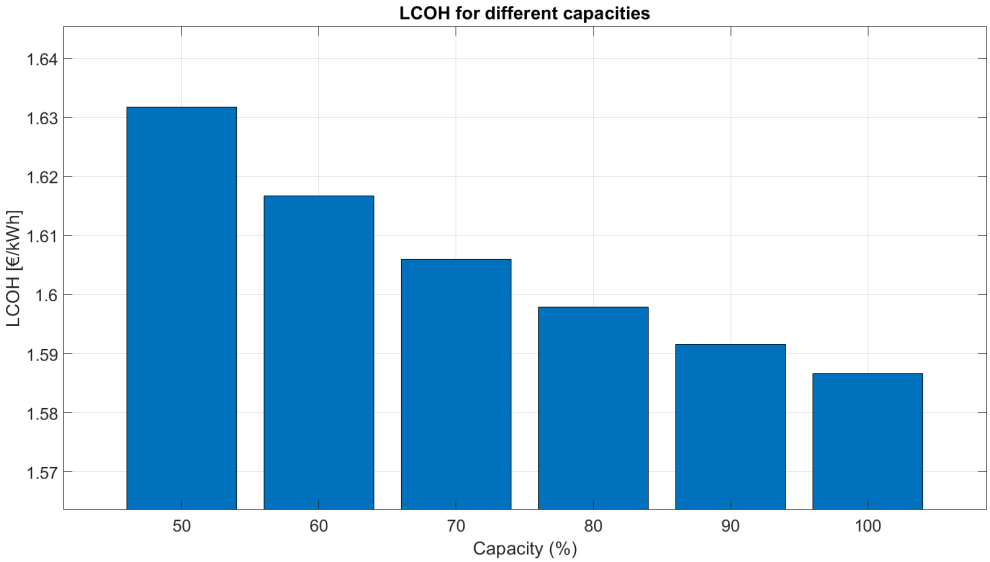

Figure 7.13: LCOH for different installed H2 production capacities

7.5. Scenario Analysis

The reference case is evaluated for four different future scenarios discussed in Section 6.5. On the basis of analyses performed in this section, the Subquestion 5: *"How do possible future scenarios affect the decision to add H2 production to offshore floating wind?"* will be answered. First the different scenarios for H2 price (7.5.1) be elaborated on, followed by scenarios for different electricity prices (7.5.2). Thereafter, Subsection 7.5.3 encompasses the analysis of scenarios for CO2 tax bonuses, introduced in Subsection 6.5.4. The section is finalised by the results of the analysis for varying CAPEX and OPEX.

7.5.1. H2 Price Scenarios

This subsection entails a better understanding of how the results of the reference case are influenced by development of the H2 prices over the lifetime of the integrated system. The applied scenarios for different H2 price development are described in Section 6.5.2 with corresponding values for H2 price and in- or decrease over the lifetime. Note that all scenario analysis are evaluated on the influence with respect to the reference case.

The anticipation was for a significant increase in revenue, even for marginal differences, as the operational schedule of the system is dominated by hours in HM. However, the observed outcome shows the system provides a hedge to variations in H2 pricing since for each of the scenarios, the annual CF is significantly higher than for a conventional OFWF.

As illustrated in Figure B.9, the gradual reduction in hydrogen prices over the years exhibits an increasing influence on the annual CF of the IS. The anticipated variations in H2 prices across different scenarios do not exhibit large differences in the beginning, resulting in a marginal variation in revenue derived from H2 sales. However, after around the 7th operational year the CF differences begin to stabilize. This phenomenon can be related to the fact that the fluctuation in H2 prices across scenarios is modest, not exceeding ¥150 (€1), thereby yielding a modest variance in revenue.

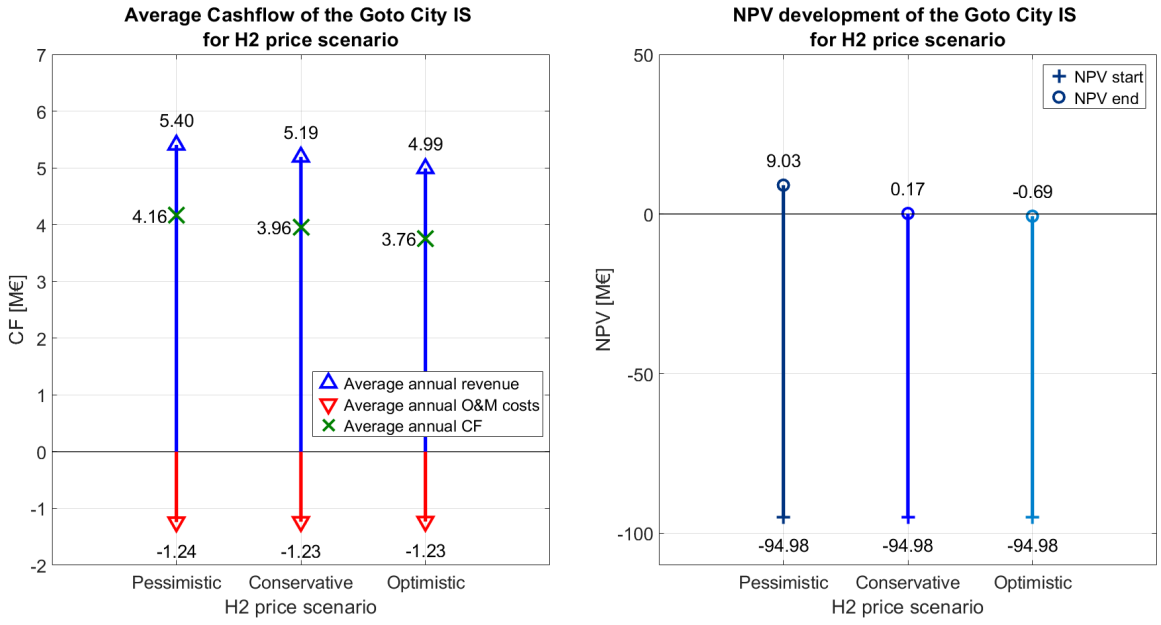

(a) Cashflow

(b) NPV

Figure 7.14: Average CF (a) and NPV development (b) of the Goto City Integrated System over its operational lifetime for different H2 price scenarios.

The marginal impact of the indifference in cash flow translates into relatively low fluctuations in the NPV of the system between the H2 price scenarios. Whether the H2 price scenario is optimistic or pessimistic, the NPV difference over the system's lifetime stays within the range of around €9 million, as illustrated in Figure 7.14b. This relatively modest variance in NPV, despite an investment exceeding €94 million, underscores the insignificance of future H2 price development perspectives on enhancing the feasibility of OFWE through integrated H2

production. This finding can be considered a positive finding since a substantial decrease in H2 sell price means that that the TEP of an integrated system still surpasses conventional OFWE, as shown in Figure B.10.

7.5.2. Power price scenario

This subsection will encompass the details on how electricity price scenarios impact the TEP of the integrated system. The applied scenarios for different electricity prices and price development are described in Section 6.5.1 with corresponding values for electricity prices and increase- or decrease over the lifetime. Note that all scenario analyses are evaluated on the influence with respect to the reference case.

As noted in Section 6.5.1, the power price scenario not only involves variations in the electricity prices of the 2022 dataset used in the reference case but incorporates prices from pessimistic and optimistic years with corresponding expectations of price development over the system's lifetime.

A notable observation in the results is the significant difference in operational hours between scenarios compared to the reference case, as depicted in Figures B.13 and B.14. The pessimistic scenario exhibits comparable hours of H2 production to the reference case, yet during grid supply hours, electricity prices are considerably higher. In contrast, the optimistic scenario shows minimal grid supply hours, with most of the operational time devoted to the integrated system. Figures B.15 and B.16 present graphs illustrating future price developments and the evolution of the switchprice for both scenarios.

CF differences stay relatively low for most of the operational lifetime. In the optimistic scenario, the CF demonstrates a decreasing trend over the system's lifetime, illustrated in Figure B.17, suggesting that the addition of an integrated system in a low power price scenario leads to decreasing profitability in later stages of operation.

For the conditions of a pessimistic power price scenario, the modeled Goto City IS performs significantly better the WF. This is evident in Figure 7.15, where the annual CF for the integrated system is significantly higher for the the largest share of the operational lifetime. The variance in annual CF is primarily caused by higher spot prices for electricity compared to the reference case.

When the resulting NPV of the scenarios, displayed in Figure 7.16, are compared, it becomes clear that addition of H2 production system to conventional OFWE increases the NPV for every scenario. This finding is less valuable for the optimistic power price scenario, since the final NPV differences are minimal here. However, on the notion that electricity prices tend to become more volatile in the future, the findings of the pessimistic scenario, where prices are more volatile, become more valuable.

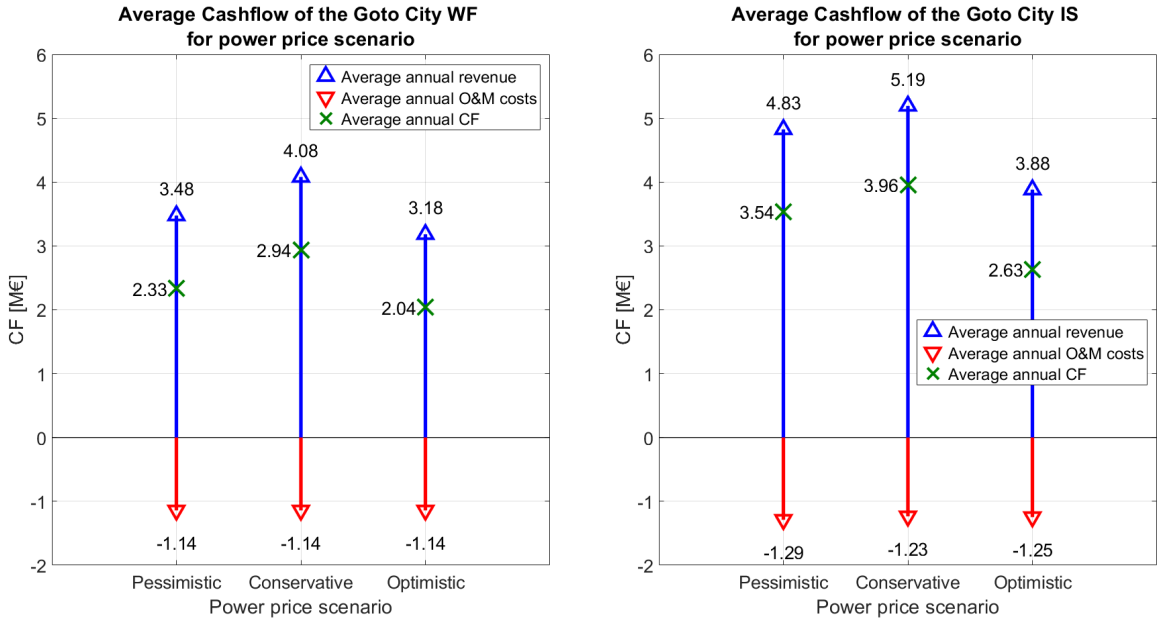

(a) Wind Farm

(b) Integrated System

Figure 7.15: Average CF of the Goto City Wind Farm (a) and the Integrated System (b) over its operational lifetime for different power price price scenarios.

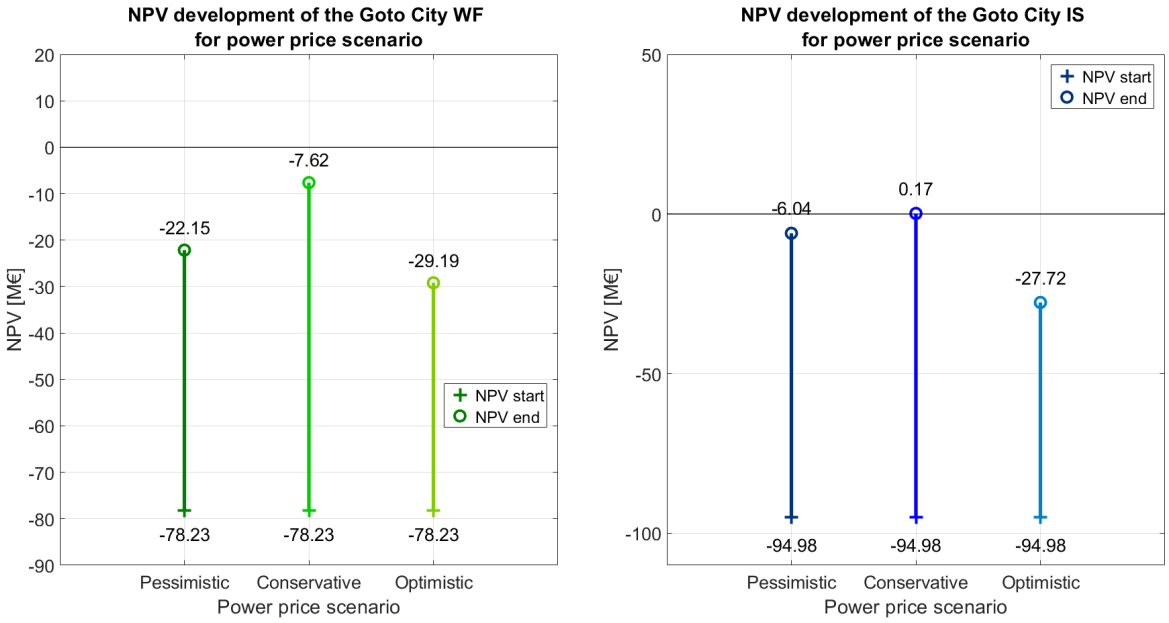

(a) Wind Farm

(b) Integrated System

Figure 7.16: NPV development of the Goto City Wind Farm (a) and the Integrated System (b) over its operational lifetime for different power price price scenarios.

7.5.3. CO2 Tax Scenario

Previously mentioned results did not incorporate a CO2 bonus, primarily because CO2 tax was not factored into the CF calculations of the system since no CO2 is generated during energy production. The resulting bonus is a conceptual addition to the TEP of the integrated system, serving to underscore the financial incentive to transition away from fossil fuels as an energy source in the future. The pessimistic case in the figures indicated the results of the reference case that does not take in to account a CO2 bonus.

To establish the REB, the CO2 emission per kWh of natural gas is estimated at approximately 0.19 kg/kWh [108, 39]. The energy output of the integrated system is then compared to the corresponding CO2 emissions of a natural gas-fired turbine. It is important to note that the energy output used in calculations represents the energy supplied to the grid in kWh and the weight of supplied CGH2 in metric tons. Electrical losses in the grid delivery and losses associated with CGH2 production are not considered in these calculations.

The emitted CO2 from a natural gas-fired turbine equivalent to the produced energy of the integrated system is matched with the corresponding CO2 tax per metric ton and subsequently added to the revenue of the integrated system. Figure 7.17a illustrates the resulting CF over the system's lifetime, reflecting an increase in revenue of approximately €0.5 million and €0.9 million annually on average due to the REB for optimistic and conservative developments of TCCM respectively. This illustrated better in the NPV graph in Figure 7.17b, where the system in the considered optimistic CO2 tax scenario results in an elevated value at the end of lifetime of €30 million.

Again, it must be stated that this analysis illustrates a fictional bonus only to emphasize the need to deviate from fossil fuel based energy sources. For that reason this scenario is not considered as a decisive measurement on concluding if the addition of a H2 production system to conventional OFWE improves its TEP.

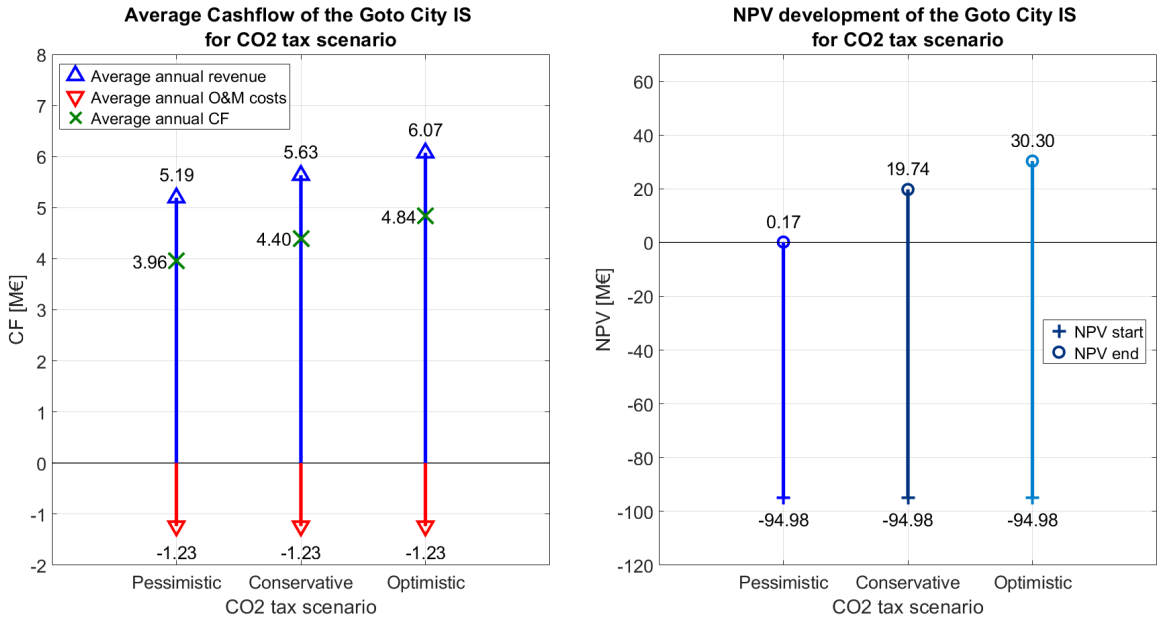

(a) Cashflow

(b) NPV

Figure 7.17: Average CF (a) and NPV development (b) of the Goto City Integrated System over its operational lifetime for different CO2 tax scenarios.

7.5.4. CAPEX Scenarios

The integrated system was assessed under two distinct CAPEX and OPEX scenarios, as outlined in Table 5.1. As previously highlighted, CAPEX and OPEX constitute major factors contributing to the negative NPV observed for both conventional OFWE at the end of their lifetime, indicating the non-viability of the project. Consequently, as depicted in Figure 7.19, the NPV is significantly increased relative to the reference case and the base case.

It is noteworthy that for each of the analysed scenarios, the NPV of both the WF and the IS amounts to positive values at the end of lifetime, indicating project viability. This underscores the necessity for a substantial improvement in the development of CAPEX and OPEX for both OFWE and H2 production to render the systems economically viable under the conditions of the reference case.

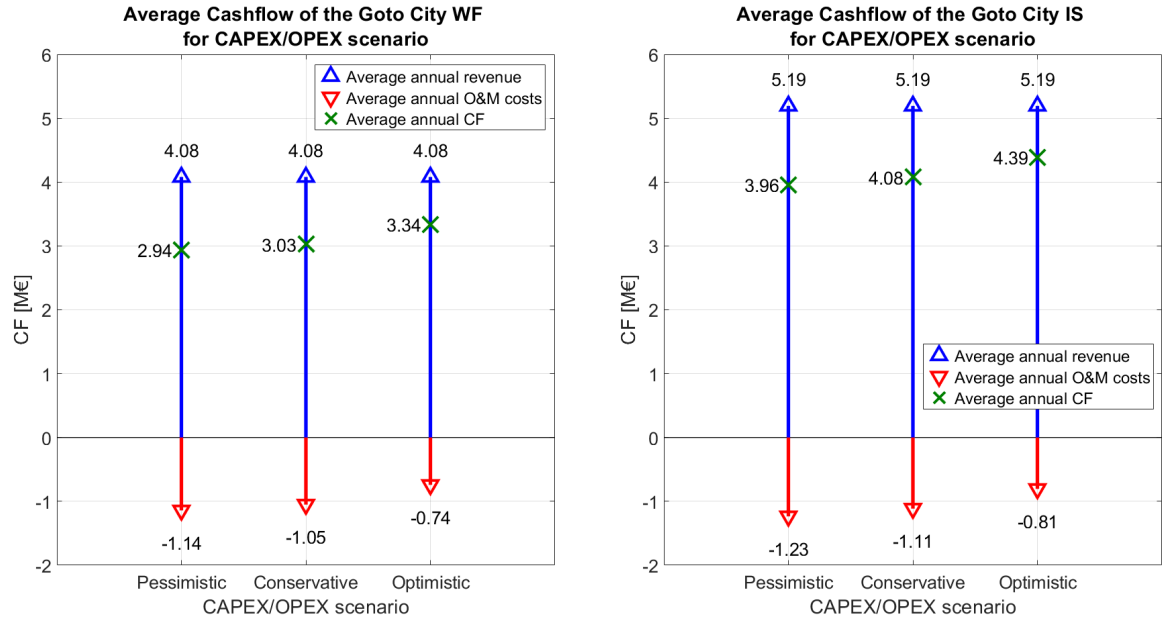

(a) Wind Farm **(b)** Integrated System

Figure 7.18: Average CF of the Goto City Wind Farm (a) and the Integrated System (b) over lifetime for different CAPEX scenarios.

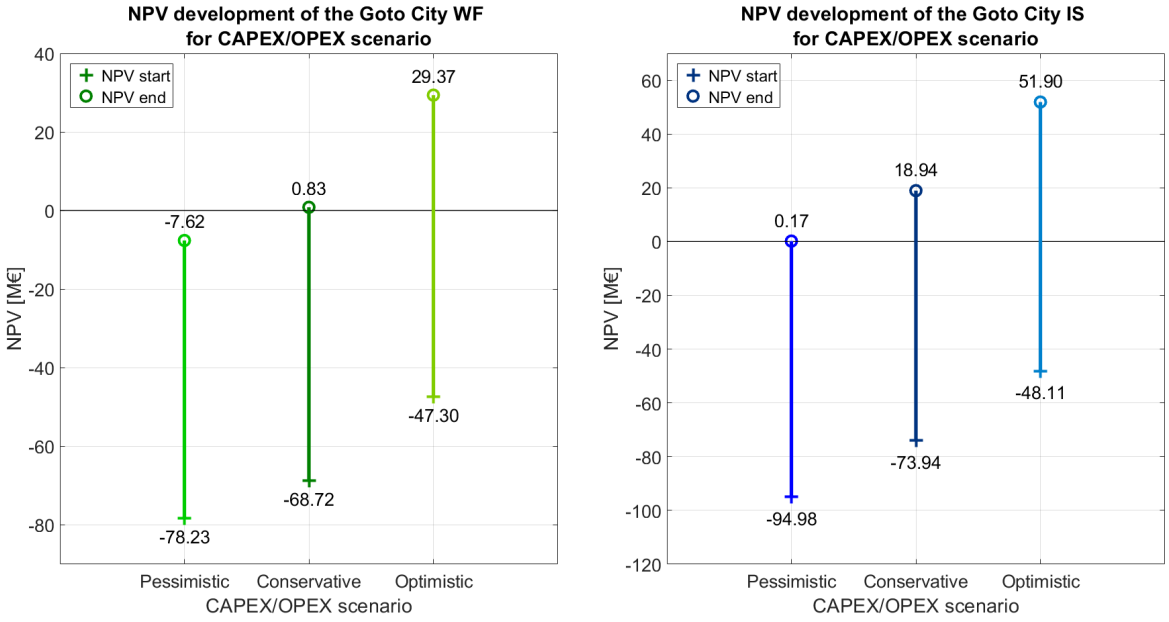

(a) Wind Farm **(b)** Integrated System

Figure 7.19: NPV development of the Goto City Wind Farm (a) and the Integrated System (b) over lifetime for different CAPEX scenarios.

7.5.5. Overview Results Scenario Analyses

	H2 Price		Power Price		CAPEX		Unit
	WF	IS	WF	IS	WF	IS	
Conservative							
LCOE	88.7	53.3	88.7	53.3	81.6	46.2	€/MWh
LCOH	-	1.59	-	1.59	-	0.91	€/kg
Total Revenue	102.0M	129.8M	102.0M	129.8M	102.0M	129.8M	€
Average CF	+2.94M	+3.96M	+2.94M	+3.96M	+3.03M	+4.08M	€
PBP	27.6	24.5	27.6	24.5	24.6	19.8	years
Final NPV	-7.62M	0.17M	-7.62M	0.17M	0.83M	18.9M	€
Optimistic							
LCOE	88.7	59.7	88.7	44.2	158.8	22.3	€/MWh
LCOH	-	1.66	-	1.42	-	0.45	€/kg
Total Revenue	102.0M	124.7M	79.6M	97.0M	102.0M	129.8M	€
Average CF	+2.94M	+3.76M	+2.04M	+2.63M	+3.34M	+4.39M	€
PBP	27.6	24.9	40.6	37.4	15.6	12.4	years
Final NPV	-7.62M	-0.69M	-29.2M	27.7M	29.4M	51.9M	€
Pessimistic							
LCOE	88.7	45.6	88.7	33.1	88.7	53.3	€/MWh
LCOH	-	1.50	-	1.05	-	1.59	€/kg
Total Revenue	102.0M	135.1M	86.9M	120.6M	102.0M	129.8M	€
Average CF	+2.94M	+4.16M	+2.33M	+3.54M	+2.94M	+3.96M	€
PBP	27.6	22.2	33.7	27.5	27.6	24.5	years
Final NPV	-7.62M	9.03M	-22.1M	-6.04M	-7.62M	0.17M	€

Table 7.2: Result comparison of the different scenario analyses between the Goto City WF and IS

7.5.6. Conclusions on Scenario Analysis

This subsection outlines the most important conclusions that can be drawn from the performed scenarios analysis. Each of these conclusions is listed below.

- **For every considered scenario the addition of a H2 production system improves the TEP with respect to conventional OFWE under the set conditions.**
- **H2 price development over lifetime of the integrated system has limited influence on the TEP of the system under the conditions of the performed analyses.**
- **Different considered power price scenarios can have a large impact on the TEP of the system, where a pessimistic scenario shows the most substantial differences in TEP between the WF and IS.**
- **The considered CAPEX/OPEX scenarios resulted to have the most influence on the TEP of the system under the set conditions, where an optimistic scenario for future expenses proved to be the most favorable of all considered scenarios.**
- **CO2 tax scenario resulted to have a significant REB, which emphasizes the urgency to switch to RES and mitigate from fossil fuels our energy supply.**

7.6. Sensitivity Analysis

This section seeks to visualize the variations in TEP under changes in parameters beyond the installed electrolyser capacity, discussed in the previous section. In this sensitivity analysis, the deviation of KPIs is assessed by modifying 17 parameters relative to the reference case, as discussed in Section 6.1. All resulting graphs on KPIs are provided in Appendix B.6. A tornado chart detailing the parameters and their impact on the NPV of the IS and the WF is also included in Appendix B.6. The objective of these charts is to address the Subquestion 7: *"Which parameters have the most impact on enhancing the concept of floating wind?"*

The outcomes of the sensitivity analysis serve to identify the effects of parameter variations on the feasibility of the integrated system. They act as a foundational step towards understanding how the TEP of the integrated system can be optimized to further contribute to the concept of OFWE. Notably, certain parameters were identified to

have a higher influence on the change in KPIs than others, particularly those linked to power output and power prices. The ensuing Subsections (7.6.1, and 7.6.2, 7.6.3) provide a detailed exploration of the results related to changes in wind speeds, power prices and wind farm capacity respectively. These parameters where chosen since each of the analyses produced remarkable results in term of operation of the IS.

7.6.1. Wind Speed

The initial parameter of interest is the wind speed at the designated location, a factor previously acknowledged in Section 3.6 as suboptimal for the OFWF. The sensitivity analysis on wind speeds aims to provide insights into the alterations in TEP for the integrated system at different locations characterized by varying wind speeds.

The increase or decrease in wind speeds impacts the power supply of the system, altering both active and passive hours of the wind farm. Consequently, this induces changes in power delivered to the grid and H2 production, resulting in a corresponding shift in revenue. This revenue change is approximately + or -€1 million annually for the IS and approximately + or -€0.8 million annually for the OFWF over the system's lifetime respectively. The observed change is reflected clearly in the CF of the system, as no modifications have been made to the fundamental characteristics of both systems, resulting in constant operating expenses for the systems in each of the analyses.

Notably, the NPV development of the system experiences a substantial variation with a 10% variation in wind speed. These outcomes underscore and reinforce the statement that the Goto City wind farm is situated in a suboptimal location. The relocation of the system to an area with more favorable wind conditions would significantly enhance the integrated system's performance.

Remarkably, the analysis also reveals that variations in wind speeds not only impact power generation during active hours of the reference case but also activate or deactivate the WTs at wind speeds slightly below or above the cut-in wind speed, respectively. This observation is evident in Figure B.25, which illustrates that the adjusted wind profile triggers the cut-in speed of the WT at the first and sixth hours of the first two days.

Also, since the biggest share of wind speeds is between cut-in and rated power. Combined with the characteristic of WTs that the function of power output is exponential to the wind speed 3.1, it is reflected that the relatively low deviation in wind speed results in a relatively large deviation for KPIs. This begs the question of whether the assumption made in Section 3.7, where the wind speeds from the retrieved dataset are assumed equal to the wind speeds at hub height, can be justified. Although the difference in wind speed between the dataset and hub height is relatively small compared to the variations examined in this analysis, it suggests that even minor deviations in wind speed can significantly affect TEP of the system over a span of 25 years.

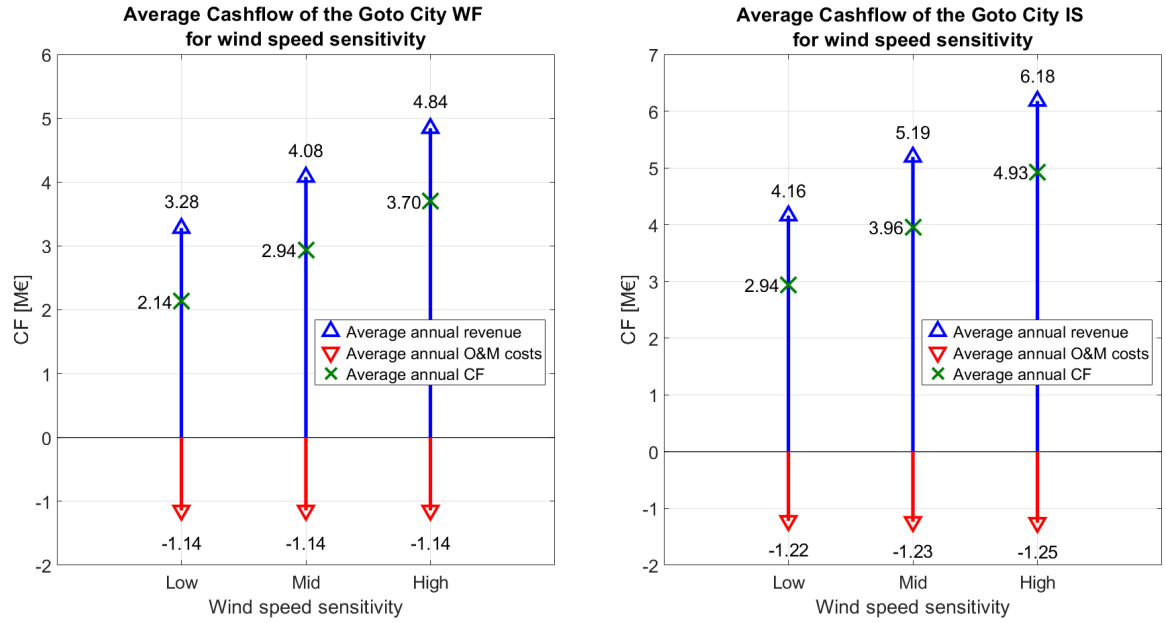

(a) Wind Farm **(b)** Integrated System

Figure 7.20: Average CF of the Goto City Wind Farm (a) and the Integrated System (b) over lifetime for wind speed sensitivity.

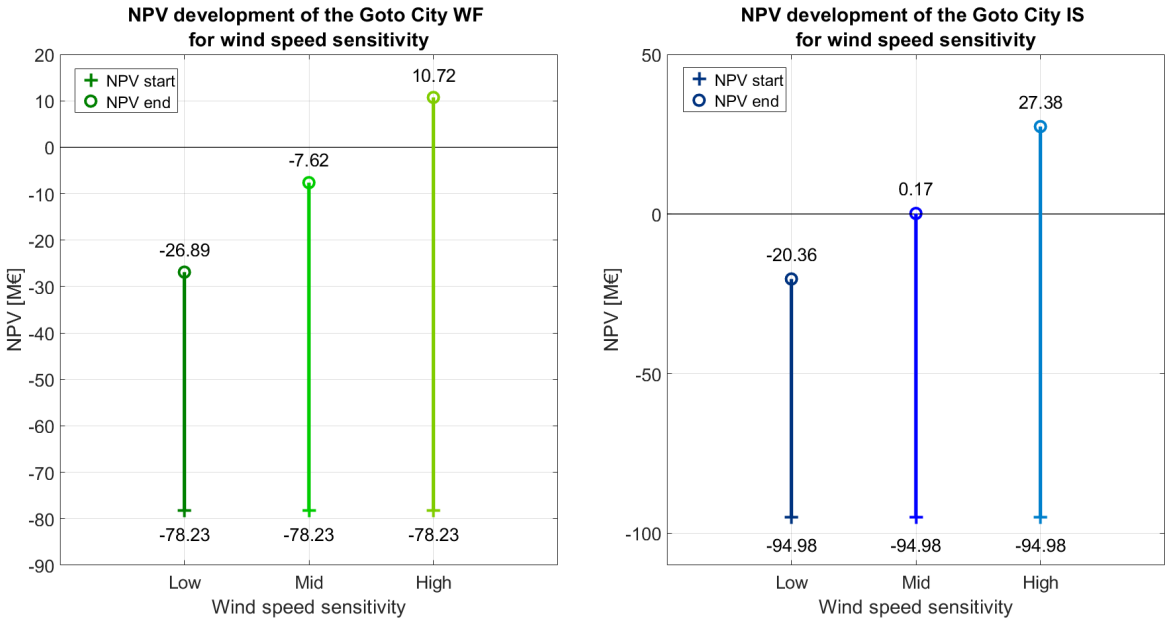

(a) Wind Farm **(b)** Integrated System

Figure 7.21: NPV development of the Goto City Wind Farm (a) and the Integrated System (b) over lifetime for wind speed sensitivity.

7.6.2. Power prices

The outcomes of the sensitivity analysis for power prices are presented in the figures below. Despite showing a notable influence on the resulting KPIs, power price variations surprisingly yield minimal changes in the Success Difference. Both increases and decreases in power prices correspond with equivalent percentage changes in all analyzed KPIs.

A reduction in the prices of hours below the switchprice should theoretically result in no revenue changes during these hours for the integrated system, as H2 production would not trigger any revenue reduction. Conversely, the

revenue for the base case would decrease by 10%. Given that nearly half of the yearly operational hours involve the system operating in HM, a significant difference in the SD was expected. The resulting differences did not align with this expectation as NPV differences between the WF and IS configurations for a low and high power price scenario are €13 million and €12 million.

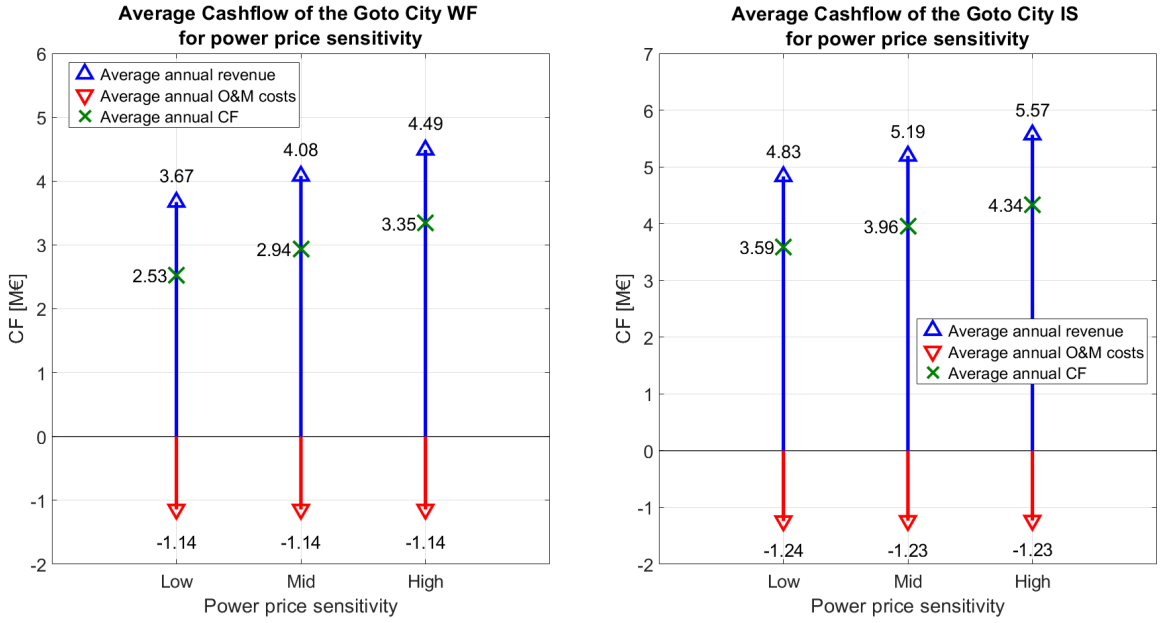

(a) Wind Farm **(b)** Integrated System

Figure 7.22: Average CF of the Goto City Wind Farm (a) and the Integrated System (b) over lifetime for power price sensitivity.

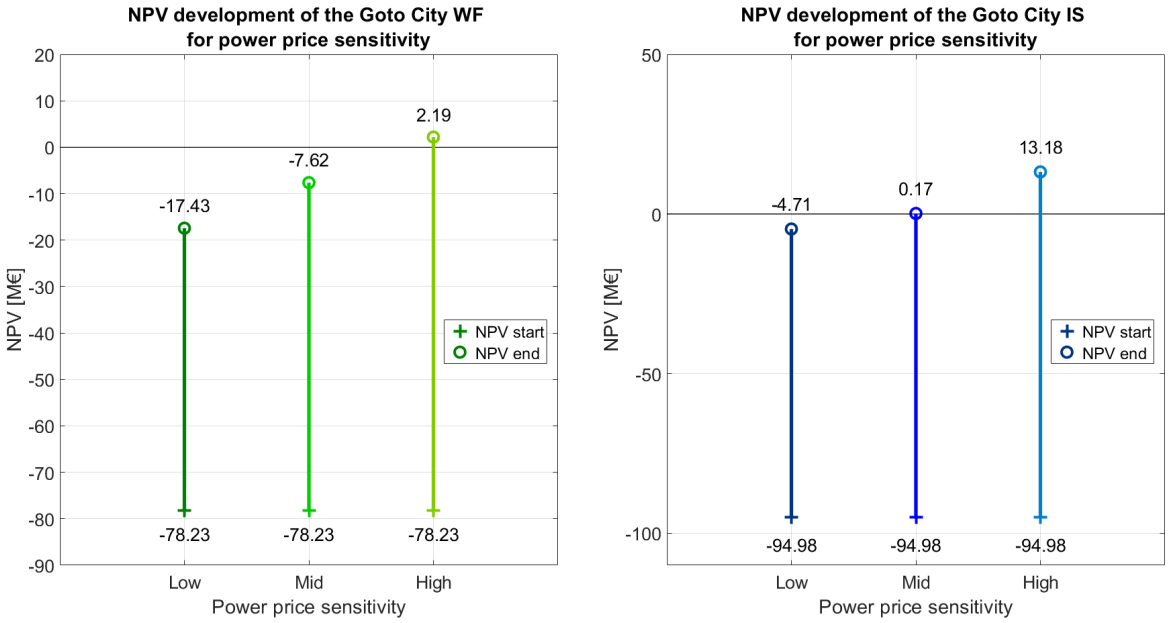

(a) Wind Farm **(b)** Integrated System

Figure 7.23: NPV development of the Goto City Wind Farm (a) and the Integrated System (b) over lifetime for power price sensitivity.

7.6.3. Wind Farm Capacity

These findings indicate that changes in wind farm capacity have the most impact as both enhancers and regressors of the KPIs. Alterations in wind farm capacity lead to the most significant deviations in TEP, aligning with expectations given the linear dependence of power output and consequently H2 production and grid supply. Together with earlier made statements that the expenses of the system are predominantly influenced by the OFWE system, TEP of the system is largely dependent by wind farm capacity. It's essential to note that the wind farm capacity sensitivity analysis divides into two distinct types of parameter changes: a). the number of installed wind turbines and b). the type of installed wind turbines. Each of these parameter changes influences the wind farm capacity and subsequently the KPIs of the system in different ways. Importantly, the installed H2 production capacity in this sensitivity analysis remains fixed at 100%, with the H2 production facility's installed capacity growing in tandem with the OFWF capacity. The insights derived from this analysis contribute to a better understanding of how wind farm capacity adjustments distinctly influence the overall performance of the integrated system.

Number of Installed Wind Turbines

This subsection encompasses the outcomes of halving and doubling the number of floating wind turbines in the Goto City wind farm, while maintaining the same characteristics of the WTs used in the previous analyses. As expected, the revenue and CF of the integrated system linearly grows with the increased number of WTs. This growth is a direct consequence of the doubled power output of the system. Notably, the CF doubles as the largest share of OPEX is attributed to the OFWF, which experiences gradually increased OPEX with the expansion of the wind turbine fleet.

However, a noteworthy observation in this analysis is that, despite the almost doubling of revenue and CF, the final NPV of the system is only slightly elevated compared to that of the reference case. This trend is consistent with the observations in the reference case, where a significant portion of the investment is attributed to the CAPEX of the OFWF. The addition of H2 production system did contribute to an improvement in NPV of the reference case, reaching a positive NPV. Doubling the number of wind turbines appears to reach a positive NPV as well, only the difference between the reference case is approximately €20 million over lifetime. Nonetheless, the outcomes of this analysis showcase improvements when compared with both the reference and base cases. Reducing the number of turbines has a reversed effect on the NPV compared to doubling it. This analysis implies that for either the Goto City WF or IS, the system would have an diminished TEP when using less wind turbines. Notably, for each of the run analyses the IS has an elevated TEP compared to the WF.

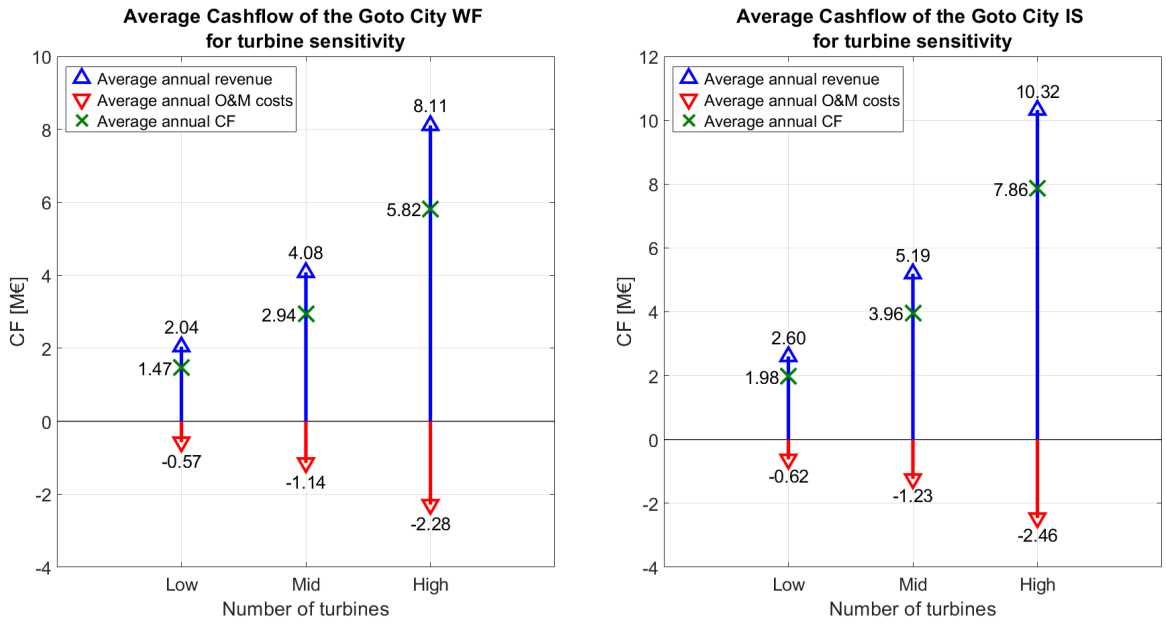

(a) Wind Farm

(b) Integrated System

Figure 7.24: Average CF of the Goto City Wind Farm (a) and the Integrated System (b) over lifetime for turbine sensitivity.

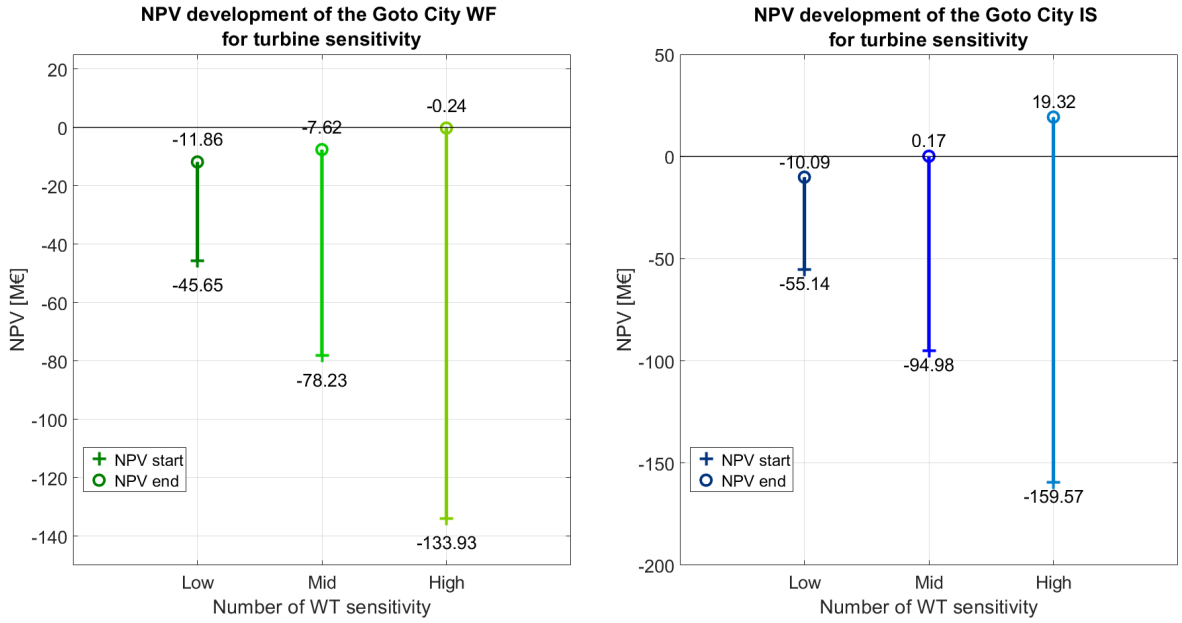

(a) Wind Farm

(b) Integrated System

Figure 7.25: NPV development of the Goto City Wind Farm (a) and the Integrated System (b) over lifetime for turbine sensitivity.

8 MW Wind Turbines

The analysis considering WTs with a significantly higher rated power resulted in noteworthy results. This analysis uses the Siemens Gamesa 8 MW, which is one of the most commonly used wind turbines in North Sea wind farms. The adoption of this turbine demonstrated a significant enhancement in the TEP of the Goto City IS. Although this enhancement is not particularly reflected in the revenue stream of the integrated system, which increased in tandem with the power output of the wind farm by approximately a factor of four. Also, the marginal SD between the conventional and integrated system remains consistent, reflected by the nearly constant increase of average CF differences for both configurations. The impact is more significant in other key metrics.

This proportionally increased CF translates into a remarkable improvement in TEP, as shown in the NPV graph provided in 7.27. Remarkably, the NPV of the project exhibits much more positive results at the end of the operational lifetime, rendering the system far above the minimum requirement for feasibility. This positive outcome is due to the proportionally lower CAPEX compared to the increase in power and the significant boost in CF. This outcome serves as a noteworthy indication that integrating H2 production into a conventional offshore floating wind farm can significantly enhance the feasibility of the concept if it is combined with the usage of high capacity WTs.

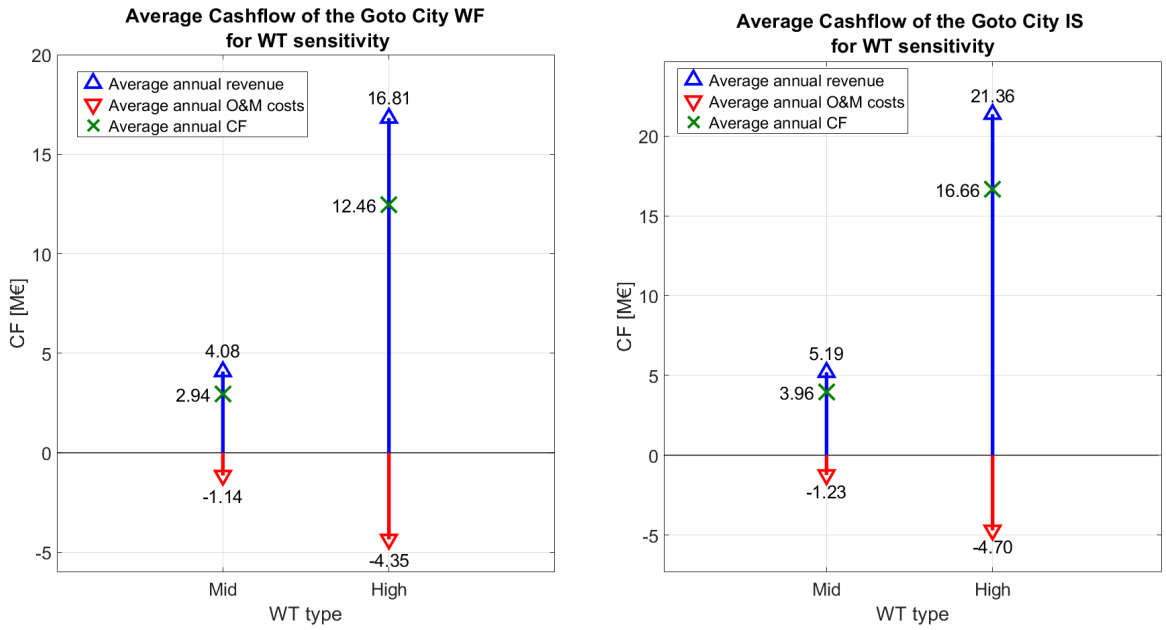

(a) Wind Farm **(b)** Integrated System

Figure 7.26: Average CF of the Goto City Wind Farm (a) and the Integrated System (b) over lifetime for WT type sensitivity.

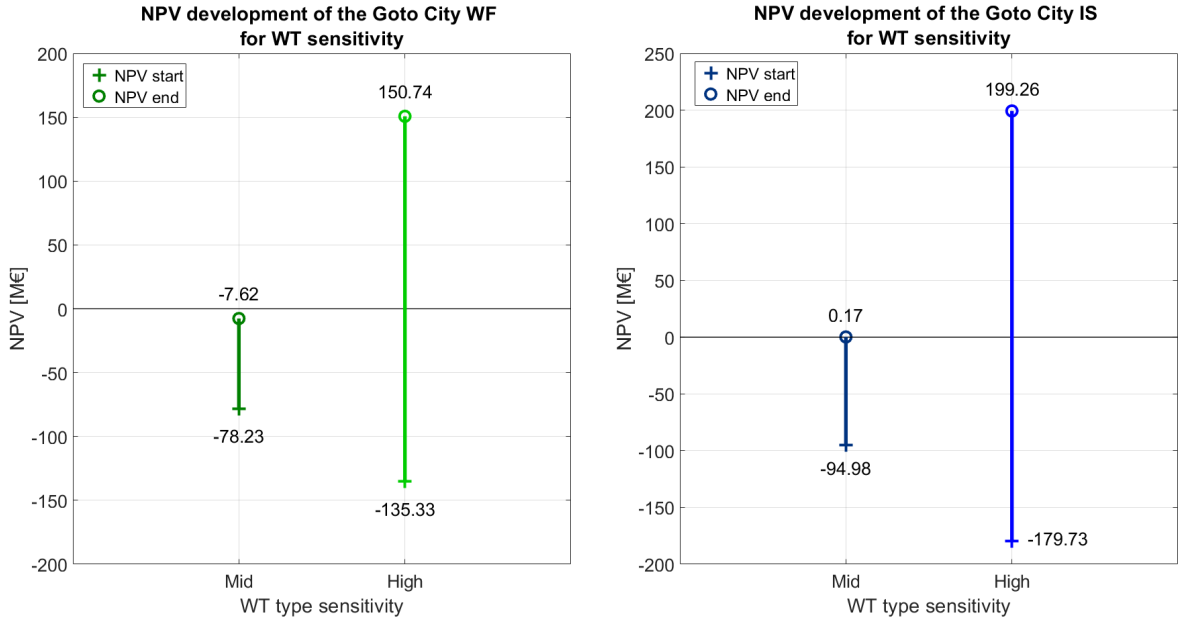

(a) Wind Farm **(b)** Integrated System

Figure 7.27: NPV development of the Goto City Wind Farm (a) and the Integrated System (b) over lifetime for WT type sensitivity.

Number of installed 8 MW turbines

The combination of the two previous analyses also results in remarkable findings. Firstly, halving the number of wind turbines in the fleet but upgrading the capacity also results in a substantially more positive NPV compared to the reference- and base case. This is particularly interesting considering that the investment is nearly equal to the reference- and base case, illustrated in Figure 7.29, while the capacity of the wind farm is now nearly doubled. Note again that the TEP of the IS is improved compared to conventional OFWE.

The system structure with double the amount of wind turbines with an increased capacity results in an even higher

difference between WF and IS NPV. This is the result of a larger required investment for the construction of the integrated system and wind farm, dominated by the expenses of the OFWF. The highly elevated power output of the system however does result in the highest NPV found in analyses.

However, even though the capacity of the system in this structure is double that of the system in the previous analysis where only the WT capacity was increased, the final NPV of the system is not doubled. This outcome suggests that achieving increased feasibility for an integrated system compared to a conventional OFWF requires finding an optimum balance between WT rated power and the number of WTs. This optimum is primarily influenced by the capacity and other internal characteristics of the WT, as the CAPEX of the OFWF are primarily determined by the number of offshore operations required for its construction, rather than the size of these operations. Therefor, finding the right balance in WT characteristics is vital for optimizing the feasibility and economic viability of the integrated system.

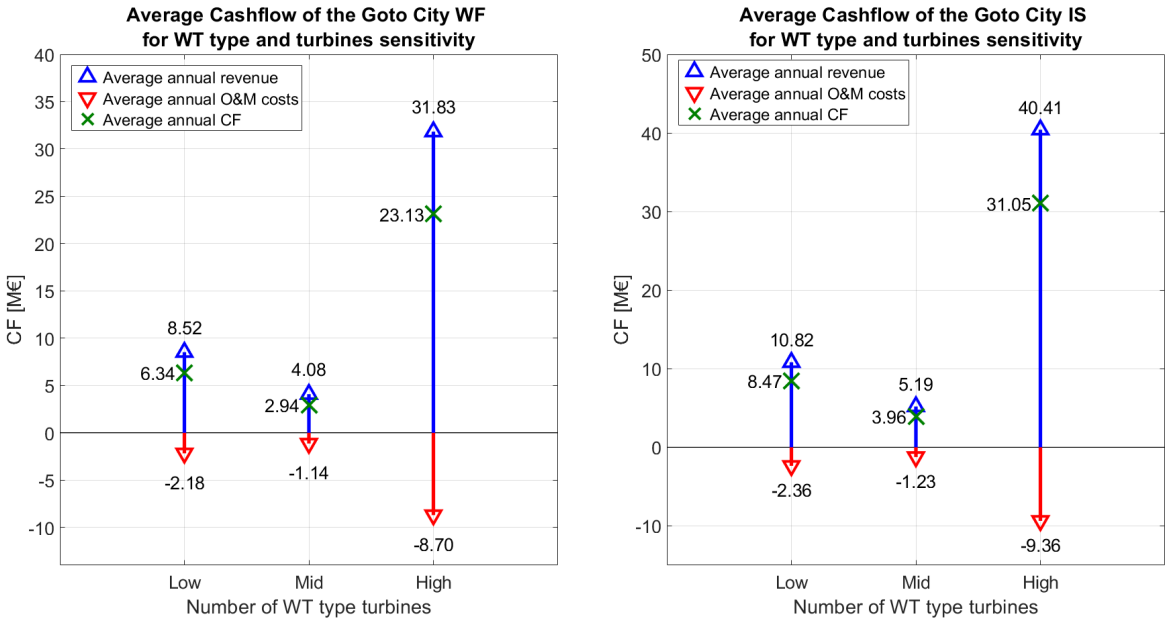

(a) Wind Farm

(b) Integrated System

Figure 7.28: Average CF of the Goto City Wind Farm (a) and the Integrated System (b) over lifetime for number of WT type sensitivity.

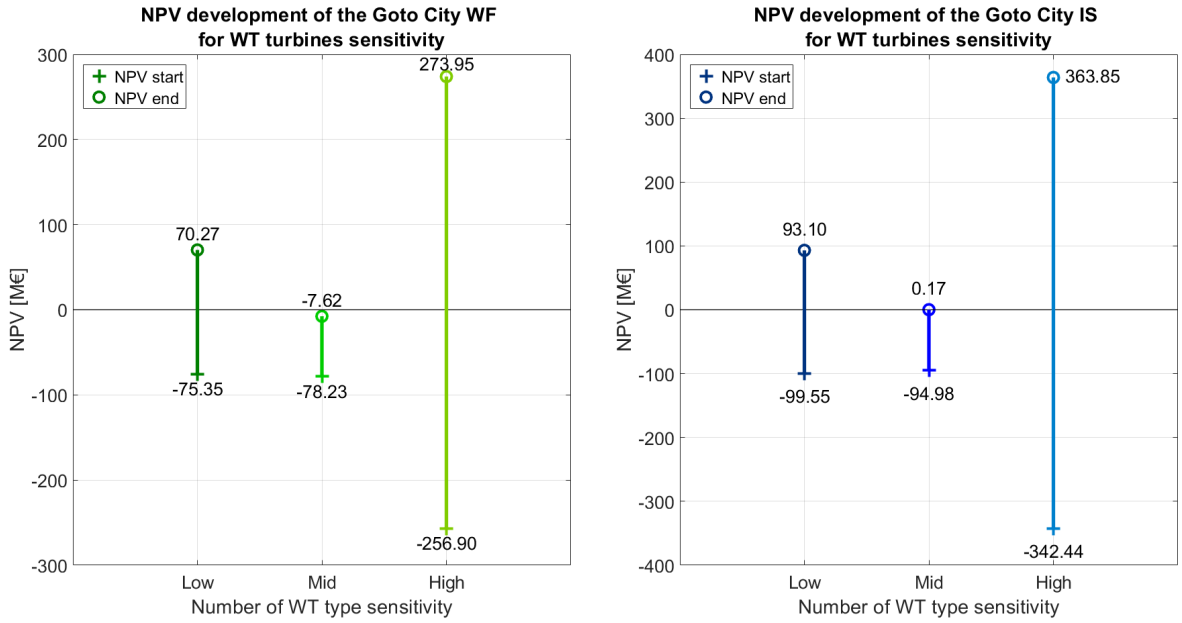

(a) Wind Farm

(b) Integrated System

Figure 7.29: NPV development of the Goto City Wind Farm (a) and the Integrated System (b) over lifetime for number of WT type sensitivity.

7.6.4. Conclusions on Sensitivity Analysis

This subsection outlines the most important conclusions that can be drawn from the performed sensitivity analysis. Each of these conclusions is listed below.

- **The installed capacity of the OFWF proved to have the largest impact on the TEP of the system of the investigated parameters, leading to a highly increased NPV for both the WF and IS configuration.**
- **The use of high capacity wind turbines is preferred over increasing the number of wind turbines for an OFWF and integrated system. The number of turbines of the OFWF has an increased influence on the CAPEX of the system for the used economics compared to turbine capacity. Installing fewer, high capacity wind turbines amounting to the same WF capacity results in more beneficial KPIs. High capacity wind turbines lead to a highly increased revenue with relatively low additional expenses.**
- **Wind speed proved to be of significant influence on the TEP of the system, questioning the assumption that the difference in hub height and dataset wind speed can be neglected since wind speed deviation is only 3.3%.**
- **Power price resulted in relatively low impact on TEP.**
- **SEC of the electrolysers proved to have one of the highest positive impacts on the TEP of the integrated system.**

7.7. Conditions for TE improvement

This study addresses the research question: ”How can hydrogen (H2) production add to offshore floating wind energy?” The results of the base case indicate that the Goto City Wind Farm alone is not economically viable in the current industry landscape. This is mainly attributed to the higher costs compared to the more prevalent fixed-bottom offshore wind energy. Given that both RES types yield the same power output and sell at the JEPX for identical prices, the NPV of the Goto City Wind Farm does not reach a positive value, rendering the project economically unfeasible.

Modeling the Goto City Wind Farm as an integrated system, however, demonstrated an increase in the TEP since the resulting KPIs of the integrated system were consistently elevated compared to the base case. Beyond the enhancement in TEP due to improved KPIs, the incorporation of a hydrogen production system serves as a risk mitigation strategy against uncertainties in OFWE parameters. Notably, it acts as a safety net, particularly in

the face of potential challenges such as low power prices, especially considering future scenarios of increased volatility in RES leading to more fluctuating power prices. Sensitivity and scenario analyses provided additional insights into other key parameters influencing the improvement in TEP. Among the most significant factors are:

- The addition of a hydrogen production system to the Goto City Wind Farm significantly improves the TEP. With current perspectives on H2 and power price development with respect to the base case, an integrated system results in an elevated revenue stream of 27.25%, elevated CF of 34.7% and an increase NPV of 33.5%.
- For power price scenario, pessimistic scenario proved to be the largest improvement on system value for OFWE by addition of H2 production (€16.11 million) compared to the conservative (€7.79 million) and optimistic (€1.47 million). Pessimistic power price scenario resulted also in the largest percentage difference in NPV between WF and IS, 46.6% compared to 33.5% (conservative) and 22.8% (optimistic).
- CAPEX scenario analyses resulted in highly improved TEP of both systems . CF differences were negligible, since OPEX contribution is relatively low compared to revenue stream, but NPV of the system was increased significantly. For an optimistic CAPEX scenario the TEP of the integrated system based on NPV is elevated by €22.53 million and for the conservative scenario €18.11 million.
- Numerous parameters influenced the ratio of improvement by addition of H2 production during the sensitivity analysis of which wind speed and wind farm capacity to the largest extend.
- Relocating the Goto City Wind Farm to a more favorable location in terms of prevailing wind speed would result in significantly improved TEP under the set conditions of the model. Prevailing wind conditions at the designated location are considered sub-optimal regarding the characteristics of the used WTs. Higher wind speeds that would reach rated wind speed more often could highly increase power generation.

7.8. Conditions for TE feasibility

The addition of a hydrogen production system which is active during hours of low electricity price does significantly improve the TEP of the integrated system, up to the point where the system turns a profit at the end of its lifetime. However, besides the conversion to an IS, TE feasibility for the Goto City WF can be achieved under alternative conditions. Sensitivity and scenario analyses have given new insight in the probability of TE feasibility for the Goto City Wind Farm. Changing the input parameters on the model for the system proved to result in some interesting findings on making the concept without an H2 system feasible. These conditions for TE feasibility, external or internal, will be discussed in this section in the following subsections.

7.8.1. Internal Conditions

Internal conditions, conditions within the region of system design play a crucial role in enhancing the TEP of the integrated system. The correct understanding of TEP involves strategic design choices, particularly the selection of WT types and capacities.

As depicted in Figure B.36, the choice of an appropriate WT type proves to be crucial in achieving a positive NPV. The analysis highlights that a significant increase in WT capacity, achieved through doubling the amount of wind turbines in the farm, does not guarantee feasibility for the Goto City WF on its own. However, the integrated system, with its additional hydrogen production functionality, does exhibit a positive NPV trajectory. This underscores the transformative impact of integrating hydrogen production into offshore wind energy systems.

Notably, the usage of a more common, higher capacity WT appeared to ensure TE feasibility for both WF and IS configurations. The significantly increased revenue as a result of elevated power generation outweighs the expenses that come with utilizing this WT type. As a result, the NPV of both WF and IS follows a highly improved trajectory, rendering both systems feasible at the end of lifetime under the modeled conditions. Even for half the number of WTs with elevated capacity both systems would still both be feasible at the end of lifetime, underscoring the self-sufficiency of this condition.

The self-sufficiency of internal conditions for feasibility implies that specific design choices can independently ensure a positive NPV. This insight is valuable for system designers and stakeholders, emphasizing the significance of incorporating such features into the design phase of conventional OFWE to enhance the TEP of the system.

In conclusion, a comprehensive understanding of both external and internal conditions is paramount for assessing

the TEP of the integrated system. External conditions are characterized by a level of uncertainty, and their strategic combination is crucial. Internal conditions underscore the transformative potential of specific design choices in ensuring economic viability.

7.8.2. External Conditions

The TEP of the integrated system is inherently tied to external conditions, specifically the prevailing wind conditions and the CAPEX of the system. These dynamic parameters play a crucial role in shaping the economic landscape of the system. The prevailing wind conditions, the key power generating factor, is characterized by unpredictability. Variations in wind conditions can significantly influence the NPV of the integrated system and wind farm. Figure 7.21 illustrates the sensitivity of system value development to deviations in wind speeds, showcasing that under more favorable environmental conditions with respect to the used dataset, both systems may exhibit positive economic returns.

Moreover, the significant increase in NPV, amounting to around €20M compared to the reference case, underscores the system's sensitivity to wind speed variations. It implies that the integrated system's TEP can be significantly strengthened by shifting operations to a more favorable location considering the prevailing wind conditions.

Notably, an examination of optimistic and conservative CAPEX conditions revealed a positive NPV for both systems. The feasibility of these systems is significantly dependent upon investment in their respective components. For the WF configuration to reach self-sufficient feasibility within the modeled conditions, an enhancement in CAPEX perspectives to a level at least as favorable as the analysed conservative scenario is crucial.

The potential for variations in wind conditions and positive CAPEX scenarios, to lead to a positive NPV is a critical observation. It suggests that strategic positioning and planning to external conditions can result in a favourable TEP. The unpredictability of wind conditions necessitates a better suitable location for the Goto City WF, which is mediocre in the current orientation. These findings emphasize the need for a dynamic and adaptable approach to external conditions, leveraging favorable scenarios and mitigating risks, to enhance the overall TEP of the integrated system.

In conclusion, a comprehensive understanding of both external and internal conditions is paramount for assessing the TEP of the integrated system. External conditions are characterized by a level of uncertainty, and their strategic combination is crucial. Internal conditions underscore the transformative potential of specific design choices in ensuring economic viability.

7.8.3. Discussion Case Study

This subsection will discuss on how specific the model is in terms of the considered case study. Some parameters used in the model are specifically bound to location or other characteristics. In other words, what elements of the model and the research are location specific and what elements are transferable.

Case Study Specific Elements

This case study considers several location-specific factors that can significantly influence the outcomes of the simulated performance. The first element is the wind conditions at the designated location. These conditions depend on the prevailing climate, surrounding terrain and seasonal changes. Therefore, any conclusions drawn from the simulations are applicable only to the wind conditions specific to Goto City. The performance of the modeled system is greatly affected by these wind conditions, as detailed in subsection 7.6.1. Consequently, the system may perform differently in other locations with varying wind conditions.

Another specific element in the model is the use of power price data from the JEPX. Power markets can be influenced largely by governmental regulations, and Japan's transition to a free, competitive power market, as explained in subsection 2.1.3, has had a significant impact on price dynamics. The revenue simulated in the model is based on this specific market structure. Results may differ in countries with different power market regulations.

Thirdly, the characteristics of the wind turbines used in the simulation are specific to this case study, with the Hitachi 2.1 MW turbine being employed. The power output of the entire wind farm is limited by the capacity of these turbines. Using turbines with different characteristics could lead to substantially different outcomes and conclusions, as demonstrated in Section 7.6.3.

Finally, several other aspects of the simulations are specific to this particular case study, contributing further to the understanding of system performance. These include factors such as site-specific operational considerations,

maintenance strategies and grid integration requirements, all of which play important roles in the outcomes and conclusions drawn from the analysis.

Transferability

The case study discussed in the research offers valuable insights into the wind farm's and integrated systems's performance in Goto City. However, whether the model can be applied to other locations depends on several factors.

Firstly, the wind conditions at Goto City, can be altered to simulate performance of the system at a different location. This is done in the verification of the wind farm system in Section 3.8. The results of this verification indicated that the model may yield reasonably accurate predictions, as the different wind speed dataset used resulted in similar power output compared to realised values. One might suggest that for this reason the transferability of the model to a case study considering different wind conditions is possible.

Secondly, the model's reliance on power price data from the JEPX can be replaced with data from other markets, as demonstrated in the analysis of alternative power price scenarios in Section 7.5.2. This flexibility allows the model to be applied to different regions with varying market dynamics.

Furthermore, the transferability of wind turbine characteristics is already discussed in Section 7.6.3, that encompasses the use of Siemens 8 MW wind turbines. Simulations show that the in terms of WT characteristics, the model can indicate system performance that utilizes a different set of wind turbines.

Considering these factors, which are deemed of large importance to whether the model is transferable based on the model, it is reasonable to conclude that the model has the potential to be transferred and applied to simulate systems in alternative locations or case studies. However, careful consideration and adjustments may be necessary to account for specific environmental, market, and technological differences.

7.8.4. Limitations

Before substantiated conclusions can be drawn from the acquired results of the various simulations, certain limitations of the model need to be addressed. The model simulated performance of the Goto City WF and IS based on assumptions, summarized in Subsection 3.7 and 6.7. However, these assumptions resulted in certain simplifications of parameters or elements of the model that need to be addressed. This subsection reviews the results and limitations of the model in light of these assumptions.

One significant limitation is the assumption that wind speed at hub height is equal to the wind speed retrieved from the dataset at 100 meters above sea level. While this assumption was based on small nominal deviations between the two values, sensitivity analysis, performed in Section 7.6.1, revealed that even a 10% deviation in wind speed can significantly influence system performance. Consequently, the fact that the model is based on the assumption that wind speed from dataset implies that the simulated power output of the wind farm has a certain degree of inaccuracy.

Another key limitation of the results from the model is the acquired revenue gained from providing the grid with power in the year after 2022. This revenue is based on the assumption that the future power prices are the similar to the first operational year, only with alterations based on the expected development of power prices. This assumptions is ofcourse inaccurate since future power prices can not be predicted and are influenced by a variety of external factors. The accuracy of hourly revenue gained from providing the grid with power in the years after 2022 from the simulations in the model is for this reason debatable.

Similarly, predictions of future wind speeds are based on the assumption that wind speeds follow a Weibull distribution. However, future wind speeds may be affected by global climate change and other external factors, potentially deviating significantly from the values used in the simulations.

Another important limitation of this model in terms of its scalability and transferability, is the fact that wake effects are not taken into account in the model. Wake, induced by turbines, has a significant effect on the performance of WTs. However, wake is not taken into account in the model since the farm consists of only 8 WTs. Consequently, its suitability for simulating the performance of wind farms with multiple rows of turbines is questionable, as wake effects are not accounted for in the power output calculations.

These limitations highlight the uncertainties associated with the simulation model, which relies on various assumptions. Simulation models are useful tools for understanding and examining complex systems. However, they are

limited by the assumptions made during their development. Recognizing these limitations and evaluating the validity of assumptions is crucial for ensuring that results are meaningful and can be substantiated.

Despite these limitations, the model demonstrates a degree of accuracy also, as results from its simulations seem to correspond with realised and predicted outcomes, previously discussed in Sections 3.8 and 7.1. Thus, while the model's limitations may pose some uncertainty into the results, can also be regarded as a realistic representation of the system's performance.

8

Conclusions and Recommendations

8.1. Conclusions

The primary objective of this research is to address the overarching question: *"How can hydrogen production add to offshore floating wind energy?"* This chapter serves to provide a response to this question and outlines the conditions under which this integration proves beneficial. Additionally, it summarizes the findings in response to the subquestions posed throughout the study. This chapter is finalized by recommendations for further research.

The four conclusions that collectively answer the above question are as follows:

1. **The results of the Goto City IS model, under the considered conditions, demonstrate that the addition of a PEMEL hydrogen production system is a financially viable enhancement to offshore floating wind energy based on NPV increase.**

   The strategic production of hydrogen during hours when the electricity price falls below a certain threshold, known as the switchprice, significantly amplifies the TEP of the Goto City WF. This approach results in an elevated and more consistent revenue stream, leading to a substantial reduction in the PBP of the system which in turn causes the system to be techno-economically feasible under the modeled conditions and with the set assumptions. Despite the increased expenditures associated with the hydrogen production system, the NPV of the Goto City WF surpasses that of the conventional wind farm after thirteen operational years under the specified conditions.

2. **Compressed Gaseous hydrogen resulted in the best option to use as a H2 carrier.**

   Among the four considered hydrogen carrier configurations, Compressed Gaseous Hydrogen, also used as the reference case, emerged as the most profitable for this case study. This preference is attributed to its streamlined production- and retail process, involving fewer steps to form and sell the final product, thereby reducing energy losses and enhancing overall profitability compared to the other carriers.

3. **The capability for switchability between hydrogen production and grid supply hedges against potential uncertainties in the future.**

   The IS not only acts as a double contributor to Japan's climate change mitigation goals but also serves as a hedge for OFWE against low power prices and power price volatility. The primary factor influencing the effectiveness of this hedge is the fluctuation in power prices, as deviations in these prices result in higher differences in the overall TEP of the IS. This observation is further supported by the fact that the TEP of the IS, with respect to conventional OFWE, did not exhibit deviations with the same magnitude in the power price scenarios. This indicates that hydrogen production could ensure higher system value for unfavourable, volatile power prices.

4. **Techno-economic feasibility is achieved through the addition of hydrogen production for the Goto City WF under the set conditions, as the NPV of the system reached positive values.**

The operational switchability provides an additional revenue stream which outweighs the increased expenditures of the additional components. The substantial increase in expenses of offshore floating wind energy, when compared to its fixed-bottom alternative, could be offset by the enhanced and more consistent revenue stream resulting from hydrogen production to achieve system feasibility without governmental subsidies.

Various configurations, parameters and scenarios were analysed in order to identify their influence on the TEP of the system. These analyses lead to the next conclusion: **Under certain conditions (identified through various analyses) TEP of the initial system and the integrated system could be enhanced, potentially rendering it feasible.**

These conditions are categorized as internal and external, with both conditions having the potential to achieve feasibility independently. The summarized conditions are presented below.

- **Internal conditions**: Section 7.8.1 emphasizes the critical role of selecting an appropriate WT type and utilizing the minimum number of turbines for ensuring a positive NPV. The sensitivity analysis demonstrates that using WTs with substantially higher power output than those in the Goto City WF significantly enhances the TEP of the system.

  However, utilizing an increased number of turbines does not guarantee economic feasibility for the conventional OFWE system for the analysed conditions. In contrast, the IS, with its additional hydrogen production functionality, results in a positive NPV.

  This underscores the impact of integrating hydrogen production into offshore wind energy systems. The emphasis is on the capacity of a singular WT, as increasing the WF's capacity by doubling the number of turbines does not result in the same proportional TEP increase as a higher capacity WT. This is due to marginally higher expenses compared to utilizing a higher capacity WT with the used economic characteristics in the model.

  The self-sufficiency of internal conditions for feasibility implies that specific design choices, particularly the integration of hydrogen production capabilities and the use of a high capacity WT, can independently ensure a positive NPV. This insight is valuable for system designers and stakeholders, underscoring the importance of incorporating such features during the design phase of conventional OFWE to enhance the TEP of the system.
- **External conditions**: The unpredictable nature of wind conditions and the expenditure landscape resulted in a highly significant influence on the TEP of the system. Section 7.8.2 describes the sensitivity of KPIs to different CAPEX scenarios and variations in wind speeds without altering additional conditions for the model. Both scenarios resulted in a notably elevated TEP, reaching positive system NPVs for both WF and IS.

In summary:

Under the analysed conditions, the addition of an H2 production system to OFWE does add to the TEP performance of the system when H2 is produced during hours of low power prices and consequently ensures system feasibility. Besides enhancing the TEP, it also mitigates risks of future uncertainties with respect to power prices. Under the condition that the OFWF uses WTs with a large capacity or the WF would be located at a location with more favorable wind conditions, feasibility can even be achieved for both the IS and the WF.

8.2. Recommendations

As outlined in the preceding section, this research serves as an illustrative example of the potential benefits of integrating hydrogen production with OFWE. The obtained results and acknowledged limitations of this study can lay the groundwork for further, more extensive research. The following summarizes the key findings and suggests areas for future exploration:

Extended Range of Locations

The case study focused on the Goto City wind farm in Japan. Future research could extend to other locations, considering diverse environmental conditions. Exploring H2 production's impact on OFWE under different conditions would further validate the generalizability of the findings.

Based on the findings derived from the modeled system, it may be suggested that the addition of hydrogen production to the Goto City WF could potentially enhance its performance or even render it economically viable in alternative locations. Notably, the current wind conditions at the designated site were identified as suboptimal. Thus, relocating the farm to a more favorable site could enhance its performance, given that power generation and subsequent revenue streams are highly dependent on the power output of the wind farm.

However, it is important to recognize that optimizing OFWE viability is dependent on a range of various parameters besides wind conditions alone. For instance, any alternative location should possess compatible electrical infrastructure and similar power market dynamics to those modeled for this research, as the operational schedule of the farm is largely influenced by prevailing power prices. Furthermore, the presence of a hydrogen-integrated economy can significantly influence the potential for system improvement. This research, in the reference case, considers a direct sale of the final hydrogen product at market prices, driven by Japan's steel industry. The absence of similar industrial sectors or other end-users of hydrogen could substantially impact the TEP of the system.

Hence, no definite claim can be made on the improvement of TEP for OFWE through hydrogen integration across different global locations, as such enhancements are dependent on a large range of parameters and external factors. To substantiate the statement that OFWE performance can be enhanced through hydrogen integration for alternative locations, a more detailed modeling of the system encompassing a variety of location and their specific conditions should be conducted.

Extrapolating Wind Speeds

This research adopted the assumption that the wind speed at hub height equals the wind speed recorded at 100 meters above sea level for the retrieved dataset. The difference between those wind speeds amounts to around 3%. However, sensitivity analyses revealed that relatively small variations in wind speed can have a substantially larger impact on the wind farm's power output. To enhance the accuracy of future research in representing power output at specific locations, extrapolating dataset wind speeds to match those at hub height is recommended. This adjustment would result in a more precise estimation of the wind farm's power output.

Power Price Prediction

This research employed historic power prices and literature-based predictions for future scenarios for the Japanese power market. Future studies could employ more sophisticated models for power price prediction to better capture the potential enhancement of OFWE in diverse future scenarios.

Influence of wave interaction

This research did not take into account the dynamic response of the floating wind turbine as a result of wave forces. The interplay between waves and floater might result in significantly higher operating and maintenance cost or even damage of system components as a result of heavy wave conditions. Further research could investigate the effect of this dynamic response to system performance.

Optimization of Operational Strategy

Analysing the best operational strategy is vital to maximise the potential of an IS. A way to optimise this operational strategy is using a module-based approach. This module-based approach would enable mode selection at each time step but would require more input from active hydrogen, power prices, wind speeds and other variables in order to optimize the system's performance.

Hydrogen System Efficiency Enhancement

Hydrogen system efficiency can be increased when more accurate and detailed models are applied with respect to the ones used in this research. This would enhance the overall system efficiency for a more accurate representation of system output. The current model uses a basic PEMEL cell with a set efficiency and degradation but more dynamics are at play with PEMEL cells which are deemed outside of the scope of this research. A more accurate H2 system efficiency would result in a more accurate representation of system performance.

Offshore Wind-to-Hydrogen Verification

This thesis represents a possible concept of an integrated offshore wind-to-hydrogen system and is not yet operational anywhere on earth. Verification of results from this and similar studies becomes challenging in the absence of actual, realized data. Future research could benefit from verification once such systems are commercially

operational, providing empirical evidence to support and strengthen the conclusions drawn from modeling.

References

[1] Iea - International Energy Agency. “Japan 2021 - Energy Policy Review”. In: (2021). URL: www.iea.org/t&c/.

[2] Irena – International Renewable Energy Agency. *FUTURE OF WIND Deployment, investment, technology, grid integration and socio-economic aspects A Global Energy Transformation paper Citation About IRENA*. IRENA, 2019. ISBN: 978-92-9260-155-3. URL: www.irena.org/publications..

[3] *(PDF) Assessment of wind resource for possibility of small wind turbine installation in Ilorin, Nigeria*. URL: https://www.researchgate.net/publication/307803793_Assessment_of_wind_resource_for_possibility_of_small_wind_turbine_installation_in_Ilorin_Nigeria.

[4] Zainul Abdin et al. “Large-scale stationary hydrogen storage via liquid organic hydrogen carriers”. In: (2021). DOI: 10.1016/j.isci. URL: https://doi.org/10.1016/j.isci..

[5] M S Adaramola and P.-Å Krogstad. “Experimental investigation of wake effects on wind turbine performance”. In: (2011). DOI: 10.1016/j.renene.2011.01.024.

[6] Faisal Alhumaidan, David Cresswell, and Arthur Garforth. “Hydrogen storage in liquid organic hydride: Producing hydrogen catalytically from methylcyclohexane”. In: *Energy and Fuels* 25.10 (Oct. 2011), pp. 4217–4234. ISSN: 08870624. DOI: 10.1021/EF200829X. URL: https://pubs.acs.org/sharingguidelines.

[7] By Amber. “A EUROPEAN HYDROGEN INFRASTRUCTURE VISION COVERING 28 COUNTRIES APRIL 2022”. In: (). URL: https://www.ehb.eu/maps.

[8] Olimpo Anaya-Lara et al. *Offshore wind energy generation: control, protection, and integration to electrical systems*. 1st ed. John Wiley & Sons, Incorporated, 2014.

[9] I Andrić et al. “Comparison of liquid hydrogen, methylcyclohexane and ammonia on energy efficiency and economy”. In: *Energy Procedia* 158 (2019), pp. 4086–4091. ISSN: 1876-6102. DOI: 10.1016/j.egypro.2019.01.827. URL: www.sciencedirect.comAvailableonlineatwww.sciencedirect.comwww.elsevier.com/locate/procedia1876-6102www.sciencedirect.comwww.elsevier.com/locate/procediawww.sciencedirect.comwww.elsevier.com/locate/procedia.

[10] Muhammad Aziz. *Liquid hydrogen: A review on liquefaction, storage, transportation, and safety*. Sept. 2021. DOI: 10.3390/en14185917.

[11] Aurélien Babarit et al. “Techno-economic feasibility of fleets of far offshore hydrogen-producing wind energy converters”. In: *International Journal of Hydrogen Energy* 43.15 (Apr. 2018), pp. 7266–7289. ISSN: 03603199. DOI: 10.1016/j.ijhydene.2018.02.144.

[12] Erin Bachynski, Maxime Thys, and Virgile Delhaye. “Dynamic response of a monopile wind turbine in waves: Experimental uncertainty analysis for validation of numerical tools”. In: (2019). DOI: 10.1016/j.apor.2019.05.002. URL: https://doi.org/10.1016/j.apor.2019.05.002.

[13] Philipp Beiter et al. “The Cost of Floating Offshore Wind Energy in California Between 2019 and 2032 Cost and Performance Results Data”. In: (). URL: www.nrel.gov/publications..

[14] David Berstad et al. “Liquid hydrogen as prospective energy carrier: A brief review and discussion of underlying assumptions applied in value chain analysis”. In: *Renewable and Sustainable Energy Reviews* 154 (Feb. 2022). ISSN: 18790690. DOI: 10.1016/j.rser.2021.111772.

[15] Camilla Nicol Bonacina, Nima Bordbar Gaskare, and Gianluca Valenti. “Assessment of offshore liquid hydrogen production from wind power for ship refueling”. In: *International Journal of Hydrogen Energy* 47.2 (Jan. 2022), pp. 1279–1291. ISSN: 03603199. DOI: 10.1016/j.ijhydene.2021.10.043.

[16] Jonathan Bosch, Iain Staffell, and Adam D. Hawkes. “Global levelised cost of electricity from offshore wind”. In: *Energy* 189 (Dec. 2019). ISSN: 03605442. DOI: 10.1016/j.energy.2019.116357.

[17] Ulf Bossel and Baldur Eliasson. *Energy Hydrogen Economy*. Tech. rep. ABB Switzerland, 2002.

[18] Giulio Buffo et al. “Energy and environmental analysis of a flexible Power-to-X plant based on Reversible Solid Oxide Cells (rSOCs) for an urban district”. In: *Journal of Energy Storage* 29 (June 2020). ISSN: 2352152X. DOI: 10.1016/j.est.2020.101314.

[19] Alexander Buttler and Hartmut Spliethoff. “Current status of water electrolysis for energy storage, grid balancing and sector coupling via power-to-gas and power-to-liquids: A review”. In: *Renewable and Sustainable Energy Reviews* 82 (Feb. 2018), pp. 2440–2454. ISSN: 18790690. DOI: 10.1016/J.RSER.2017.09.003.

[20] BVG Associates. *Wind farm costs | Guide to a floating offshore wind farm*. URL: https://guidetofloatingoffshorewind.com/wind-farm-costs/.

[21] Gonçalo Calado and Rui Castro. *Hydrogen production from offshore wind parks: Current situation and future perspectives*. June 2021. DOI: 10.3390/app11125561.

[22] Upeksha Caldera and Christian Breyer. “Learning Curve for Seawater Reverse Osmosis Desalination Plants: Capital Cost Trend of the Past, Present, and Future”. In: *Water Resources Research* 53.12 (Dec. 2017), pp. 10523–10538. ISSN: 19447973. DOI: 10.1002/2017WR021402.

[23] Laura Castro-Santos et al. “Economic feasibility of floating offshore wind farms”. In: *Energy* 112 (Oct. 2016), pp. 868–882. ISSN: 0360-5442. DOI: 10.1016/J.ENERGY.2016.06.135.

[24] Simonas Cerniauskas et al. “Future hydrogen markets for transportation and industry: The impact of CO2 taxes”. In: *Energies* 12.24 (Dec. 2019). ISSN: 19961073. DOI: 10.3390/en12244707.

[25] Yu Lin K. Chang et al. “July 2020 heavy rainfall in Japan: effect of real-time river discharge on ocean circulation based on a coupled river-ocean model”. In: *Ocean Dynamics* 73.5 (May 2023), pp. 249–265. ISSN: 16167228. DOI: 10.1007/s10236-023-01551-1.

[26] Chenyang Chu et al. “Hydrogen storage by liquid organic hydrogen carriers: Catalyst, renewable carrier, and technology-A review”. In: (2023). DOI: 10.1016/j.crcon.2023.03.007. URL: https://doi.org/10.1016/j.crcon.2023.03.007.

[27] William I.F. David et al. “Hydrogen production from ammonia using sodium amide”. In: *Journal of the American Chemical Society* 136.38 (Sept. 2014), pp. 13082–13085. ISSN: 15205126. DOI: 10.1021/JA5042836. URL: https://pubs.acs.org/sharingguidelines.

[28] *Day Ahead Market | Trading Market Data | Trading Information | JEPX*. URL: https://www.jepx.jp/en/electricpower/market-data/spot/.

[29] Ronald M. Dell, Patrick T. Moseley, and David A.J. Rand. “Hydrogen, Fuel Cells and Fuel Cell Vehicles”. In: *Towards Sustainable Road Transport*. Elsevier, 2014, pp. 260–295. DOI: 10.1016/b978-0-12-404616-0.00008-6.

[30] Van Nguyen Dinh et al. “Development of a viability assessment model for hydrogen production from dedicated offshore wind farms”. In: *International Journal of Hydrogen Energy* 46.48 (July 2021), pp. 24620–24631. ISSN: 03603199. DOI: 10.1016/j.ijhydene.2020.04.232.

[31] *Dolphyn Hydrogen*. URL: https://www.dolphynhydrogen.com/.

[32] *Electrical system*. URL: https://www.wind-energy-the-facts.org/electrical-system-7.html.

[33] ENERdata. *Japan sets feed-in tariff levels for renewable projects in 2022-2023 | Enerdata*. URL: https://www.enerdata.net/publications/daily-energy-news/japan-sets-feed-tariff-levels-renewable-projects-2022-2023.html.

[34] International Energy Agency. “Electricity Market Report_Update 2023”. In: (2023). URL: www.iea.org.

[35] *ERA5 hourly data on single levels from 1940 to present*. URL: https://cds.climate.copernicus.eu/cdsapp#!/dataset/reanalysis-era5-single-levels?tab=overview.

[36] “European Hydrogen Backbone HOW A DEDICATED HYDROGEN INFRASTRUCTURE CAN BE CREATED”. In: (2020). URL: https://transparency.entsog.eu/.

[37] Domenico Ferrero et al. “Power-to-Gas Hydrogen: Techno-economic Assessment of Processes towards a Multi-purpose Energy Carrier”. In: *Energy Procedia*. Vol. 101. Elsevier Ltd, Nov. 2016, pp. 50–57. DOI: 10.1016/j.egypro.2016.11.007.

[38] *Floating Substations: the next challenge on the path to commercial scale floating windfarms*. URL: https://www.dnv.com/article/floating-substations-the-next-challenge-on-the-path-to-commercial-scale-floating-windfarms-199213#.

[39] *Frequently Asked Questions (FAQs) - U.S. Energy Information Administration (EIA)*. URL: https://www.eia.gov/tools/faqs/faq.php?id=74&t=11.

[40] Alessandro Giampieri, Janie Ling-Chin, and Anthony Paul Roskilly. "Techno-economic assessment of offshore wind-to-hydrogen scenarios: A UK case study". In: *International Journal of Hydrogen Energy* (2023). ISSN: 03603199. DOI: 10.1016/J.IJHYDENE.2023.01.346.

[41] Dolf Gielen, Emanuele Taibi, and Raul Miranda. "HYDROGEN: A RENEWABLE ENERGY PERSPECTIVE". In: (2019). URL: www.irena.org.

[42] GlobalData. *Power plant profile: Goto Floating Wind Farm, Japan*. URL: https://www.power-technology.com/marketdata/power-plant-profile-goto-floating-wind-farm-japan/.

[43] Hemangi Gokhale. "Japan's carbon tax policy: Limitations and policy suggestions." In: *Current Research in Environmental Sustainability* 3 (2021), p. 100082. DOI: 10.1016/j.crsust.2021.100082. URL: https://doi.org/10.1016/j.crsust.2021.100082.

[44] Mika Goto and Toshiyuki Sueyoshi. "Electric power market reform in Japan after Fukushima Daiichi nuclear plant disaster Issues and future direction". In: *International Journal of Energy Sector Management* 9.3 (2015), pp. 336–360. DOI: 10.1108/IJESM-05-2014-0009. URL: www.emeraldinsight.com/1750-6220.htm.

[45] Muhammad Haris Hamayun et al. "Simulation study to investigate the effects of operational conditions on methylcyclohexane dehydrogenation for hydrogen production". In: *Energies* 13.1 (Jan. 2020). ISSN: 19961073. DOI: 10.3390/en13010206.

[46] *Hitachi, Ltd. HTW2.1-80A - 2,10 MW - Wind turbine*. URL: https://en.wind-turbine-models.com/turbines/2141-hitachi-ltd.-htw2.1-80a.

[47] Cassidy Houchins and Brian D James. "Hydrogen Storage Cost Analysis". In: (2022).

[48] *How Do Wind Turbines Survive Severe Storms? | Department of Energy*. URL: https://www.energy.gov/eere/articles/how-do-wind-turbines-survive-severe-storms.

[49] John Humphreys, Rong Lan, and Shanwen Tao. "Development and Recent Progress on Ammonia Synthesis Catalysts for Haber–Bosch Process". In: *Advanced Energy and Sustainability Research* 2.1 (Jan. 2021), p. 2000043. ISSN: 2699-9412. DOI: 10.1002/AESR.202000043.

[50] Timothy D. Hutty, Siyuan Dong, and Solomon Brown. "Suitability of energy storage with reversible solid oxide cells for microgrid applications". In: *Energy Conversion and Management* 226 (Dec. 2020). ISSN: 01968904. DOI: 10.1016/J.ENCONMAN.2020.113499.

[51] *Hywind Scotland - the world's first floating wind farm - Equinor*. URL: https://www.equinor.com/energy/hywind-scotland.

[52] *Hywind Tampen - Equinor*. URL: https://www.equinor.com/energy/hywind-tampen.

[53] Omar S. Ibrahim et al. *Dedicated large-scale floating offshore wind to hydrogen: Assessing design variables in proposed typologies*. May 2022. DOI: 10.1016/j.rser.2022.112310.

[54] Jussi Ik et al. "Power-to-ammonia in future North European 100 % renewable power and heat system". In: (2018). DOI: 10.1016/j.ijhydene.2018.06.121. URL: https://doi.org/10.1016/j.ijhydene.2018.06.121.

[55] Sung Ju Im et al. "Techno-economic evaluation of an element-scale forward osmosis-reverse osmosis hybrid process for seawater desalination". In: *Desalination* 476 (Feb. 2020), p. 114240. ISSN: 0011-9164. DOI: 10.1016/J.DESAL.2019.114240.

[56] The International Renewable Energy Agency. *GREEN HYDROGEN COST REDUCTION SCALING UP ELECTROLYSERS TO MEET THE 1.5° C CLIMATE GOAL H 2 O 2*. IRENA, 2020. ISBN: 9789292602956. URL: www.irena.org/publications.

[57] The International Renewable Energy Agency. "GREEN HYDROGEN COST REDUCTION SCALING UP ELECTROLYSERS TO MEET THE 1.5°C CLIMATE GOAL H 2 O 2". In: (2020). URL: www.irena.org/publications.

[58] *Japan readies to lead the world in offshore wind*. URL: https://www.energymonitor.ai/renewables/japan-readies-to-lead-the-world-in-offshore-wind/.

[59] *Japan sets feed-in tariff levels for renewable projects in 2022-2023 | Enerdata*. URL: https://www.enerdata.net/publications/daily-energy-news/japan-sets-feed-tariff-levels-renewable-projects-2022-2023.html.

[60] *Japan steelmakers lay out road map for a hydrogen-electric future - Nikkei Asia*. URL: https://asia.nikkei.com/Business/Materials/Japan-steelmakers-lay-out-road-map-for-a-hydrogen-electric-future.

[61] *Japan: estimated green hydrogen production cost per kilogram 2050 | Statista*. URL: https://www.statista.com/statistics/1304507/japan-green-hydrogen-production-cost-per-kilogram/.

[62] *Japan: Goto City Aims to Become 'Islands of Energy' by Harnessing Offshore Wind*. URL: https://www.renewableenergyworld.com/baseload/hydropower/japan-goto-city-aims-to-become-islands-of-energy-by-harnessing-offshore-wind/#gref.

[63] *Japan's coastal sea floor topography - Stock Image - C008/9969 - Science Photo Library*. URL: https://www.sciencephoto.com/media/152655/view/japan-s-coastal-sea-floor-topography.

[64] *Japan's Big Bet on Hydrogen – ESG Investor*. URL: https://www.esginvestor.net/japans-big-bet-on-hydrogen/.

[65] Morten Kofoed Jensen. "LCOE Update and Recent Trends - Offshore Wind". In: (2022).

[66] Johan Meyers. "Optimal turbine spacing in fully developed wind farm boundary layers". In: *Wind energy* 15.2 (2012), pp. 305–317.

[67] Mert Kaptan et al. "Analysis of spar and semi-submersible floating wind concepts with respect to human exposure to motion during maintenance operations". In: *Marine Structures* 83 (May 2022). ISSN: 09518339. DOI: 10.1016/J.MARSTRUC.2021.103145.

[68] M. A. Khan et al. "Seawater electrolysis for hydrogen production: A solution looking for a problem?" In: *Energy and Environmental Science* 14.9 (Sept. 2021), pp. 4831–4839. ISSN: 17545706. DOI: 10.1039/d1ee00870f.

[69] Hirokazu Kojima et al. "Methylcyclohexane production under fluctuating hydrogen flow rate conditions". In: (2021). DOI: 10.1016/j.ijhydene.2020.12.117. URL: https://doi.org/10.1016/j.ijhydene.2020.12.117.

[70] Søren Krohn, Poul-Erik Morthorst, and Shimon Awerbuch. "The Economics of Wind Energy A report by the European Wind Energy Association". In: (). URL: www.inextremis.be.

[71] Padmavathi Lakshmanan, Ruijuan Sun, and Jun Liang. "Electrical Collection Systems for Offshore Wind Farms: A Review". In: *CSEE JOURNAL OF POWER AND ENERGY SYSTEMS* 7.5 (2021). DOI: 10.17775/CSEEJPES.2020.05050. URL: https://orcid.org/0000-0002-4525-2741.

[72] Han Soo Lee et al. "STORM SURGE IN SETO INLAND SEA WITH CONSIDERATION OF THE IMPACTS OF WAVE BREAKING ON SURFACE CURRENTS". In: *Coastal Engineering Proceedings* 32 (Jan. 2011), p. 17. ISSN: 0589-087X. DOI: 10.9753/ICCE.V32.CURRENTS.17.

[73] William C Leighty and John H Holbrook. "Alternatives to Electricity for Transmission, Firming Storage, and Supply Integration for Diverse, Stranded, Renewable Energy Resources: Gaseous Hydrogen and Anhydrous Ammonia Fuels via Underground Pipelines Selection and/or peer-review under responsibility of Canadian Hydrogen and Fuel Cell Association". In: *Energy Procedia* 29 (2012), pp. 332–346. DOI: 10.1016/j.egypro.2012.09.040. URL: www.sciencedirect.com.

[74] Markus Lerch, Mikel De-Prada-Gil, and Climent Molins. "Collection Grid Optimization of a Floating Offshore Wind Farm Using Particle Swarm Theory". In: *Journal of Physics: Conference Series*. Vol. 1356. 1. Institute of Physics Publishing, Oct. 2019. DOI: 10.1088/1742-6596/1356/1/012012.

[75] *Liquid Storage Vessels | Hydrogen Tools*. URL: https://h2tools.org/bestpractices/liquid-storage-vessels.

[76] Baolong Liu and Jianxing Yu. "Dynamic Response of SPAR-Type Floating Offshore Wind Turbine under Wave Group Scenarios". In: *Energies* 15.13 (July 2022). ISSN: 19961073. DOI: 10.3390/en15134870.

[77] Boming Liu et al. “Estimating hub-height wind speed based on a machine learning algorithm: Implications for wind energy assessment”. In: *Atmospheric Chemistry and Physics* 23.5 (Mar. 2023), pp. 3181–3193. ISSN: 16807324. DOI: 10.5194/ACP-23-3181-2023.

[78] Yichao Liu et al. *Developments in semi-submersible floating foundations supporting wind turbines: A comprehensive review*. July 2016. DOI: 10.1016/j.rser.2016.01.109.

[79] *Lower and Higher Heating Values of Fuels | Hydrogen Tools*. URL: https://h2tools.org/hyarc/calculator-tools/lower-and-higher-heating-values-fuels.

[80] Yuehong Lu et al. “A Critical Review of Sustainable Energy Policies for the Promotion of Renewable Energy Sources”. In: *Sustainability 2020, Vol. 12, Page 5078* 12.12 (June 2020), p. 5078. ISSN: 2071-1050. DOI: 10.3390/SU12125078. URL: https://www.mdpi.com/2071-1050/12/12/5078/htm%20https://www.mdpi.com/2071-1050/12/12/5078.

[81] Zhibin Luo et al. “Hydrogen production from offshore wind power in South China”. In: *International Journal of Hydrogen Energy* 47.58 (July 2022), pp. 24558–24568. ISSN: 03603199. DOI: 10.1016/j.ijhydene.2022.03.162.

[82] Kai-Tung Ma et al. “Mooring design”. In: *Mooring System Engineering for Offshore Structures*. Elsevier, 2019, pp. 63–83. DOI: 10.1016/b978-0-12-818551-3.00004-1.

[83] Jun Maekawa et al. “The Effect of Renewable Energy Generation on the Electric Power Spot Price of the Japan Electric Power Exchange”. In: (). DOI: 10.3390/en11092215. URL: www.mdpi.com/journal/energies.

[84] C. Maienza et al. “A life cycle cost model for floating offshore wind farms”. In: *Applied Energy* 266 (May 2020). ISSN: 03062619. DOI: 10.1016/j.apenergy.2020.114716.

[85] André Månsson. “Energy, conflict and war: Towards a conceptual framework”. In: *Energy Research & Social Science* 4 (2014), pp. 106–116. DOI: 10.1016/j.erss.2014.10.004. URL: http://dx.doi.org/10.1016/j.erss.2014.10.004.

[86] Ahmad Mayyas et al. *Manufacturing Cost Analysis for Proton Exchange Membrane Water Electrolyzers*. Tech. rep. National Renewable Energy Laboratory, 2019. URL: https://www.nrel.gov/docs/fy10osti/72740.pdf..

[87] Eric R. Morgan, James F. Manwell, and Jon G. McGowan. *Sustainable Ammonia Production from U.S. Offshore Wind Farms: A Techno-Economic Review*. Nov. 2017. DOI: 10.1021/acssuschemeng.7b02070.

[88] Anders Myhr et al. “Levelised cost of energy for offshore floating wind turbines in a life cycle perspective”. In: (2014). DOI: 10.1016/j.renene.2014.01.017. URL: http://dx.doi.org/10.1016/j.renene.2014.01.017.

[89] R M Nayak-Luke et al. “Techno-Economic Aspects of Production, Storage and Distribution of Ammonia”. In: (2021). DOI: 10.1016/B978-0-12-820560-0.00008-4. URL: https://doi.org/10.1016/B978-0-12-820560-0.00008-4.

[90] Mojtaba Nedaei. “Wind resource assessment in abadan airport in Iran”. In: *International Journal of Renewable Energy Development* 1.3 (Oct. 2012), pp. 87–97. ISSN: 22524940. DOI: 10.14710/IJRED.1.3.87-97.

[91] NEL. *NEL Containerized PEM Electrolyser*. May 2023.

[92] *NREL Floats New Offshore Wind Cost Optimization Vision | News | NREL*. URL: https://www.nrel.gov/news/program/2020/nrel-floats-new-offshore-wind-cost-optimization-tool.html.

[93] T. Numazawa et al. “Magnetic refrigerator for hydrogen liquefaction”. In: *Cryogenics* 62 (2014), pp. 185–192. ISSN: 00112275. DOI: 10.1016/J.CRYOGENICS.2014.03.016.

[94] *Offshore Construction Starts on Japan’s First Floating Wind Farm | Offshore Wind*. URL: https://www.offshorewind.biz/2022/10/18/offshore-construction-starts-on-japans-first-floating-wind-farm/.

[95] *Offshore grid connection Borssele Beta ready to land offshore wind power - TenneT*. URL: https://netztransparenz.tennet.eu/tinyurl-storage/detail/offshore-grid-connection-borssele-beta-ready-to-land-offshore-wind-power/.

[96] "Outline of Strategic Energy Plan Agency for Natural Resources and Energy". In: (2021).

[97] *Outline of Transaction | Trading Information | Japan Electric Power Exchange (JEPX)*. URL: https://www.jepx.jp/en/electricpower/outline/.

[98] "Overview of Basic Hydrogen Strategy Background and overall view of updated Basic Hydrogen Strategy". In: (2023).

[99] Dionissios D Papadias, Jui-Kun Peng, and Rajesh K Ahluwalia. "Hydrogen carriers: Production, transmission, decomposition, and storage". In: (2021). DOI: 10.1016/j.ijhydene.2021.05.002. URL: https://doi.org/10.1016/j.ijhydene.2021.05.002.

[100] Michael Penev, Jarett Zuboy, and Chad Hunter. "Economic analysis of a high-pressure urban pipeline concept (HyLine) for delivering hydrogen to retail fueling stations". In: *Transportation Research Part D: Transport and Environment* 77 (Dec. 2019), pp. 92–105. ISSN: 1361-9209. DOI: 10.1016/J.TRD.2019.10.005.

[101] *Plan for Public Tender for Occupancy for the Offshore Wind Power Generation Project in Goto City, Nagasaki Prefecture Has Been Certified*. URL: https://www.meti.go.jp/english/press/2022/0426_002.html.

[102] *Princess Amalia | Windpowernl*. URL: https://windpowernl.com/2021/02/23/princess-amalia-offshore-wind-farm/.

[103] *Reverse Osmosis Desalination Systems | Crystal Quest – Crystal Quest Water Filters*. URL: https://crystalquest.com/pages/reverse-osmosis-desalination-systems.

[104] Jochen M Schmittmann. *The Financial Impact of Carbon Taxation on Corporates Japan*. Tech. rep.

[105] Giuseppe Sdanghi et al. "Towards non-mechanical hybrid hydrogen compression for decentralized hydrogen facilities". In: *Energies* 13.12 (June 2020). ISSN: 19961073. DOI: 10.3390/en13123145.

[106] Tomoharu Senjyu and Kohei Shiota. "Revisit the Upper Portion of the Japan Sea Proper Water: A Recent Structural Change and Freshening in the Formation Area". In: *Journal of Geophysical Research: Oceans* 128.1 (Jan. 2023). ISSN: 21699291. DOI: 10.1029/2022JC019094.

[107] Hyun Kyu Shin and Sung Kyu Ha. *A Review on the Cost Analysis of Hydrogen Gas Storage Tanks for Fuel Cell Vehicles*. July 2023. DOI: 10.3390/en16135233.

[108] Priyadarshi R Shukla et al. "Climate Change 2022 Mitigation of Climate Change Working Group III Contribution to the Sixth Assessment Report of the Intergovernmental Panel on Climate Change Summary for Policymakers Edited by". In: (2022). URL: www.ipcc.ch.

[109] Alessandro Singlitico, Jacob Østergaard, and Spyros Chatzivasileiadis. "Onshore, offshore or in-turbine electrolysis? Techno-economic overview of alternative integration designs for green hydrogen production into Offshore Wind Power Hubs". In: *Renewable and Sustainable Energy Transition* 1 (2021), p. 100005. DOI: 10.1016/j.rset.2021.100005. URL: https://doi.org/10.1016/j.rset.2021.100005.

[110] *Small-scale ammonia: where the economics work and the technology is ready – Ammonia Energy Association*. URL: https://www.ammoniaenergy.org/articles/small-scale-ammonia-where-the-economics-work-and-the-technology-is-ready/.

[111] *Structural Defects Delay Japan's First Floating Offshore Wind Farm | Offshore Wind*. URL: https://www.offshorewind.biz/2023/09/22/structural-defects-delay-japans-first-floating-offshore-wind-farm/.

[112] *Sustainability | Energy from green hydrogen will be expensive, even in 2050*. URL: https://sustainability.crugroup.com/article/energy-from-green-hydrogen-will-be-expensive-even-in-2050.

[113] Daniel Teichmann, Wolfgang Arlt, and Peter Wasserscheid. "Liquid Organic Hydrogen Carriers as an efficient vector for the transport and storage of renewable energy". In: (2012). DOI: 10.1016/j.ijhydene.2012.08.066. URL: http://dx.doi.org/10.1016/j.ijhydene.2012.08.066.

[114] *The history of wind energy subsidies | World Economic Forum*. URL: https://www.weforum.org/agenda/2015/01/the-history-of-wind-energy-subsidies/.

[115] Juan Tomasini et al. "Assessment of the Potential for Hydrogen Production from Bottom Fixed Offshore Wind in Uruguay". In: *Proceedings of the Annual Offshore Technology Conference*. Offshore Technology Conference, 2022. ISBN: 9781613998526. DOI: 10.4043/31879-MS.

[116] Agung Tri Wijayanta et al. “Liquid hydrogen, methylcyclohexane, and ammonia as potential hydrogen storage: Comparison review”. In: (2019). DOI: 10.1016/j.ijhydene.2019.04.112. URL: https://doi.org/10.1016/j.ijhydene.2019.04.112.

[117] *Types of Fuel Cells | Department of Energy*. URL: https://www.energy.gov/eere/fuelcells/types-fuel-cells.

[118] *Understanding the cost drivers of SWRO | Danfoss*. URL: https://www.danfoss.com/en/about-danfoss/articles/dhs/understanding-the-cost-drivers-of-swro/.

[119] UNFCCC. *Climate Plans Remain Insufficient: More Ambitious Action Needed Now | UNFCCC*. URL: https://unfccc.int/news/climate-plans-remain-insufficient-more-ambitious-action-needed-now.

[120] UNFCCC. *The Paris Agreement | UNFCCC*. URL: https://unfccc.int/process-and-meetings/the-paris-agreement.

[121] B. Van Eeckhout et al. “Economic comparison of VSC HVDC and HVAC as transmission system for a 300MW offshore wind farm”. In: *European Transactions on Electrical Power* 20.5 (July 2010), pp. 661–671. ISSN: 1430144X. DOI: 10.1002/etep.359.

[122] *Vestas V80-2.0 - 2,00 MW - Wind turbine*. URL: https://en.wind-turbine-models.com/turbines/19-vestas-v80-2.0.

[123] *Volume to Weight conversions for common substances and materials*. URL: https://www.aqua-calc.com/calculate/volume-to-weight.

[124] Piotr Wais. “A review of Weibull functions in wind sector”. In: (2016). DOI: 10.1016/j.rser.2016.12.014. URL: http://dx.doi.org/10.1016/j.rser.2016.12.014.

[125] Ganzhou Wang, Alexander Mitsos, and Wolfgang Marquardt. “Conceptual design of ammonia-based energy storage system: System design and time-invariant performance”. In: *AIChE Journal* 63.5 (May 2017), pp. 1620–1637. ISSN: 15475905. DOI: 10.1002/AIC.15660.

[126] Hanchu Wang, Prodromos Daoutidis, and Qi Zhang. “Harnessing the Wind Power of the Ocean with Green Offshore Ammonia”. In: *ACS Sustainable Chemistry and Engineering* 9.43 (Nov. 2021), pp. 14605–14617. ISSN: 21680485. DOI: 10.1021/acssuschemeng.1c06030.

[127] “Wave Loads on Ships”. In: *Elsevier Ocean Engineering Series* 4.C (Jan. 2001), pp. 123–178. ISSN: 1571-9952. DOI: 10.1016/S1571-9952(01)80006-4.

[128] *Will wind-wake slow industry’s ambitions offshore? | Recharge*. URL: https://www.rechargenews.com/wind/will-wind-wake-slow-industrys-ambitions-offshore-/2-1-699430.

[129] *Wind farm costs – Guide to an offshore wind farm*. URL: https://guidetoanoffshorewindfarm.com/wind-farm-costs.

[130] *World’s first offshore green hydrogen production platform inaugurated in France - Offshore Energy*. URL: https://www.offshore-energy.biz/worlds-first-offshore-green-hydrogen-production-platform-inaugurated-france/.

[131] Yamin Yan et al. “Roadmap to hybrid offshore system with hydrogen and power co-generation”. In: *Energy Conversion and Management* 247 (Nov. 2021). ISSN: 01968904. DOI: 10.1016/j.enconman.2021.114690.

[132] Andreas Zauner et al. “Innovative large-scale energy storage technologies and Power-to-Gas concepts after optimization Analysis on future technology options and on techno-economic optimization”. In: (2019).

[133] Tongtong Zhang et al. *Hydrogen liquefaction and storage: Recent progress and perspectives*. Apr. 2023. DOI: 10.1016/j.rser.2023.113204.

[134] Jinyang Zheng et al. “Development of high pressure gaseous hydrogen storage technologies”. In: (2011). DOI: 10.1016/j.ijhydene.2011.02.125.

[135] E I Zountouridou et al. “Offshore floating wind parks in the deep waters of Mediterranean Sea”. In: (2015). DOI: 10.1016/j.rser.2015.06.027. URL: http://dx.doi.org/10.1016/j.rser.2015.06.027.

A

Appendix: Flow Diagrams

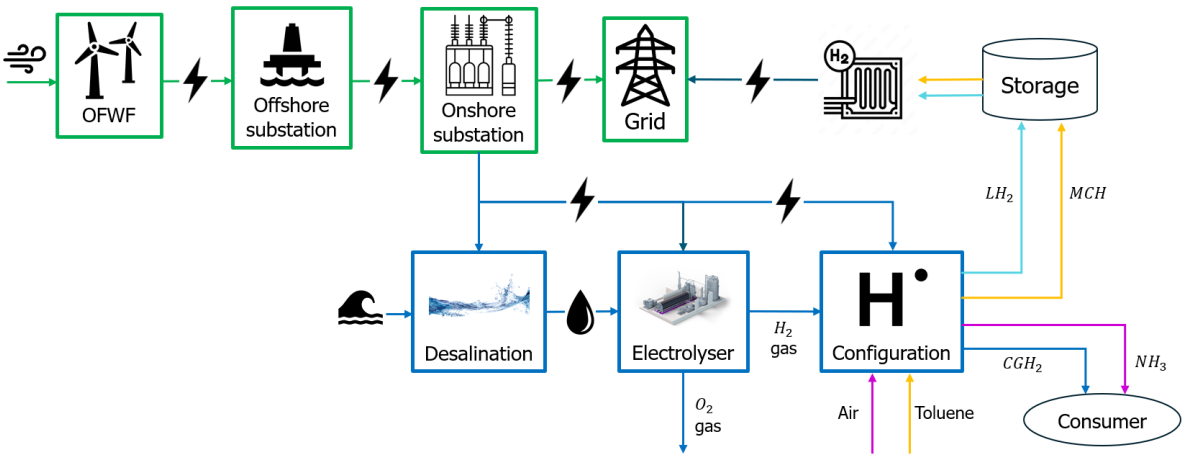

Figure A.1: System build-up in conventional OFWF mode (Green) and in W2H mode (Blue)

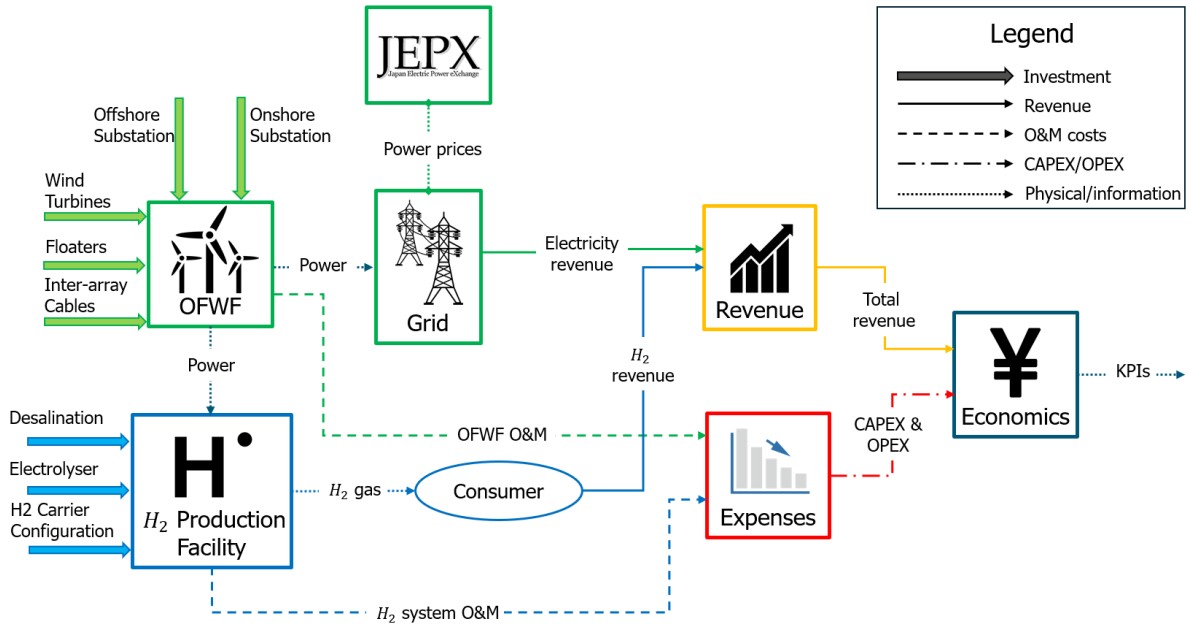

Figure A.2: Flow diagram of the economics of the OFWF (Green) and the integrated system (Blue). Striped lines indicate expenses and solid lines indicate income. Dotted lines indicate physical flows or information.

B

Appendix:Analysis Figures

B.1. Base Case

The section includes the yearly cash flow and NPV development graph from the model for the base case. Cash flow figures illustrate the total gained revenue and operating expenses from both the WF and IS and the resulting cash flow of the year. NPV figures illustrate the annual development of system value over its operational lifetime.

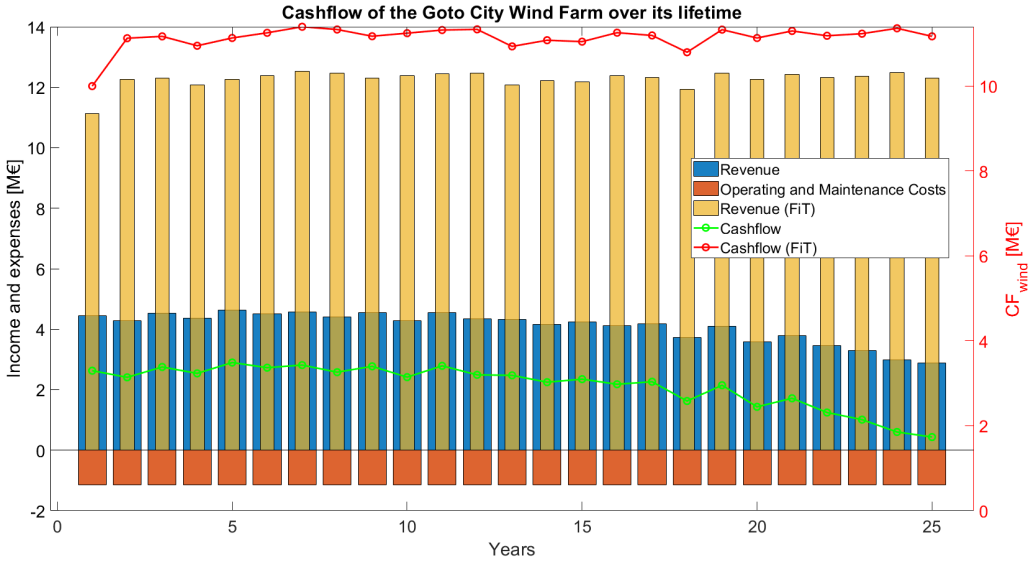

Figure B.1: Cash Flow of the Goto City Wind Farm over the operational lifetime with and without a governmental FiT

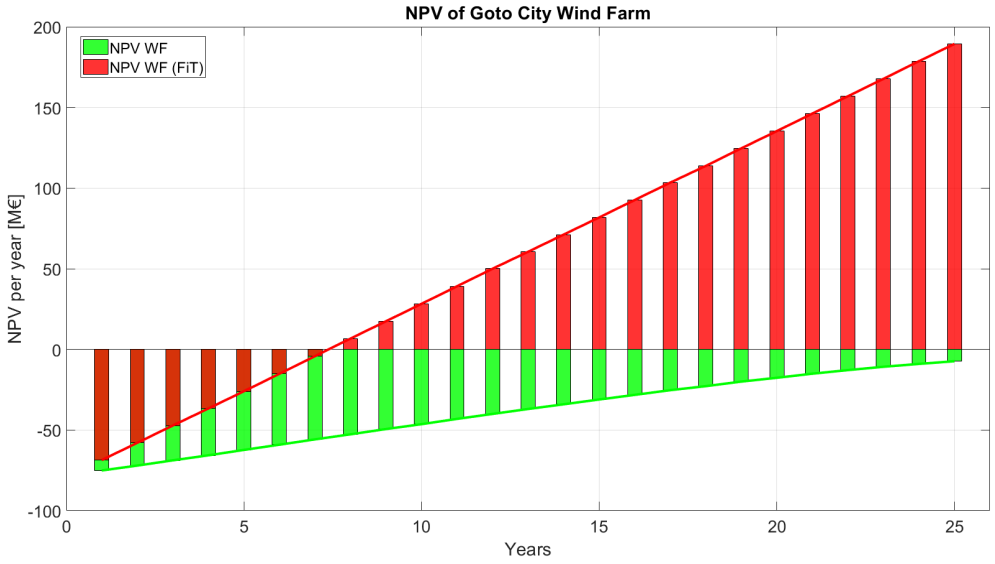

Figure B.2: NPV of the Goto City Wind Farm over the operational lifetime with and without a governmental FiT

B.2. Reference Case

The section includes the yearly cash flow and NPV development graph from the model for the reference case. Cash flow figures illustrate the total gained revenue and operating expenses from both the WF and IS and the resulting cash flow of the year. NPV figures illustrate the annual development of system value over its operational lifetime.

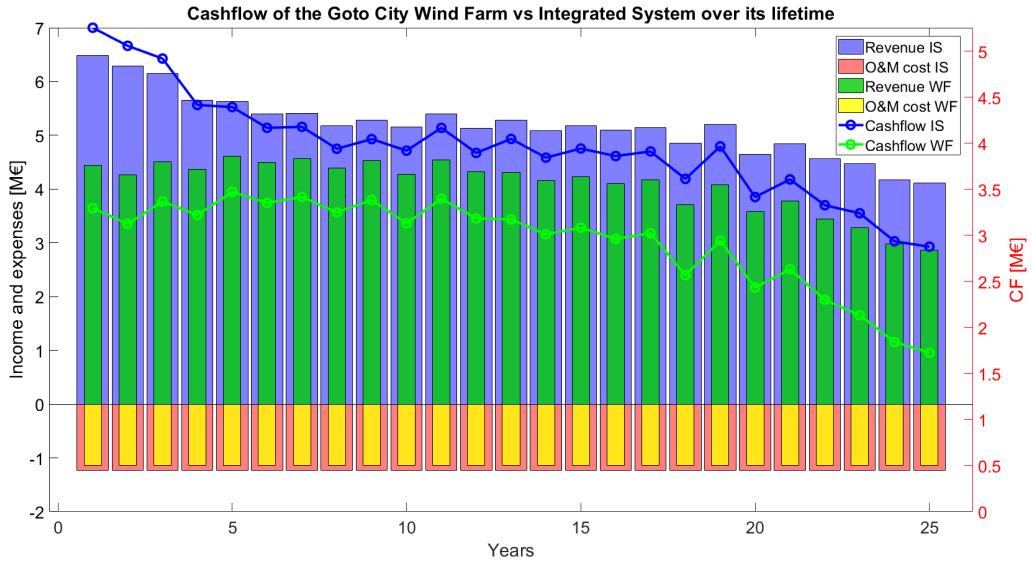

Figure B.3: Cash Flow over total lifetime of the integrated system compared to conventional OFWF

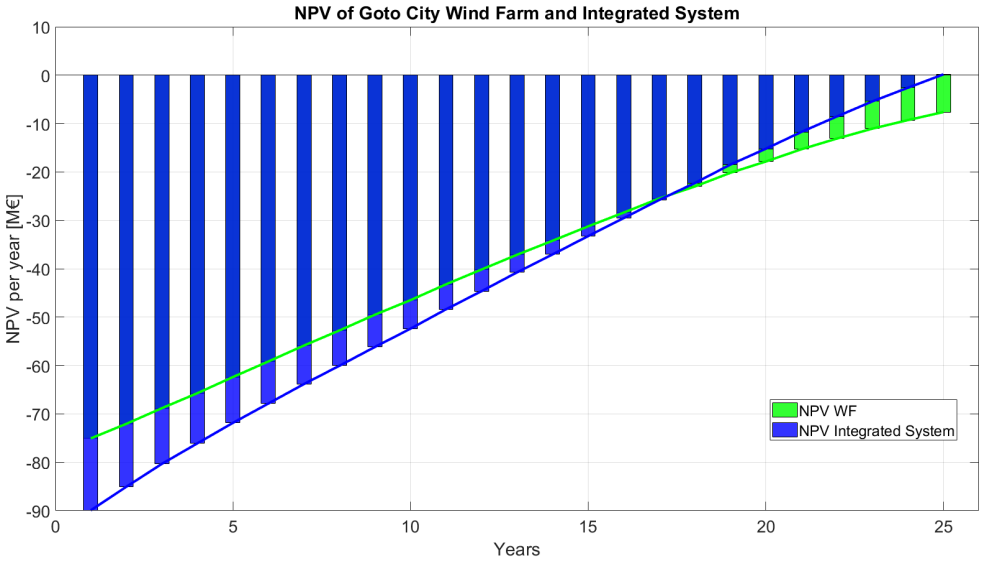

Figure B.4: NPV over total lifetime of the integrated system compared to conventional OFWF

B.3. Configuration Analysis

The section includes the yearly cash flow and NPV development graph from the model for the configuration analysis. Cash flow figures illustrate the total gained revenue and operating expenses from both the WF and IS and the resulting cash flow of the year. NPV figures illustrate the annual development of system value over its operational lifetime.

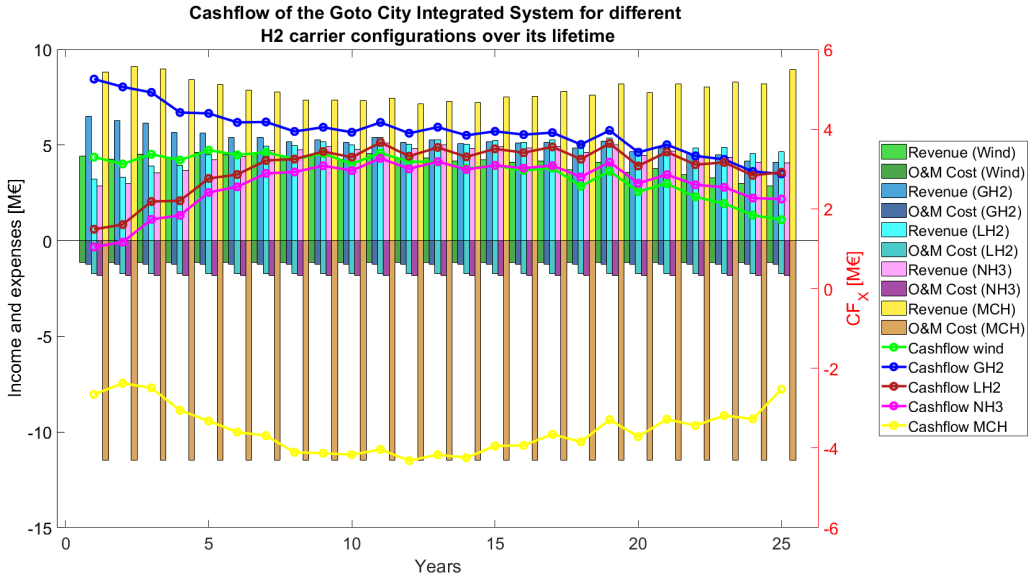

Figure B.5: Cashflow for different hydrogen carrier configurations.

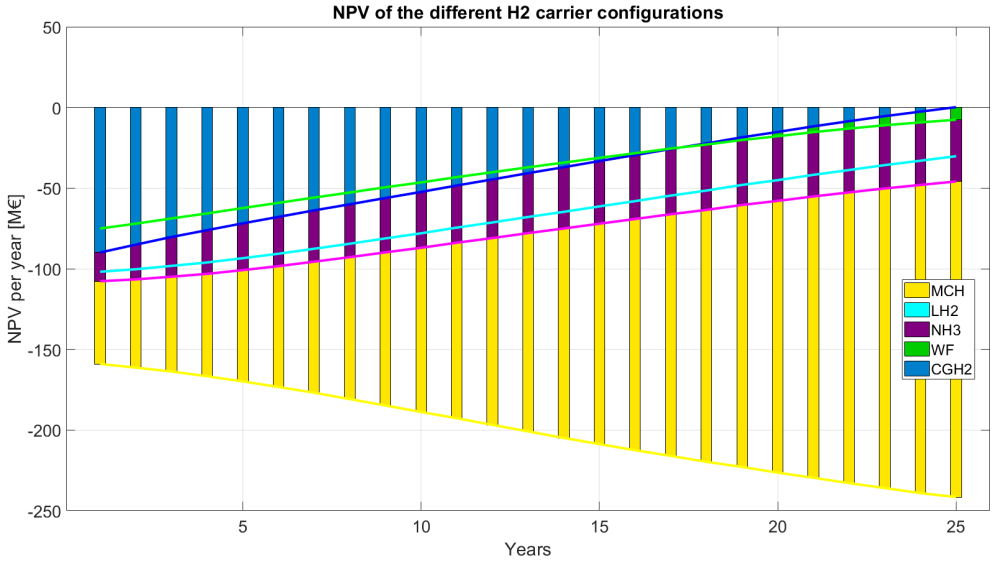

Figure B.6: NPV for different hydrogen carrier configurations.

B.4. Capacity Analysis

The section includes the yearly cash flow and NPV development graph from the model for the capacity analysis. Cash flow figures illustrate the total gained revenue and operating expenses from both the WF and IS and the resulting cash flow of the year. NPV figures illustrate the annual development of system value over its operational lifetime.

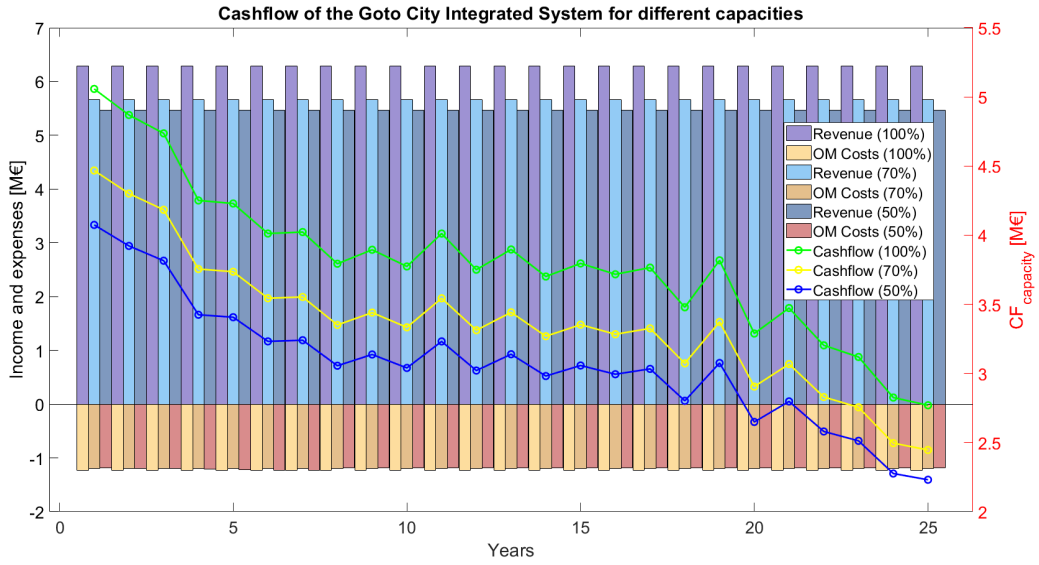

Figure B.7: Cash Flow of the integrated system over its lifetime for different installed H2 production capacities

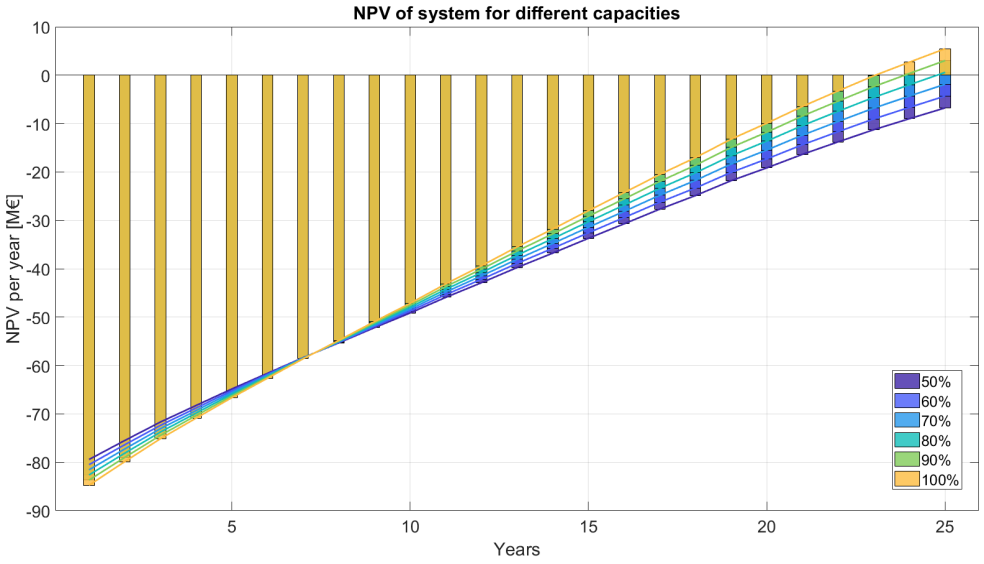

Figure B.8: NPV of the integrated system over its lifetime for different installed H2 production capacities

B.5. Scenario Analyses

The section includes the yearly cash flow and NPV development graph from the model for the scenario analyses. Cash flow figures illustrate the total gained revenue and operating expenses from both the WF and IS and the resulting cash flow of the year. NPV figures illustrate the annual development of system value over its operational lifetime.

B.5.1. H2 price scenario

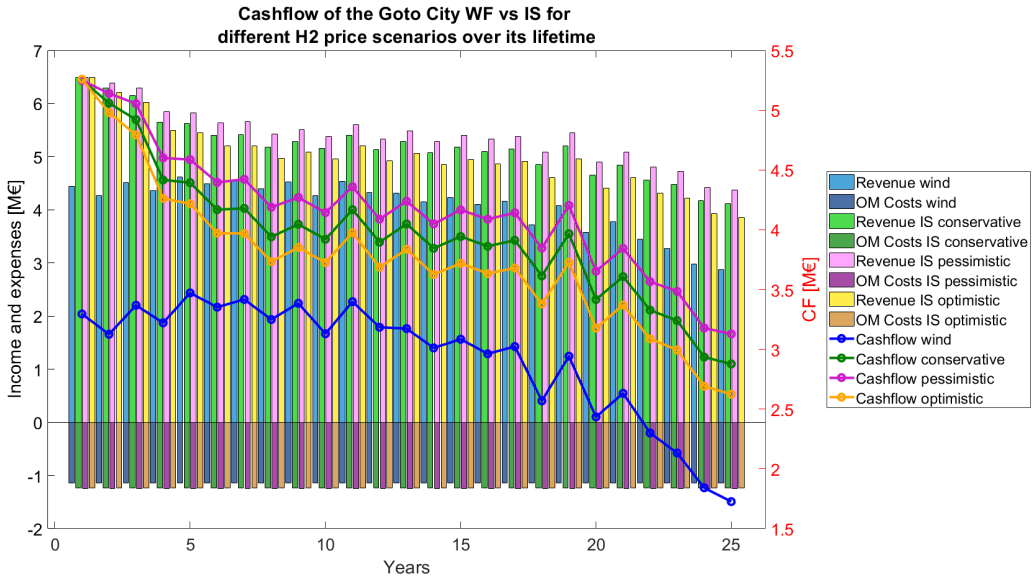

Figure B.9: The Cashflow of the integrated system over the lifetime for different scenarios for H2 price.

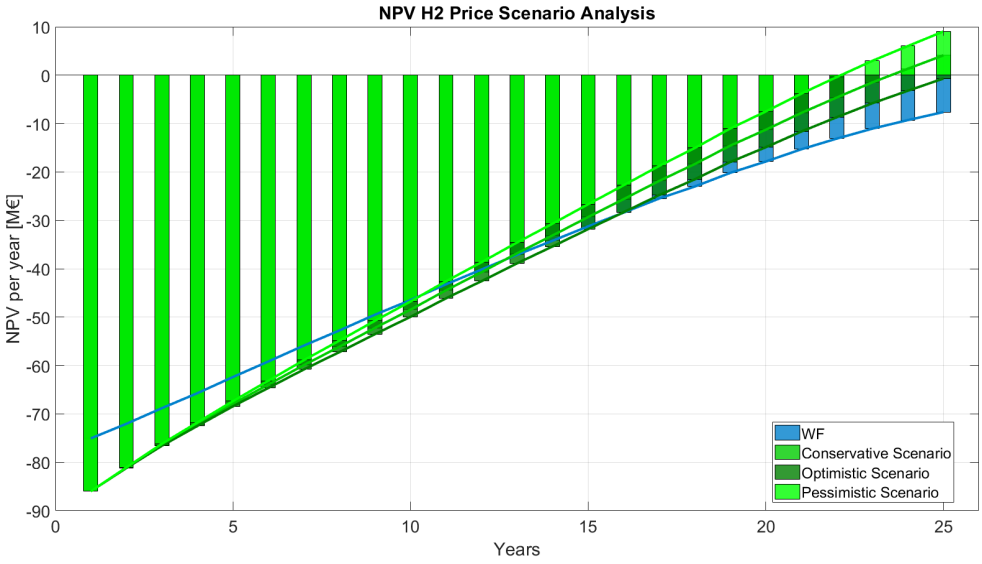

Figure B.10: The NPV of the integrated system over the lifetime for different scenarios for H2 price.

B.5.2. Power Price Scenario

Power Price Datasets

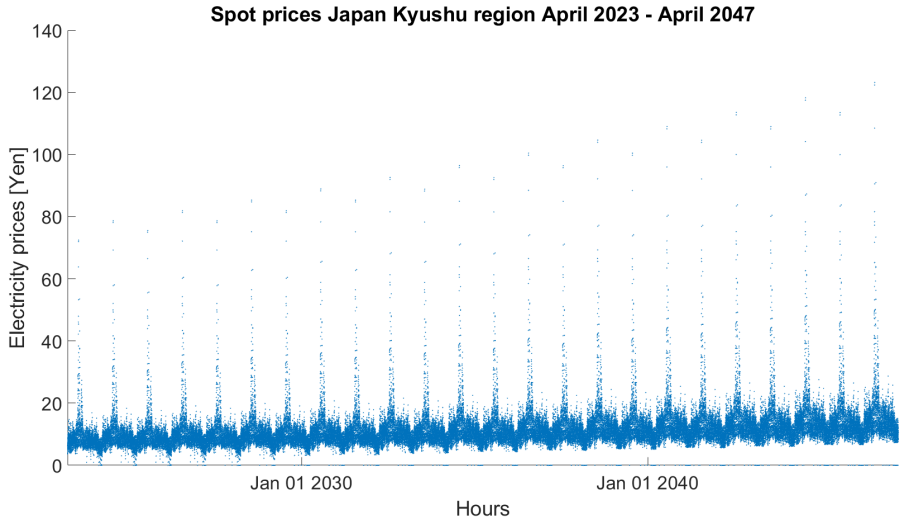

Figure B.11: Prediction on the future electricity prices for Japan during the lifetime of the Goto City Wind Farm for the optimistic scenario

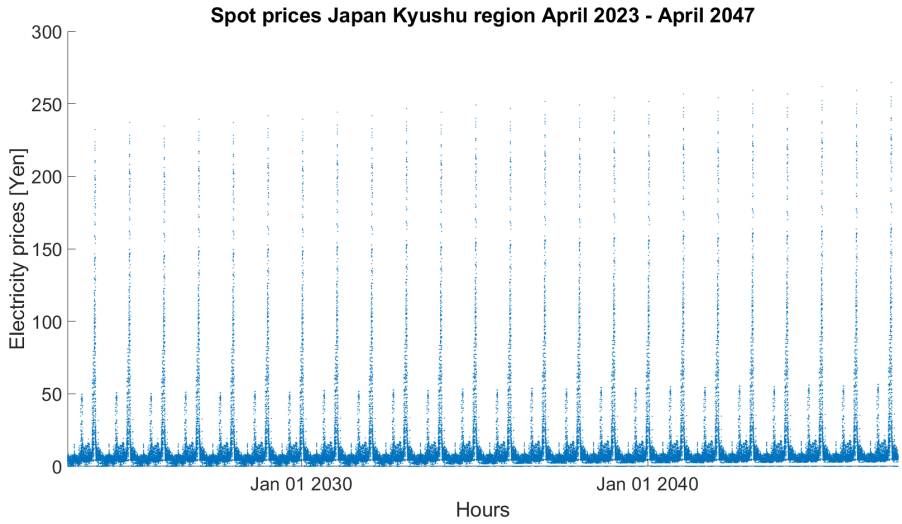

Figure B.12: Prediction on the future electricity prices for Japan during the lifetime of the Goto City Wind Farm for the pessimistic scenario

Operational Schedules

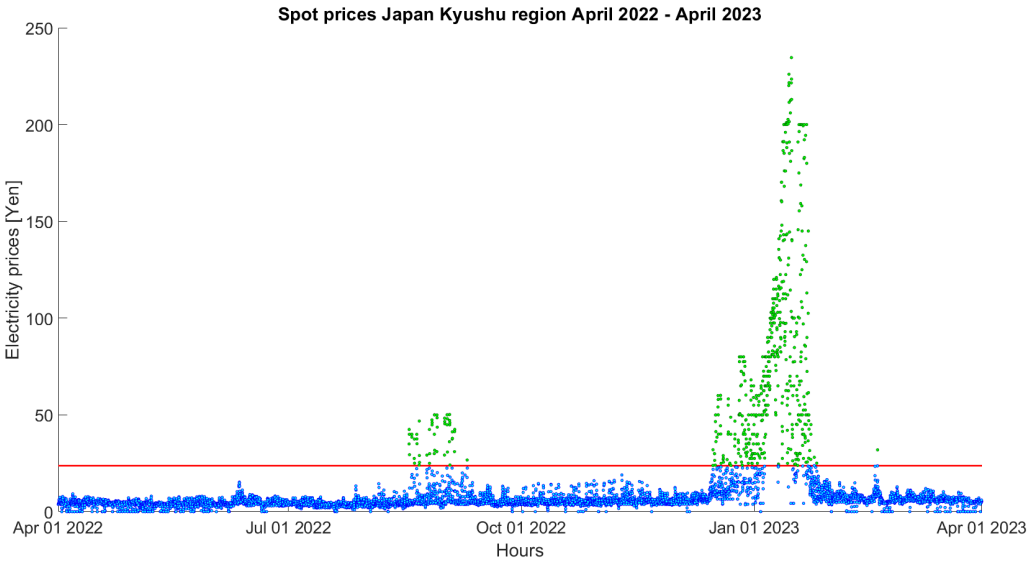

Figure B.13: Operational hours in the first year of Goto City Wind Farm for a pessimistic power price scenario

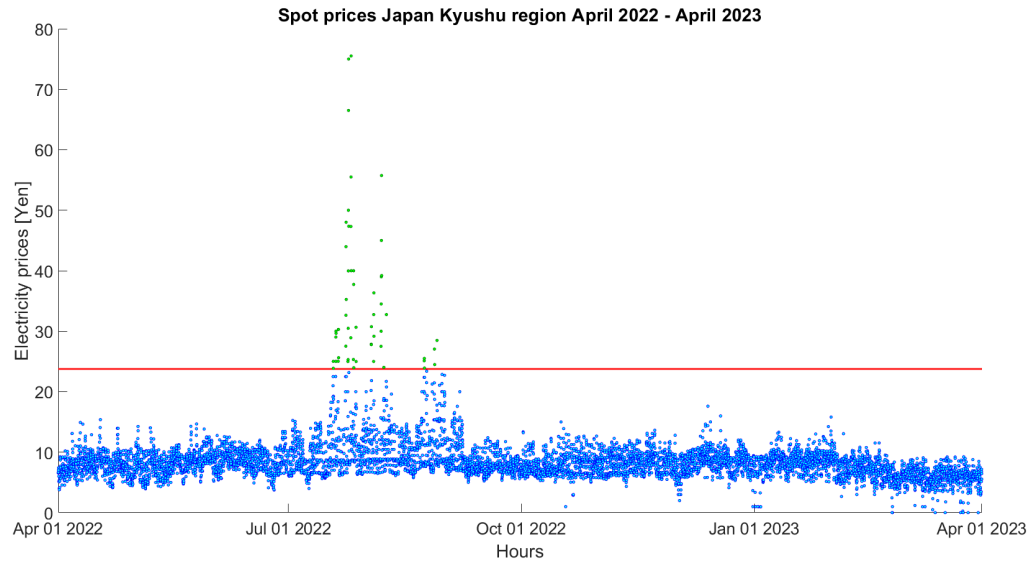

Figure B.14: Operational hours in the first year of Goto City Wind Farm for an optimistic power price scenario

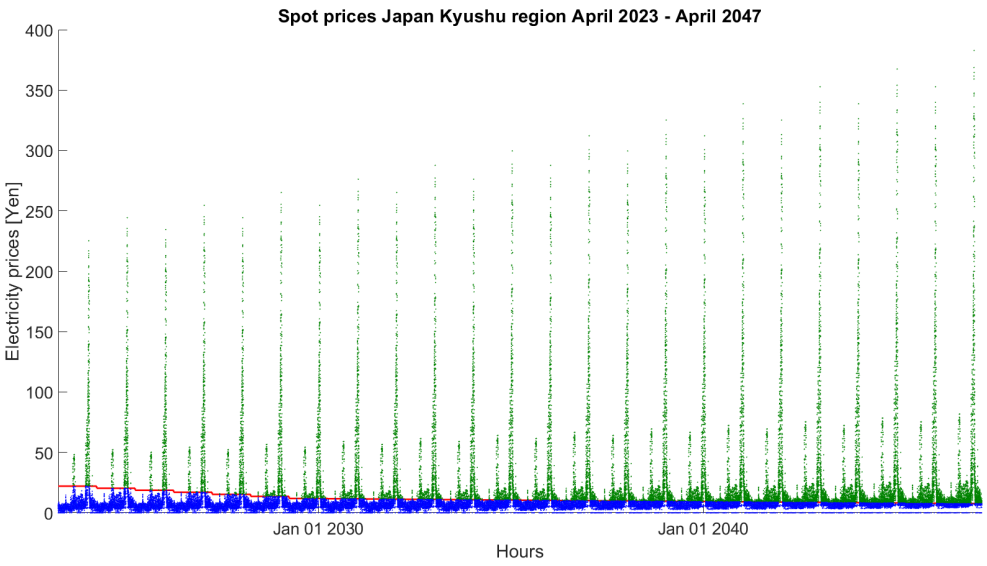

Figure B.15: Operational hours of Goto City Wind Farm for a pessimistic power price scenario

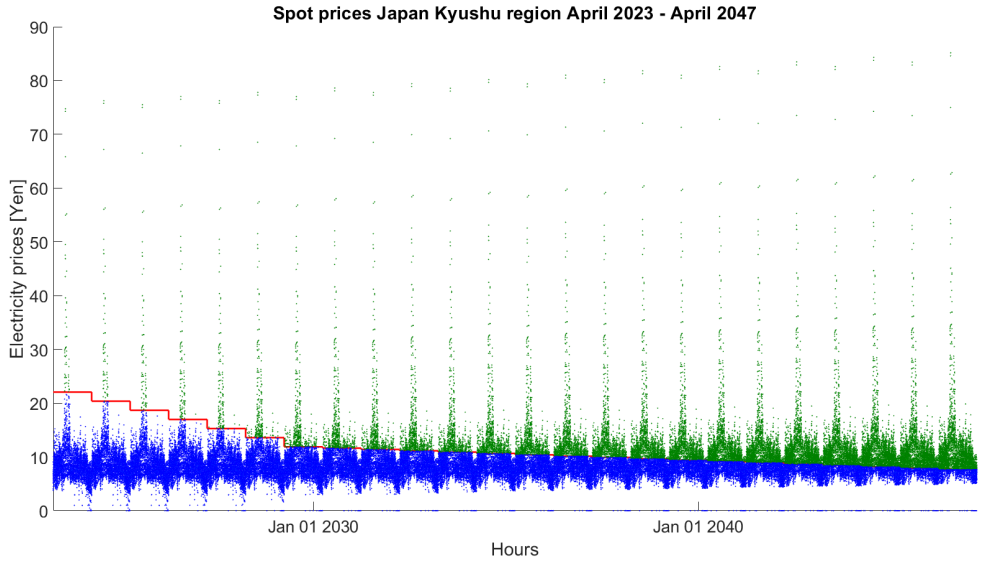

Figure B.16: Operational hours of Goto City Wind Farm for an optimistic power price scenario

KPI figures

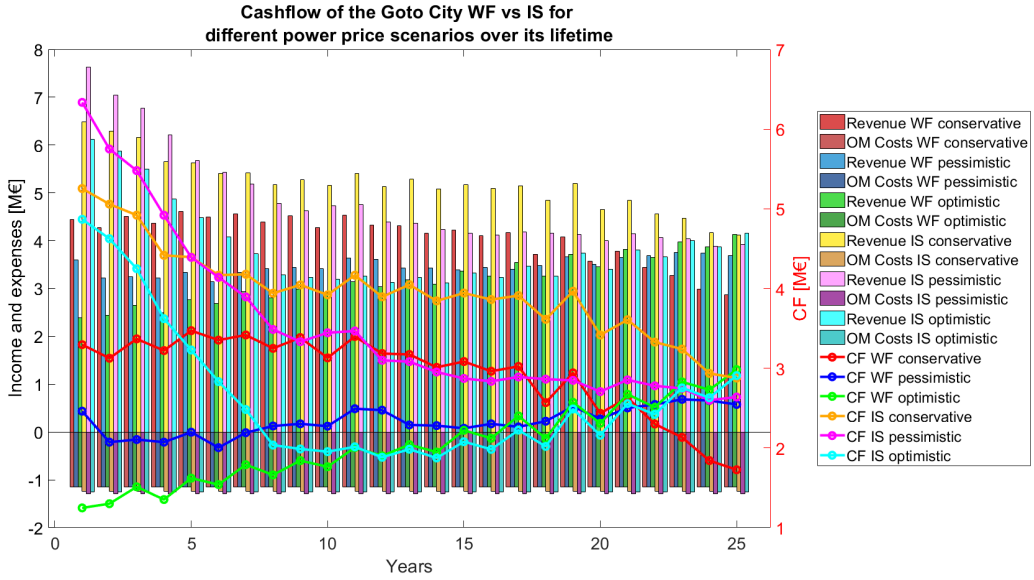

Figure B.17: Cashflow over lifetime for different power price scenarios

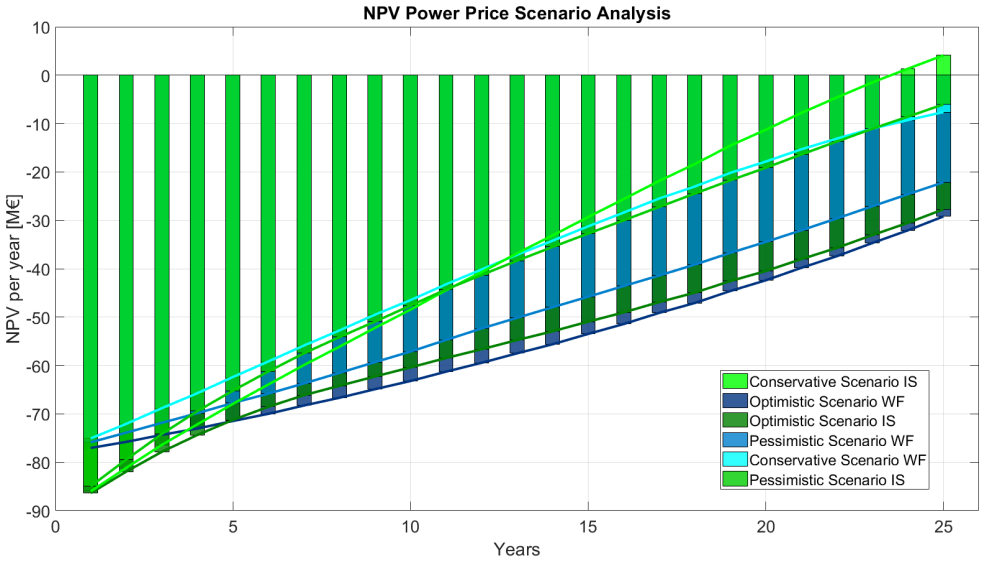

Figure B.18: NPV over lifetime for different power price scenarios

B.5.3. CO2 scenario

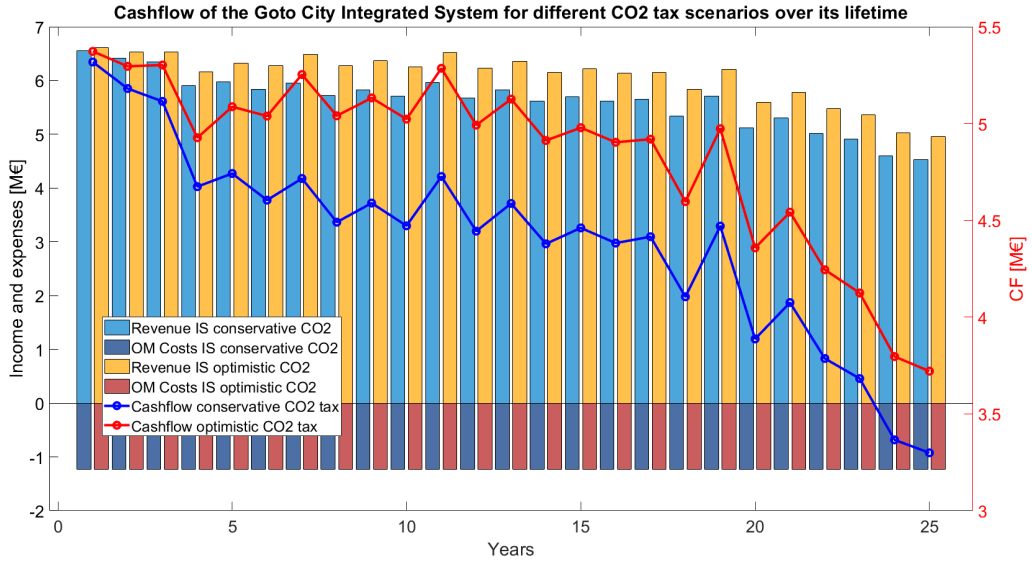

Figure B.19: Cashflow over lifetime for different CO2 tax scenarios

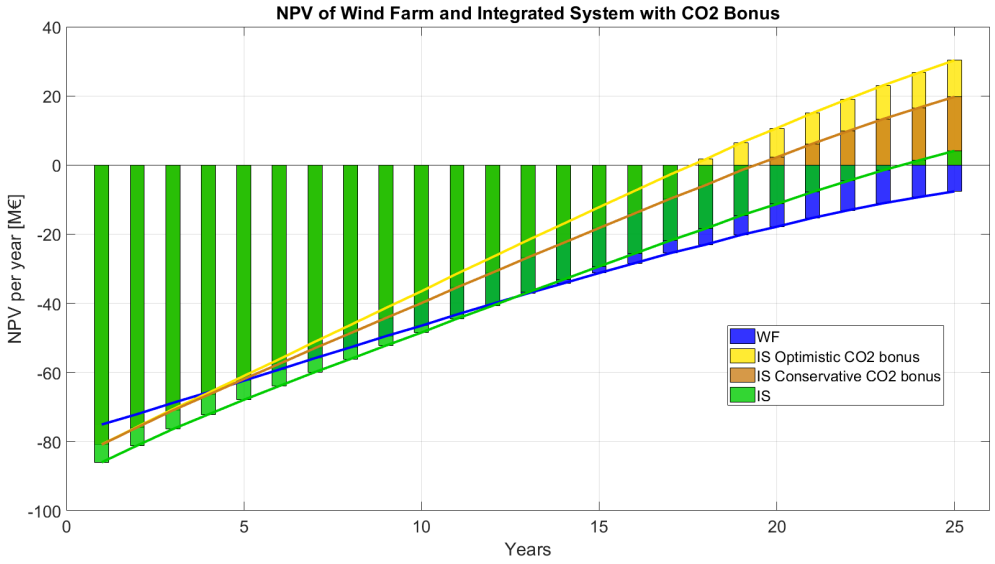

Figure B.20: NPV over lifetime for different CO2 tax scenarios

B.5.4. CAPEX/OPEX scenarios

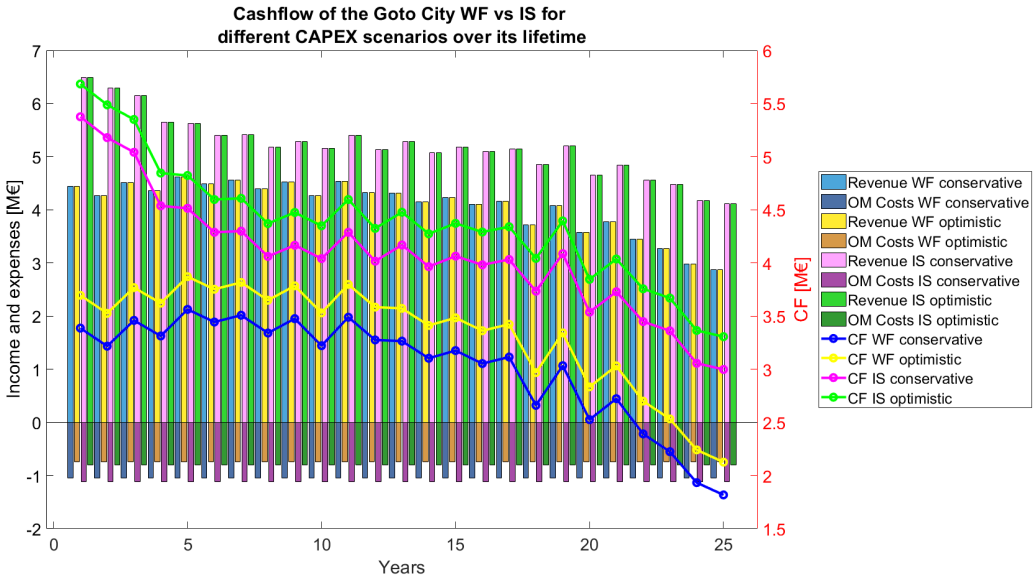

Figure B.21: CF over lifetime for different CAPEX scenarios

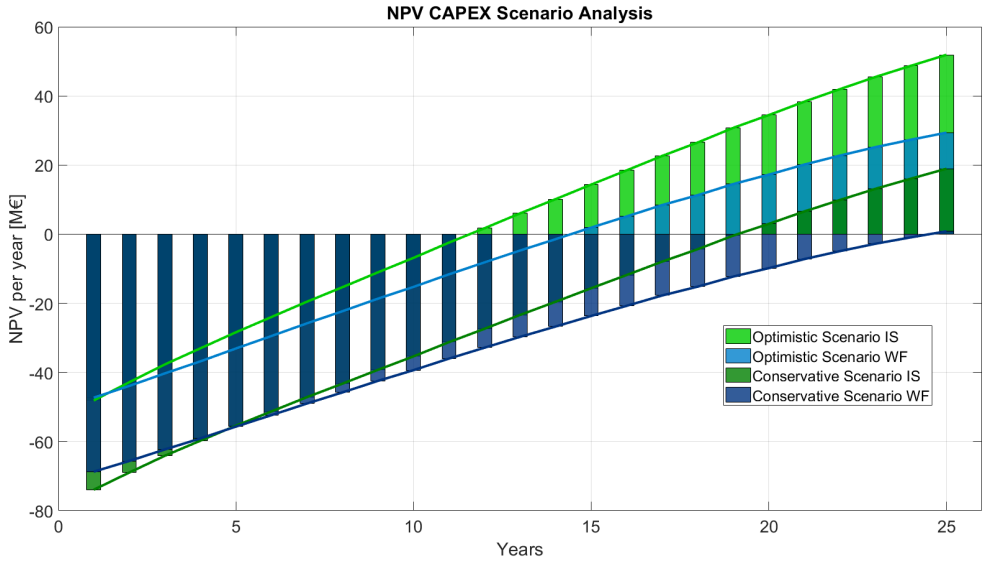

Figure B.22: NPV over lifetime for different CAPEX scenarios

B.6. Sensitivity Analyses

The section includes the yearly cash flow and NPV development graph from the model for the sensitivity analyses. Cash flow figures illustrate the total gained revenue and operating expenses from both the WF and IS and the resulting cash flow of the year. NPV figures illustrate the annual development of system value over its operational lifetime.

B.6.1. Wind Speed

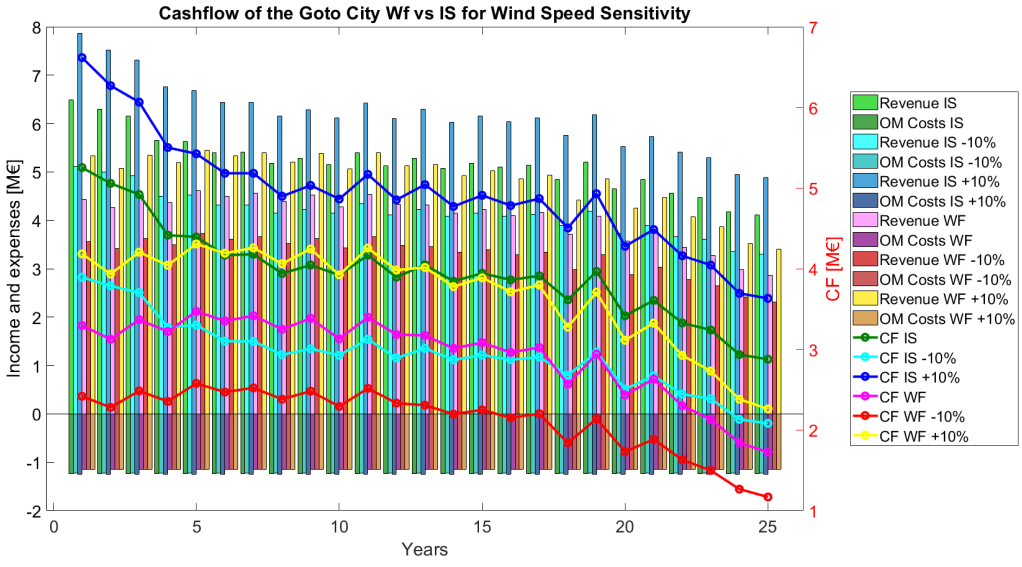

Figure B.23: CF over the lifetime of the WF and IS for wind speed sensitivity analysis

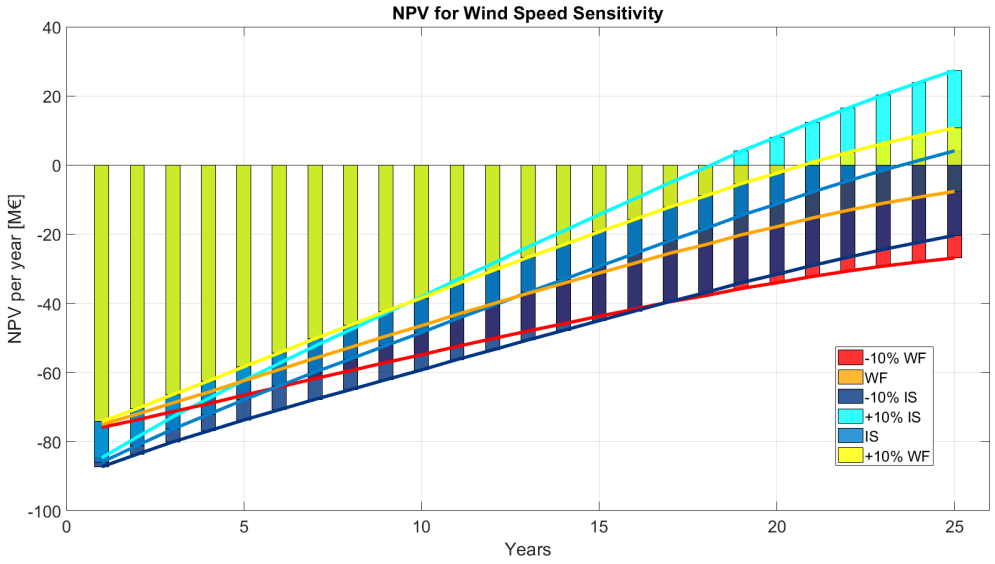

Figure B.24: NPV over the lifetime of the WF and IS for wind speed sensitivity analysis

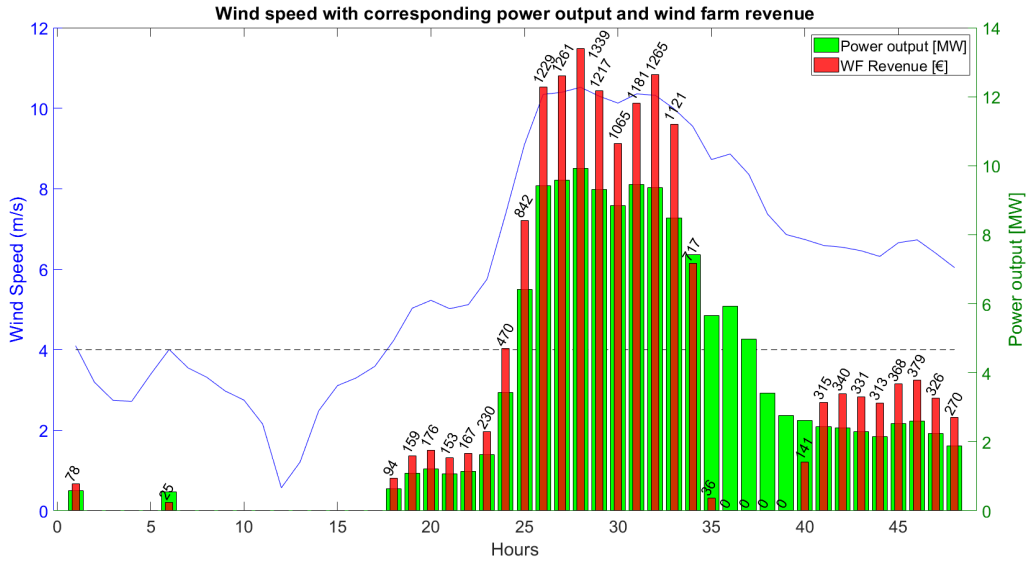

Figure B.25: Hourly power generation and revenue of the system over a two day time period for the high wind speed sensitivity analysis

B.6.2. Power price

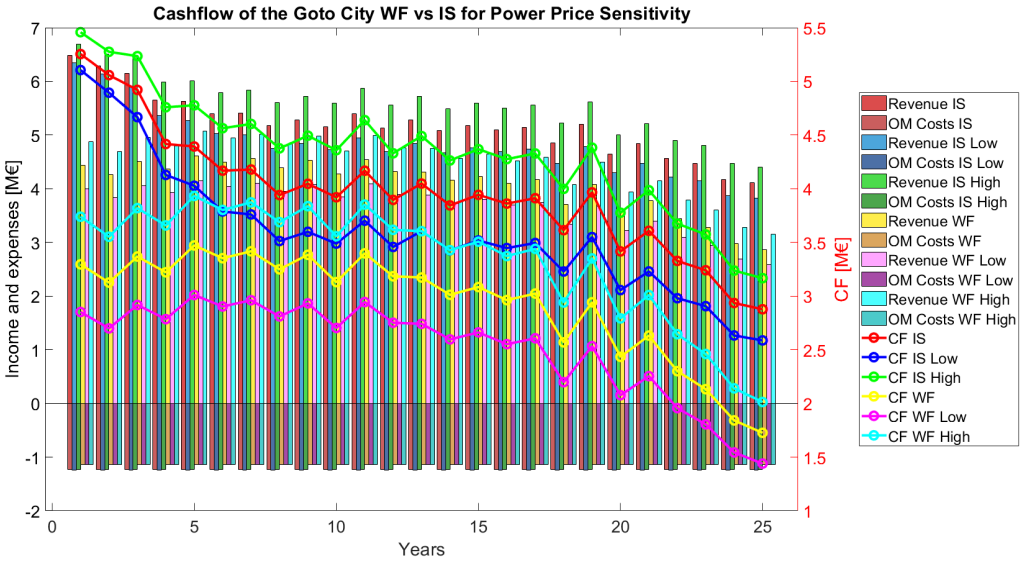

Figure B.26: Cashflow of the Goto City WF and IS for power price sensitivity analyses

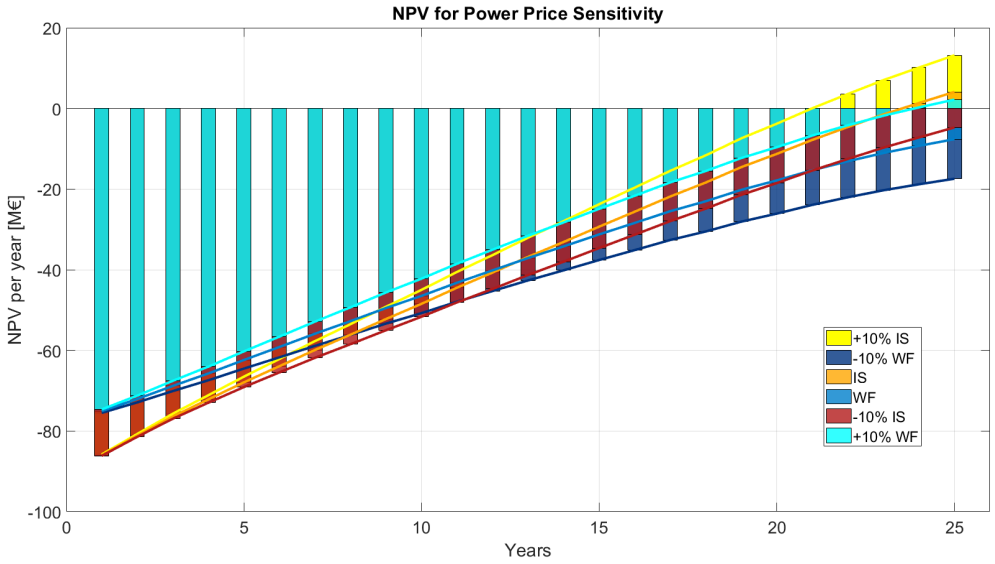

Figure B.27: NPV of the Goto City WF and IS for power price sensitivity analyses

B.6.3. Turbines

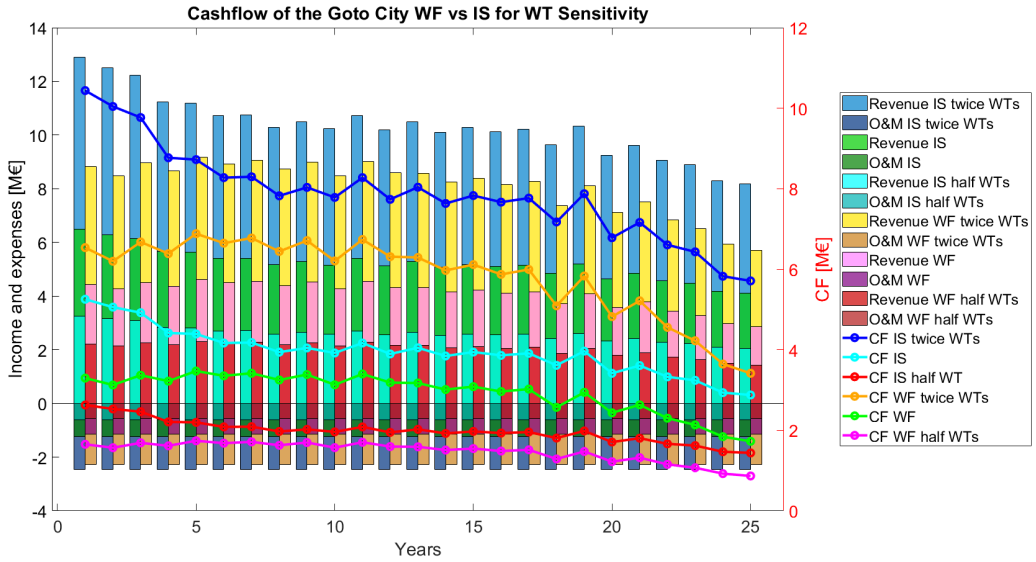

Figure B.28: Cashflow of the Goto City WF and IS for wind farm capacity sensitivity analysis considering the number of installed WTs in the wind farm

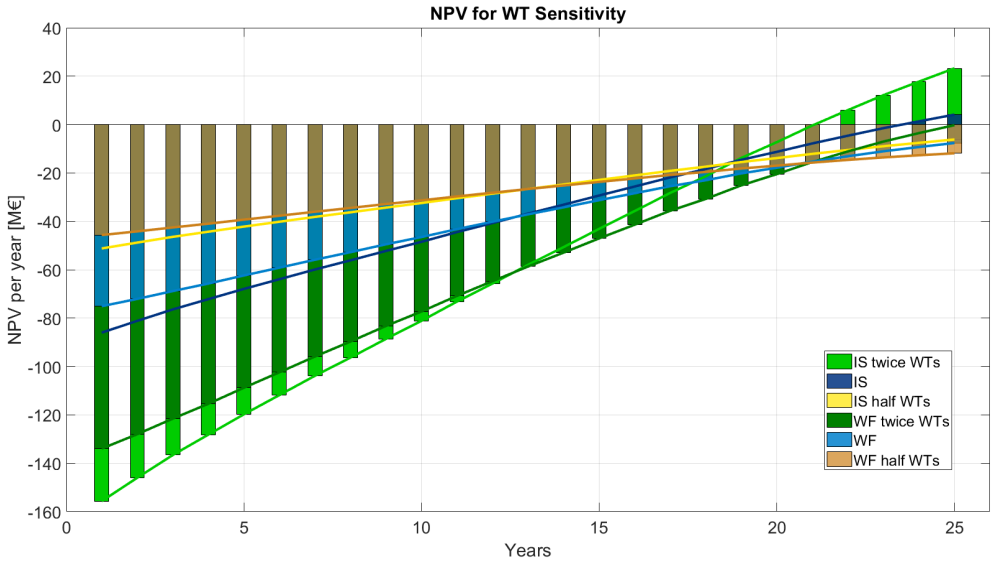

Figure B.29: NPV of the Goto City WF and IS for wind farm capacity sensitivity analysis considering the number of installed WTs in the wind farm

B.6.4. WT Type

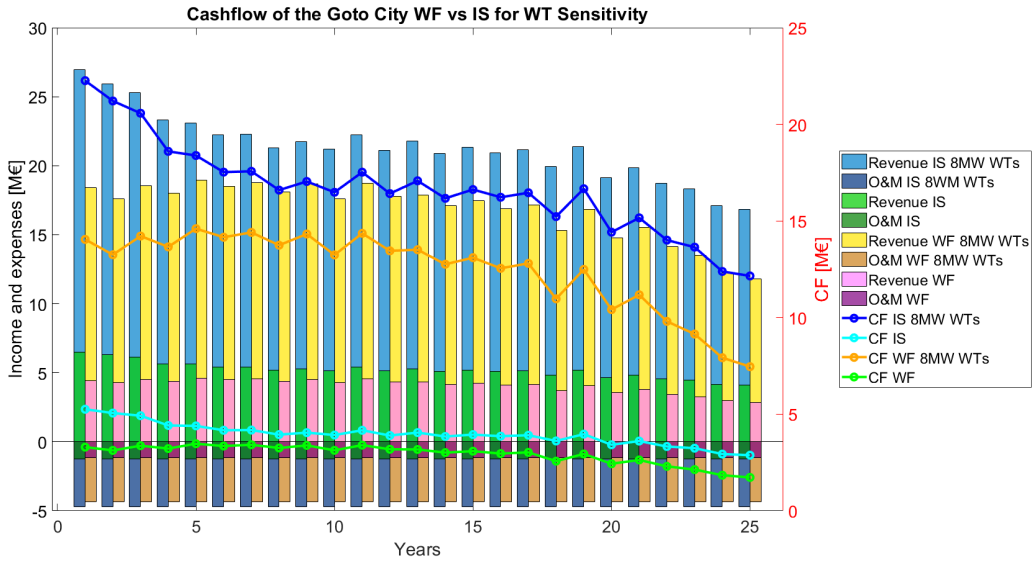

Figure B.30: Cashflow of the Goto City WF and IS for wind farm capacity sensitivity analysis considering the installed WT type in the wind farm

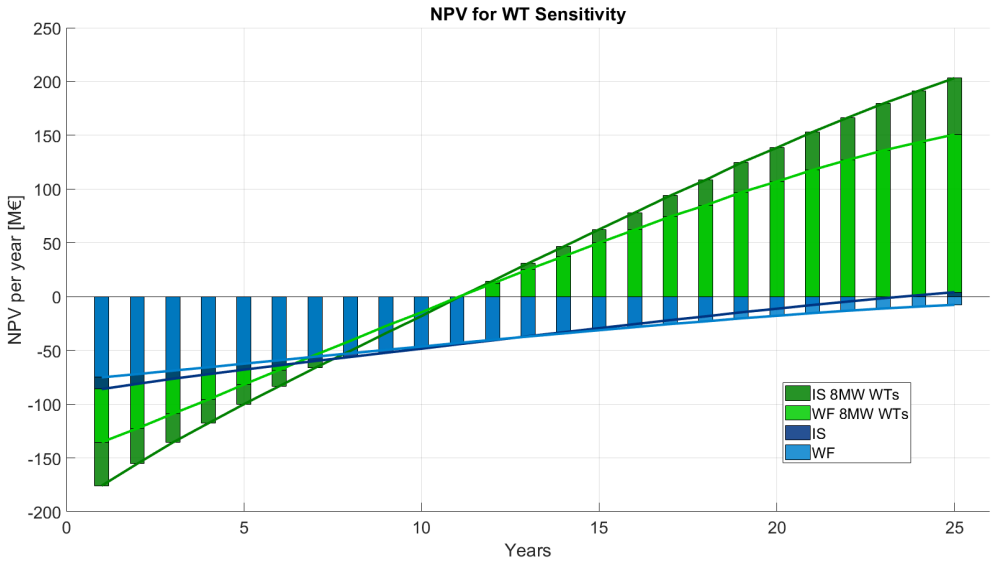

Figure B.31: NPV of the Goto City WF and IS for wind farm capacity sensitivity analysis considering the installed WT type in the wind farm

B.6.5. Number of WT type

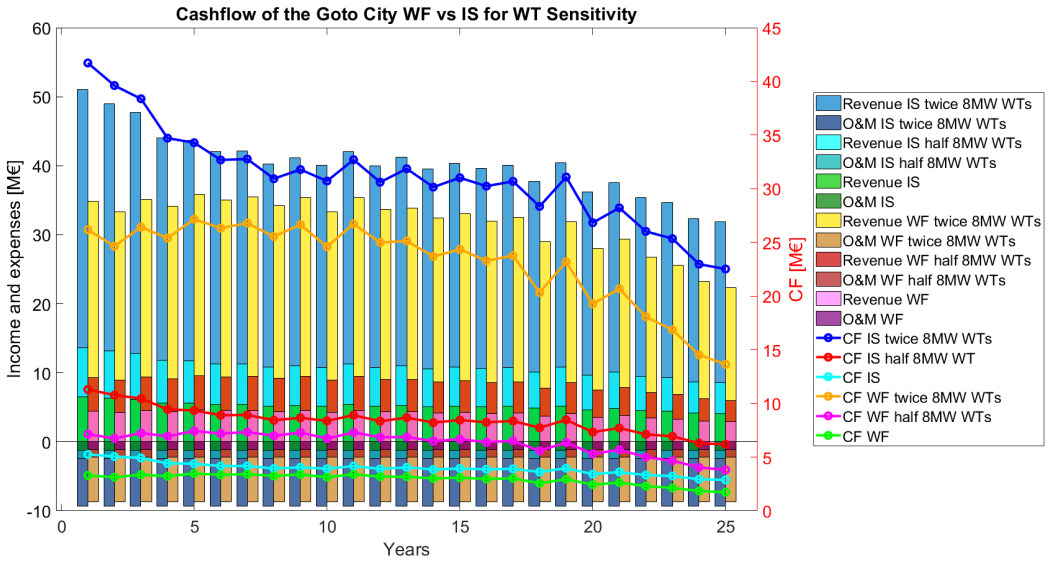

Figure B.32: Cashflow of the Goto City WF and IS for wind farm capacity sensitivity analysis considering the number of installed WT type in the wind farm

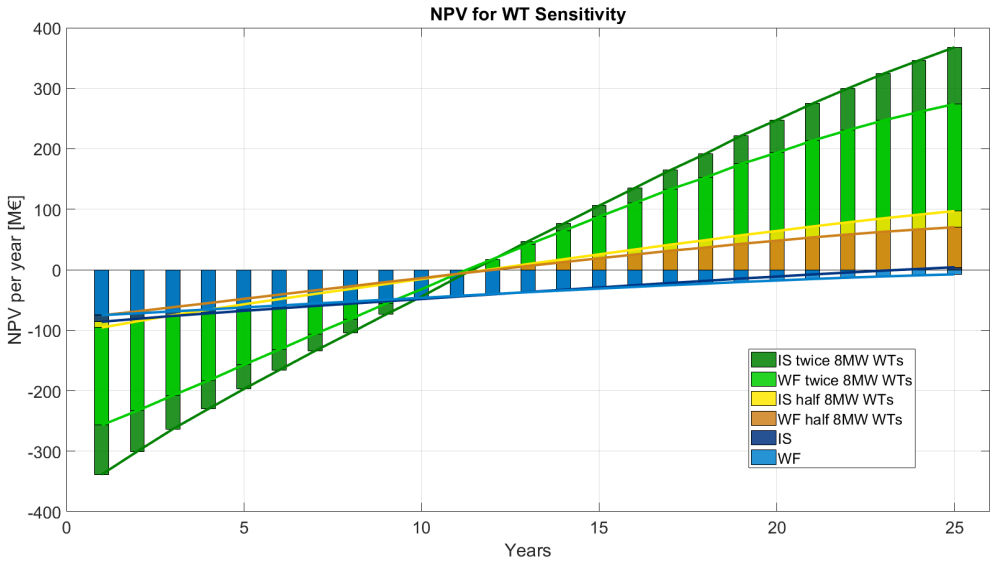

Figure B.33: NPV of the Goto City WF and IS for wind farm capacity sensitivity analysis considering the number of installed WT type in the wind farm

B.6.6. Tornado Charts Deviations

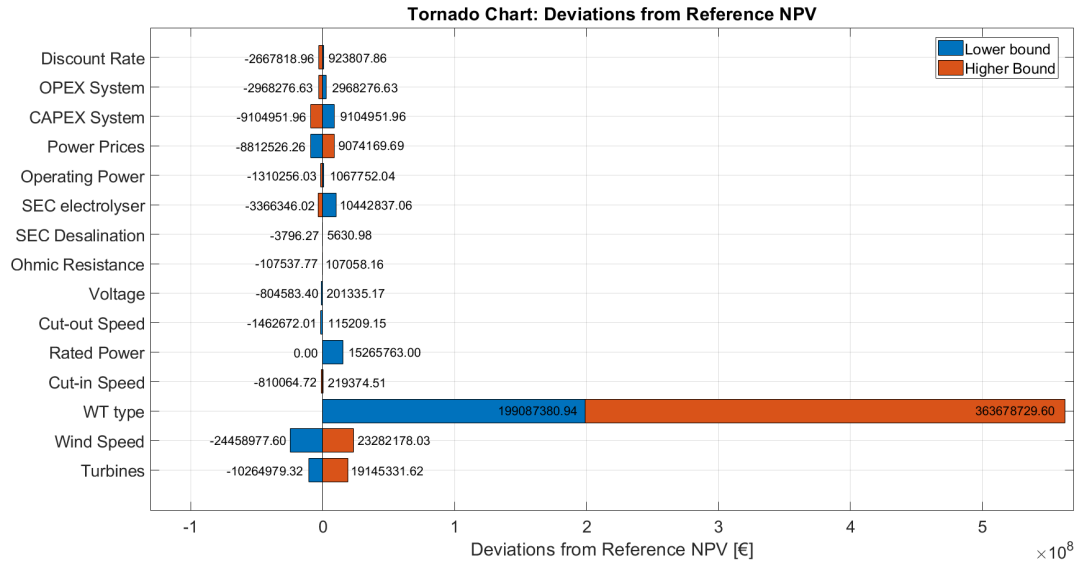

Figure B.34: Tornado chart for each of the deviations with respect to the NPV of the IS for each of the analysed sensitivity parameters

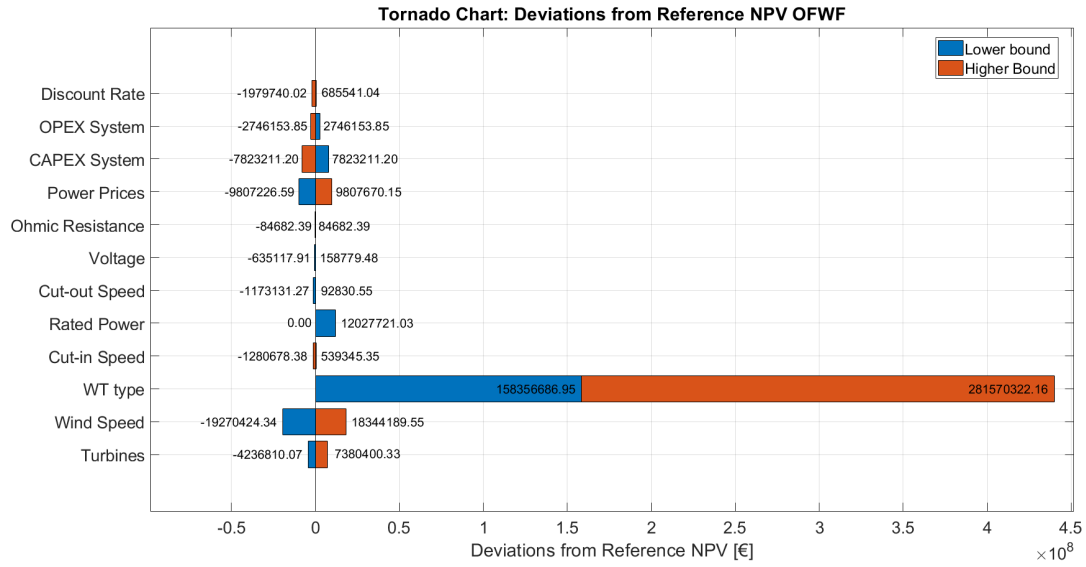

Figure B.35: Tornado chart for each of the deviations with respect to the NPV of the WF for each of the analysed sensitivity parameters

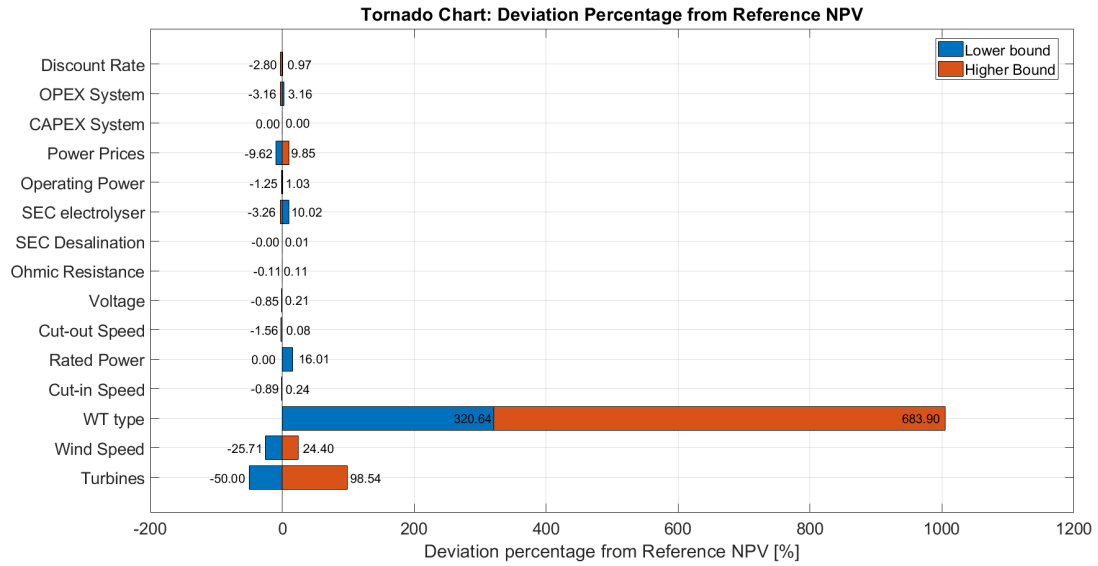

Figure B.36: Tornado chart for each of the deviation percentages with respect to the NPV of the IS for each of the analysed sensitivity parameters

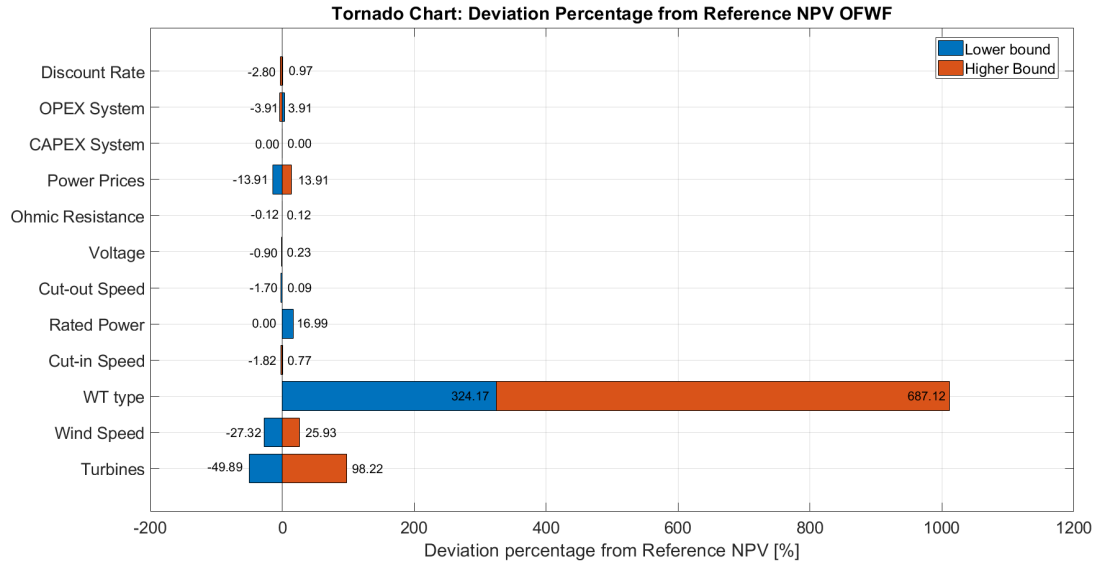

Figure B.37: Tornado chart for each of the deviation percentages with respect to the NPV of the WF for each of the analysed sensitivity parameters